

# Hallucination Engineering: From Neuroscience Robotics to Hallucinations in Health and Disease

Présentée le 8 septembre 2020

à la Faculté des sciences de la vie  
Chaire Fondation Bertarelli de neuroprothétique cognitive  
Programme doctoral en neurosciences

pour l'obtention du grade de Docteur ès Sciences

par

**Eva BLONDIAUX**

Acceptée sur proposition du jury

Prof. F. C. Hummel, président du jury  
Prof. O. Blanke, Prof. D. N. A. Van De Ville, directeurs de thèse  
Prof. A. Cronin-Golomb, rapporteuse  
Prof. M. Schaer, rapporteuse  
Prof. J.-Ph. Thiran, rapporteur



---

## **Abstract**

My thesis focuses on a psychotic symptom called the presence hallucination (PH). PHs are defined as the false perception that someone is nearby when no one is actually present. PHs can occur in various populations, ranging from healthy subjects (when exposed to extreme conditions) to neurological (e.g. epileptic, Parkinson's disease patients) and psychiatric patients (e.g. schizophrenia). Our group has designed a robotic device that allows to safely induce PH in healthy subjects, in a controlled manner, using different sensorimotor conflicts (Blanke et al., 2014). The aim of my thesis was to unravel the brain regions and mechanisms associated with PH and explore how the neuroscientific understanding of PH can improve diagnostics of different clinical populations with hallucinations.

In Chapter 2, I investigated the brain networks associated with a category of complex phenomena named autoscopic phenomena (AP). AP include PHs and three other forms: autoscopic hallucinations, heautoscopies, and out-of-body experiences. AP are rare phenomena, defined as illusory reduplication involving a double of one's own body seen or felt in extrapersonal space. Lesion network mapping analysis was used to identify the brain networks associated to each AP. My data showed that each AP is characterised by specific connectivity networks consistent with their phenomenology. All AP also share common brain connectivity.

In Chapter 3, using an MR-compatible robot able to induce PH, I investigated the brain regions and mechanisms of robot-induced PH in healthy subjects using fMRI. I combined these data with the results of my lesion network mapping analysis in neurological patients with focal brain damage associated with PH (Chapter 3). Both networks (i.e. robot-induced PH-network in healthy subjects and symptomatic PH-network) were merged together to identify the key regions involved in PH, defining a common PH-network. The relevance of this common PH-network was then assessed and confirmed in patients with Parkinson's disease (PD), revealing a difference in functional connectivity within this network between PD patients experiencing symptomatic PH compared to patients without such symptoms.

Further, I studied the functional connectivity within the common PH-network in 22q11.2 deletion syndrome (DS) subjects (i.e. subjects with high risks (30%) of developing schizophrenia) (Chapter 4) and in psychotic patients with passivity

---

experiences (Chapter 5). Studying PH in these population is relevant since PH is frequent in schizophrenia. In both populations, a reduced functional connectivity in the common PH-network was revealed. In Chapter 4, I also assessed the sensitivity to the sensorimotor conflicts and the proneness to experience robot-induced PH in 22q11DS subjects and age-matched controls. Results showed a lack of sensitivity in sensorimotor modulation for the sense of agency, further corroborated by a lack of delay dependency in experiencing robot-induced PH in 22q11DS subjects compared to controls.

In summary, by coupling robotic technology with neuroimaging, a common PH-network was delineated and was found relevant in different clinical populations. These findings are important since PH can be present at early stages before the apparition of more severe symptoms. Therefore, our results can lead to more robust diagnostic tools and early treatment intervention, which might significantly improve prognosis in those patients.

**Keywords:** presence hallucination, autoscopic phenomena, fMRI, resting state functional connectivity, 22q11.2 deletion syndrome, Parkinson's disease, lesion network mapping

---

## Résumé

Ma thèse porte sur un symptôme psychotique appelé l'hallucination de présence (HP). L'HP se caractérise par la sensation d'une présence à proximité (à côté ou derrière soi) alors que personne n'est réellement là. Les HP peuvent se produire dans diverses populations, allant des sujets sains (lors de conditions extrêmes) aux patients neurologiques (épilepsie, maladie de Parkinson) et psychiatriques (la schizophrénie). Notre laboratoire a conçu un dispositif robotique permettant d'induire en toute sécurité et de manière non-invasive les HP chez des sujets sains, de manière contrôlée, en utilisant des conflits sensorimoteurs (Blanke et al., 2014). L'objectif de ma thèse est d'identifier les régions du cerveau et les mécanismes associés à l'HP et de déterminer comment une meilleure compréhension de ce phénomène peut améliorer le diagnostic de différentes populations cliniques présentant des hallucinations.

Au Chapitre 1, j'expose les réseaux cérébraux associés aux phénomènes autoscopiques (PA). Les PA sont des phénomènes illusoire rares durant lesquelles un double de son propre corps est perçu dans l'environnement. Les PA incluent les HP et trois autres phénomènes : les hallucinations autoscopiques, les héautoscopies et les expériences extracorporelles. En utilisant une méthode de cartographie des réseaux neuronaux à partir de lésions de patients neurologiques ayant des AP, mes analyses ont montré que chaque PA est caractérisé par des réseaux de connectivité spécifique, en accord avec leur phénoménologie. Les PA partagent également une connectivité cérébrale commune.

Dans le chapitre 2, à l'aide d'un dispositif robotique capable d'induire l'HP, j'ai étudié les régions du cerveau associées à l'HP chez des sujets sains en utilisant l'IRMf. J'ai combiné ces données avec le réseau associé à l'HP trouvé précédemment (Chap. 1). Les deux réseaux ont été fusionnés pour identifier les régions importantes impliquées dans l'HP. La pertinence de ce réseau neuronal a été ensuite évaluée et confirmée chez des patients atteints de la maladie de Parkinson, révélant une différence de connectivité fonctionnelle au sein de ce réseau entre les patients présentant l'HP comparé à ceux qui n'ont pas ce symptôme.

J'ai également étudié la connectivité fonctionnelle au sein du réseau neuronal associé à l'HP chez des sujets atteints du syndrome de microdélétion 22q11.2 (22q11DS) (des

---

sujets ayant un risque élevé de développer la schizophrénie) (Chap. 3) et chez des patients psychotiques présentant des symptômes de passivité (Chap. 4). L'étude de l'HP dans ces populations est pertinente puisque l'HP est fréquente chez les schizophrènes. Dans les deux populations, une connectivité fonctionnelle réduite dans le réseau neuronal associé à l'HP a été révélée. Au chapitre 3, j'ai également évalué la sensibilité des sujets 22q11DS aux conflits sensorimoteurs et leur susceptibilité à avoir l'HP pendant notre manipulation robotique comparé à un groupe contrôle.

En résumé, en couplant la technologie robotique à la neuroimagerie, un réseau neuronal associé à l'HP a été délimité et s'est avéré pertinent dans différentes populations cliniques. Ces résultats sont importants, car l'HP peut être présente à des stades précoces avant l'apparition de symptômes plus graves. Par conséquent, nos résultats peuvent conduire à des outils de diagnostic plus robustes et à une intervention thérapeutique précoce, ce qui pourrait améliorer considérablement le pronostic des patients.

**Mots-clés:** hallucination de présence, phénomènes autoscopiques, IRMf, connectivité fonctionnelle au repos, syndrome de microdélétion 22q11.2, maladie de Parkinson, cartographie des réseaux de lésions

---

## **Table of Content**

<b>Chapter 1: General Introduction.....</b>	<b>1</b>
<b>1.1 Motivation and overview .....</b>	<b>1</b>
<b>1.2 Bodily self-consciousness .....</b>	<b>3</b>
<b>1.3 Altered bodily states: Autoscopic phenomena .....</b>	<b>4</b>
1.3.1 Definition and phenomenology.....	4
1.3.2 Etiology of AP.....	6
1.3.3 Theoretical considerations .....	7
<b>1.4 Brain lesions: tools to study brain function .....</b>	<b>8</b>
1.4.1 Traditional lesion analysis.....	8
1.4.2 Lesion network mapping analysis.....	9
<b>1.5 Presence hallucination .....</b>	<b>11</b>
1.5.1 Definition .....	11
1.5.2 PH classification within AP.....	12
1.5.3 Etiology.....	12
1.5.3.1 PH in Parkinson’s Disease .....	13
1.5.3.2 PH in Schizophrenia .....	13
1.5.4 Brain regions involved in PH.....	14
1.5.5 Agency and sensorimotor integration .....	15
1.5.6 Experimental procedures .....	17
<b>Chapter 2: Common and distinct brain networks of four autoscopic phenomena .</b>	<b>20</b>
Abstract .....	21
Introduction .....	22
Methods .....	27
Results .....	30
Autoscopic hallucinations.....	30
Heautoscopy.....	31
Out-of-body experiences.....	31
Presence hallucinations.....	31
Common lesion network .....	34
Discussion .....	36
References .....	44
Supplementary information of Common and distinct brain networks of four autoscopic phenomena.....	50
<b>Chapter 3: Sensorimotor hallucinations in Parkinson’s disease .....</b>	<b>56</b>
Abstract .....	57
Introduction .....	58
Results .....	60
riPH in patients with PD (study1.1) .....	60
riPH in PD-PH patients depend on sensorimotor delay (study1.2) .....	63
Brain mechanisms of PH.....	64
Brain mechanisms of riPH in healthy participants using MR-compatible robotics (study2.1) .....	64
Common PH-network for sPH and riPH (study2.2).....	66
Disrupted functional connectivity in cPH-network accounts for sPH Parkinson’s disease (study3.1).....	68

Functional disconnection within the cPH-network correlates with cognitive decline for PD-PH (study3.2).....	69
Discussion .....	71
Methods .....	73
References .....	81
Supplementary Information of Sensorimotor hallucinations in Parkinson’s disease.....	85
<b>Chapter 4: Individuals with the 22q11.2 deletion syndrome show lack of sensitivity to sensorimotor conflicts .....</b>	<b>117</b>
Abstract .....	118
Introduction .....	119
Methods .....	122
Results .....	128
Occurrence of PH in 22q11DS .....	128
Experiment 1: robot-induced PH and PE through sensorimotor stimulations .....	129
Experiment 2: robot-induced PH and PE based on varying degrees of sensorimotor conflicts .	131
Experiment 3: resting-state functional connectivity within the PH-network.....	132
Correlations with clinical and neuropsychological scores .....	132
Discussion .....	135
References .....	138
<b>Chapter 5: Fronto-temporal functional disconnection within the presence hallucination network in psychotic patients with passivity experiences .....</b>	<b>141</b>
Abstract .....	142
Introduction .....	143
Methods .....	145
Results .....	150
Functional disconnection within the presence hallucination network .....	150
Extended PH-network functional connectivity changes.....	152
Discussion .....	155
References .....	157
Supplementary information of fronto-temporal functional disconnection within the PH-network in psychotic patients with passivity experiences .....	160
<b>Chapter 6: General Discussion.....</b>	<b>163</b>
<b>6.1 Summary of scientific contributions.....</b>	<b>163</b>
6.1.1 Studying AP towards a better understanding of BSC .....	163
6.1.1.1 Outlook.....	164
6.1.2 PH brain network across populations.....	165
<b>6.2 Induction of PH in healthy subjects .....</b>	<b>167</b>
<b>6.3 PH and PE: independent processes?.....</b>	<b>170</b>
<b>6.4 Current and future studies in healthy subjects .....</b>	<b>172</b>
6.4.1 Using dynamic functional connectivity .....	172
6.4.2 Whole versus body parts .....	172
<b>6.5 PH across clinical populations .....</b>	<b>173</b>



---

6.5.1	Fronto-temporal disconnection.....	174
6.5.2	Future studies in patients.....	176
<b>6.6</b>	<b>Conclusion .....</b>	<b>176</b>
<b>7.</b>	<b><i>References</i> .....</b>	<b>177</b>
<b>8.</b>	<b><i>Annexes</i> .....</b>	<b>186</b>
8.1	Psycho-physiological analysis .....	186
8.2	Distinct neural mechanisms of temporal and spatial prediction in peripersonal space .....	189
	<b><i>Acknowledgments</i>.....</b>	<b>236</b>
	<b><i>Curriculum Vitae</i>.....</b>	<b>237</b>

---

## Abbreviations

PH = presence hallucination

AP = autoscopic phenomena

AH = autoscopic hallucination

HAS = heautoscopy

OBE = out-of-body experience

BSC = bodily self-consciousness

TPJ = temporo-parietal junction

IFG = inferior frontal gyrus

pMTG = posterior middle temporal gyrus

vPMC = ventral premotor cortex

fMRI = functional magnetic resonance imaging

rsfMRI = resting state functional magnetic resonance imaging

PD = Parkinson's disease

22q11DS = 22q11 deletion syndrome

PE = passivity experience

LoA = loss of agency

## Chapter 1: General Introduction

### 1.1 Motivation and overview

*« Je hâtai le pas, inquiet d'être seul dans ce bois, apeuré sans raison, stupidement, par la profonde solitude. Tout à coup, il me sembla que j'étais suivi, qu'on marchait sur mes talons, tout près, à me toucher. Je me retournai brusquement. J'étais seul. »*

Guy de Maupassant, Le Horla.

Have you ever felt this sensation that someone is behind you? A sensation so strong that you feel the need to turn back to see, and surprisingly find out no one is actually there? This sensation, referred in this thesis as the presence hallucination (PH), has been extensively described in folklore and literature over the centuries (Critchley, 1955; Geiger, 2009; de Maupassant, 1886; Messner, 2003; Smythe, 1940). PH was more recently classified as part of autoscopic phenomena (AP), defined as illusions involving the feeling or the visual reduplication of one's own body in the extrapersonal space (i.e. space outside the reaching space around the body). AP consist of four main forms including PH, namely autoscopic hallucinations (AH), heautoscopy (HAS) and out-of-body experiences (OBE) (Blanke et al., 2004; Brugger et al., 1997). AP are rare and spontaneous phenomena that have been reported in different types of populations, e.g., from healthy subjects to neurological and psychiatric patients; and yet the brain mechanisms associated to AP have not been fully understood (Brugger et al., 1999; Critchley, 1950; Devinsky et al., 1989; Fénelon et al., 2011; Hécaen and Ajuriaguerra, 1952; Jaspers, 1913; Lippman, 1992; Llorca et al., 2016; Menninger-Lerchenthal, 1935).

My thesis aimed at unravelling the brain networks underlying such complex phenomena. Those objectives have been addressed through experimental paradigms merging robotics, cognitive neuroscience and neuroimaging methods. In addition, this thesis demonstrates that the observed neuroscientific insights can improve understanding and diagnosis of different clinical populations with PH symptoms such as in Parkinson's disease (PD). A particular focus was given to PH which, until recently, was not systematically assessed in clinical populations despite being very common in psychiatric and neurological patients (up to 46 % of patients with the schizophrenia and 40% of patients with PD experience such hallucinations) Indeed,

PH, in the case of Parkinson's disease, can appear before the onset of more complex hallucinations (e.g. visual structured hallucination) and sometimes even before the onset of the first motor-symptoms (Ffytche et al., 2017; Pagonabarraga et al., 2016), providing an opportunity to detect and diagnose those cases at a very early stage. In this thesis, we investigated these two clinical populations in which the occurrence of PH is frequent, but also a third population which is well-known to be at high risk of developing schizophrenia, young individuals with the 22q11.2 deletion syndrome (22q11DS). In those individuals, the sensitivity to experience PH could be studied at early stages before the apparition of more severe psychotic symptoms, potentially leading to early therapeutic interventions. Therefore, better understanding the brain mechanisms of PH and identifying neural and/or behavioural biomarkers are highly relevant clinically, e.g., to provide more robust diagnostic tools.

In **Chapter 2**, I describe the work I carried out to investigate the brain networks associated with each AP of neurological origin using a novel neuroimaging method that combines lesion data and a normative database containing data of healthy subjects. In **Chapter 3**, I present the study on the brain regions associated with PH in healthy subjects using an MR-compatible robotic device that can induce PH in a safe, non-invasive and controlled manner. Brain activity of participants was recorded throughout the experiment, allowing to identify brain regions associated to PH. In addition, by merging these brain regions with the brain network obtained from the above-mentioned neurological patients (symptomatic PH-network, **Chapter 3**), I have identified a more specific brain network, the PH-network, involved in both populations (i.e. healthy subjects and neurological patients with focal brain damage causing PH). The relevance of this network was further confirmed in another independent clinical population experiencing PH, patients with PD. In those patients, the functional connectivity (i.e. the temporal dependency between spatially separated brain regions) within the PH-network differed depending on whether the patient experienced PH in their daily life or not. In **Chapter 4**, I present the study on the robot-induced PH and passivity experiences (defined as the sensation of not being in control of one's own actions) in a clinical population at high risk of developing schizophrenia (subjects with the 22q11DS). The functional connectivity during rest in the PH-network was also reduced for the individuals with 22q11DS compared to age-matched controls. Finally, in **Chapter 5**, the functional connectivity within the PH-network was also investigated

in psychotic patients with and without passivity experiences and again reduced functional connectivity was observed in this network.

In the next sections, I will introduce and provide the general background and methods needed for a good understanding of the present thesis. I will start by defining and explaining autoscopic phenomena, including the different symptoms, the theoretical considerations and the etiology. Then, I will continue by providing a more detailed introduction of PH, focusing on the etiology, its link to sensorimotor processing. I will finish by presenting the experimental methods used to assess PH.

### **1.2 Bodily self-consciousness**

Bodily self-consciousness (BSC) is defined as the conscious experience of being a self inside a body and to have control over that body (agency) (Blanke, 2012; Blanke et al., 2015; Jeannerod, 2003). In other words, BSC is the “I” of conscious experience also known as the “minimal self” as opposed to other more cognitive aspects of the self (e.g. the social self, the narrative self) (Blanke and Metzinger, 2009; Gallagher, 2000). BSC relies on three important aspects: (1) self-identification, the experience of owning a body (can also be referred as body-ownership); (2) first person perspective, i.e. the experience of the position and perspective from where the world is perceived and (3) self-location, the experience of where the self is located in space (Blanke, 2012; Blanke and Metzinger, 2009; Blanke et al., 2015). BSC has been suggested to depend on multisensory perception of external and bodily-related signals such as visual, tactile, proprioceptive, audition, vestibular and visceral information (Blanke, 2012; Blanke et al., 2015). Evidence for the importance of multisensory mechanisms in BSC has been gathered through the observation of neurological and psychiatric patients presenting disorders of body representation, in which self-identification and/or self-location and first-person perspective had been altered (Critchley, 1950). Examples of such disorders include somatoparaphrenia, in which a body part is no longer considered as one’s own (i.e. abnormal feeling of disownership toward a body part, usually the hand or arm) (Bottini et al., 2002; Vallar and Ronchi, 2009), and AP, which affect the whole body (i.e. full body disorder) (Blanke et al., 2004; Brugger et al., 1997; Case et al., 2020). AP will be described in more detailed in the next section of this introduction.

Over the last 20 years, researchers have designed novel paradigms aiming at manipulating multisensory signals and altering the different aspects of BSC. This was mainly done using technological tools such as virtual reality and robotics, leading to a better understanding of BSC brain mechanisms (Ehrsson, 2007; Guterstam et al., 2015; Ionta et al., 2011; Lenggenhager et al., 2007, 2009; Petkova et al., 2011; Tsakiris et al., 2006, 2007, 2010). For example, one of the widely used paradigms is the full body illusion during which the participant is touched on the back while seeing an avatar being stroked synchronously (Ehrsson, 2007; Lenggenhager et al., 2007). This creates visuo-somatosensory conflicts that results in a shift in self-location towards the avatar and induces self-identification for the avatar. Induction of the full body illusion enables to experimentally investigate the important aspects of whole BSC as opposed to body parts only. Studying the whole BSC is relevant to understand the essential aspects of a unitary and global representation of the self. The full body illusion paradigm was further adapted to the more restrictive environment of magnetic resonance imaging (MRI) scanner in order to investigate the associated brain regions (Guterstam et al., 2015; Ionta et al., 2011; Petkova et al., 2011; Tsakiris et al., 2010).

### **1.3 Altered bodily states: Autoscopic phenomena**

#### ***1.3.1 Definition and phenomenology***

AP originate from the Greek “Autos” (self) and “skopeo” (looking at) and are disorders involving body representation. AP are defined as illusory reduplications of one’s own body involving a double of one’s own body seen or felt in the extrapersonal space (Menninger-Lerchenthal, 1935). Over the years, AP have been classified in four main types: autoscopic hallucination (AH), heautoscopy (HAS), out-of-body experience (OBE) and feeling of a presence or PH (Blanke and Mohr, 2005; Brugger et al., 1997; Devinsky et al., 1989). A brief definition of each AP will be given in this part but more details about the brain correlates will be found in **Chapter 2**.

AH is characterized by the visual reduplication of one’s own body in the extrapersonal space as if one was looking in the mirror (Figure 1.1A) (Blanke and Mohr, 2005; Brugger et al., 1997; Devinsky et al., 1989). Self-identification, self-location and first person-perspective remain intact in AH: the patients report seeing the world from the physical body as well as being located and identify themselves with the physical body.

HAS is similar to AH with the difference that subjects have difficulties in reporting the localization of their centre of awareness (whether it is located on the physical body or in the double, the autoscopic body) and whether they are disembodied or not (Figure 1.1B) (Blanke and Mohr, 2005; Brugger et al., 1997; Menninger-Lerchenthal, 1935). HAS is characterized by the alternating self-location between the physical body and the autoscopic body and the unstable visuo-spatial perspective. In addition, patients report the experience of echopraxia which is the experience of sharing movements and body postures with the autoscopic body as well as sharing thoughts and verbal communication with the autoscopic body (Brugger et al., 2006; Lukianowicz, 1958). HAS was also associated with negative intense feelings such as suicidal thoughts, fear and despair (Brugger et al., 1994; Lukianowicz, 1958).

During OBE, patients report seeing their own body from an elevated mostly down-looking perspective (Figure 1.1C) (Blanke and Mohr, 2005; Brugger et al., 1997; Devinsky et al., 1989). Therefore, during OBE, the self-location as well as the first-person perspective are abnormal (both are located at the illusory double, feeling of disembodiment). In addition, patients identify themselves to the illusory double rather than to their physical body (i.e., abnormal self-identification).

PH is the sensation that someone is nearby when actually no one is present and it has been classified as being a non-visual AP (Figure 1.1D) (Blanke et al., 2004; Brugger et al., 1997). A more detailed description will be given in **section 1.4** of this introduction since **Chapter 3, 4 and 5** focus on this hallucination.

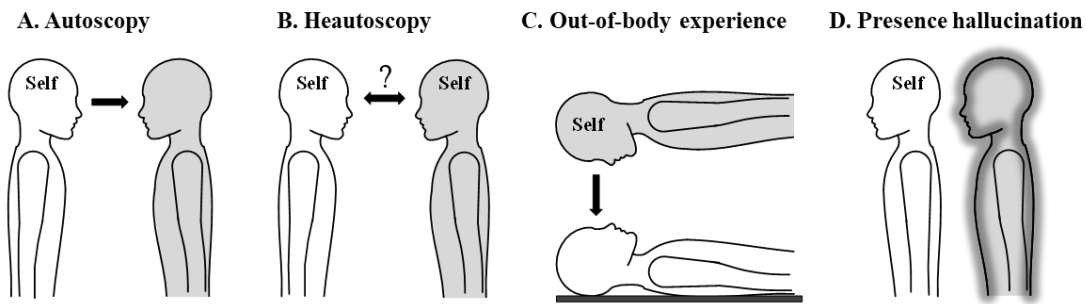


**Figure 1.1:** Autoscopic phenomena. Autoscopic phenomena represents a unique opportunity to investigate the key aspects of BSC: self-identification, self-location and first-person perspective, since those aspects are altered differently across the phenomena. **A.** In autoscopy, patients report seeing an autoscopic body (second illusory own body) in front of them from their physical body (intact self-identification, self-location and first-person perspective). **B.** In heautoscopy, patients report ambiguous location between the physical body and the autoscopic body as well as alternating visuo-spatial perspective between the two bodies. Self-identification either refers to the physical body or to the autoscopic body or to both. **C.** In out-of-body experiences, patients report seeing their physical body from an elevated down-looking perspective. Self-identification refers to the autoscopic body. **D.** In presence hallucination, patients report the sensation that someone is behind them even so no one is present. Self-identification, self-location and first-person perspective are intact in presence hallucination. The autoscopic bodies are represented in grey and the physical body in white. The arrows represent the visuo-spatial perspective and “Self” indicates where the patients locate themselves.

### ***1.3.2 Etiology of AP***

AP have been described in very different clinical populations, including patients with neurological disorders (i.e. epilepsy, migraine (Devinsky et al., 1989; Lippman, 1992; Podoll and Robinson, 1999)), infection disorders (Lhermitte, 1939), psychiatric disorders (schizophrenia (Critchley, 1950; Menninger-Lerchenthal, 1935) as well as depression (Lukianowicz, 1958).

AP have also been described in healthy subjects (Brugger et al., 1999; Devinsky et al., 1989; Hécaen et al., 1952; Lhermitte, 1951). Finally, OBE have been reported in healthy subjects after a near-death experience and 10% of the general population experience such phenomena (Blackmore, 1982, 1986).



### *1.3.3 Theoretical considerations*

Blanke and colleagues have proposed that AP arise from a failure to integrate multisensory signals, i.e., from a disintegration of proprioceptive, tactile, vestibular and visual body-related signals in the personal space (space within reaching distance) (Blanke and Mohr, 2005; Blanke et al., 2004). To create a unified representation of one's own body, the different sensory signals must be integrated and weighted properly by the brain in order to form a coherent information from those sensory signals and minimise uncertainty (Alais and Burr, 2004; Ernst and Banks, 2002). Such process can lead to discarding of inconsistent sensory signals, e.g., by temporarily considering them as noise. It is proposed that a failure in this multisensory integration can lead to AP (Blanke and Mohr, 2005; Blanke et al., 2004).

It was suggested that the different types of AP arise from a double disintegration of multisensory signals. The first one is in personal space, due to conflicting proprioceptive, tactile, kinaesthetic and visual information, and the second is between the personal space and the extrapersonal space, due to conflicting vestibular and visual information (Blanke and Mohr, 2005; Blanke et al., 2004). The former disintegration in the personal space varies depending on the AP, with dysfunction between proprioceptive and visual signals in AH, HAS and OBE and dysfunction between proprioceptive and motor signals in PH (Blanke and Mohr, 2005; Blanke et al., 2008). The second disintegration has been suggested to vary across AP according to the strength and type of vestibular and visual dysfunction. Indeed, OBE is associated with a strong alteration of vestibular signals, HAS and PH with moderate alteration of vestibular signals and AH with low or absent alteration of vestibular signals. For AH, it was instead proposed that alterations of visual signals were more responsible for the disintegration in the personal and extrapersonal space (Blanke and Mohr, 2005; Blanke et al., 2004, 2008).

The theoretical considerations described above were founded on the phenomenology and neural-based evidence of each AP, derived mostly from single case reports of neurological patients (Anzellotti et al., 2011; Blanke and Mohr, 2005; Blanke et al., 2004; Brugger et al., 1997; Devinsky et al., 1989; Hécaen and Ajuriaguerra, 1952; Heydrich et al., 2011; Lhermitte, 1939; Lukianowicz, 1958; Lunn, 1970; Maillard et al., 2004; Menninger-Lerchenthal, 1935; Zamboni et al., 2005). For the last ten years,

researchers have used novel methods to analyse lesions and attribute a particular symptom to a precise brain location (Bates et al., 2003; Rorden et al., 2007). In the next section, I will briefly review traditional lesion analysis methods and the insights it provided about the brain regions involved in AP.

### **1.4 Brain lesions: tools to study brain function**

#### ***1.4.1 Traditional lesion analysis***

One historical approach to better understand and infer brain function was to study patients with focal brain damage. In this manner, many brain regions were associated with different functions. For example, Broca associated the left inferior frontal gyrus with language at the end of the nineteenth century by inspecting, post mortem, the brain of one of his patients only able to reproduce one syllable (Brocca, 1865). Since then, novel techniques to infer human brain functions have emerged such as magnetic resonance imaging (MRI) that allows identifying brain structures non-invasively in humans. Traditional lesion overlap analysis consists in overlapping different brain lesions from patients experiencing the same symptom and trying to find a common overlapping brain region implicated in most/all of the patients (Rorden and Karnath, 2004). In addition, to ensure that this overlapping region is not a brain region that might be more vulnerable to injury (due to high vascularity for example), the lesions associated with the symptom of interest were compared to a control group of patients with focal brain damage but who did not experience the particular symptom of interest (Rorden and Karnath, 2004). Over the years, different statistical methods have emerged to assess the specificity of the overlapping brain region to a particular symptom (beyond subtraction analysis with a control group of lesioned patients). One relevant method is voxel-based lesion symptom mapping (VLSM) (Bates et al., 2003; Karnath et al., 2018; Rorden et al., 2007). VLSM is a statistical test that identifies voxels that are more affected in the patients with lesions causing the symptom of interest compared to the control group of patients. It is a mass-univariate analysis where the statistical test is applied independently to every single voxel in the brain (Bates et al., 2003; Rorden et al., 2007).

Using these methods, OBE was associated with brain damage to the right angular gyrus, HAS to the left posterior insula, AH to the right superior occipital cortex/cuneus

and PH to the insula, the superior parietal cortex and the temporo-parietal junction (TPJ) (Blanke et al., 2014; Heydrich and Blanke, 2013; Ionta et al., 2011).

However, traditional lesion analysis has several limitations: similar symptoms do not always localize to the same brain region, but are sometimes heterogeneously distributed in the brain. Many complex symptoms can also arise without any focal brain lesions, like in the case of psychiatric conditions. This suggests that in the case of complex symptoms, networks rather than a single brain region might be involved. Such networks would be extremely difficult to capture with traditional lesion analysis. In this respect, new methods have emerged to extend traditional lesion analysis using normative connectome data such as lesion network mapping (using functional MRI (fMRI) to measure brain function during rest) or network modification (NEMO) tool using structural connectome (tractograms from healthy subjects) (Boes et al., 2015; Karnath et al., 2018; Kuceyeski et al., 2013).

### *1.4.2 Lesion network mapping analysis*

Boes and colleagues developed a method called lesion network mapping analysis consisting in finding the brain networks associated to a particular symptom without the need of functional neuroimaging data in patients. This is important because acquiring a large set of neuroimaging data including connectivity measures is rarely possible in clinics (Boes et al., 2015; Fox, 2018). The approach relies on normative resting state functional magnetic resonance imaging (rsfMRI) data of healthy subjects from publicly available databases and investigates how in healthy brains the maps of the lesions are connected to the rest of the brain.

To this aim, the lesions are considered as seed regions of interest (ROIs) in a rsfMRI analysis. Their mean time course is correlated with the mean time course of the whole brain voxels in order to find which brain regions have the same pattern of activity. Therefore, the lesion network mapping consists in three main steps (Figure 1.2): 1. Translating the lesion in a normalized brain template (Montreal Neurological Institute (MNI) space) 2. Using the lesion as a seed ROI in the rsfMRI analysis and finding its functional connectivity pattern that will result in one map per subject, 3. Thresholding and binarizing the maps of all the subjects for each lesion to obtain

one map per lesion, and finally, 4. Overlap all the lesions' map to identify the brain regions connected to all the lesion locations.

The method is largely being used to assess different types of lesions causing different types of symptoms such as visual and auditory hallucinations, pain, aphasia, coma-causing lesion, loss of consciousness, hemichorea-hemiballismus, freezing of gait, criminal behaviour, delusional misidentifications, free will, prosopagnosia, hemiplegia, hallucinations cervical dystonia, parkinsonism, impaired decision making, impaired self-attribution and amnesia (Boes et al., 2015; Cohen et al., 2019; Corp et al., 2019; Darby et al., 2017a, 2017b, 2018; Fasano et al., 2017; Ferguson et al., 2019; Fischer et al., 2016; Joutsa et al., 2018; Kim et al., 2019; Klingbeil et al., 2020; Laganiere et al., 2016; Snider et al., 2020; Sutterer et al., 2016; Wawrzyniak et al., 2018).

In the case of AP, which are complex phenomena, even though traditional lesion analysis provided some insights about the brain associated to each AP, not all lesions were overlapping (refer to **Chapter 2** for more details), suggesting next to the complex multisensory nature of AP a network implication rather than a single brain region. Therefore, one aim of my thesis was to investigate the brain networks underlying each AP as well as the common parts of their networks using lesion network mapping analysis (see **Chapter 2**).

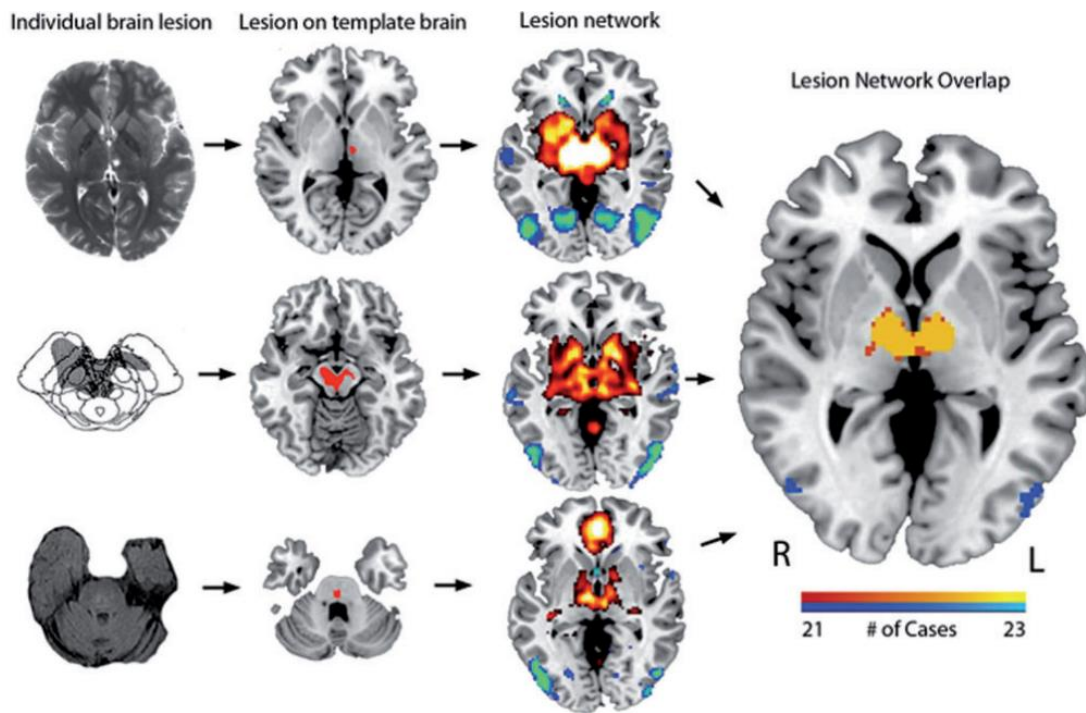


**Figure 1.2:** Lesion network mapping analysis. The method, which uses a normative database of healthy subjects, is composed of three main steps: 1. Mapping the lesion into a template brain (Montreal Neurological Institute (MNI) space), 2. Computing the whole brain connectivity during resting state of this lesion used as region of interest (ROI) and threshold these maps and 3. Overlap all the maps obtained (one per lesion) to obtain a mapping of the brain regions connected to most of the lesions. Here, the color code will correspond to how many lesions overlap in the brain regions. Figure from (Boes et al., 2015)

## 1.5 Presence hallucination

### 1.5.1 Definition

Presence hallucination (PH) refers to the persuasive sensation that somebody is close by although nobody is around (Brugger et al., 1996; Critchley, 1950, 1955; Fénelon et al., 2000; Jaspers, 1913; Lhermitte, 1939). PH was initially described by Karl Jaspers as “*patients who have a certain feeling (in the mental sense) or awareness that someone is close by, behind them or above them, someone that they can in no way perceive with the external senses, yet whose actual/concrete presence is clearly experienced*” (Jaspers, 1913). PH was later referred to as “*l’hallucination du compagnon*” (Lhermitte, 1939), “*idea of a presence*” (Critchley, 1950), or more recently “*feeling of a presence*” (Blanke et al., 2003; Brugger et al., 1996; Fénelon et al., 2000). PH can present different magnitudes of vividness, from highly realistic and

vivid to dreamlike and ephemeral, and be of different durations, from transient to persistent. Individuals who experience PH are typically unable to see or hear the “presence” per se (Blanke et al., 2003; Brugger et al., 1996), but are nonetheless convinced it is here, and can locate it in space accurately (Brugger et al., 1996; James, 1961).

### *1.5.2 PH classification within AP*

PH has been classified among AP despite the fact that no visual autoscopic body is involved and that the felt presence is generally experienced as another human (Blanke et al., 2008; Brugger et al., 1996; Critchley, 1950, 1955). It has, however, also been described as “a shadow” at a glimpse of vision (Arzy et al., 2006; Brugger et al., 1996) that can occur jointly with AH, HAS and OBE (Blanke et al., 2004; Brugger et al., 1996; Lukianowicz, 1958; Maillard et al., 2004; Martínez-Horta et al., 2020). Furthermore, PH often shares similar characteristics with HAS involving own body perceptions (e.g. psychological affinity towards the autoscopic body and sharing of body postures and actions with the autoscopic body (Arzy et al., 2006; Brugger et al., 1996; Critchley, 1955)) and has been described as an “heautoscopy without optical image” or as an “invisible” double (Brugger et al., 1996; Menninger-Lerchenthal, 1935). In addition, a few patients have reported to feel the presence of a second own body next to them (Brugger et al., 1996; Critchley, 1950, 1955).

### *1.5.3 Etiology*

PH is not limited to a single etiology, but has been described in psychiatric disorders like schizophrenia (Jaspers, 1913) as well as in neurological disorders like epilepsy (e.g., Ardila & Gómez, 1988; Blanke et al., 2003; Brugger et al., 1996; Critchley, 1950, 1955), Parkinson’s disease (Fénelon et al., 2000; Llorca et al., 2016; Williams et al., 2008; Wood et al., 2015), dementia with Lewy bodies (Nagahama et al., 2010; Nicastro et al., 2018), or focal brain lesions (Blanke et al., 2003, 2008, 2014; Brugger, 1994; Brugger et al., 1996). PH is also present in healthy subjects in case of extreme conditions (e.g. mountaineers, solitary sailors) when performing repetitive and monotonous movements, but also during bereavement (Barnby and Bell, 2017; Brugger et al., 1999; Bychowski, 1943; Hayes and Leudar, 2016; Keen et al., 2013; Nightingale, 1982; Rees, 1971; Rohde et al., 2014; Suedfeld and Mocellin, 1987).

### 1.5.3.1 *PH in Parkinson's Disease*

Parkinson's disease (PD) is a neurodegenerative disorder associated with motor symptoms such as tremor, rigidity, bradykinesia. Non-motor symptoms (e.g. apathy and sleep disorders) are also present in PD and include PD psychosis which is a spectrum of psychotic symptoms (abnormal condition of the self characterized by hallucination and delusions) that occur at different stages of the disease (Fénelon and Alves, 2010; Ravina et al., 2007). Among the psychotic symptoms, minor hallucinations include visual illusions, passage hallucinations (sensation that someone or an animal is passing in the peripheral visual field) and PH (Pagonabarraga et al., 2016). These so-called minor hallucinations can be present before the onset of motor symptoms (Pagonabarraga et al., 2016). PH occurs in approximately 40% of patients (Fénelon and Alves, 2010; Llorca et al., 2016), however, in clinical practices, it is still understudied due to the reticence of patients to talk about it and the difficulty to diagnose and classify such hallucinations, or because PH is simply not assessed by clinicians (Holroyd et al., 2001; Ravina et al., 2007). The phenomenology of PH in PD is complex and heterogeneous. However, we can retain that it can last for a few seconds, and the insight<sup>1</sup> in most of the cases is preserved and if it was not the case, no delusional component is observed as it is seen in psychiatric patients (Fénelon et al., 2011), but delusions can still occur at advanced stages of the illness (Ffytche et al., 2017). The presence is often reported on the side or behind the patients without any predominant side and is rarely associated with distress. **Chapter 3** will characterise PH in PD using a robotic paradigm and will investigate neural markers of PH in order to identify new objective tools to assess PH in PD.

### 1.5.3.2 *PH in Schizophrenia*

Schizophrenia is a severe psychiatric disorder that comprises a wide range of debilitating symptoms including positive symptoms: hallucinations, loss of agency and other passivity experiences (i.e. sensation of not being in control of one's own actions), delusions, thought disorders (American Psychiatric Association, 2013; WHO, 2018). Among the hallucinations, PH has been reported in up to 46% in schizophrenia patients (Llorca et al., 2016). The onset of schizophrenia is usually during early adolescence or late adulthood. Schizophrenia has been described as a disorder of the self where the

---

<sup>1</sup> Insight: metacognitive ability to analyse, criticise and put to a distance ideas, beliefs, perceptions or any other anomalous experiences.

boundaries between the self and the external world are altered (Frith, 2000; Parnas and Handest, 2003). The disconnection hypothesis, meaning altered functional connectivity between different network, has been proposed to explain schizophrenia (Friston, 1999; Friston and Frith, 1995; Friston et al., 2016; Van Den Heuvel and Fornito, 2014; Li et al., 2019; McGuire and Frith, 1996; Northoff and Duncan, 2016; Rubinov and Sporns, 2010; Woodward et al., 2012). In particular, many studies have found a fronto-temporal disconnection in patients with schizophrenia (Crossley et al., 2009; Lawrie et al., 2002; Wolf et al., 2007). **Chapter 5** will investigate the network related to PH in this population.

A human model allowing to study schizophrenia is the 22q11.2 deletion syndrome (22q11DS) population, which is a neurodevelopmental disorder caused by chromosomal microdeletion of 1.5 to 3 million base pairs on chromosome 22 band q11.2 (McDonald-McGinn et al., 2015; Murphy et al., 1999). It has been estimated in one over 4000 live birth and is associated with complex somatic, cognitive and neuropsychological phenotype (Biswas and Furniss, 2016). This population has a major risk (up to 25%) for developing schizophrenia, and in 30% of them, the onset of schizophrenia occurs before the age of 18 years old (Bassett and Chow, 1999; Murphy et al., 1999; Schneider et al., 2014). Psychosis in 22q11DS subjects has been described as a continuum of psychotic experiences with increasing severity, and hallucinations have been reported to happen earlier than delusions (Schneider et al., 2014). Therefore, better characterizing PH in 22q11DS subjects would provide insights on the development of prodromal signs of psychosis at a very early stage before the onset of definite symptoms of schizophrenia (see **Chapter 4**).

### *1.5.4 Brain regions involved in PH*

While early lesion analyses reported broad lesions in the parietal, temporal and occipital lobes that could lead to PH (Brugger et al., 1996; Critchley, 1979; Hécaen and Ajuriaguerra, 1952), a more recent case-report showed that electrical stimulation in the temporo-parietal cortex triggered PH in an epileptic patient (Arzy et al., 2006). This result is supported by a recent lesion analysis in 12 neurological patients with PH, showing the implication of the temporo-parietal cortex, as well as insula and fronto-parietal cortex (Blanke et al., 2014). Apart from those findings, little is known about the neural mechanisms of PH in the different clinical populations.



Before going into details of the experimental paradigms used to induce and assess PH and its related brain regions, definitions of agency and sensorimotor integration will be provided in the next section.

### *1.5.5 Agency and sensorimotor integration*

Integration of sensory feedback signals (tactile, proprioceptive and motor signals) with movement related signals is fundamental for our interactions with the external world. Agency has been defined as the feeling of being the agent of an action and is another important aspect of BSC, which enables to distinguish whether certain sensory signals are self-generated (i.e. consequences of our actions) or externally produced (Blanke and Metzinger, 2009; Gallagher, 2000; Jeannerod, 2003). Agency has been studied by applying sensorimotor conflicts: inserting temporal and/or spatial conflicts between the movement and sensory feedback (Kannape et al., 2010; Tsakiris et al., 2010). Most of the studies have investigated BSC with respect to ownership and agency for the upper limb (Ehrsson et al., 2005; Kalckert and Ehrsson, 2012; Pozege et al., 2014; Rohde et al., 2014). In terms of neural correlates, a large cortical network has been involved in agency comprising mainly the ventral premotor cortex (vPMC), the supplementary motor area (SMA and pre-SMA), the cerebellum, the dorsolateral prefrontal cortex (DLPFC), the posterior parietal cortex (PPC), the posterior segment of the superior temporal sulcus (pSTS), the extrastriate body area (EBA) and the insula (Blakemore and Sirigu, 2003; David et al., 2008; Ehrsson, 2007; Farrer and Frith, 2002; Farrer et al., 2003; Fink et al., 1999; Jastorff et al., 2011; Leube et al., 2003a; Nahab et al., 2011; Sperduti et al., 2011; Yomogida et al., 2010).

One prominent model for motor control and conscious bodily experience is the internal forward model where efferent copies based on motor and other related signal commands are used to predict the sensory consequences of one's own action (Britain et al., 1996; Miall and Wolpert, 1996; Wolpert et al., 1995). If these predictive signals match the current sensory input, movements are perceived as self-generated (Figure 1.3). However, if there is a difference between the prediction and the actual sensory feedback, the action is considered as externally produced. This model was extended to propose an explanation to hallucinations and passivity experiences suggesting that failure in the predictive mechanisms of one's own actions could lead to abnormal perceptions (hallucinations) (Blakemore et al., 2000a; Fletcher and Frith, 2009; Friston

and Frith, 1995; Frith, 1992, 2005; Graham-Schmidt et al., 2017; Pynn and DeSouza, 2013).

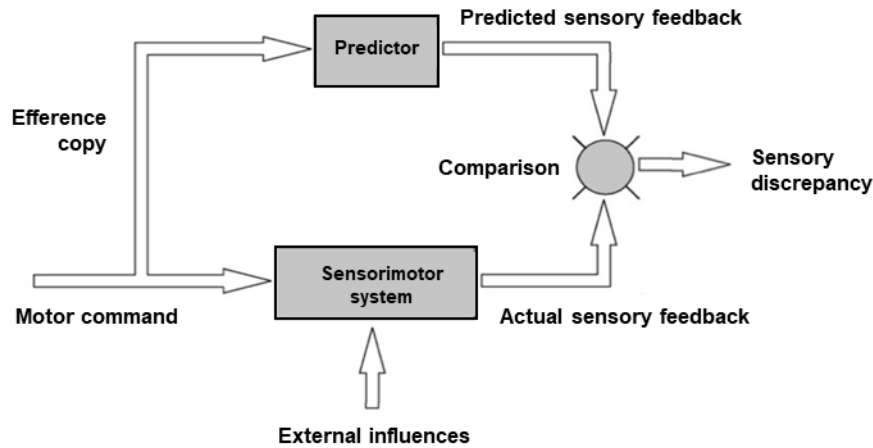


**Figure 1.3: Internal forward model scheme.** Once a motor command is generated, an efference copy is also sent and used to make a prediction about the sensory consequence of the action. The predicted sensory feedback and the actual sensory feedback are then compared. If they are matched then the movement is considered as self-generated, however if there is a discrepancy, the movement is attributed to an external factor, which could be an external agent. Figure adapted from (Blakemore et al., 2000a).

It has been shown that under normal conditions when an action is considered as self-generated, the sensory feedback is attenuated both at the behavioural and neural levels (Blakemore et al., 1998, 2000b; Shergill et al., 2005, 2013; Weiskrantz et al., 1971). One of the classical examples illustrating attenuation was done by Blakemore and colleagues where they showed that when a tactile stimulus is self-produced it is perceived as less ticklish than external tactile stimulus. At the neural level, reduced brain activity in the secondary somatosensory cortex and increased activity in the cerebellum were observed. The authors also showed that activity in the somatosensory (primary and secondary) cortex and thalamus was modulated by the cerebellum during self-produced tactile stimuli only (Blakemore et al., 1998, 1999). These results suggested that the cerebellum plays an important role in sensorimotor prediction and somatosensory cortex attenuation and were further confirmed by a recent study (Kilteni and Ehrsson, 2020). Self-monitoring deficits were found in psychiatric patients. In schizophrenia, the sensory attenuation has been shown to be altered and has been suggested to lead to abnormal perceptions (Blakemore et al., 2000a; Ford et al., 2005, 2008; Leube et al., 2010; Lindner et al., 2005; Shergill et al., 2014). For the

22q11DS individuals, self-monitoring deficits have also been observed but only a few studied assessed the link with psychotic symptoms (Debbané et al., 2006, 2010).

### *1.5.6 Experimental procedures*

As mentioned previously, it is suggested that PH is a disorder of own body perception and has been related to body posture and movement (tactile, proprioceptive, and motor cues) were found to be important to induce PH (Blanke et al., 2014). This finding is compatible with the observation that PH are a frequent manifestation in motor diseases such as Parkinson's Disease (Fénelon et al., 2000; Williams et al., 2008; Wood et al., 2015). The idea that PH is a disorder of own body perception is also compatible with a prominent account of hallucinations in schizophrenia positing that illusions and hallucinations such as passivity experiences and loss of agency (the feeling of not being the author of a given action) may be associated with faulty sensorimotor prediction mechanisms (Fletcher and Frith, 2009; Frith, 1992).

Based on these findings, the clinical data mentioned above, and recent experimental advances of multisensory own-body illusions (Blakemore et al., 2000b; Ehrsson et al., 2005; Ionta et al., 2011), Blanke and colleagues recently developed a robotic system able to generate sensorimotor conflicts, resulting in the induction of PH in healthy subjects under controlled laboratory conditions (Blanke et al., 2014). Participants were asked to perform repeated tapping movements with their right index finger using a robot situated in front of them. The movements were recorded and then electronically transmitted to a second robot providing tactile feedback to the participants' back in different delay conditions (i.e. synchronous with 0 ms delay and asynchronous with 500 ms delay between the movement performed and the touch received on the back). The synchronous condition was characterised by a spatial conflict between the movement participants were performing in their front space and the sensory consequence of their movement on their back (Figure 1.4A). Under a condition of strong sensorimotor conflicts (i.e. asynchronous condition characterized by an additional spatio-temporal conflict due to the delay between the movement and the feedback), participants experienced being in the presence of another person, situated behind them (Blanke et al., 2014). This indicated that disrupting the integration of specific sensorimotor bodily signals including the trunk is sufficient to induce PH. In

addition to PH, participants reported experiencing passivity experiences in the asynchronous condition (Figure 1.4B).

In **Chapter 3** and **Chapter 4**, this paradigm was tested in Parkinsonian patients and 22q11 subjects.

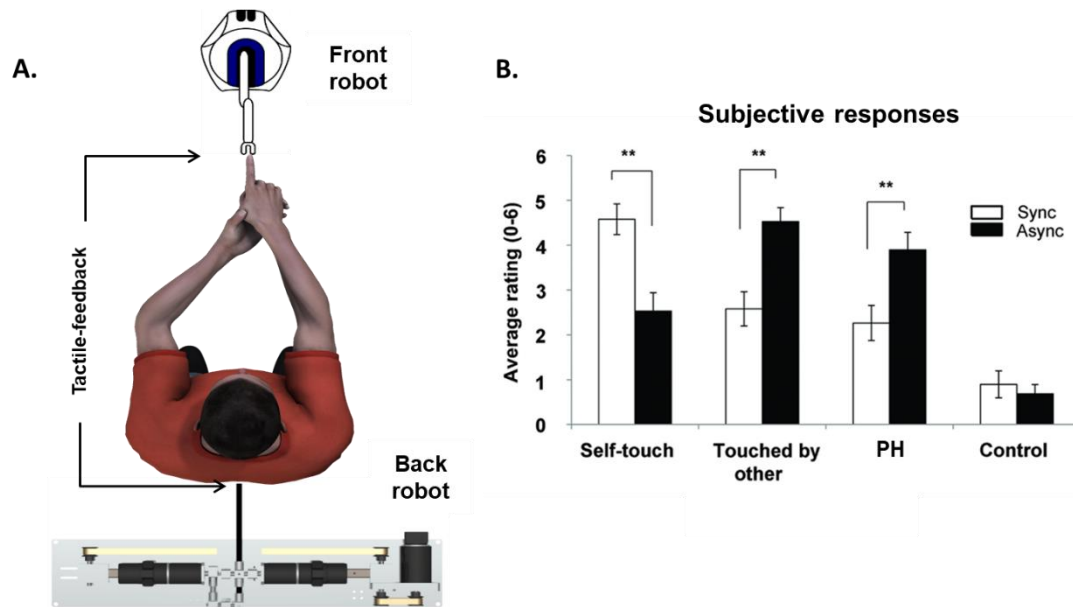


**Figure 1.4: Robot-induced presence hallucination.** **A.** Robotic device able to induce in a safe and controlled manner PH in healthy participants. Participants were asked to perform repetitive movement with their right index finger. Their movement was translated onto a back robot that either reproduced their movement synchronously or asynchronously. **B.** When strong sensorimotor conflicts were present (i.e. the asynchronous condition), subjects reported higher PH ratings and higher passivity experiences. \*\*:  $p < 0.01$ . Figures adapted from (Blanke et al., 2014).

The brain mechanisms responsible for robotically-induced PH in healthy subjects and their relation with mechanisms of sensorimotor integration are currently unknown. Accordingly, the relation between the brain regions responsible for the robotically-induced PH in healthy subjects and those involved in pathological conditions remain elusive. Resolving this lack of understanding is particularly important as the development of a systematic neuroscientific understanding of PH requires to link both the phenomenology and the neural underpinnings of the robotically-induced PH to the PH spontaneously occurring under pathological or extreme conditions. These issues are addressed here by combining recent advances in MR-compatible robotics with advanced lesion network mapping analysis to identify a PH-network (see **Chapter 3**). Furthermore, the relevance of this PH-network was assessed in different clinical

population: in Parkinson's disease for validation (**Chapter 3**), in 22q11DS subjects, which is a population at high risk to develop schizophrenia (**Chapter 4**) and finally in patients with psychosis (schizophrenia spectrum) (**Chapter 5**).

## Chapter 2: Common and distinct brain networks of four autoscopic phenomena

**Authors:** Eva Blondiaux<sup>1</sup>, Lukas Heydrich<sup>2</sup> & Olaf Blanke<sup>1,3</sup>

**Status:** in preparation

***Affiliations:***

**1.** Laboratory of Cognitive Neuroscience, Center for Neuroprosthetics and Brain Mind Institute, Swiss Federal Institute of Technology (EPFL), Switzerland. **2.** CORE Lab, Psychosomatic Competence Center, Department of Neurology, Inselspital, Bern University Hospital, University of Bern, Switzerland. **3.** Department of Neurology, University of Geneva, Switzerland

**Personal contributions:** Study design, data analysis, writing

### Abstract

Autoscopic phenomena (AP) are illusory and multisensory own body reduplications characterized by the perception of a second own body in extrapersonal space, and include four main forms: autoscopic hallucination (AH), heautoscopy (HAS), out-of-body-experience (OBE), and presence hallucination (PH). Past research showed that lesions were heterogeneously distributed and affected many different brain regions within and across patients, while small case series suggested that AP lesions converge in temporo-parietal and parieto-occipital cortex. As only very few studies investigated each form of AP separately, it is not known whether the four AP are characterized by common and distinct brain mechanisms and how this relates to focal brain damage versus abnormal functional connectivity patterns. Here, we applied lesion network analysis in 38 neurological AP patients and determined their common and distinct functional connectivity patterns. We report that all AP include interference with a common network region at the bilateral TPJ, arguably reflecting their main common element: illusory reduplication of one's own body. This TPJ connectivity was further associated with specific patterns of functional connectivity, defining each type of AP. OBE resulted from a brain network connected to bilateral angular gyrus, right precuneus, and right inferior frontal gyrus, differing from AH with a brain network connected to bilateral precuneus, inferior temporal gyrus, and cerebellum. A third pattern emerged for HAS, which resulted from a brain network connected to left inferior frontal gyrus and left parahippocampus, while PH were not associated with a specific brain network. The present data describe the TPJ as a common core region for AP and highlight the different sensorimotor and self-related sub-networks for each AP, linking AP to latest advances in human neuroscience and accounting for the diverse etiological and neuroanatomical causes of AP.

**Keywords:** Lesion network mapping, multisensory processing, bodily self-consciousness, temporo-parietal junction

### Introduction

Autoscopic phenomena (AP) are illusory and multisensory own body perceptions that have been reported in various neurological and psychiatric conditions as well as in the healthy population (Menninger-Lerchenthal, 1935; Critchley, 1950; Hécaen and Ajuriaguerra, 1952; Lippman, 1953; Devinsky *et al.*, 1989; Brugger *et al.*, 1999; Fénelon *et al.*, 2011). AP are characterized by the illusory perception of one's own body in extrapersonal space and classified among disorders of the body schema (i.e. Hécaen & Ajuriaguerra, 1952; Menninger-Lerchenthal, 1935; Brugger, Regard, & Landis, 1997; Devinsky, Feldmann, Burrowes, & Bromfield, 1989) and have sparked broad academic interest across many disciplines beyond medicine, including philosophy (i.e. Blanke and Metzinger, 2009), psychology, but also occultism, fiction, and religion (Rank, 1925; Menninger-Lerchenthal, 1946; Todd and Dewhurst, 1955; Sheils, 1978). AP have recently been the target of neuroscientific investigations due to their relevance for self and self-consciousness and related multisensory bodily processing (bodily self-consciousness; i.e. Blanke, 2012; Blanke and Metzinger, 2009; Blanke *et al.*, 2015). Neurological case descriptions highlighted the involvement of a wide variety of brain regions, including temporal, parietal and occipital cortex (Menninger-Lerchenthal, 1935; Lhermitte, 1939; Hécaen and Ajuriaguerra, 1952; Lunn, 1970; Devinsky *et al.*, 1989; Denning and Berrios, 1994; Brugger *et al.*, 1996, 1997; Blanke and Mohr, 2005), whereas subsequent analyses of small groups of patients with AP delimited lesion overlap to temporo-parietal cortex (i.e. Blanke, Landis, Spinelli, & Seeck, 2004; Hoepner *et al.*, 2013) or parieto-occipital regions (Maillard *et al.*, 2004).

AP include four main forms, consisting of autoscopic hallucination (AH), heautoscopy (HAS), out-of-body-experience (OBE), and feeling of a presence (or presence hallucination, PH) (Devinsky *et al.*, 1989; Brugger *et al.*, 1997; Brugger, 2002; Blanke *et al.*, 2004) and more recent research has investigated the brain mechanisms of each AP separately. During AH, subjects report seeing a second own (autoscopic) body in extrapersonal space, which most often consists of the upper body parts (face and/or torso) that is seen in front-view, as if they were looking in a mirror. The subject's center of awareness remains within the physical body and they see the world and the autoscopic body from their habitual body-centered visuo-spatial viewpoint (Fig.1A).



Patients do not report feelings of disembodiment (i.e. the conscious experience of being located outside one's body) that is typical for OBE (see below). Studies of AH cases of neurological origin highlighted damage or interference to occipital, occipito-temporal, or occipito-parietal cortex (Kolmel, 1985; Bhaskaran *et al.*, 1990; Maillard *et al.*, 2004; Zamboni *et al.*, 2005; Blanke and Castillo, 2007; Bolognini *et al.*, 2011; Ochoa *et al.*, 2015). Research using lesion overlap analysis associated AH with damage in right occipito-parietal cortex, including the superior occipital gyrus and the cuneus (Heydrich and Blanke, 2013). This posterior location has also been observed in patients undergoing presurgical epilepsy evaluation by showing that electrical stimulation in right medial occipito-parietal cortex, including the precuneus, repeatedly elicited AH (Jonas *et al.*, 2014).

Subjects experiencing OBE also report seeing a second own body in extrapersonal space, but from an elevated visuo-spatial perspective, which is characteristically associated with the conscious experience of disembodiment. The center of awareness during OBE is located at the elevated visuo-spatial perspective and patients may also report vestibular sensations of elevation, floating or flying (Fig.1C) (Devinsky *et al.*, 1989; Brugger, 2002; Blanke *et al.*, 2004). A meta-analysis regrouping several neurological patients with OBE suggested a right hemispheric dominance and involvement of the parietal and temporal cortex (Blanke and Arzy, 2005; Blanke and Mohr, 2005), based on single case reports (Daly, 1958; Blanke *et al.*, 2004; Maillard *et al.*, 2004; Brandt *et al.*, 2005; Heydrich *et al.*, 2011; Fang *et al.*, 2014). Lesion overlap analysis in a group of OBE patients converged on damage to the right angular gyrus and the posterior superior temporal gyrus (pSTG) (Ionta *et al.*, 2011). This focal origin was supported by the finding that electrical stimulation (in patients undergoing presurgical epilepsy evaluation) of the right angular gyrus and pSTG induced repeated OBE in several patients (Blanke *et al.*, 2002; De Ridder *et al.*, 2007; Bos *et al.*, 2016).

HAS is defined as an intermediate AP, between AH and OBE, with elements of disembodiment and perspective changes while subjects also report seeing a second own body in extrapersonal space. Compared to AH, a complete (not only upper) autoscopic body is seen, often in various side- and back-views. Moreover, subjects have difficulties to determine their center of awareness and the origin of the visuo-spatial perspective, which may be experienced at their physical body, at the location

of the hallucinated body, or at alternating locations (Fig.1B). Thus, HAS is often associated with the feeling of bi-location and strong self-identification and close emotional affinity with the autoscopic body (Devinsky et al., 1989; Brugger, 2002; Blanke and Mohr, 2005), which may even persist if the autoscopic body only partly reflects the patient's visual bodily appearance. HAS is less investigated compared to OBE and AH, and, although case reports linked HAS to damage in temporal and parietal cortex (Brugger *et al.*, 1994, 2006; Blanke and Mohr, 2005; Tadokoro *et al.*, 2006; Arias *et al.*, 2007; Anzellotti *et al.*, 2011), lesion overlap analysis in a group of HAS patients suggested a different brain region and converged on the left posterior insula (Heydrich and Blanke, 2013).

The fourth AP is PH, defined as the sensation that someone is present nearby, either behind or to the side of the subject, although nobody is physically present (Fig.1D) (Brugger, Regard, & Landis, 1996; Critchley, 1950, 1955; Jaspers, 1913; Lhermitte, 1939). The felt presence is generally experienced as *another* human, although some patients have also reported to feel the presence of a second own body next to them (Critchley, 1950, 1955; Brugger *et al.*, 1996). In some patients PH may occur jointly with AH, HAS or OBE and, accordingly, most classical authors (i.e. an influential early textbook described PH as "heautoscopy without optical image"; Menninger-Lerchenthal, 1935) have classified PH among AP although PH do not involve the visual hallucination of an autoscopic body (Menninger-Lerchenthal, 1935; Lhermitte, 1939; Hécaen and Ajuriaguerra, 1952; Lukianowicz, 1958; Critchley, 1979; Brugger *et al.*, 1996, 1997) (for a detailed discussion of PH and AP see Blanke, Arzy, & Landis, 2008; Brugger *et al.*, 1996). Studies of PH cases of neurological origin highlighted damage to posterior parietal and temporal cortex (Critchley, 1950; Hécaen and Ajuriaguerra, 1952; Nightingale, 1982) more particularly to temporo-parietal cortex (Brugger, 1994; Brugger *et al.*, 1996; Blanke *et al.*, 2003, 2008). This focal origin was further supported by the finding that electrical stimulation (in patients undergoing presurgical epilepsy evaluation) in TPJ induced repeated PH in several patients (Arzy *et al.*, 2006; Zijlmans *et al.*, 2009). However, other regions have also been proposed such as the left insular cortex (Picard, 2010; Landtblom *et al.*, 2011) and lesion overlap analysis in a group of neurological patients with PH revealed involvement of three cortical regions: temporo-parietal cortex, superior parietal cortex, and the posterior insula (Blanke *et al.*, 2014).

Despite these lesion overlaps that differed for each AP, most of the studies mentioned above found that brain damage was heterogeneously distributed and affected many different brain regions within and across patients. For example, in AH, even though the lesions were centered in the right parieto-occipital cortex, some lesions affected the left hemisphere as well as inferior parietal and temporal cortex (Denning and Berrios, 1994; Maillard *et al.*, 2004; Heydrich and Blanke, 2013). For HAS, even though the insular cortex and the TPJ were shown to be involved and mostly localized in the left hemisphere, several patients also suffered from right brain damage and involvement of the superior parietal cortex (Blanke *et al.*, 2004; Blanke and Mohr, 2005; Anzellotti *et al.*, 2011; Heydrich and Blanke, 2013). Similar observations hold for OBE and PH (OBE: Blanke *et al.*, 2004; Bos *et al.*, 2016; Greyson, Fountain, Derr, & Broshek, 2014; PH: Arzy *et al.*, 2006; Zijlmans *et al.*, 2009; Blanke *et al.*, 2014). These data suggest that AP, despite being associated with damage to one or several posterior brain regions, may emerge from dysfunctional brain networks rather than only damage to a single or limited number of brain regions. Moreover, the number of tested patients remained low and AP occur in many different patient populations, involving psychiatric diseases such as schizophrenia and depression (Menninger-Lerchenthal, 1935; Critchley, 1950; Lukianowicz, 1958; Blackmore, 1986) and many neurological diseases such as epilepsy, migraine, stroke, brain tumors, and infections (Lhermitte, 1939; Lippman, 1953; Devinsky *et al.*, 1989; Brugger *et al.*, 1994; Blanke *et al.*, 2004; Ionta *et al.*, 2011). Importantly, many of these diseases are not associated with focal brain damage. Moreover, AP have been linked to alterations in multisensory perception, based on altered integration of information from somatosensory, visual, motor, and vestibular brain regions (Ionta *et al.*, 2011; Blanke, 2012; Ronchi *et al.*, 2018), and also occur in healthy subjects, a finding that is also compatible with our hypothesis that AP are associated with alterations in functional brain connectivity (Lhermitte, 1951; Hécaen and Ajuriaguerra, 1952; Blackmore, 1986; Suedfeld and Mocellin, 1987; Brugger *et al.*, 1999).

New lesion network analysis methods have been developed recently and enable to uncover brain networks associated with specific neurological symptoms by using normative resting state data from healthy subjects in order to determine the brain regions functionally connected to each patients' lesion location (Boes *et al.*, 2015; Fox,

2018). Lesion network analysis does not require the acquisition of functional neuroimaging data from patients and allows to determine whether heterogeneously distributed lesions causing the same symptom are part of the same network. The method has already been applied to several neurological symptoms, including phenomena of comparable complexity to AP such as delusional misidentification syndromes, auditory and visual hallucinations, and prosopagnosia among others (Boes *et al.*, 2015, Darby *et al.*, 2017b; Cohen *et al.*, 2019; Kim *et al.*, 2019), but never to AP.

Here, we applied lesion network analysis to 38 neurological patients with AH, HAS, OBE or PH caused by focal brain damage. We sought to investigate the networks involved in each AP and determined their common and distinct network patterns. On the one hand, we hypothesized that AH, OBE, HAS and PH would share parts of their networks because they all share an altered self-representation characterized by an illusory reduplication of their body (Brugger *et al.*, 1997; Blanke *et al.*, 2004). On the other hand, we hypothesized that each form of AP would recruit additional specific networks, based on previous work associating each form with different sensory, motor, and cognitive mechanisms (Blanke *et al.*, 2004; Maillard *et al.*, 2004; Heydrich and Blanke, 2013).

## Methods

### Patients

The lesion masks of patients experiencing the different AP were taken from previously published studies (Ionta *et al.*, 2011; Heydrich and Blanke, 2013; Blanke *et al.*, 2014; Bernasconi *et al.*, 2020) to which we added two unpublished cases, one with HAS and one with OBE. This led to a total of 38 patients: seven with AH cases, ten with HAS (Heydrich and Blanke, 2013), ten with OBE (Ionta *et al.*, 2011) and eleven with PH (Blanke *et al.*, 2014; Bernasconi *et al.*, 2020) (Supplementary Table S1).

### Lesion network mapping

For each patient we identified the lesion-derived network from each seed region of interest (ROI) following the lesion network mapping approach as described previously (Boes *et al.*, 2015; Laganiere *et al.*, 2016, Darby *et al.*, 2017b, a, 2018; Fasano *et al.*, 2017; Joutsa *et al.*, 2018). The method consists in three main steps: (1) mapping each lesion into standard MNI space, (2) computing its functional connectivity at rest in a normative resting state database of healthy subjects, (3) and overlapping each of the binarized lesion-derived network together.

### MRI acquisition

For this we used the resting state and T1-weighted structural data from 151 healthy participants obtained from the publicly available Enhanced Nathan Kline Institute Rockland Sample (Nooner *et al.*, 2012). All participants were right handed and aged between 19 to 40 years ( $25.8 \pm 5.5$  years, 83 females). Scans were acquired with a 3T Siemens Magnetom TrioTim syngo. For the resting state data, a multiband EPI sequence was used (multiband factor=4, 64 continuous slices, TR=1.4s, TE=30ms, flip angle=65°, slice thickness=2mm) and 404 scans were collected. For each participant, an anatomical image was recorded using a T1-weighted MPRAGE sequence (TR=1.9s, TE=2.52ms, Inversion time=900ms, flip angle=9°, 1mm isotropic voxels, 176 slices per slab and FOV=250mm).

### **Image pre-processing**

The pre-processing steps were performed using Matlab (R2018b, MathWorks) with Statistical Parametric Mapping (SPM12, Wellcome Trust Centre for Neuroimaging, London). The first four functional scans were discarded from the analysis to allow for magnetic saturation effects therefore the analysis was performed on the 400 scans remaining. The standard pre-processing pipeline was applied and included slice-timing correction, spatial realignment and co-registration of the anatomical images to the mean functional image. The functional and anatomical scans were then normalized to the Montreal Neurological Institute space (MNI space). Finally, the functional scans were spatially smoothed with a 5mm full-width at half-maximum isotropic Gaussian kernel. The anatomical T1-weighted image was segmented into grey and white matter and cerebrospinal fluid (CSF). The data were filtered with a bandwidth of 0.008 Hz to 0.09 Hz. The six motion parameters and their first-degree derivative were included as nuisance regressors in addition to the bold activity in the white matter and the cerebrospinal fluid. Subjects with excessive motion were excluded from the analysis, this comprised 25 subjects which had more than 15% of scans affected by movement as calculated by the framewise displacement (Power *et al.*, 2012). In total, 126 subjects were included for the analysis.

### **Resting state analysis**

The resting state data was analyzed using the CONN-fMRI Functional Connectivity toolbox (v.18.a, <http://www.nitrc.org/projects/conn>, Whitfield-Gabrieli & Nieto-Castanon, 2012). The lesion masks were used as seed ROIs and their mean time course was extracted and correlated to all other brain voxels, limiting our analysis to voxels within the grey matter. Finally, the brain network derived from each seed lesion was thresholded at  $T > 4.25$  with  $p < 0.00005$  FWE peak-level whole brain corrected similar to previous literature (Boes *et al.*, 2015; Fischer *et al.*, 2016; Laganier *et al.*, 2016, Darby *et al.*, 2017b). The lesion network maps were then binarized and overlapped together to determine the regions of shared positive and negative correlations.

Five different lesion network mapping analyses were performed. First, we applied lesion network mapping analysis for each AP separately to identify the brain networks associated with AH, HAS, OBE, and PH (networks were thresholded at 100% of the cases to be as restrictive as possible given the limited number of patients per AP). The

lesion network mapping analysis was previously applied to PH using the same patient's lesions (Bernasconi *et al.*, 2020); for the present study thresholding was performed as for the other AP. Next, we applied lesion network mapping analysis including all patients with AP. This was done in order to determine all regions functionally connected to the lesion locations of neurological patients with APs. Here, we applied a more liberal threshold of 85% due to the higher number of patients for the analysis. For all analyses, only clusters larger than 10 voxels were considered. The anatomical regions were labeled according to the AAL atlas (Tzourio-Mazoyer *et al.*, 2002) implemented in MRICron (<http://www.mccauslandcenter.sc.edu/mricro/mricron>) and the Anatomy toolbox (Eickhoff *et al.*, 2005, 2006, 2007).

### **Specificity**

In a further analysis step, we assessed whether the regions connected for AH, HAS, OBE, and PH were specific to each AP. To this aim, we compared the lesion network maps of each AP against all others using a Lieberman statistical test, using voxel-based lesion symptom mapping (VLSM) (Rorden *et al.*, 2007). This method enabled us to identify those voxels, in which the connectivity was significantly altered in a particular symptom compared to the voxels altered by another symptom. The analysis was performed on the binary maps (separately for positive and negative maps). We corrected for multiple comparisons using FWE correction ( $p < 0.01$  and 1000 permutations) and only the voxels altered in 15% of the patients were included. For this analysis, we only considered voxels within 100% of the lesion network map in order to determine only the brain regions specific for each AP.

We performed additional statistical analysis (a one-way ANOVA including all AP group as a factor) to compare the number of voxels connected to each lesion of each AP to ensure all AP lesions were functionally connected to the same number of voxels.

### **Data availability**

All data are available from the corresponding authors upon request.

## Results

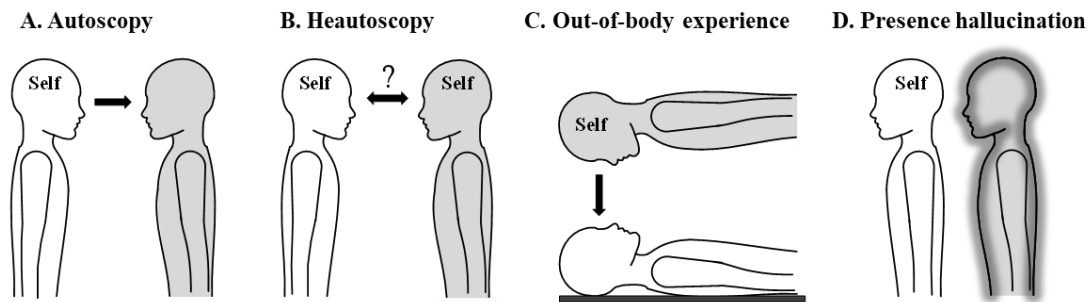


**Figure 1: Phenomenology of autoscopic phenomena (AP).** Phenomenology of the different AP: autoscopic hallucination (A), heautoscopy (B), out-of-body experience (C) and presence hallucination (D). **A.** During AH, patients report seeing an autoscopic body in extrapersonal space from their habitual body-centered self-location and perspective (indicated by *Self*). **B.** During HAS, patients report alternating self-location and first-person perspective between the physical body and the autoscopic body. **C.** In OBE, patients report disembodiment (i.e. the experience of being located outside the physical body) and to be located with an elevated position and perspective. **D.** In PH, patients report the strong sensation that someone is behind them even though no one is present. *Self* in each depiction represents experienced self-location and the arrow represents the experienced direction of the first-person perspective, for each AP separately (for more detail see main text). The grey body represents the location of the illusory autoscopic body. For PH, the shadow surrounding the grey body indicates that the illusory body is not seen, but felt.

### ***Autoscopic hallucinations***

Lesions causing AH were mainly positively connected to a large cluster in bilateral precuneus and adjacent regions in superior occipital cortex and superior parietal cortex, as well as bilateral occipito-temporal cortex (posterior inferior temporal cortex (pITG)) and bilateral cerebellum (Fig.2A, Supplementary Table S2 and Fig.S1A). Several much smaller clusters also showed negative functional connectivity with lesions causing AH (Supplementary Table S2-S3).

When comparing the AH network maps with the network maps of the three other AP, we found that bilateral precuneus, cerebellum and pITG were specifically connected to the lesions causing AH, but not in any of the other three forms of AP.



### *Heautoscopy*

Lesions causing HAS were positively connected to large bilateral clusters in middle and superior temporal gyrus (MTG/STG), parahippocampal gyrus (PHC), inferior temporal gyrus (Fig.2B and Fig.S1B). Smaller clusters were found in left inferior frontal gyrus (IFG), left precentral gyrus, and left thalamus (Fig.2B) (Supplementary Table S4 and Fig.S1B). The left caudate nucleus was found negatively connected to lesions causing HAS (Supplementary Table S4).

When comparing the HAS network maps with the network maps of the other AP, we found that only left hemispheric clusters in the left IFG and the left parahippocampal gyrus/hippocampus were specific to HAS compared to the other three forms of AP (Supplementary Table S3).

### *Out-of-body experiences*

Lesions causing OBE were all mainly positively connected to bilateral SMG/angular gyrus, bilateral posterior MTG, the right IFG (Fig.2C) (Supplementary Table S5 and Fig.S1C). No negative correlations were found with lesions causing OBE.

When comparing the OBE network maps with the network maps of the other AP, we found four clusters being specific to OBE compared to the other three forms of AP, mainly the bilateral angular gyrus, the right IFG and the right precuneus (Supplementary Table S3).

### *Presence hallucinations*

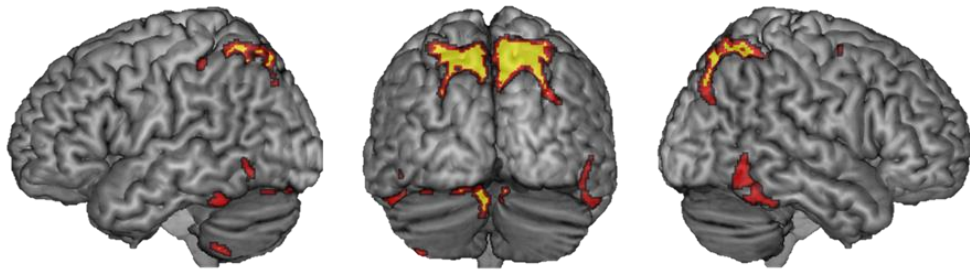
Lesions causing PH were positively connected to the right posterior STG and right supramarginal gyrus (SMG). Additional clusters were found in right IFG, bilateral insula, left middle cingulate cortex (MCC) and left postcentral gyrus (Fig.2D) (Supplementary Table S6 and Fig.S1D). No negative correlations were found with lesions causing PH.

When comparing the PH network maps with the network maps of the other AP, none of the PH regions were shown to be specifically connected to the lesion locations causing PH (no cluster survived the FWE correction and voxel extend bigger than 10 voxels). This was found even though the lesions causing PH were on average

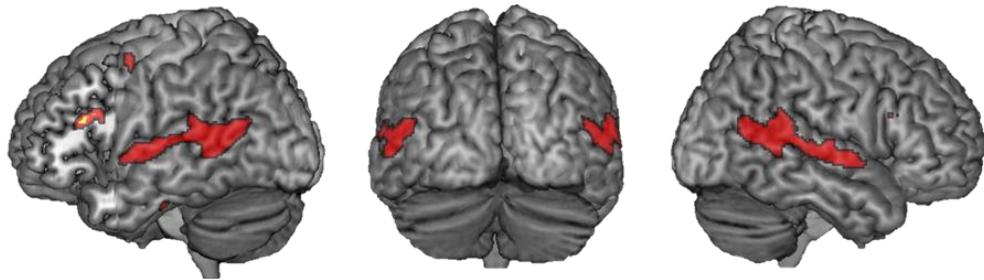
connected to the same number of voxels than the lesions causing the other three other AP ( $F(3,34) = 0.69$  ,  $p\text{-value} = 0.56$ ).

When overlapping all four AP, we observed visually that HAS, OBE and PH had relatively similar brain network connectivity with common bilateral activations of the TPJ, while AH also elicited a bilateral parietal-occipital network (Fig.3). There was limited overlap across AP.

**A. Autoscopy**



**B. Heautoscopy**



**C. Out-of-body experience**



**D. Presence hallucination**

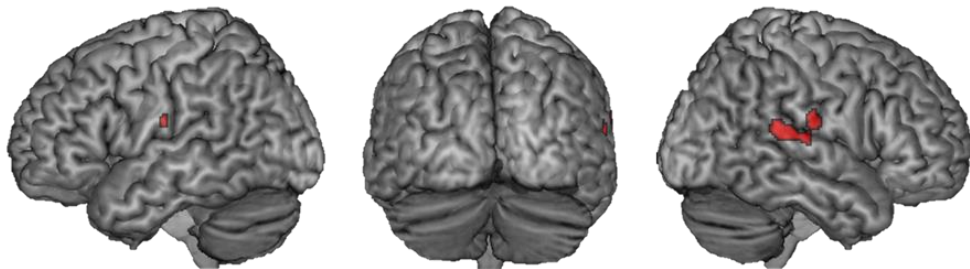


**Figure 2: Lesion derived network for each AP.** Brain networks connected to lesions causing autistic hallucinations (AH) (A), heautoscopy (HAS) (B), out-of-body experiences (OBE) (C) and presence hallucinations (PH) (D). Brain networks for each AP are depicted in red. The yellow regions indicate those brain regions that are specific for each AP as compared to the other three AP (Liebermeister test; see methods and results for further detail).

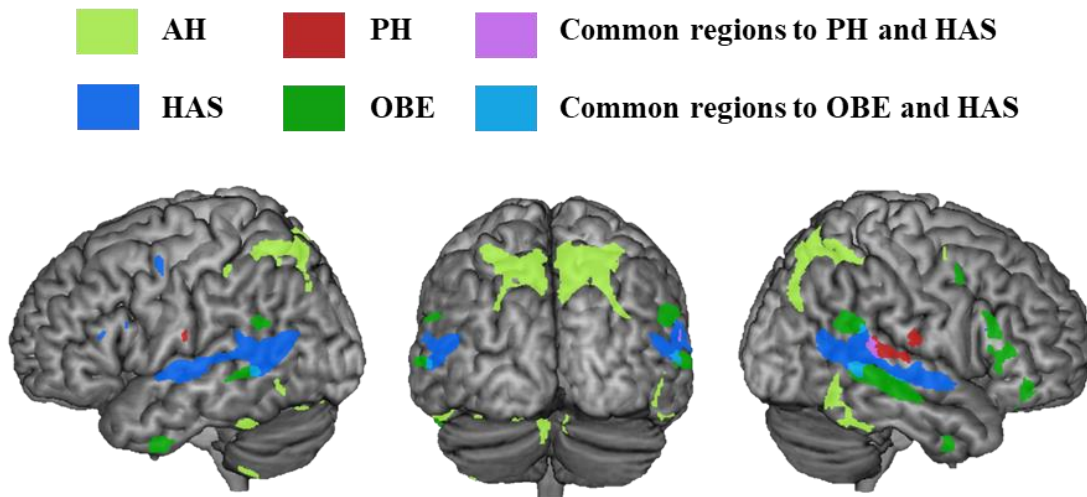


**Figure 3: Overlap of all AP network together.** The brain networks of each AP were overlap and displayed onto a common template brain to reveal common and distinct network components. HAS is shown in blue, OBE in green, AH in light green, and PH in red. Shared brain networks were observed between HAS and OBE (overlap indicated in light blue) and between HAS and PH (overlap in pink). Both overlaps were located in TPJ.

### ***Common lesion network***

To search for brain regions that were commonly involved in all AP, we considered all AP cases together and applied lesion network mapping analysis to all 38 AP patients. We found that lesions causing AP were positively connected to the bilateral TPJ, involving the bilateral posterior MTG, the right posterior STG as well as the bilateral ventral occipito-temporal cortex (fusiform gyrus close to the fusiform face area, FFA) (Fig.4) (Supplementary Table S7 for smaller clusters). Negative connections were

found with one subcortical region (right caudate nucleus) (Supplementary Table S7).

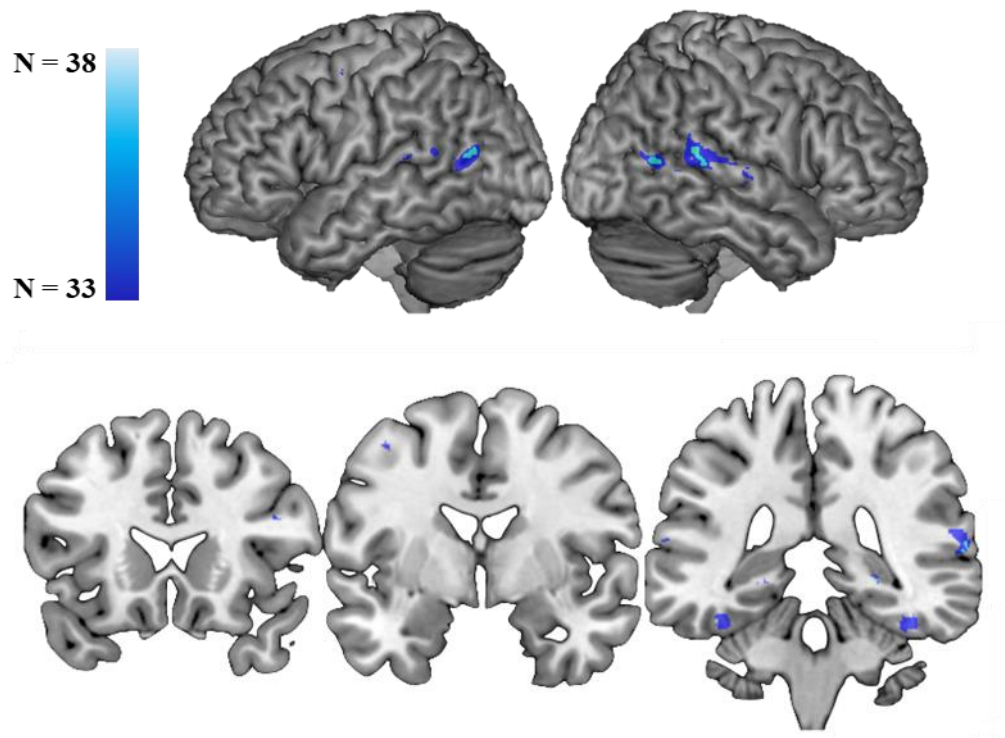


**Figure 4: Common brain regions involved in AP.** 85% of the lesions causing AP were connected to a brain network including bilateral TPJ (in bilateral pMTG and right STG) as well as bilateral temporo-occipital cortex (in proximity to the fusiform face area).

## Discussion

We investigated the brain networks underlying complex illusory own body experiences, AP, and defined their common and distinct patterns of network connectivity. Our lesion network analysis show that all AP share common network connections with two posterior brain regions: bilateral TPJ and ventral temporo-occipital cortex. We also provide evidence for specific network connections for three of the investigated AP that were characterized by specific connectivity networks (no specific network compared to the other AP was found for PH). Below we discuss the specific and common AP networks and the relevance of these data for clinical neurology and for neuroscience research on self-consciousness.

### **AH derived network**

Lesions causing AH occur in brain regions functionally connected to bilateral regions involving the precuneus, the inferior temporal gyrus and the cerebellum. Our analysis also revealed several other regions, but these were smaller and not found to be specific for AH. The AH network differed most strongly from the networks found for the other AP. The present data show that AH-lesions are connected to specific regions consisting of bilateral precuneus, pITG and cerebellum, providing new evidence that AH result from interference with a larger cortical and subcortical network. We argue that this reflects the involvement of self-related as well as visual mechanisms. Concerning visual mechanisms, AH is a complex structured visual hallucination of the patient's face or upper body and often associated with more elementary visual hallucinations (Blanke and Mohr, 2005). Accordingly, AH are mostly described as visual pseudo-hallucinations, differing further from the other AP, which are reported as highly realistic experiences (Blanke *et al.*, 2004; Blanke and Mohr, 2005; see next sections). Previous work found that most of the present patients with AH had lesion overlap in the right superior occipital gyrus and the right cuneus in extrastriate visual cortex (Heydrich and Blanke, 2013). The present connectivity data confirm the importance of visual mechanisms in AH by revealing the involvement of extrastriate visual cortex, thereby extending the lesion overlap data by Heydrich & Blanke (2013) who showed that AH share aspects with complex visual hallucination and revealed the involvement of extrastriate visual cortex in AH patients. Extrastriate visual cortex contains brain regions specialized for the visual processing of body and face stimuli such as the

extrastriate body area (EBA) and the fusiform face area (FFA) (Allison *et al.*, 1994; Kanwisher *et al.*, 1997; Downing and Kanwisher, 2001; Astafiev *et al.*, 2004). The present data extend these earlier lesion data by revealing altered connectivity with ventral stream regions (Ungerleider and Haxby, 1994; Bevil R. Conway and Conway, 2018) at the level of the pITG (located somewhat anterior to the EBA and in proximity to the FFA), which has been associated with face recognition, including the own face (Allison *et al.*, 1994; Sugiura *et al.*, 2008; Apps *et al.*, 2012; Rolls, 2017). Functional connectivity (as found for AH) with the cerebellum has also been associated with visual hallucinations (Kim *et al.*, 2019) and the cerebellum has been involved in spatial processing (i.e. mental rotation of objects: (Stoodley, 2012), mirror perception (Van Overwalle *et al.*, 2014) and visual-somatosensory processing of body parts (Ehrsson *et al.*, 2005; Brozzoli *et al.*, 2011; Gentile *et al.*, 2013)).

Another novel observation was our finding that AH lesions showed connectivity with the bilateral precuneus/superior parietal cortex, which is part of the dorsal stream (Ungerleider and Haxby, 1994) relevant for spatial perception and sensorimotor integration and planning (Ungerleider and Haxby, 1994; Bevil R. Conway and Conway, 2018). The precuneus, in particular, has also prominently been involved in many self-related functions, including own face perception, self-location, and self-projection (Ruby and Decety, 2001; Cavanna and Trimble, 2006; Northoff *et al.*, 2006; Peer *et al.*, 2015). A meta-analysis on self-face recognition highlighted the role of the precuneus, which is coherent with our finding of precuneus involvement\$ only in AH patients, as only the latter patients among all AP patients often report seeing their own face during the AP and, in addition, may report seeing their face as clearly as if they were looking in a mirror. Further work has linked the precuneus to own-face and own-body processing (Platek *et al.*, 2008; Devue and Brédart, 2011; Dohle *et al.*, 2011). To conclude, we argue that AH result from a disrupted bilateral cortical network characterized by connectivity with ventral (pITG) and dorsal stream regions (precuneus), as well as the cerebellum. These findings are distinct from the three other types of AP, linking AH to a disruption of local and distributed regions that involve visual and self-related processing in extrastriate cortex and precuneus, respectively.

### HAS derived network

We found that lesions causing HAS are part of a common brain network functionally connected to large bilateral STG/MTG clusters, but also to clusters in fronto-temporal cortex as well as subcortical regions. From these areas only two left hemispheric regions were found to be specifically linked to HAS: the left IFG and the PHC. In HAS, compared to the other AP, patients experience a mental state that is characterized by a strong alteration of bodily self-consciousness with alternating self-location, visuo-spatial perspective and self-identification between the physical body and the autoscopic body (Lunn, 1970; Brugger *et al.*, 1994; Brugger, 2002; Blanke *et al.*, 2004; Blanke and Mohr, 2005; Heydrich and Blanke, 2013). Here, we found that HAS was associated with left IFG and left PHC. The left IFG has been involved in several self-related processes (Morin and Michaud, 2007) such as face and body identification (Uddin *et al.*, 2005; Platek *et al.*, 2008; Hodzic *et al.*, 2009) coherent with HAS phenomenology where the patients report abnormal and strong self-identification with the autoscopic body (Heydrich and Blanke, 2013). In addition, the left IFG is involved in inner speech and language processing (McGuire *et al.*, 1996; Shergill *et al.*, 2001; Morin and Michaud, 2007; Geva *et al.*, 2011; Liakakis *et al.*, 2011), which has been argued to be in line with the report of thought and verbal communication with the autoscopic body. Another experiential feature, that distinguishes HAS from AH and OBE, is the experience of echopraxia (the experienced sharing of movement and body postures with the autoscopic body) (Lukianowicz, 1958; Brugger *et al.*, 2006) and disconnection from left IFG may reflect such echopraxia-related aspects of HAS, due to interference with sensorimotor processing, conscious action monitoring (i.e. agency: Fink *et al.*, 1999; Nahab *et al.*, 2011) and action observation (Iacoboni, 1999; Johnson-Frey *et al.*, 2003; Molnar-Szakacs *et al.*, 2005; Buccino *et al.*, 2013).

We also found that HAS was associated with PHC, which has not been reported before. The PHC is a key region for episodic memory, autobiographical memory, and spatial navigation (Ranganath and Ritchey, 2012; Aminoff *et al.*, 2013), as well as viewpoint-specific local scene processing (Epstein *et al.*, 2003; Epstein, 2008; Mullally and Maguire, 2011; Ranganath and Ritchey, 2012). Guterstam and colleagues also found this region to be associated with self-location (Guterstam *et al.*, 2015), in line with observations by HAS patients reporting alternating self-location and visuo-spatial perspective between the physical body and the autoscopic body. Previous lesion



analysis has linked HAS to the left posterior insula (Heydrich and Blanke, 2013), here we extend this result by showing the involvement of the left IFG, which is connected to the insula (Deen *et al.*, 2011; Cerliani *et al.*, 2012), and the left PHC. The present lesion network analysis confirmed a left hemispheric dominance associated with HAS, which has been hypothesized before (Brugger *et al.*, 1997; Blanke and Mohr, 2005; Lopez *et al.*, 2008) and is coherent with HAS phenomenology involving experienced speech and thought communication with the autoscopic body. Even though, the present data show that HAS is associated with bilateral networks and that lesions occurring in the right hemisphere (Heydrich and Blanke, 2013) can also cause HAS, only left functional connections at left IFG and left PHC were specific for HAS, highlighting the importance of the left hemisphere in HAS. To conclude, HAS result from disrupted left cortical connectivity with IFG and PHC. These findings are distinct from the three other types of AP, arguably linking HAS to a disruption of sensorimotor, language and prominent self-related processes, including self-identification and first-person perspective in the left hemisphere.

### **OBE derived network**

Lesions causing OBE are part of a common brain network functionally connected to bilateral angular gyrus, bilateral MTG and inferior temporal cortex, right precuneus and several clusters in right prefrontal cortex, mostly IFG. Several of these regions were specific to OBE and included the bilateral angular gyrus, right IFG, right precuneus, right MTG, and left inferior temporal gyrus. Compared to other AP, only OBE patients report seeing their own body from an elevated visuo-spatial perspective that is associated with prominent vestibular sensations (Blanke *et al.*, 2004) and being located at this elevated position (i.e. abnormal self-location and disembodiment). Here, we found involvement of the angular gyrus of TPJ, a multisensory area involved in visuo-tactile and vestibular processing (Brandt & Dieterich, 1999; Ionta *et al.*, 2011; Tsakiris, Longo, & Haggard, 2010; Ventre-Dominey, 2014). This result is also in line with lesion analysis highlighting the right TPJ (including the angular gyrus) (Ionta *et al.*, 2011) and single case reports (Lunn, 1970; Devinsky *et al.*, 1989; Maillard *et al.*, 2004; Brandt *et al.*, 2005; Bunning and Blanke, 2005; Hoepner *et al.*, 2012). In addition, vestibular processing is thought to arise from a network of connected regions around the core regions of TPJ and parieto-insular vestibular cortex (PIVC): these include frontal and temporal regions such as IFG and ITG, which were also highlighted

in the present analysis (Fasold *et al.*, 2002; Lopez *et al.*, 2012; Ventre-Dominey, 2014). TPJ involvement (bilateral angular gyrus) in OBEs is also compatible with data in healthy subjects when experiencing experimentally-induced changes in self-location and elevated visuo-spatial perspective (Ionta *et al.*, 2011), and the prominent involvement of the TPJ in self-consciousness more generally (Ruby and Decety, 2001; Vogeley and Fink, 2003; Vogeley *et al.*, 2004; Schwabe *et al.*, 2009).

We also report the new findings that the OBE network also included connectivity with the right precuneus and the IFG. PET imaging revealed recruitment of the precuneus in a single case of stimulation-induced OBE (De Ridder *et al.*, 2007), likely reflecting this structure's role in visual-spatial processing and in self-related processing (Ruby and Decety, 2001; Cavanna and Trimble, 2006; Northoff *et al.*, 2006; Peer *et al.*, 2015) and third-person perspective taking (Ruby and Decety, 2001; Vogeley *et al.*, 2004), which are disrupted in OBE. We note that the precuneus activation associated with OBE was more ventral compared to the more dorsal-posterior precuneus activation found in AH and has been previously found functionally connected to the angular gyrus compared to the dorsal posterior precuneus, which is more connected to the visual cortex (Margulies *et al.*, 2009; Zhang and Li, 2012). Concerning the connectivity with the IFG, only the right IFG was associated with OBE (compare with left IFG in HAS) and we argue that this likely reflects the IFG's role in self-processing and self-recognition (Uddin *et al.*, 2005; Hodzic *et al.*, 2009), with conflict monitoring, and self-other distinction (Fink *et al.*, 1999; Nahab *et al.*, 2011), as well third-person perspective views coherent with OBE phenomenology (Vogeley *et al.*, 2004). Future work should investigate how these self-related processes in right vs left IFG are associated with OBE vs. HAS, respectively. To conclude, we find that OBE result from disrupted bilateral cortical connectivity involving bilateral angular gyrus, right IFG, right precuneus, right MTG, and left ITG, compatible with symptomatic and experimentally-induced OBE (Ehrsson, 2007; Lenggenhager *et al.*, 2007, 2009; Ionta *et al.*, 2011, 2014) and altered spatial self-related processing involving first-person perspective and self-location.

### **PH derived network**

PH were linked to a common brain network functionally connected to the right STG/SMG, right IFG, bilateral insula, left MCC and left postcentral gyrus. However, compared to the other AP, none of these regions were found to be specifically linked to PH. PH differs from the aforementioned AP by the lack of a hallucinated autoscopic visual body and is defined as the non-visual sensation that someone is present nearby (Brugger, Regard, & Landis, 1996; Critchley, 1950, 1955; Jaspers, 1913; Lhermitte, 1939). Because, the felt presence may rarely be experienced as a second *own* body (Critchley, 1950, 1955; Brugger *et al.*, 1996) and may occur jointly with AH, HAS or OBE, most classical authors classified PH with AP. In an influential early textbook, Menninger-Lerchenthal (1935) described PH as “heautoscopy without optical image” and the present network data revealed highly similar patterns between PH and HAS such as bilateral STG/MTG and insula. The insula is a multisensory region integrating tactile, visual, auditory, viscerosensitive and vestibular signals (Augustine, 1996; Flynn *et al.*, 1999; Heydrich *et al.*, 2018) and has frequently been involved in bodily self-consciousness (Tsakiris *et al.*, 2007; Serino *et al.*, 2013). The bilateral STG was found in all AP (see next section) and the IFG was present in PH, HAS, and OBE, underlining the involvement of prefrontal functions highlighted above. Finally, non-specific involvement of the postcentral gyrus was only found for PH and may be compatible with the frequent somatosensory manifestations in PH patients that are absent in the other three AP. We can only speculate why we did not find a specific PH network. Although PH lack the seen autoscopic body that is characteristic for all other three AP, PH are characterized by an illusory second body, a felt presence that is generally neither seen, heard, or felt. This reduplicative element of one’s own body has been revealed also in stimulation-induced PH (Arzy *et al.*, 2006) and experimentally-induced PH (Blanke *et al.*, 2014) and is therefore present in all four AP (Blanke *et al.*, 2008). Based on these and the present findings, we argue that reduplication is a common phenomenological element of all AP and that PH may present a minimal form of AP associated with the common network.

### **Common regions involved in AP and conclusion**

An important finding of the present lesion network data is that, in addition to these different networks, our data also show that lesions causing AP share connectivity with

bilateral TPJ. This is in agreement with current classification of all four symptoms as AP and the proposed idea of continuum between AP experiences (Hécaen and Ajuriaguerra, 1952; Maillard *et al.*, 2004) where all AP are associated with illusory reduplication of one's own body, which result from interference with distinct functional sub-systems (Brugger, 2002; Blanke *et al.*, 2004). Thus, although each AP results from a different lesion location and different altered network connectivity, which are distributed across temporal, parietal, frontal, and occipital cortices for the different AP (Fig.2), they all include interference with a common network region at the bilateral TPJ (Fig.4). We argue that the TPJ involvement reflects the main common element of AP: the illusory reduplication of one's own body that is either seen (AH, HAS, OBE) or felt (PH)). Of note, even during HAS the "autoscopic" body is not always clearly perceived as one's own body (Blanke and Mohr, 2005) and may also be variable in OBEs (Blanke *et al.*, 2004). The TPJ connectivity is further associated with the specific patterns of brain damage and altered functional connectivity that defines each type of AP. AH are visual AP, OBE have prominent vestibular and spatial components associated with disembodiment and perspective changes, HAS has prominent interoceptive, motor, and language-related aspects, some of which are shared with PH. The present connectivity findings may also explain why some patients reported experiencing more than one AP, as for example in the case of an AP of epileptic origin the involved network may differ depending on the spread of ictal activity in a given seizure: Maillard *et al.*, 2004; Tadokoro *et al.*, 2006; for other diseases: Arias *et al.*, 2007; Martínez-horta *et al.*, 2020). To conclude, the present data converge towards TPJ being a common core region for AP, but also highlight the different functional sub-networks for each AP by linking all forms to specific self-related networks.

The combined origin of focal brain damage and altered network connectivity accounts well for the multiple medical causes of AP, which include various focal and generalized diseases of the central nervous system. AP following focal brain damage emerge from a large variety of etiologies including focal epilepsy (Devinsky *et al.*, 1989; Blanke *et al.*, 2004; Maillard *et al.*, 2004), traumatic brain damage (Todd and Dewhurst, 1955), migraine (Lippman, 1953), vascular brain damage (Kolmel, 1985; Blanke *et al.*, 2004), neoplasia (Todd, 1955), dysembryoblastic neuroepithelial tumor (Blanke *et al.*, 2004), and arteriovenous malformation (Devinsky *et al.*, 1989). The present data accounts for this wide variety of pathological brain mechanisms and

provides a combined lesion- and connectivity-based framework, making it possible to explain AP caused by migraine, epilepsy, or stroke within a single framework. Importantly, it may also extend to AP in generalized neurological etiologies (encephalitis, intoxications, generalized epilepsies; Blanke *et al.*, 2004). In particular, AP may be more prominent than currently thought in neurodegenerative disease. Thus, although it is known that PH are very frequent in Parkinson's disease (Fénelon *et al.*, 2011; Llorca *et al.*, 2016; Pagonabarraga *et al.*, 2016; Bernasconi *et al.*, 2020) and Lewy body dementia (Nicastro *et al.*, 2018) it is not known whether the other AP are also present in Parkinson's disease.

Beyond the relevance for neurological research and practice, the present data are of relevance for neuroscience research of consciousness. A large number of current and past studies investigated multisensory and sensorimotor mechanisms of the upper limb and its altered states of bodily self-consciousness, including phantom limbs (i.e. Ramachandran and Hirstein, 1998; Halligan *et al.*, 2002; Kikkert *et al.*, 2018) and chronic limb pain (Solcà *et al.*, 2018). This field of research described some of the underlying cortical and subcortical mechanisms for limb representations and created new lab-based research paradigms (Botvinick and Cohen, 1998; Ehrsson *et al.*, 2004), leading to an improvement of models of corporeal awareness and bodily self-consciousness (Halligan, 2002; Brugger *et al.*, 2000; Ramachandran and Hirstein, 1998) and novel procedures to treat complex regional pain syndrome (Solcà *et al.*, 2018) and phantom limb pain (Rognini *et al.*, 2019). These advances, however, are limited to body part representations, mostly the upper limb. The scientific value of a thorough understanding of AP, their neural basis, and etiological origin, which differs from those for the upper limb (Blanke *et al.*, 2015) can thus not be overstated for neurological and psychiatric disease and normal brain functions related to corporeal awareness, embodiment, and self-consciousness (Seth and Tsakiris, 2018; Park and Blanke, 2019) and may further provide novel treatment options by targeting global self-representations.

## References

- Allison T, Ginter H, McCarthy G, Nobre AC, Puce A, Luby M, et al. Face recognition in human extrastriate cortex. *J Neurophysiol* 1994; 71: 821–825.
- Aminoff EM, Kveraga K, Moshe B. The role of the parahippocampal cortex in cognition. *Trends Cogn Sci* 2013; 17: 379–390.
- Anzellotti F, Onofri V, Maruotti V, Ricciardi L, Franciotti R, Bonanni L, et al. Autoscopic phenomena: case report and review of literature. *Behav Brain Funct* 2011; 7: 2.
- Apps, Tajadura-Jiménez A, Turley G, Tsakiris M. The different faces of one’s self: An fMRI study into the recognition of current and past self-facial appearances. *Neuroimage* 2012; 63: 1720–1729.
- Arias M, Constela IR, Iglesias S, Arias-Rivas S, Dapena D, Sesar Á. The autoscopic phenomena in neurological clinic: A study of two cases. *J Neurol Sci* 2007; 263: 223–225.
- Arzy S, Seeck M, Ortigue S, Spinelli L, Blanke O. Induction of an illusory shadow person. *Nature* 2006; 443: 287.
- Astafiev S V., Stanley CM, Shulman GL, Corbetta M. Extrastriate body area in human occipital cortex responds to the performance of motor actions. *Nat Neurosci* 2004; 7: 542–548.
- Augustine JR. Circuitry and functional aspects of the insular lobe in primates including humans. *Brain Res Rev* 1996; 22: 229–244.
- Bernasconi F, Blondiaux E, Potheegadoo J, Stripeikyte G, Bejr-kasem H, Pagonabarraga J, et al. Sensorimotor hallucinations in Parkinson’s disease. 2020
- Bevil R. Conway, Conway BR. The Organization and Operation of Inferior Temporal Cortex. *Annu Rev Vis Sci* 2018; 4: 381–402.
- Bhaskaran R, Kumar A, Nayar P. Autoscopy in the hemianopic field. *J Neurol Neurosurg Psychiatry* 1990; 53: 1016–1017.
- Blackmore. Out-of-body experiences in schizophrenia. A questionnaire survey. *J Nerv Ment Dis* 1986; 174: 615–619.
- Blanke O. Multisensory brain mechanisms of bodily self-consciousness. *Nat Rev Neurosci* 2012; 13: 556–571.
- Blanke O, Arzy S. The out-of-body experience: Disturbed self-processing at the temporo-parietal junction. *Neuroscientist* 2005; 11: 16–24.
- Blanke O, Arzy S, Landis T. Illusory perceptions of the human body and self. *Neuropsychology* 2008; 88: 429–458.
- Blanke O, Castillo V. Clinical Neuroimaging in Epileptic Patients with Autoscopic Hallucinations and Out-of-Body Experiences. *Epileptologie* 2007: 90–96.
- Blanke O, Landis T, Spinelli L, Seeck M. Out-of-body experience and autoscopy of neurological origin. *Brain* 2004; 127: 243–258.
- Blanke O, Metzinger T. Full-body illusions and minimal phenomenal selfhood. *Trends Cogn Sci* 2009; 13: 7–13.
- Blanke O, Mohr C. Out-of-body experience, heautoscopy, and autoscopic hallucination of neurological origin: Implications for neurocognitive mechanisms of corporeal awareness and self-consciousness. *Brain Res Rev* 2005; 50: 184–199.
- Blanke O, Ortigue S, Coeytaux A, Martory M-D, Landis T. Hearing of a Presence. *Neurocase* 2003; 9: 329–339.
- Blanke O, Ortigue S, Landis T, Seeck M. Stimulating illusory own-body perceptions. *Nature* 2002; 419: 269–270.
- Blanke O, Pozeg P, Hara M, Heydrich L, Serino A, Yamamoto A, et al. Neurological and Robot-Controlled Induction of an Apparition. *Curr Biol* 2014; 24: 2681–2686.
- Blanke O, Slater M, Serino A. Behavioral, Neural, and Computational Principles of Bodily Self-Consciousness. *Neuron* 2015; 88: 145–166.
- Boes AD, Prasad S, Liu H, Liu Q, Pascual-Leone A, Caviness VS, et al. Network localization of neurological symptoms from focal brain lesions. *Brain* 2015; 138: 3061–3075.
- Bolognini N, Làdavas E, Farnè A. Spatial Perspective and Coordinate Systems in Autoscopy : A Case Report of a “ Fantome de Profil ” in Occipital Brain Damage. 2011: 1741–1751.
- Bos EM, Spoor JKH, Smits M, Schouten JW, Vincent AJPE. Out-of-Body Experience During Awake Craniotomy. *World Neurosurg* 2016; 92: 586.e9-586.e13.
- Botvinick M, Cohen J. Rubber hands ‘feel’ touch that eyes see. *Nature* 1998; 391: 756.
- Brandt, Brechtelsbauer D, Bien CG, Reiners K. ‘Out-of-body experience’ als mögliches anfallssymptom bei einem patienten mit rechtsparietaler läsion. *Nervenarzt* 2005; 76: 1259–1262.
- Brandt T, Dieterich M. The vestibular cortex. *Ann N Y Acad Sci* 1999: 293–312.

- Brozzoli, Gentile G, Petkova VI, Ehrsson HH. fMRI adaptation reveals a cortical mechanism for the coding of space near the hand. *J Neurosci* 2011; 31: 9023–9031.
- Brugger. Reflective mirrors: Perspective-taking in autoscopic phenomena. *Cogn Neuropsychiatry* 2002; 7: 179–194.
- Brugger P. Are “Presences” Preferentially Felt along the Left Side of One’s Body? *Percept Mot Skills* 1994; 79: 1200–1202.
- Brugger P, Agosti R, Regard M, Wieser HG, Landis T. Heautoscopy, epilepsy, and suicide. *J Neurol Neurosurg Psychiatry* 1994; 57: 838–839.
- Brugger P, Blanke O, Regard M, Bradford DT, Landis T. Polyopic heautoscopy: Case report and review of the literature. *Cortex* 2006; 42: 666–674.
- Brugger P, Regard M, Landis T. Unilaterally Felt ‘Presences’: The Neuropsychiatry of One’s Invisible Doppelgänger. *Neuropsychiatry Neuropsychol Behav Neurol* 1996; 9: 114–122.
- Brugger P, Regard M, Landis T, Oelz O. Hallucinatory experiences in extreme-altitude climbers. *Neuropsychiatry Neuropsychol Behav Neurol* 1999; 12: 67–71.
- Brugger, Regard M, Landis T. Illusory Reduplication of One’s Own Body: Phenomenology and Classification of Autoscopic Phenomena. *Cogn Neuropsychiatry* 1997; 2: 19–38.
- Buccino G, Binkofski F, Fink GR, Fadiga L, Fogassi L, Gallese V, et al. Action observation activates premotor and parietal areas in a somatotopic manner: An fMRI study. *Soc Neurosci Key Readings* 2013; 9780203496: 133–142.
- Bunning S, Blanke O. The out-of-body experience: Precipitating factors and neural correlates. *Prog Brain Res* 2005; 150: 331–350.
- Cavanna AE, Trimble MR. The precuneus: A review of its functional anatomy and behavioural correlates. *Brain* 2006; 129: 564–583.
- Cerliani L, Thomas RM, Jbabdi S, Siero JCW, Nanetti L, Crippa A, et al. Probabilistic tractography recovers a rostrocaudal trajectory of connectivity variability in the human insular cortex. *Hum Brain Mapp* 2012; 33: 2005–2034.
- Cohen AL, Soussand L, Corrow SL, Martinaud O, Barton JJS, Fox MD. Looking beyond the face area: lesion network mapping of prosopagnosia. *Brain* 2019; 142: 3975–3990.
- Cook CM, Persinger MA. Experimental induction of the ‘sensed presence’ in normal subjects and an exceptional subject. *Percept Mot Skills* 1997; 85: 683–693.
- Critchley M. The body-image in neurology. *Lancet* 1950; 1: 335–340.
- Critchley M. The idea of a presence. *Acta Psychiatr Scand* 1955; 30: 155–168.
- Critchley M. *The divine banquet of the brain and other essays*. Raven Press, New York; 1979
- Daly D. Ictal affect. *Am j ournal psychiatry* 1958: 97–108.
- Darby RR, Horn A, Cushman F, Fox MD. Lesion network localization of criminal behavior. *Proc Natl Acad Sci* 2017: 201706587.
- Darby RR, Joutsa J, Burke MJ, Fox MD. Lesion network localization of free will. *Proc Natl Acad Sci* 2018; 115: 10792–10797.
- Darby RR, Laganiere S, Pascual-Leone A, Prasad S, Fox MD. Finding the imposter: Brain connectivity of lesions causing delusional misidentifications. *Brain* 2017; 140: 497–507.
- Deen B, Pitskel NB, Pelphrey KA. Three systems of insular functional connectivity identified with cluster analysis. *Cereb Cortex* 2011; 21: 1498–1506.
- Denning TR, Berrios GE. Autoscopic phenomena. *Br J Psychiatry* 1994; 165: 808–817.
- Devinsky O, Feldmann E, Burrowes K, Bromfield E. Autoscopic phenomena with seizures. *Arch Neurol* 1989; 46: 1080–1088.
- Devue C, Brédart S. The neural correlates of visual self-recognition. *Conscious Cogn* 2011; 20: 40–51.
- Dohle C, Stephan KM, Valvoda JT, Hosseiny O, Tellmann L, Kühlen T, et al. Representation of virtual arm movements in precuneus. *Exp Brain Res* 2011; 208: 543–555.
- Downing P, Kanwisher N. A cortical area specialized for visual processing of the human body. *J Vis* 2001; 1: 2470–2474.
- Ehrsson HH. The Experimental Induction of Out-of-Body Experiences. *Science (80- )* 2007; 317: 1048–1048.
- Ehrsson HH, Holmes NP, Passingham RE. Touching a rubber hand: feeling of body ownership is associated with activity in multisensory brain areas. *J Neurosci* 2005; 25: 10564–73.
- Ehrsson HH, Spence C, Passingham RE. That’s my hand! Activity in premotor cortex reflects feeling of ownership of a limb. *Science* 2004; 305: 875–7.
- Eickhoff SB, Heim S, Zilles K, Amunts K. Testing anatomically specified hypotheses in functional imaging using cytoarchitectonic maps. *Neuroimage* 2006; 32: 570–582.
- Eickhoff SB, Paus T, Caspers S, Grosbras MH, Evans AC, Zilles K, et al. Assignment of functional activations to probabilistic cytoarchitectonic areas revisited. *Neuroimage* 2007; 36: 511–521.

- Eickhoff SB, Stephan KE, Mohlberg H, Grefkes C, Fink GR, Amunts K, et al. A new SPM toolbox for combining probabilistic cytoarchitectonic maps and functional imaging data. *Neuroimage* 2005; 25: 1325–1335.
- Epstein. Parahippocampal and retrosplenial contributions to human spatial navigation. *Trends Cogn Sci* 2008; 12: 388–396.
- Epstein, Graham KS, Downing PE. Viewpoint-specific scene representations in human parahippocampal cortex. *Neuron* 2003; 37: 865–876.
- Fang T, Yan R, Fang F. Spontaneous out-of-body experience in a child with refractory right temporoparietal epilepsy. *J Neurosurg Pediatr* 2014; 14: 396–399.
- Fasano A, Laganieri SE, Lam S, Fox MD. Lesions causing freezing of gait localize to a cerebellar functional network. *Ann Neurol* 2017; 81: 129–141.
- Fasold O, Von Brevern M, Kuhberg M, Ploner CJ, Villringer A, Lempert T, et al. Human vestibular cortex as identified with caloric stimulation in functional magnetic resonance imaging. *Neuroimage* 2002; 17: 1384–1393.
- Fénelon G, Soulas T, Cleret de Langavant L, Trinkler I, Bachoud-Lévi A-C. Feeling of presence in Parkinson's disease. *J Neurol Neurosurg Psychiatry* 2011; 82: 1219–1224.
- Fink GR, Marshall JC, Halligan PW, Frith CD, Driver J, Frackowiak RSJ, et al. The neural consequences of conflict between intention and the senses. *Brain* 1999; 122: 497–512.
- Fischer D, Boes A, Demertzi A, Evrard H, Laureys S, Edlow B, et al. A human brain network based on coma-causing brainstem lesions. *Neurology* 2016; 87: 2427–2434.
- Flynn FG, Benson DF, Ardila A. Anatomy of the insula - Functional and clinical correlates. *Aphasiology* 1999; 13: 55–78.
- Fox MD. Mapping Symptoms to Brain Networks with the Human Connectome. *N Engl J Med* 2018; 379: 2237–2245.
- Gentile G, Guterstam A, Brozzoli C, Ehrsson HH. Disintegration of multisensory signals from the real hand reduces default limb self-attribution: an fMRI study. *J Neurosci* 2013; 33: 13350–66.
- Geva S, Jones PS, Crinion JT, Price CJ, Baron JC, Warburton EA. The neural correlates of inner speech defined by voxel-based lesion-symptom mapping. *Brain* 2011; 134: 3071–3082.
- Greyson B, Fountain NB, Derr LL, Broshek DK. Out-of-body experiences associated with seizures. *Front Hum Neurosci* 2014; 8: 1–11.
- Guterstam A, Björnsdotter M, Gentile G, Ehrsson HHH. Posterior Cingulate Cortex Integrates the Senses of Self-Location and Body Ownership. *Curr Biol* 2015; 25: 1416–1425.
- Halligan SL, Clark DM, Ehlers A. Cognitive processing, memory, and the development of PTSD symptoms: Two experimental analogue studies. *J Behav Ther Exp Psychiatry* 2002; 33: 73–89.
- Hécaen H, Ajuriaguerra J. *Meconnaissances et Hallucinations Corporelles: Intégration et Désintégration de la Somatognosie*. Masson (in French); 1952
- Heydrich L, Aspell JE, Marillier G, Lavanchy T. Cardio-visual full body illusion alters bodily self-consciousness and tactile processing in somatosensory cortex. *Sci Rep* 2018: 1–8.
- Heydrich L, Blanke O. Distinct illusory own-body perceptions caused by damage to posterior insula and extrastriate cortex. *Brain* 2013; 136: 790–803.
- Heydrich L, Lopez C, Seeck M, Blanke O. Partial and full own-body illusions of epileptic origin in a child with right temporoparietal epilepsy. *Epilepsy Behav* 2011; 20: 583–586.
- Hodzic A, Kaas A, Muckli L, Stirn A, Singer W. Distinct cortical networks for the detection and identification of human body. *Neuroimage* 2009; 45: 1264–1271.
- Hoepner R, Labudda K, Hoppe M, Schoendienst M, Schulz R, Tomka-Hoffmeister M, et al. Unilateral autoscopic phenomena as a lateralizing sign in focal epilepsy. *Epilepsy Behav* 2012; 23: 360–363.
- Hoepner R, Labudda K, May TW, Schoendienst M, Woermann FG, Bien CG, et al. Ictal autoscopic phenomena and near death experiences: A study of five patients with ictal autoscopies. *J Neurol* 2013; 260: 742–749.
- Iacoboni M. Cortical Mechanisms of Human Imitation. *Science* (80-) 1999; 286: 2526–2528.
- Ionta S, Heydrich L, Lenggenhager B, Mouthon M, Fornari E, Chappuis D, et al. Multisensory mechanisms in temporo-parietal cortex support self-location and first-person perspective. *Neuron* 2011; 70: 363–74.
- Ionta S, Martuzzi R, Salomon R, Blanke O. The brain network reflecting bodily self-consciousness: a functional connectivity study. [Internet]. *Soc Cogn Affect Neurosci* 2014[cited 2014 Aug 13] Available from: <http://www.ncbi.nlm.nih.gov/pubmed/24396007>
- Jaspers K. Über leibhaftige Bewusstheiten (Bewusstheitstäuschungen), ein psychopathologisches Elementarsymptom. *Zeitschrift für Pathopsychologie* 1913; 2: 150–161.
- Johnson-Frey SH, Maloof FR, Newman-Norlund R, Farrer C, Inati S, Grafton ST. Actions or hand-object interactions? Human inferior frontal cortex and action observation. *Neuron* 2003; 39: 1053–1058.



- Jonas J, Maillard L, Frismand S, Colnat-Coulbois S, Vespignani H, Rossion B, et al. Self-face hallucination evoked by electrical stimulation of the human brain. *Neurology* 2014; 83: 336–338.
- Joutsa J, Horn A, Hsu J, Fox MD. Localizing parkinsonism based on focal brain lesions. *Brain* 2018; 2445–2456.
- Kanwisher N, McDermott KB, Chun MM. The Fusiform Face Area: A Module in Human Extrastriate Cortex Specialized for Face Perception. *J Neurosci* 1997; 17: 4302–4311.
- Kikkert S, Johansen-Berg H, Tracey I, Makin TR. Reaffirming the link between chronic phantom limb pain and maintained missing hand representation. *Cortex* 2018; 106: 174–184.
- Kim NY, Hsu J, Talmasov D, Joutsa J, Soussand L, Wu O, et al. Lesions causing hallucinations localize to one common brain network [Internet]. *Mol Psychiatry* 2019 Available from: <http://dx.doi.org/10.1038/s41380-019-0565-3>
- Kolmel HW. Complex visual hallucinations in the hemianopic field. *J Neurol Neurosurg Psychiatry* 1985; 48: 29–38.
- Laganieri S, Boes AD, Fox MD. Network localization of hemichorea-hemiballismus. *Neurology* 2016; 86: 2187–2196.
- Landtblom AM, Lindehammar H, Karlsson H, Craig ADB. Insular cortex activation in a patient with ‘sensed presence’/ecstatic seizures. *Epilepsy Behav* 2011; 20: 714–718.
- Lenggenhager B, Mouthon M, Blanke O. Spatial aspects of bodily self-consciousness. *Conscious Cogn* 2009; 18: 110–117.
- Lenggenhager B, Tadi T, Metzinger T, Blanke O. Video ergo sum: manipulating bodily self-consciousness. *Science* 2007; 317: 1096–9.
- Lhermitte J. *L’image de notre corps*. Paris: Edi. 1939
- Lhermitte J. Visual Hallucination of the Self. *Br Med J* 1951: 431–434.
- Liakakis G, Nickel J, Seitz RJ. Diversity of the inferior frontal gyrus-A meta-analysis of neuroimaging studies. *Behav Brain Res* 2011; 225: 341–347.
- Lippman CW. Hallucinations of physical duality in migraine. *J Nerv Ment Dis* 1953; 117: 345–350.
- Llorca PM, Pereira B, Jardri R, Chereau-Boudet I, Brousse G, Misdrahi D, et al. Hallucinations in schizophrenia and Parkinson’s disease: an analysis of sensory modalities involved and the repercussion on patients. *Sci Rep* 2016; 6: 38152.
- Lopez, Blanke O, Mast FW. The human vestibular cortex revealed by coordinate-based activation likelihood estimation meta-analysis. *Neuroscience* 2012; 212: 159–79.
- Lopez C, Halje P, Blanke O. Body ownership and embodiment: Vestibular and multisensory mechanisms. *Neurophysiol Clin* 2008; 38: 149–161.
- Lukianowicz. Autoscopic phenomena. *Arch Neurol Psychiatry* 1958; 80: 199.
- Lunn V. Autoscopic phenomena. *Acta Psychiatr Scand* 1970; 46: 118–125.
- Maillard L, Vignal JP, Anxionnat R, Taillandier L, Vespignani H. Semiologic Value of Ictal Autoscopy. *Epilepsia* 2004; 45: 391–394.
- Margulies DS, Vincent JL, Kelly C, Lohmann G, Uddin LQ, Biswal BB, et al. Precuneus shares intrinsic functional architecture in humans and monkeys. *Proc Natl Acad Sci U S A* 2009; 106: 20069–20074.
- Martínez-Horta S, Perez-Perez J, Pagonabarraga J, Sampedro F, Horta-Barba A, Blanke O, et al. Autoscopic phenomena as an atypical psychiatric presentation of Huntington’s disease: A case report including longitudinal clinical and neuroimaging data. *Cortex* 2020; 125: 299–306.
- McGuire PK, Silbersweig DA, Murray RM, David AS, Frackowiak RSJ, Frith CD. Functional anatomy of inner speech and auditory verbal imagery. *Psychol Med* 1996; 26: 29–38.
- Menninger-Lerchenthal E. *Das Truggebilde der eigenen Gestalt (Heautoscopy, Doppelgänger)*. Berlin, Karger; 1935
- Menninger-Lerchenthal E. *Der eigene Doppelgänger*. Bern: Huber; 1946
- Molnar-Szakacs I, Iacoboni M, Koski L, Mazziotta JC. Functional segregation within pars opercularis of the inferior frontal gyrus: Evidence from fMRI studies of imitation and action observation. *Cereb Cortex* 2005; 15: 986–994.
- Morin A, Michaud J. Self-awareness and the left inferior frontal gyrus: Inner speech use during self-related processing. *Brain Res Bull* 2007; 74: 387–396.
- Mullally SL, Maguire EA. A new role for the parahippocampal cortex in representing space. *J Neurosci* 2011; 31: 7441–7449.
- Nahab FB, Kundu P, Gallea C, Kakareka J, Pursley R, Pohida T, et al. The neural processes underlying self-agency. *Cereb Cortex* 2011; 21: 48–55.
- Nicastro N, Eger AF, Assal F, Garibotto V. Feeling of presence in dementia with Lewy bodies is related to reduced left frontoparietal metabolism [Internet]. *Brain Imaging Behav* 2018 Available from: <http://link.springer.com/10.1007/s11682-018-9997-7>
- Nightingale S. Somatoparaphrenia: A Case Report. *Cortex* 1982; 18: 463–467.

- Nooner KB, Colcombe SJ, Tobe RH, Mennes M, Benedict MM, Moreno AL, et al. The NKI-Rockland Sample: A Model for Accelerating the Pace of Discovery Science in Psychiatry. *Front Neurosci* 2012; 6: 1–11.
- Northoff G, Heinzel A, de Greck M, Bermpohl F, Dobrowolny H, Panksepp J. Self-referential processing in our brain—A meta-analysis of imaging studies on the self. *Neuroimage* 2006; 31: 440–457.
- Ochoa JF, Ascencio JL, Zapata JF. Conectividad funcional en un paciente con alucinaciones complejas. Un caso de autoscopia. *Acta Neurológica Colomb* 2015; 31: 423–431.
- Van Overwalle F, Baetens K, Mariën P, Vandekerckhove M. Social cognition and the cerebellum: A meta-analysis of over 350 fMRI studies. *Neuroimage* 2014; 86: 554–572.
- Pagonabarraga J, Martínez-Horta S, Fernández de Bobadilla R, Pérez J, Ribosa-Nogué R, Marín J, et al. Minor hallucinations occur in drug-naïve Parkinson’s disease patients, even from the premotor phase. *Mov Disord* 2016; 31: 45–52.
- Park H, Blanke O. Coupling Inner and Outer Body for self-consciousness. *Trends Cogn Sci* 2019; 23: 377–388.
- Peer M, Salomon R, Goldberg I, Blanke O, Arzy S. Brain system for mental orientation in space, time, and person. *Proc Natl Acad Sci U S A* 2015; 112: 11072–11077.
- Picard F. Epileptic feeling of multiple presences in the frontal space. *Cortex* 2010; 46: 1037–1042.
- Platek SM, Wathne K, Tierney NG, Thomson JW. Neural correlates of self-face recognition: An effect-location meta-analysis. *Brain Res* 2008; 1232: 173–184.
- Power JD, Barnes KA, Snyder AZ, Schlaggar BL, Petersen SE. Spurious but systematic correlations in functional connectivity MRI networks arise from subject motion. *Neuroimage* 2012; 59: 2142–2154.
- Ramachandran VS, Hirstein W. The perception of phantom limbs. The D. O. Hebb lecture. *Brain* 1998; 121: 1603–1630.
- Ranganath C, Ritchey M. Two cortical systems for memory-guided behaviour. *Nat Rev Neurosci* 2012; 13: 713–726.
- Rank O. *Der Doppelgänger. Eine psychoanalytische Studie.* Rank O. *Der Doppelgänger. Eine psychoanalytische Studie.* Leipzig: Internationaler Psychoanalytischer Verlag; 1925
- De Ridder D, Van Laere K, Dupont P, Menovsky T, Van de Heyning P. Visualizing out-of-body experience in the brain. *N Engl J Med* 2007; 357: 1829–1833.
- Rognini G, Petrini FM, Raspopovic S, Valle G, Granata G, Strauss I, et al. Multisensory bionic limb to achieve prosthesis embodiment and reduce distorted phantom limb perceptions. *J Neurol Neurosurg Psychiatry* 2019; 90: 833–836.
- Rolls ET. Face processing in different brain areas and face recognition. *Encycl Anim Cogn Behav* 2017: 1–11.
- Ronchi R, Park HD, Blanke O. *Bodily self-consciousness and its disorders.* 1st ed. Elsevier B.V.; 2018
- Rorden C, Karnath H-O, Bonilha L. Improving lesion-symptom mapping. *J Cogn Neurosci* 2007; 19: 1081–1088.
- Ruby P, Decety J. Effect of subjective perspective taking during simulation of action: A PET investigation of agency. *Nat Neurosci* 2001; 4: 546–550.
- Schwabe L, Lenggenhager B, Blanke O. The timing of temporoparietal and frontal activations during mental own body transformations from different visuospatial perspectives. *Hum Brain Mapp* 2009; 30: 1801–1812.
- Serino A, Alsmith A, Costantini M, Mandrigin A, Tajadura-Jimenez A, Lopez C. Bodily ownership and self-location: Components of bodily self-consciousness. *Conscious Cogn* 2013; 22: 1239–1252.
- Seth AK, Tsakiris M. Being a Beast Machine: The Somatic Basis of Selfhood. *Trends Cogn Sci* 2018; 22: 969–981.
- Sheils D. A Cross-Cultural Study of Beliefs in out-of-the-Body Experiences, Waking and Sleeping. *J Soc Psych Res* 1978; 49: 697–741.
- Shergill SS, Bullmore ET, Brammer MJ, Williams SCR, Murray RM, McGuire PK. A functional study of auditory verbal imagery. *Psychol Med* 2001; 31: 241–253.
- Solcà M, Ronchi R, Bello-Ruiz J, Schmidlin T, Herbelin B, Luthi F, et al. Heartbeat-enhanced immersive virtual reality to treat complex regional pain syndrome. *Neurology* 2018; 91: e1–e11.
- Stoodley CJ. The cerebellum and cognition: Evidence from functional imaging studies. *Cerebellum* 2012; 11: 352–365.
- Suedfeld P, Mocellin JSSP. The ‘Sensed Presence’ in Unusual Environments. *Environ Behav* 1987; 19: 33–52.
- Sugiura M, Sassa Y, Jeong H, Horie K, Sato S, Kawashima R. Face-specific and domain-general characteristics of cortical responses during self-recognition. *Neuroimage* 2008; 42: 414–422.
- Tadokoro Y, Oshima T, Kanemoto K. Postictal autoscopia in a patient with partial epilepsy. *Epilepsy Behav* 2006; 9: 535–540.

- Todd J, Dewhurst K. The double: its psycho-pathology and psycho-physiology. *J Nerv Ment Dis* 1955; 122: 47–55.
- Tsakiris M, Hesse MD, Boy C, Haggard P, Fink GR. Neural signatures of body ownership: A sensory network for bodily self-consciousness. *Cereb Cortex* 2007; 17: 2235–2244.
- Tsakiris M, Longo MR, Haggard P. Having a body versus moving your body: Neural signatures of agency and body-ownership. *Neuropsychologia* 2010; 48: 2740–2749.
- Tzourio-Mazoyer N, Landeau B, Papathanassiou D, Crivello F, Etard O, Delcroix N, et al. Automated anatomical labeling of activations in SPM using a macroscopic anatomical parcellation of the MNI MRI single-subject brain. *Neuroimage* 2002; 15: 273–289.
- Uddin LQ, Kaplan JT, Molnar-Szakacs I, Zaidel E, Iacoboni M. Self-face recognition activates a frontoparietal ‘mirror’ network in the right hemisphere: An event-related fMRI study. *Neuroimage* 2005; 25: 926–935.
- Ungerleider LG, Haxby J V. ‘What’ and ‘where’ in the human brain. *Curr Opin Neurobiol* 1994; 4: 157–165.
- Ventre-Dominey J. Vestibular function in the temporal and parietal cortex: Distinct velocity and inertial processing pathways. *Front Integr Neurosci* 2014; 8: 1–13.
- Vogeley, Fink GR. Neural correlates of the first-person- perspective. *Trends Cogn Sci* 2003; 7: 3–7.
- Vogeley, May M, Ritzl A, Falkai P, Zilles K, Fink GR. Neural correlates of first-person perspective as one constituent of human self-consciousness. *J Cogn Neurosci* 2004; 16: 817–827.
- Whitfield-Gabrieli S, Nieto-Castanon A. Conn: A Functional Connectivity Toolbox for Correlated and Anticorrelated Brain Networks. *Brain Connect* 2012; 2: 125–141.
- Zamboni G, Budriese C, Nichelli P. ‘Seeing oneself’: A case of autoscopia. *Neurocase* 2005; 11: 212–215.
- Zhang S, Li C shan R. Functional connectivity mapping of the human precuneus by resting state fMRI. *Neuroimage* 2012; 59: 3548–3562.
- Zijlmans M, Van Eijsden P, Ferrier CH, Kho KH, Van Rijen PC, Leijten FSS. Illusory shadow person causing paradoxical gaze deviations during temporal lobe seizures. *J Neurol Neurosurg Psychiatry* 2009; 80: 686–688.

Supplementary information of Common and distinct brain networks of  
four autistic phenomena

Supplementary tables:

Table S1: Information on lesions causing AP included in the analysis.

Patient	Diagnosis	Lesion site	Lesion side	Lesion analysis	Reported by
AH 1	Epilepsy (glioblastoma)	Parieto-occipital lobe	Left	MRI, EEG	Heydrich et al., 2013
AH 2	Epilepsy (focal dysplasia)	Parietal lobe	Right	MRI, EEG	Maillard et al., 2004
AH 3	Ischaemic lesion (eclampsia)	Occipital lobe	Right	MRI	Zamboni et al., 2005
AH 4	Epilepsy (parasitical lesion)	Occipital lobe	Right	MRI, EEG	Blanke et al., 2007
AH 5	Epilepsy (intracerebral haematoma)	Parieto-occipital lobe	Right	MRI, EEG	Maillard et al., 2004
AH 6	Epilepsy (oligodendroglioma)	Occipital lobe	Right	MRI, EEG	Maillard et al., 2004
AH 7	Tumor (postoperative lesion)	Occipital lobe	Right	MRI	Bogni et al., 2011
HAS 1	Epilepsy (dysembryoblastic tumor)	Temporal lobe, insula	Left	MRI, EEG, PET	Heydrich et al., 2013
HAS 2	Epilepsy	Temporal lobe, insula	Left	MRI, iEEG	Heydrich et al., 2013
HAS 3	Epilepsy (dysembryoblastic tumor)	Temporal lobe, mesio-basal	Left	MRI, EEG, PET	Heydrich et al., 2013
HAS 4	Epilepsy (focal dysplasia, after resection)	Temporo-parietal lobe, insula	Left	MRI, iEEG	Heydrich et al., 2013
HAS 5	Migraine (atrophy)	Parieto-occipital lobe	Bilateral	MRI	Heydrich et al., 2013
HAS 6	Epilepsy (lesional)	Insula and temporo-parieto-occipital lobe	Left	MRI, EEG	Heydrich et al., 2013
HAS 7	Epilepsy (astrocytoma)	Temporal lobe, insula	Right	CT, MRI, EEG, PET	Heydrich et al., 2013
HAS 8	Epilepsy (astrocytoma)	Temporal lobe, insula	Left	CT, EEG	Heydrich et al., 2013
HAS 9	Epilepsy (hippocampal sclerosis)	Temporal lobe, mesial	Left	MRI, SPECT	Heydrich et al., 2013
HAS 10	Hemorrhagic stroke	Temporo-occipital	Right	CT, MRI, EEG	
OBE 1	Ischemic lesion	Temporo-parietal	Right	MRI, PET	Ionta et al., 2011
OBE 2	Epilepsy (focal dysplasia)	Parietal	Right	MRI, EEG	Maillard et al., 2004
OBE 3	Epilepsy (focal dysplasia)	Parietal	Right	MRI	Brandt et al., 2005
OBE 4	Traumatic brain injury	Temporo-parietal	Right	MRI, EEG	Ionta et al., 2011
OBE 5	Epilepsy (focal dysplasia)	Temporo-parietal	Left	MRI, sEEG	Blanke et al., 2004
OBE 6	Tinnitus (no structural lesion)	Temporo-parietal	Right	Intracranial stimulation, MRI PET	De Ridder et al., 2007
OBE 7	Subarachnoid bleeding (post operative lesion)	Temporo-parietal	Right	MRI	Ionta et al., 2011
OBE 8	Epilepsy (dysembryoblastic neuroepithelial tumor)	Parieto-occipital	Right	MRI, EEG, SPECT	Blanke et al., 2004
OBE 9	Epilepsy (no structural lesion)	Temporo-parietal	Right	Intracranial stimulation, MRI	Blanke et al., 2004
OBE 10	Epilepsy	Temporal lobe	Left	MRI, EEG	
PH 1	Neurocystercosis	Frontoparietal cortex	Right	MRI	Blanke et al., 2014
PH 2	Epilepsy, status post ischemic stroke, vasculitis	Occipitoparietal cortex, frontoparietal cortex	Right	MRI, EEG	Blanke et al., 2014
PH 3	Epilepsy	Frontoparietal cortex	Left	MRI, EEG, PET, SPECT, iEEG	Blanke et al., 2014
PH 4	Epilepsy, status post resection of capillary angioma in the left insula	Insula, Frontoparietal cortex	Left	MRI, EEG, PET, SPECT, cortical stimulation	Blanke et al., 2014
PH 5	Intracerebral hematoma, ischemic stroke	Temporal lobe, frontal lobe, insula	Right	MRI	Blanke et al., 2014
PH 6	Epilepsy, cerebral histiocytosis	Thalamocapsular-caudate region, insula	Right	MRI, EEG	Blanke et al., 2014
PH 7	Epilepsy status post capsulolenticular haemorrhagic stroke	Insula, capsulolenticular region	Right	MRI, EEG	Blanke et al., 2014
PH 8	Epilepsy, hemiplegic migraine	Insula, parietooccipital cortex	Left	MRI, EEG	Blanke et al., 2014
PH 9	Epilepsy	Mesial temporal lobe, anterior temporal lobe	Left	MRI, PET, SPECT, iEEG	Blanke et al., 2014
PH 10	Epilepsy, status post resection of a left temporal dysplastic lesion	Temporoparietal cortex	Left	MRI, EEG, PET, SPECT, cortical stimulation	Blanke et al., 2014
PH 11	Epilepsy	Posterior temporal lobe	Left	MRI, cortical stimulation	Blanke et al., 2014
PH 12	Epilepsy, intracerebral hematoma	Temporoparietooccipital cortex	Left	MRI, EEG	Blanke et al., 2014

Table S2: Brain regions connected to all lesions causing autoscopic hallucinations (AH).

Brain regions	Voxel size	Coordinates (center of gravity)		
		x	y	z
<i>Positive correlations</i>				
R. superior parietal cortex/ precuneus/superior occipital gyrus/	3109	21	-63	48
L. superior parietal cortex/ precuneus/superior occipital gyrus	2086	-21	-63	49
L. cerebellum	265	-9	-75	-21
	68	-41	-47	-54
	13	-37	-74	-21
R. inferior temporal gyrus	203	53	-50	-17
L. inferior temporal gyrus	89	-56	-46	-26
	51	-50	-59	-7
R. middle frontal gyrus	85	31	0	52
R. precuneus	55	5	-41	49
L. inferior parietal lobe	24	-45	-36	50
R. middle cingulate cortex	24	11	-22	38
L. Thalamus	22	-2	-19	-3
R. cerebellum	20	7	-72	-24
<i>Negative correlations</i>				
R. caudate nucleus	137	18	13	18
L. parahippocampal gyrus	46	-15	-13	-15
L. fornix	31	-1	0	2
R. parahippocampal gyrus	15	20	-16	-15

Table S3: Brain regions selectively connected to each AP.

Brain regions	Voxel size	MNI coordinates			Intensity (Z-max)
		x	y	z	
<b><i>Autoscopy - positive correlations</i></b>					
R. Precuneus/Superior Parietal Lobe (SPL)	2400	17	-62	41	4.36
L. Precuneus/Superior Parietal Lobe (SPL)	1801	-3	-75	45	4.36
L. Cerebellum	260	-15	-89	-20	4.15
	40	-39	-50	-59	3.25
	13	-35	-75	-21	3.76
R. Cerebellum	20	8	-71	-26	4.15
L. inferior temporal gyrus	25	-59	-51	-27	3.42
R. inferior temporal gyrus	14	60	-47	-27	3.25
<b><i>Autoscopy - negative correlations</i></b>					
L. hippocampus	24	-18	-14	-15	4.36
L. fornix	16	-3	2	2	3.76
<b><i>Heautoscopy - positive correlations</i></b>					
L. inferior frontal gyrus (pars triangularis)	152	-47	29	15	3.43
L. parahippocampus/hippocampus	33	-20	-15	-27	3.25
<b><i>Out-of-body - positive correlations</i></b>					
R. angular gyrus	201	63	-53	30	4.19
R. inferior frontal gyrus (pars orbitalis)	74	48	41	-11	3.61
R. middle frontal gyrus	52	35	5	42	3.8
L. angular gyrus	47	-63	-56	26	3.8
R. inferior frontal gyrus (IFG)	41	56	23	30	3.8
	28	57	26	9	3.43
	10	39	14	33	3.8
R. precuneus	40	12	-56	45	3.99
	40	11	-45	41	3.99
R. middle temporal gyrus (MTG)	26	60	-23	-12	3.43
	11	54	-47	-3	3.43
L. inferior temporal gyrus	25	-57	-6	-38	3.61

Table S4: Brain regions connected to all lesions causing heautoscopy hallucinations.

Brain regions	Voxel size	Coordinates (center of gravity)		
		x	y	z
<b>Positive correlations</b>				
L. middle temporal gyrus	2797	-53	-44	10
R. superior temporal gyrus	2177	56	-39	10
L. parahippocampal gyrus	425	-26	-28	-12
R. parahippocampal gyrus/hippocampus	214	27	-33	-7
	36	26	-15	-22
L. inferior frontal gyrus	198	-43	18	23
R. inferior frontal gyrus (IFG)	74	42	19	22
L. inferior temporal gyrus	143	-43	-25	-24
R. inferior temporal gyrus	14	46	-20	-26
L. precentral gyrus	91	-40	-2	50
L. putamen	40	-36	-11	-9
L. thalamus	22	-12	-30	-1
<b>Negative correlations</b>				
L. caudate nucleus	16	-17	21	14

Table S5: Brain regions connected to all lesions causing out-of-body experiences.

Brain regions	Voxel size	Coordinates (center of gravity)		
		x	y	z
<b>Positive correlations</b>				
R. posterior middle temporal gyrus (MTG)	1219	62	-32	-3
R. supramarginal gyrus (SMG)/angular gyrus	646	53	-49	26
L. supramarginal gyrus	87	-56	-52	27
R. inferior frontal gyrus (IFG)	422	47	22	24
	97	50	40	-9
	116	54	28	9
	11	43	35	-21
R. precuneus	151	9	-51	44
L. anterior inferior temporal gyrus	113	-45	-25	-25
	106	-55	-2	-36
L. posterior middle temporal gyrus	152	-64	-46	1
R. anterior inferior temporal gyrus	103	52	0	-36
R. precentral gyrus	83	40	6	47

Table S6: Brain regions connected to all lesions causing presence hallucinations.

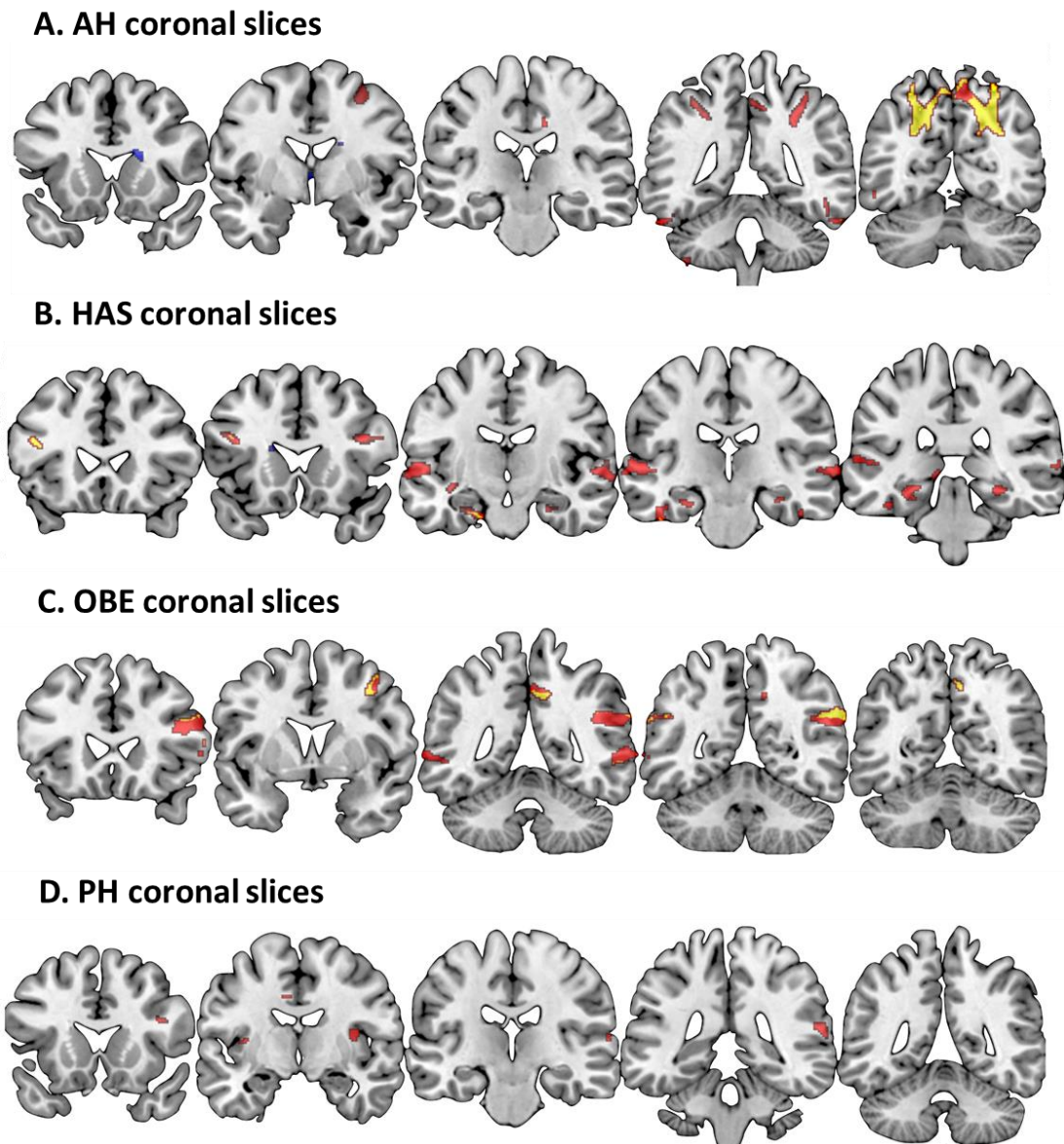
Brain regions	Voxel size	Coordinates (center of gravity)		
		x	y	z
<b>Positive correlations</b>				
R. superior temporal gyrus (STG)	164	62	-32	14
R. supramarginal gyrus (SMG)	34	66	-16	20
R. insula	38	37	-7	12
L. insula	24	-37	-5	6
L. middle cingulate cortex (MCC)	32	-9	-12	37
L. postcentral gyrus	15	-60	-15	20
R. inferior frontal gyrus (IFG)	12	41	18	22

Table S7: Brain regions connected to 85% of the lesion causing AP.

Brain regions	maximum overlap within the cluster	Voxel size	Coordinates (center of gravity)		
			x	y	z
<b>Positive correlations</b>					
L. middle temporal gyrus (MTG)	35/38	1237	-51	-65	14
R. superior temporal gyrus (STG)	35/38	997	63	-36	9
R. middle temporal gyrus (MTG)	35/38	417	51	-53	9
R. inferior frontal gyrus (IFG)	35/38	46	44	18	24
R. hippocampus	35/38	39	27	-36	-3
L. precentral gyrus	35/38	34	-42	-3	54
L. superior temporal gyrus (STG)	34/38	50	-50	-20	2
L. fusiform gyrus	34/38	1349	-41	-35	-26
R. fusiform gyrus	34/38	1311	39	-36	-26
L. hippocampus	34/38	35	-23	-35	-6
L. thalamus	34/38	24	-14	-29	-3
L. middle cingulate cortex (MCC)	33/38	29	-8	-12	37
R. postcentral gyrus	33/38	12	65	-11	27
<b>Negative correlations</b>					
R. Caudate Nucleus	34/38	12	17	20	14



Supplementary figure:



Supplementary Figure S1: Coronal slices of AP network activations. **A.** AH slices,  $Y = 24$ ,  $Y = 19$ ,  $Y = -12$ ,  $Y = -21$ ,  $Y = -30$  **B.** HAS coronal slices :  $Y = 16$ ,  $Y = -2$ ,  $Y = -22$ ,  $Y = -42$ ,  $Y = -63$ , **C.** OBE coronal slices,  $Y = 24$ ,  $Y = 4$ ,  $Y = -46$ ,  $Y = -52$  and  $Y = -58$  and **D.** PH coronal slices,  $Y = 18$ ,  $Y = -8$ ,  $Y = -21$ ,  $Y = -37$  and  $Y = -46$ . In yellow, the clusters that are specific for each AP and in red the network for each AP.

## Chapter 3: Sensorimotor hallucinations in Parkinson's disease

**Authors:** Fosco Bernasconi<sup>\*1</sup>, **Eva Blondiaux**<sup>\*1</sup>, Jevita Potheegadoo<sup>1</sup>, Giedre Stripeikyte<sup>1</sup>, Javier Pagonabarraga<sup>2,3,4,5</sup>, Helena Bejr-Kasem<sup>2,3,4,5</sup>, Michela Bassolino<sup>1</sup>, Michel Akselrod<sup>1,6</sup>, Saul Martinez-Horta<sup>2,3,4,5</sup>, Fred Sampedro<sup>2,3,4,5</sup>, Masayuki Hara<sup>9</sup>, Judit Horvath<sup>7</sup>, Matteo Franza<sup>1</sup>, Stéphanie Konik<sup>1,6</sup>, Matthieu Bereau<sup>7,8</sup>, Joseph-André Ghika<sup>10</sup>, Pierre R. Burkhard<sup>7</sup>, Dimitri Van De Ville<sup>12,13</sup>, Nathan Faivre<sup>1,11</sup>, Giulio Rognini<sup>1</sup>, Paul Krack<sup>14</sup>, Jaime Kulisevsky<sup>2,3,4,5\*\*</sup>, and Olaf Blanke<sup>1,7\*\*</sup>

(\*, \*\*) These authors contributed equally to the paper

**Status:** Submitted and Accessible on BioRxiv

<https://doi.org/10.1101/2020.05.11.054619>

### *Affiliations*

**1.** Laboratory of Cognitive Neuroscience, Center for Neuroprosthetics & Brain Mind Institute, Ecole Polytechnique Fédérale de Lausanne (EPFL), Geneva, Switzerland. **2.** Movement Disorders Unit, Neurology Department Sant Pau Hospital, Barcelona, Spain. **3.** Universitat Autònoma de Barcelona (UAB), Spain. **4.** Centro de Investigación en Red-Enfermedades Neurodegenerativas (CIBERNED), Spain. **5.** Biomedical Research Institute (IIB-Sant Pau), Barcelona, Spain. **6.** University Hospital of Lausanne, CHUV, Lausanne, Switzerland. **7.** Department of Neurology, Geneva University Hospitals, Geneva, Switzerland. **8.** Department of Neurology, Besançon University Hospital, Besançon, France. **9.** Graduate School of Science and Engineering, Saitama University, Japan. **10.** Department of Neurology, Hôpital du Valais, Sion, Switzerland. **11.** Laboratoire de Psychologie et Neurocognition, LPNC, CNRS 5105 Université Grenoble Alpes, France. **12.** Medical Image Processing Laboratory, Institute of Bioengineering, Ecole Polytechnique Fédérale de Lausanne (EPFL), Lausanne, Switzerland. **13.** Department of Radiology and Medical Informatics, University of Geneva, Geneva, Switzerland. **14.** Department of Neurology, Inselspital, University Hospital and University of Bern, Bern, Switzerland.

**Personal contributions:** Experimental design, data collection, data analysis of study 2 and writing.

### **Acknowledgments**

We thank Dr. Didier Genoud and Dr. Vanessa Fleury for their contribution in recruiting patients.

#### Abstract

Hallucinations in Parkinson's disease (PD) are one of the most disturbing non-motor symptoms, affect half of the patients, and constitute a major risk factor for adverse clinical outcomes such as psychosis and dementia. Here we report a robotics-based approach, enabling the induction of a specific clinically-relevant hallucination (presence hallucination, PH) under controlled experimental conditions and the characterization of a PD subgroup with enhanced sensorimotor sensitivity for such robot-induced PH. Using MR-compatible robotics in healthy participants and lesion network mapping analysis in neurological non-PD patients, we identify a fronto-temporal network that was associated with PH. This common PH-network was selectively disrupted in a new and independent sample of PD patients and predicted the presence of symptomatic PH. These robotics-neuroimaging findings determine the behavioral and neural mechanisms of PH and reveal pathological cortical sensorimotor processes of PH in PD, identifying a more severe form of PD associated with psychosis and cognitive decline.

**Keywords:** Parkinson's disease, Hallucinations, Sensorimotor, fMRI, Cognitive decline

## Introduction

The vivid sensation that somebody is nearby when no one is actually present and can neither be seen nor heard (i.e. sense of presence or presence hallucination, PH), has been reported from time immemorial and found its way into the language and folklore of virtually all cultures<sup>1-3</sup>. Following anecdotal reports of PH by extreme mountaineers<sup>4</sup>, solo-sailors and shipwreck survivors<sup>5</sup>, PH have also been described in a variety of medical conditions including schizophrenia<sup>1,6</sup>, epilepsy, stroke, brain tumors<sup>7-9</sup> and Parkinson's disease (PD)<sup>10-12</sup>.

Whereas PH are rare manifestations in most medical conditions, they are frequent and may occur regularly, even on a daily basis, in patients with PD. Hallucinations, including PH, are not only frequent, occurring in up to 60% of PD patients, but increase in frequency and severity with disease progression and are one of the most disturbing non-motor symptoms<sup>11-13</sup>. Importantly, PH and other hallucinations in PD are associated with major negative clinical outcomes such as chronic psychosis, cognitive decline and dementia, as well as higher mortality<sup>10,11,14-16</sup>. PH are generally grouped with so-called minor hallucinations and are the most prevalent and earliest type of hallucination in PD<sup>11,12</sup>, often preceding the onset of structured visual hallucinations<sup>17</sup>, and may even be experienced, by one-third of patients, before the onset of first motor symptoms<sup>18</sup>. Despite their high prevalence and strong association with major negative clinical outcome, PH (and other hallucinations) remain underdiagnosed<sup>12,14,19,20</sup>, caused by patients' reluctance to report hallucinations and difficulties to diagnose and classify them<sup>21,22</sup>.

Past research described changes in visual function, cognitive deficits and related brain mechanisms in PD patients with hallucinations, yet these studies focused on patients with structured visual hallucinations<sup>23</sup>. Comparable studies are rare or lacking for PH (or other minor hallucinations) and very little is known about the early brain dysfunction of PH in PD and how they lead to more severe and disabling structured visual hallucinations and cognitive deficits<sup>11,24</sup>. Early neurological work investigated PH following focal brain damage and classified PH among disorders of the body schema, suggesting that they are caused by abnormal self-related bodily processes<sup>9,25</sup>.

More recent data corroborated these early findings and induced PH repeatedly by electrical stimulation of a cortical region involved in sensorimotor processing<sup>8</sup>. By integrating these clinical observations with human neuroscience methods inducing bodily illusions<sup>27–30</sup>, we have designed a method able to robotically induce PH (robot-induced PH or riPH) in healthy participants<sup>26</sup>. This research demonstrated that specific sensorimotor conflicts, including bodily signals from the arm and trunk, are sufficient to induce mild to moderate PH in healthy participants, linking PH to the misperception of the source and identity of sensorimotor signals of one's own body.

Here, we adapted our robotic procedure to PD patients and elicited riPH, allowing us to characterize a subgroup of patients that is highly sensitive to the sensorimotor procedure, and to identify their aberrant sensorimotor processes (study 1). We next determined the common PH-network in frontal and temporal cortex, by combining MR-compatible robotics in healthy participants with brain network analysis in neurological non-PD patients with PH (study 2). Finally, we recorded resting-state fMRI data in a new and independent sample of PD patients and identified pathological functional connectivity patterns within the common PH-network, which were predictive for the occurrence of PD-related PH (study 3).

## Results

### *riPH in patients with PD (study1.1)*

Based on semi-structured interviews, patients with PD were grouped into those who reported symptomatic PH, sPH (PD-PH; n=13), and those without sPH (PD-nPH; n=13) (Supplementary S1-2, Tab.S1-2). Patients were asked to actuate a robotic device and were exposed to repetitive sensorimotor stimulation that has been shown to induce PH in healthy participants in a controlled way<sup>26</sup>. In study1.1, we assessed whether robotic sensorimotor stimulation induces PH in patients with PD and whether such riPH differ between PD-PH and PD-nPH, hypothesizing that PD-PH patients are more sensitive to the robotic procedure.

In the robotic sensorimotor paradigm, participants were asked to perform repetitive movements to operate a robot placed in front of them, which was combined with a back robot providing tactile feedback to participants' backs (Fig.1A). Based on previous data<sup>26,28,31</sup>, tactile feedback was delivered either synchronously with patients' movements (synchronous control condition, a spatial conflict is present between movement in front and touch on the back) or with a 500ms delay (asynchronous condition) associated with an additional spatio-temporal sensorimotor conflict shown previously to induce PH<sup>26,36</sup> (Supplementary S3).

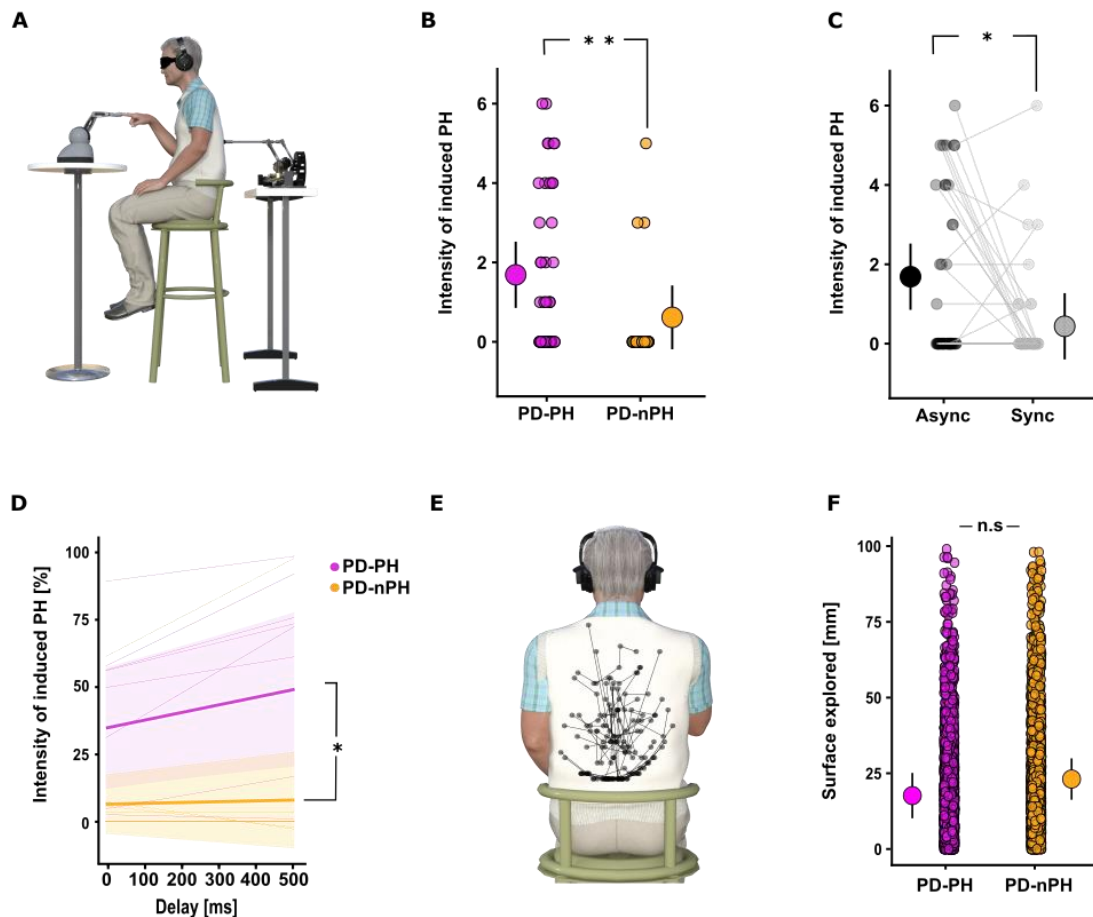


**Figure 1. Robot-induced PH (PD patients).** **A.** Setup for study 1. Responses in synchronous and asynchronous conditions are shown. During the asynchronous condition, the sensorimotor feedback on the participants' back was delayed by 500 ms (study1.1) or with a random delay (0-500ms, steps of 100ms) (study1.2). **B.** Study1.1. riPH in PD-PH are stronger than in PD-nPH. Each dot indicates the individual rating of the intensity of the riPH (PD-PH (purple) and PD-nPH (yellow)). The dot with the bar on the left and right side indicate the mixed effects linear regression between PD-PH and PD-nPH. Error bar represent 95% confidence interval. **C.** Study1.1. Asynchronous condition induced stronger riPH. Each dot indicates the individual rating of the intensity of the riPH. The dot with the bar on the left and right side indicate the mixed effects linear regression between Asynchronous (black) and Synchronous (gray) sensorimotor stimulation. Error bars represent 95% confidence interval. **D.** Study1.2. riPH were modulated by delay (permutation p-value=0.014) and PD-PH vs. PD-nPH were more sensitive to the sensorimotor stimulation (slope permutation p-value=0.039, intercept p-value=0.016). The thicker line indicates the mean of the fitted models, the shaded are indicates the 95% confidence interval, thinner lines indicate single subject fit. **E.** Study1.2. Exemplary movements executed by one patient during sensorimotor stimulation. **F.** Study1.2. Mixed effects linear regression between the Euclidean distance between pokes for PD-PH (purple) and PD-nPH (yellow). Error bar represent 95% confidence interval.

The robotic procedure was able to induce PH in patients with PD. Importantly, PD-PH patients rated the intensity of riPH higher than PD-nPH patients (main effect of Group: permutation p-value=0.01) (Fig.1B). Confirming the general importance of conflicting asynchronous sensorimotor stimulation<sup>26</sup> for riPH, both sub-groups gave higher PH ratings in the asynchronous versus synchronous condition (main effect of Synchrony: permutation p-value=0.045) (Fig.1C) (Supplementary S4 for additional results). Other robot-induced bodily experiences (e.g. illusory self-touch) also confirmed previous findings<sup>26</sup> (Supplementary S5) and no differences were observed for the control items (all permutation p-values>0.05). These results show that PH can be safely induced by the present robotic procedure under controlled conditions in patients with PD. Such riPH were modulated by sensorimotor stimulation with asynchronous robotic stimulation resulting in higher ratings in all tested groups, and, importantly, PD-PH (vs. PD-nPH) reported stronger riPH, linking the patients' usual sPH to experimental riPH and showing that PD-PH patients were more sensitive to our robotic procedure.

Post-experiment debriefing revealed 38% of PD-PH patients who reported riPH that were comparable (or even stronger) in intensity to the patients' usual sPH in daily life. One PD-PH patient, for example, described his riPH as "an adrenaline rush. Like something or someone was behind me, although there is no possibility to have someone behind" (Video S1, for additional reports Supplementary S6). Interestingly, all such instances were reported after asynchronous stimulation. Moreover, PD-PH patients often experienced riPH on their side (and not on their back, where tactile feedback was applied), revealing a further phenomenological similarity between riPH and PD patients' usual sPH<sup>10</sup> and suggesting that we induced a mental state that mimics sPH (Supplementary S7-8).

Data from study1.1 reveal that riPH can be safely induced by the present procedure, are stronger in patients who report sPH (PD-PH), and that such riPH share phenomenological similarities with PD-related sPH. These findings cannot be related to a general response bias related to PD, because riPH were absent or weaker in PD-nPH and because the control items showed no effects in any of the participant groups.



*riPH in PD-PH patients depend on sensorimotor delay (study1.2)*

Previous work investigated the effects of systematically varied sensorimotor conflicts (i.e. delays) on somatosensory perception, enabling the induction and modulation of different somatic experiences and illusions<sup>31-33</sup>. Sensorimotor processing and the forward model of motor control<sup>34,35</sup> are prominent models of hallucinations<sup>36,37</sup> and it has been proposed that deficits in predicting sensory consequences of actions causes abnormal perceptions and hallucinations<sup>36-38</sup>. In study1.2, we assessed whether riPH depend on the degree of conflict applied during sensorimotor stimulation, by inserting variable delays between the movements of the front robot (capturing movements of the forward-extended arm) and the back robot (time of tactile feedback on the back). In each trial, participants (Supplementary S9) were exposed to a randomly chosen delay (0-500ms, steps of 100ms). After each trial, participants were prompted whether they experienced a riPH or not (yes-no response, Supplementary S10). We investigated whether the intensity of riPH increases with increasing delays in PD patients (showing that PH are modulated by increasing spatio-temporal conflicts) and whether PD-PH have a higher spatio-temporal delay sensitivity than PD-nPH.

As predicted, study1.2 shows that the intensity of riPH increased with increasing spatio-temporal conflict (main effect of delay: permutation p-value=0.014) and that this delay dependency differed between the two patient groups, showing a higher delay sensitivity in PD-PH patients (interaction Group\*delay: permutation p-value=0.039) (Fig.1D) (Supplementary S11, Fig.S1). Control analysis (Supplementary S12) (Fig.1E-F, Fig.S2) allowed us to exclude that the observed differences (in riPH ratings between patient groups) are due to differences in movements of the arm and related tactile feedback during the robot actuation (Supplementary S13). In addition, these differences in riPH between PD-PH and PD-nPH cannot be explained by differences in demographic or clinical variables (including anti-parkinsonian medication, motor impairment; all permutation p-values>0.05) (Supplementary S14, Tab.S1).

Based on previous results using robotics and conflicting sensorimotor stimulation to alter somatosensory perception<sup>31-33</sup>, these data extend those of study1.1 and reveal abnormal perceptual processes in PD-PH patients when exposed to different sensorimotor conflicts, characterized by experiencing stronger riPH and a higher sensorimotor sensitivity. These findings are compatible with an alteration of

sensorimotor brain processes associated with the forward model and its role in hallucinations in PD-PH patients<sup>36,37,39</sup>.

#### ***Brain mechanisms of PH***

Neuroimaging work on sPH and other minor hallucinations in PD patients has described structural alterations and aberrant functional connectivity in different cortical regions<sup>24,40</sup>. Despite these clinical neuroimaging findings, it is not known whether the regions associated with sPH of neurological non-parkinsonian origin<sup>26</sup> are also altered in PD patients with PH. Moreover, because the brain networks of riPH have never been investigated, it is also not known whether the abnormal sensorimotor mechanisms described in PD-PH patients (study1) are associated with a disruption of brain networks of riPH. To determine the brain mechanisms of PH, we first adapted an MR-compatible robot<sup>41</sup> (Supplementary S15) and applied sensorimotor stimulations while recording fMRI during riPH in healthy participants and identified the associated brain networks (study2.1). We then combined this network with evidence from sPH of neurological non-parkinsonian origin (study 2.2) and, finally, applied this common network to PD patients (study 3).

#### ***Brain mechanisms of riPH in healthy participants using MR-compatible robotics***

##### ***(study2.1)***

Based on behavioral pilot data (Supplementary S16-S17, Tab.S5), we exposed 25 healthy participants to asynchronous and synchronous robotic stimulation while recording fMRI (Fig.2A, Video S2, Supplemental S15, Fig.S3). Our behavioral data replicated previous results (<sup>26</sup>, study1 and pilot study) and we found that asynchronous vs. synchronous robotic stimulation induces stronger PH (main effect of Synchrony: permutation p-value=0.0082, Fig.2B) and another bodily experience (Tab.S6), but did not modulate control items (all permutation p-values>0.08, Supplementary S18, Tab.S6). As for study1.2, riPH were not related to movement differences across conditions (permutation p-value=0.99) (Fig.2C), confirming that sensorimotor stimulation (and not movement differences) applied with the MR-compatible robot modulated PH intensity across conditions.

To identify the neural mechanisms of riPH, we determined brain regions that were (1) more activated during the asynchronous vs. synchronous condition (spatio-temporal sensorimotor conflict) and (2) activated by either of the sensorimotor conditions (synchronous, asynchronous) vs. two control conditions (motor and touch) (Supplementary S19, conjunction analysis). Regions more activated during asynchronous vs. synchronous sensorimotor stimulation were restricted to cortical regions (Fig.2D, Tab.S7) and included the inferior frontal gyrus (IFG), anterior insula, medial prefrontal cortex (mPFC) and the posterior part of the middle temporal gyrus (pMTG, bordering on angular gyrus and adjacent occipital cortex). Conjunction analysis (between contrast synchronous>motor+touch and contrast asynchronous>motor+touch) (Supplementary S20, Fig.S4) revealed a subcortical-cortical network in left sensorimotor cortex (contralateral to the hand moving the robot, including M1, S1 and adjacent parts of premotor cortex and superior parietal lobule), in bilateral supplementary motor area (SMA), right inferior parietal cortex, left putamen, and right cerebellum (Fig.2E, Tab.S8).

Collectively, these fMRI results constitute the first delineation of the neural underpinnings of riPH in healthy participants that is unrelated to movement differences across conditions and distinct from activations in two control conditions, revealing a network of brain regions that have been shown to be involved in sensorimotor processing and in agency (such as M1-S1, pMTG<sup>42,43</sup>, PMC<sup>44,45</sup>, SMA<sup>43,46</sup>, IPS<sup>47,48</sup>, as well as the cerebellum<sup>42,49</sup> and putamen).

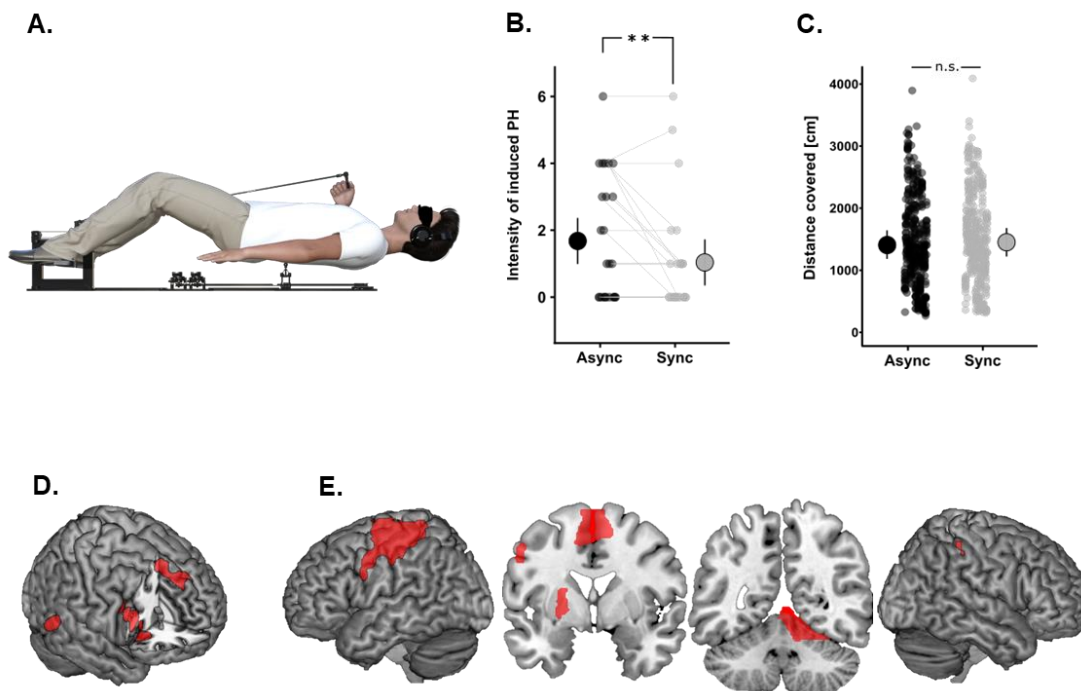


**Figure 2. Neuroimaging results of robot-induced PH (healthy participants).** **A.** MR-compatible robotic system is shown. Participants were instructed to move the front robot with their right hand and the back robot delivered the touch to the participant's back either synchronously or asynchronous (500ms delay between their movement and the sensory feedback received on the back). **B.** Asynchronous vs. synchronous condition induced stronger riPH. Each dot indicates the individual rating of the intensity of the riPH in healthy participants. The dot with the bar on the left and right side indicate the mixed effects linear regression between asynchronous (black) and synchronous (gray) sensorimotor stimulation. Error bar represents 95% confidence interval. **C.** Movement data from the fMRI experiment: no movement differences were found between the two conditions. **D.** Brain regions sensitive to the delay. **E.** Brain areas present in the conjunction analysis between the contrast synchronous>motor+touch and the contrast asynchronous>motor+touch. The coronal slices are at Y = -1 and Y = -53. There was no anatomical overlap between both networks (**D** and **E**).

***Common PH-network for sPH and riPH (study2.2)***

To determine neural similarities between riPH and sPH and confirm the sensorimotor contribution to sPH, we first applied lesion network mapping (Supplementary S21) and identified network connectivity mapping in neurological non-parkinsonian patients, in whom sPH were caused by focal brain damage (study2.2), and then determined the common network (cPH-network) between the riPH and sPH. Lesion network mapping<sup>50</sup> extends classical lesion symptom mapping by considering each lesion as a seed (region of interest, ROI) and computing its connectivity map (in

normative resting state fMRI data, publicly available database, 126 healthy participants<sup>51</sup>) (Fig.S5).

This analysis revealed that all lesions had functional connectivity with bilateral posterior superior temporal gyrus/temporo-parietal junction (pSTG/TPJ), bilateral middle cingulate cortex (MCC), bilateral insula, and right IFG, constituting the sPH-network (Fig.3A, for all regions see Tab.S9) and did not overlap with connectivity patterns of a control hallucination network (Supplementary S22-S23, Tab.S10). We then determined the common regions between the sPH-network (non-parkinsonian neurological patients) and the riPH network (healthy participants). This cPH-network consisted of three regions, including right IFG, right pMTG, and left vPMC (Fig.3B, Supplementary S24) and is the first neuroimaging evidence that riPH and sPH recruit similar brain regions, even if both types of PH differ in several aspects such as frequency, intensity, trigger mechanism, supporting a link between sensorimotor robotics inducing hallucinatory states with neuroimaging in healthy participants and in patients.

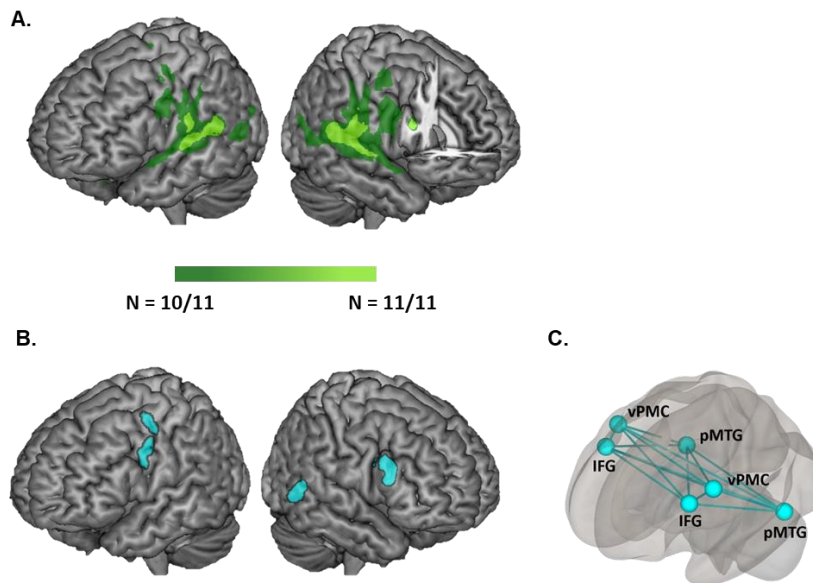


**Figure 3. Symptomatic PH-network and common PH-network.** **A.** sPH network connectivity in neurological non-parkinsonian patients. **B.** Common regions between the riPH-network and sPH-network (cPH-network) were found in three regions: left vPMC, right IFG and right pMTG. **C.** Schematic display of the cPH-network projected bilaterally.

*Disrupted functional connectivity in cPH-network accounts for sPH Parkinson's disease (study3.1)*

To assess the relevance of the cPH-network for PD patients' usual sPH in daily life, we analyzed resting state fMRI data in a new group of PD patients and investigated whether functional connectivity of the cPH-network (as defined in study2, projected bilaterally, Fig.3C) differed between PD-PH and PD-nPH (new cohort of 30 PD patients) (Supplementary S25-26, Tab.S11). Based on the disconnection hypothesis of hallucinations<sup>52</sup>, evidence of decreased connectivity for hallucinations of psychiatric origin<sup>37</sup>, and aberrant functional connectivity in PD patients with minor hallucinations including PH<sup>24</sup>, we predicted that the functional connectivity within the cPH-network differs between both PD patient groups and that the connectivity within the cPH-network is reduced in PD-PH vs. PD-nPH patients. We found that the functional connectivity within the cPH-network, predicted with 93.7% accuracy whether a patient was clinically classified as PD-PH (kappa:0.86, permutation p-value=0.0042). Moreover, within the cPH-network, the functional connectivity between the left IFG and left pMTG contributed mostly to the classification of the two sub-groups (Tab.S12). PD-PH had reduced IFG-pMTG connectivity (permutation p-value<0.0001; Fig.4A-B). These changes were selective because (1) the same analysis in a control network (Fig.S7) (same size, same number of connections) did not predict the occurrence of hallucinations based on the functional connectivity (accuracy:27.7%, kappa:-0.43, permutation p-value=0.24) and (2) no changes in functional connectivity were observed when analyzing whole brain connectivity. These data show that reduced fronto-temporal connectivity within the cPH-network distinguishes PD patients with sPH from those without hallucinations, in accordance with the disconnection hypothesis of hallucinations<sup>52-54</sup>.

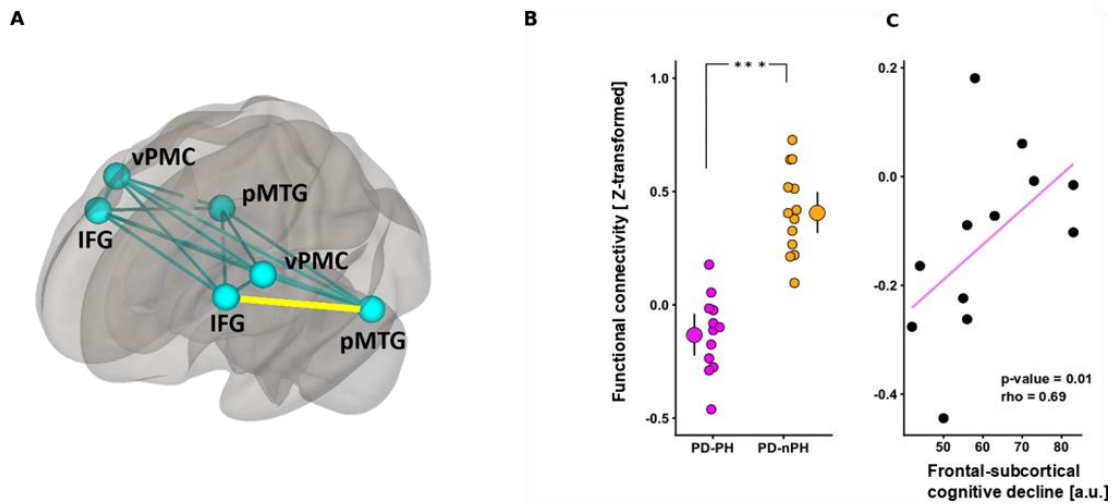


**Figure 4. Functional connectivity in the sensorimotor network.** **A.** Connections showing differences in functional connectivity between PD-PH vs. PD-nPH within the cPH-network are shown (yellow). **B.** Mixed effects linear regression between the functional connectivity for PD-PH (purple) and PD-nPH (yellow) between left IFG and left pMTG is shown. PD-PH vs. PD-nPH patients have a significantly reduced functional connectivity. Error bar represents 95% confidence interval, and the dot represents the mean functional connectivity. Dots represent the functional connectivity for each patient. **C.** Degree of functional disconnection is correlated with the cognitive decline (fronto-cortical sub-score of PD-CRS) in PD-PH patients. Lower connectivity was correlated with lower frontal cognitive fronto-subcortical abilities.

***Functional disconnection within the cPH-network correlates with cognitive decline for PD-PH (study3.2).***

It has been suggested that PH (and minor hallucinations) are indicative of a more severe and rapidly advancing form of PD, evolving towards structured visual hallucinations and psychosis<sup>11,17</sup>, as well as faster cognitive deterioration including dementia<sup>16,55-57</sup>. We therefore tested whether functional connectivity between the left IFG and the left pMTG within the cPH-network relates to cognitive dysfunction in the present PD-PH patients. Results show that stronger decreases in left IFG-pMTG connectivity are associated with stronger cognitive decline (PD-CRS<sup>58</sup>), reflecting differences in frontal-subcortical function (p-value=0.01, rho=0.69, Fig.4C), but not on posterior-cortical function (p-value=0.66, rho=-0.15, the two correlations differed significantly:  $t=3.87$ , p-value<0.01). These results reveal an association between fronto-subcortical cognitive alterations and specific decreases in fronto-temporal

connectivity within the cPH-network in PD-PH patients, compatible with a more severe form of PD associating PH and cognitive decline.



## Discussion

Having developed a robotic procedure that can induce PH in PD patients under safe and controlled sensorimotor conditions, we report that PD patients with sPH are highly sensitive to the procedure and reveal abnormal sensorimotor mechanisms leading to PH. Using MR-compatible robotics in healthy participants combined with lesion network mapping analysis in patients with sPH of neurological non-parkinsonian origin, we identify the common network associated with PH and show that fronto-temporal connectivity within this cPH-network is selectively disrupted in a new and independent sample of PD patients. Disruption of the cPH-network was only found in PD patients suffering from sPH (PD-PH) and the degree of this disruption further predicted the severity of cognitive decline.

The present behavioural findings show that stronger sensorimotor conflicts result in stronger riPH, supporting and extending previous evidence in favor of an alteration of self-related sensorimotor processing as a fundamental mechanism underlying PH<sup>33</sup>. Importantly, we show that this mechanism is especially vulnerable in PD-PH patients, revealed by their stronger bias and sensitivity when exposed to conflicting sensorimotor stimulation. These results extend the sensorimotor forward model to hallucinations in PD-PH patients<sup>36,37,39</sup> and support earlier evidence in neurological non-PD patients that PH are self-related body schema disorders associated with altered sensorimotor self-monitoring<sup>7-9</sup>.

By including fMRI data from healthy participants experiencing riPH and from non-parkinsonian neurological patients with sPH, we mapped common brain structures between both types of PH, which we showed to be selectively disrupted in PD patients with sPH. The imaging results within this cPH-network further revealed aberrant functional connectivity decreases between fronto-temporal regions that have been associated with outcome processing of sensorimotor signals and the forward model<sup>54,59</sup>, further linking PH in PD to the fronto-temporal hallucination disconnection model<sup>52,54,60</sup>. The present account - involving sensorimotor mechanisms and brain structures in fronto-temporal cortex rather than posterior brain functions and regions - is functionally and conceptually distinct from earlier proposals that hallucination in PD are caused by visuo-spatial deficits<sup>23</sup> or that sPH are caused by abnormal social-cognitive brain mechanisms<sup>10</sup> in parietal or occipital cortex<sup>23,61,62</sup>. Our finding that the

decreased fronto-temporal connectivity within the cPH-network is associated with stronger cognitive decline of PD-PH patients in fronto-subcortical (but not posterior-cortical, functions) lends support to clinical suggestions about the importance of PH (and other minor hallucinations) as a major risk factor not only for the occurrence of structured visual hallucinations and psychosis<sup>17</sup>, but also for a more severe and rapidly advancing form of PD<sup>11,16,55,57</sup>.

Because the phenomenology of riPH resembles those of sPH and PD-PH patients were found to be more sensitive to riPH, the present procedure provides researchers and clinicians with new objective possibilities to assess the occurrence and intensity of subjective hallucinatory phenomena by quantifying delay-sensitivity and the repeated online induction of hallucinatory states across controlled conditions in PD patients, as well as the association of these measures with cPH-network activity. This is not possible in current clinical practice that is based on clinically important, but post-hoc interviews between physician and patient, often about hallucinations that have occurred many days or weeks ago, and that many patients hesitate to speak about<sup>21</sup>. The detection of specific behavioural and imaging changes associated with specific hallucinatory states that are observed online during the robotic procedure will improve the quantification and prediction of a patient's proneness for hallucinations and psychosis and may facilitate targeted pharmacological interventions that limit side effects<sup>63</sup>.

### Methods

#### *Study 1*

##### **Participants (study1.1-1.2)**

All participants provided written informed consent prior to the experiments. The study was approved by the Cantonal Ethics Committee of Geneva (Commission Cantonale d'Ethique de la Recherche sur l'Être Humain), the Cantonal Ethics Committee of Vaud. Participants of study1 consisted of patients with PD (n=26) and age-matched healthy controls (HC, n=21) (Supplementary S1-S4). Based on an extensive semi-structured interview (conducted after the experimental sessions) about hallucinations (including sPH), PD patients were separated into two sub-groups: patients who reported sPH as part of their PD (PD-PH) (n=13) and PD patients without sPH (PD-nPH) (n=13). Patients were considered as having sPH if they answered affirmatively to the question that previous investigators have used: “do you sometimes feel the presence of somebody close by when no-one is there?” The hallucinated presence could be located behind, on the side (left or right) of the patient, or in another room and was generally not seen (see <sup>2,7,8,10,26</sup>). All PD patients, who were included in study1 presented idiopathic PD diagnosed by trained neurologists. No patient was suffering from a neurological disorder other than PD (more details in Supplementary S2).

##### **General experimental procedure (study1)**

Each PD patient underwent study1 at a similar time (10am), after having received their usual anti-parkinsonian medication and were in their “best ON” state. To investigate riPH, we adapted the experimental method and device as our previous research<sup>26</sup>. Briefly, sensorimotor stimulation was administered with a robotic system consisting of two robotic components (front-robot, back-robot) that has previously been used to induce PH. For each experimental session, we applied the following conditions: synchronous sensorimotor stimulation (the participants were asked to move the front-robot via either their right or left hand that was actuating the movements of the back-robot to apply tactile feedback to their back); asynchronous sensorimotor stimulation (same as synchronous stimulation, but with an additional temporal delay between the front-robot and the back-robot; see below for details of each experiment; Fig.1A). During sensorimotor stimulation, participants were always asked to keep their eyes

closed and were exposed to continuous white noise through headphones (Supplementary S3).

#### **Procedure, design, and analysis (study1.1)**

Participants were asked to insert their index finger in the haptic front-robot and carry out repeated poking movements while they received tactile cues on their backs, delivered by the back-robot. Thus, sensorimotor stimulation included motor, tactile, and proprioceptive signals from the upper limb moving the front-robot and additional tactile signals from the back-robot. Stroking was applied either synchronously (0ms delay) or asynchronously (500ms delay) (*Synchrony*: asynchronous vs. synchronous). Additionally, we measured the effect of the side of the body (i.e. hand moving the front-robot) that was most strongly affected by PD versus the other hand (*Side*) to investigate if the hemisphere predominantly affected by PD influenced riPH<sup>64,65</sup>. The factors (*Synchrony*; *Side*) and the order of testing were randomized across participants. Each participant randomly started with one *Side* first, for which the two *Synchrony* conditions (random order) were tested, and then the second *Side* was tested with the two *Synchrony* conditions (random order). In total, each participant performed four sessions (one per condition) lasting two minutes each. At the end of each of the four sensorimotor stimulation conditions, all participants filled a questionnaire (see below). Each PD-PH, PD-nPH, and HC included in the study was able to perform the entire study1.1.

#### **PH and other subjective ratings**

To measure PH and other illusions, we administered a questionnaire (6 questions) that was adapted from<sup>26</sup>. Participants were asked to indicate on a 7-point Likert scale, how strongly they felt the sensation described by each item (from 0 = not at all, to 6 = very strong). For questions see Supplementary S5.

#### **Data analysis**

Each question was analyzed with linear mixed effects models (lme4 and lmerTest both R packages<sup>66,67</sup>). Models were performed on the subjective ratings in each of the four conditions with *Synchrony* (synchronous vs. asynchronous), *Groups* (i.e., PD-PH vs. PD-nPH, and PD-PH vs. HC) and *Side* as fixed effects, and random intercepts for each

subject. The significance of fixed effects was estimated with a permutation test (5000 iterations; predictmeans<sup>68</sup> R package).

#### **Procedure, design, and analysis (study1.2)**

To complement and extend study1.1, we applied a Yes/No task, following sensorimotor stimulation, in which participants were asked to report whether they experienced a PH or not, on a trial-by-trial basis. On each sensorimotor stimulation trial, the delay between the movement and the stroking on the back was randomly chosen from a delay between 0 and 500ms (steps of 100m). One trial started with an acoustic signal (400 Hz tone, 100ms duration) indicating the beginning of the trial: at this point the participant started with the poking movements. Once the number of pokes reached a total of six (automatically counted), two consecutive tones (400 Hz, 100ms duration) indicated to the participant to stop the movements and to verbally answer with either a “Yes” or a “No” to the PH question, (Question: “Did you feel as if someone was standing close by (behind you or on one side)?”). The investigators were always placed > 4 meters away and in front from the participants during the experiment. Each participant was asked to perform three sessions; each session consisted of 18 trials (3 repetitions per delay (9 repetitions in total)). Between each session, the participant could take a break according to his/her needs (Supplementary S10).

#### **riPH rating analysis**

First, to investigate how the degree of sensorimotor conflict modulates PH, we analyzed the behavioral responses as a function of different delays (i.e., 0-500ms, steps of 100ms) across groups (i.e., PD-PH vs. PD-nPH). Here, the data was analyzed with a linear model, fitted for each participant independently. We assessed (1) the main effect of the delay (on the intensity of riPH) with a permutation test (5000 iterations) between slopes of the individual fit vs. zero; (2) the difference between the slopes of PD-PH vs. PD-nPH with a permutation test between the slopes of the two subgroups; (3) the main effect of group with a permutation test on the intercepts between the two subgroups.

## *Study 2*

### **Participants, ethics, and informed consent (study2.1)**

All healthy participants had no history of neurological or psychiatric disorders. All participants provided written informed consent prior to the experiment. The study was approved by the Cantonal Ethics Committee of Geneva (Commission Cantonale d'Ethique de la Recherche sur l'Être Humain - CCER). Twenty-five healthy participants (10 women, mean age $\pm$ SD: 24.6 $\pm$ 3.7 years old; age range: 18-32 years old, Edinburg Handedness Inventory mean index: 64.8 $\pm$ 23.7 and range: 30-100) took part in study2.1.

### **Experimental procedure (study2.1)**

The experimental procedure was based on a pilot study performed in a mock scanner (Supplementary S16). Participants were blindfolded during the task and received auditory cues through earphones to start (1 beep) and to stop (2 beeps) the movement. The paradigm was implemented using an in-house software (ExpyVR, <http://Inco.epfl.ch/expyvr>) and Visual studio 2013 interface (Microsoft) was used to control the robotic system.

Participants underwent two runs of 12 min each, during which they repeatedly had to move the front robot for 30s with their right hand followed by 20s of rest for a total of 16 repetitions per condition (8 repetitions for the motor and touch control tasks) (Supplementary S15-S19 and Fig.S3). Synchronous and the asynchronous conditions were randomized across runs. The questionnaire was presented at the end of the scanning session and after a randomized repetition of 30s of each condition. The questionnaire was based on the pilot study (Supplementary S16-S18) and on a previous study<sup>26</sup>. Participants were asked to indicate on a 7-point Likert scale, how strongly they felt the sensation described by each item (from 0 = not at all, to 6 = very strong).

### **Questionnaire analysis**

Questionnaire data were analyzed in the same way as in study1.1. Synchrony (synchronous and asynchronous) was used as a fixed effect and the subjects as random intercepts.

### **fMRI experiment**

#### fMRI data acquisition

The imaging data was acquired with a 3T Siemens Magnetom Prisma MR scanner at Campus Biotech MR Platform (Geneva). The functional data were acquired using an Echo Planar Imaging (EPI) sequence with a full brain coverage (43 continuous slices, FOV=230mm, TR=2.5s, TE=30ms, flip angle=90°, in-plane resolution=2.5x2.5mm<sup>2</sup>, slice thickness=2.5mm using a 64-channel head-coil) containing 320 volumes for the experimental runs and 160 volumes for the localizer runs. For each participant, an anatomical image was recorded using a T1-weighted MPRAGE sequence (TR=2.3s, TE=2.32 ms, Inversion time=900ms, flip angle=8°, 0.9mm isotropic voxels, 192 slices per slab and FOV=240mm).

#### fMRI data analysis

All the fMRI data analysis reported were pre-processed using SPM12 toolbox (Wellcome Department of Cognitive Neurology, Institute of Neurology, UCL, London, UK) in Matlab (R2016b, Mathworks). Slice timing correction and spatial realignment was applied to individual functional images. The anatomical image was then co-registered with the mean functional image and segmented into grey matter, white matter and cerebro-spinal fluid (CSF) tissue. Finally, the anatomical and the functional images were normalized to the Montreal Neurological Institute (MNI) brain template. Functional images were then smoothed with a Gaussian kernel with full-width half-maximum of 6mm. Head motion was assessed based on framewise displacement (FD) calculation<sup>69</sup>. All participants had a mean FD value inferior to 0.50mm (mean FD=0.12±0.05 mm). The two experimental runs were filtered with a high-pass filter at 1/300 Hz to remove low frequency confounds, while the two localizers were filtered with a high-pass filter at 1/100 Hz.

#### Activation contrasts

The experimental runs and functional localizers were submitted to a general linear model (GLM) analysis. In all runs, the periods corresponding to a given robotic stimulation (i.e., synchronous, asynchronous, motor task, touch task (Supplementary S19 and Fig.S3)) and the periods corresponding to the auditory cues were modelled as separated regressors. The six realignment parameters were modelled for each run as

regressors of no interest. In order to avoid confounding effects due to the amount of movement performed in each trial, the quantity of movement of the front robot (synchronous and asynchronous for the experimental runs and movement condition for the motor localizer, see above) was included as parametric modulators of each condition (see above).

Second-level analyses were performed using the first-level contrasts defined for each subject. In order to determine which brain regions were involved in sensorimotor conflicts (spatio-temporal conflict and fixed spatial conflict), the following contrasts were computed: asynchronous>motor+touch and synchronous>motor+touch. A conjunction between those two contrasts was performed to identify the regions involved in the fixed spatial sensorimotor conflicts. For the experimental runs, two sample t-tests (asynchronous>synchronous and synchronous>asynchronous) were performed to assess brain activations activated during a specific sensorimotor conflict. Results were thresholded at  $p < 0.001$  at voxel level and only the clusters surviving  $p < 0.05$  FWE-corrected for multiple comparison were reported as significant. The obtained clusters were labelled using the AAL atlas<sup>70</sup> and the Anatomy toolbox<sup>71</sup>.

#### **Lesion network mapping analysis (study2.2)**

In order to identify the brain regions functionally connected to each lesion location causing PH in neurological patients, we used lesion network mapping analysis<sup>50,72</sup>. Briefly, this method uses normative resting state data from 151 healthy subjects obtained from the publicly available Enhanced Nathan Kline Institute Rockland Sample<sup>51</sup> and uses the lesion locations as seed ROI. The fMRI acquisition parameters are described in the Supplementary S21.

#### Resting state fMRI analysis

For the pre-processing steps see above and Supplementary S21. The anatomical T1-weighted image was segmented into grey and white matter and CSF. Spatial realignment was applied to individual functional images. The six realignment parameters and their first-degree derivatives were added in addition to the averaged signals of the white matter and cerebro-spinal fluid. Subjects with the excessive motion were excluded from the analysis, this comprised 25 subjects which had a mean FD higher than 0.5mm and where more than 15% of scans were affected by movement. In



total, 126 subjects were included for the analysis. Then, fMRI data was bandpass-filtered in the range of 0.008-0.09Hz.

The resting state data was analyzed using the CONN-fMRI Functional Connectivity toolbox<sup>73</sup> (v.18.a, <http://www.nitrc.org/projects/conn>). The lesion masks were used as seed ROIs and their mean time course was extracted and correlated to all other brain voxels. Each lesion-seed yielded a brain network thresholded at  $p < 0.001$  ( $t \pm 3.37$ ) with  $p < 0.05$  whole brain FWE peak level corrected. The 11 networks were then binarized and overlapped to determine the regions of shared positive and negative correlations (Fig.S5). The network overlap was thresholded at 90% (at least 10 cases out of 11) with a minimal cluster extent of 50 voxels. This procedure was repeated with the visual hallucinations (VH) lesions (Supplementary S22-S23 for further analyses).

#### *Study 3*

##### **Participants (study3.1)**

Data from thirty PD patients were analyzed in this study. All patients were prospectively recruited from a sample of outpatients regularly attending to the Movement Disorders Clinic at Hospital de la Santa Creu i Sant Pau (Barcelona) based on the fulfilling of MDS new criteria for PD. Informed consent to participate in the study was obtained from all participants. The study was approved by the local Ethics Committee. Patients were diagnosed by a neurologist with expertise in movement disorders. Each patient was interviewed regarding years of formal education, disease onset, medication history, current medications, and dosage (levodopa daily dose). Motor status and stage of illness were assessed by the MDS-UPDRS-III. All participants were on stable doses of dopaminergic drugs during the 4 weeks before inclusion. Patients were included if the hallucinations remained stable during the 3 months before inclusion in the study. No participant had used or was using antipsychotic medication (Supplementary S24). Details of image acquisition and data processing are in Supplementary S25.

### Regions of interest

The cPH-network as defined in Study 2 (right posterior middle temporal gyrus (pMTG;  $x = 54$ ,  $y = -54$ ,  $z = 0$ ), the right inferior frontal gyrus (IFG;  $x = 51$ ,  $y = 18$ ,  $z = 29$ ) and the left ventral premotor cortex (vPMC;  $x = -53$ ,  $y = 1$ ,  $z = 37$ ) was transposed bilaterally to ensure that the cPH-network is not affected by any effects of movement-related laterality of activation observed in the riPH-networks (Fig.3B). Clusters were built using FSL (<https://fsl.fmrib.ox.ac.uk/fsl/>). A control network was derived by shifting each region ( $x \pm 0/20$ ;  $y + 30$ ;  $z - 15$ ) of the cPH-network (Fig.S7). This approach allowed controlling for the exact same shape and number of voxels as original cPH-network areas.

### Statistical analyses

To assess whether the functional connectivity of the cPH-network predicted if a patient was clinically classified PD-PH (or PD-nPH), we conducted a leave one out cross-validation procedure with a linear discriminant analysis (LDA) (using Caret R packages<sup>81</sup>). To ensure that the kappa value was above chance-level we conducted a permutation test (5000 iterations). At each iteration, functional connectivity values were permuted between sub-groups and the cross-validation procedure was repeated. Post-hoc analyses for the between group differences were performed using a permutation tests (5000 iterations) on the connection which mostly contributed to the decoding. Connectivity outliers (8.75% of all data points) were identified based on 1.5 IQR from the connectivity median value for each connection. Spearman 2-tailed correlation analyses were performed between functional connectivity within cPH-network areas and neuropsychological measures of the PD-CRS (Parkinson's disease – Cognitive Rating Scale). Significance between the two correlations was assessed using the Steiger Tests (psych R package<sup>76</sup>).

#### References

1. Jaspers, K. *Über leibhaftige Bewusstheiten (Bewusstheitstäuschungen), ein psychopathologisches Elementarsymptom. Zeitschrift für Pathopsychologie* **2**, 150–161 (1913).
2. Critchley, M. *The idea of a presence. Acta Psychiatrica Scandinavica* **30**, 155–168 (1955).
3. Arzy, S., Seeck, M., Ortigue, S., Spinelli, L. & Blanke, O. Induction of an illusory shadow person. *Nature* **443**, 287 (2006).
4. Messner, R. *The Naked Mountain*. (Seattle: Cambridge University Press, 2003).
5. Geiger, J. *The Third Man Factor: Surviving the Impossible*. (New York: Weinstein Books, 2009).
6. Llorca, P. M. *et al.* Hallucinations in schizophrenia and Parkinson's disease: an analysis of sensory modalities involved and the repercussion on patients. *Scientific Reports* **6**, 38152 (2016).
7. Brugger, P., Regard, M. & Landis, T. Unilaterally Felt 'Presences': The Neuropsychiatry of One's Invisible Doppelgänger. *Neuropsychiatry, neuropsychology, and behavioral neurology* **9**, 114–122 (1996).
8. Arzy, S., Seeck, M., Ortigue, S., Spinelli, L. & Blanke, O. Induction of an illusory shadow person. *Nature* **443**, 287 (2006).
9. Critchley, M. *The divine banquet of the brain and other essays*. (Raven Press, 1979).
10. Fénelon, G., Soulas, T., De Langavant, L. C., Trinkler, I. & Bachoud-Lévi, A.-C. Feeling of presence in Parkinson's disease. *J Neurol Neurosurg Psychiatry* **82**, 1219–1224 (2011).
11. Lenka, A., Pagonabarraga, J., Pal, P. K., Bejr-Kasem, H. & Kulisevsky, J. Minor hallucinations in Parkinson disease: A subtle symptom with major clinical implications. *Neurology* (2019) doi:10.1212/WNL.0000000000007913.
12. Ffytche, D. H. *et al.* The psychosis spectrum in Parkinson disease. *Nat Rev Neurol* **13**, 81–95 (2017).
13. Fénelon, G., Soulas, T., Zenasni, F. & De Langavant, L. C. The changing face of Parkinson's disease-associated psychosis: a cross-sectional study based on the new NINDS-NIMH criteria. *Mov Disord* **25**, 755–759 (2010).
14. Diederich, N. J., Fénelon, G., Stebbins, G. & Goetz, C. G. Hallucinations in Parkinson disease. *Nat Rev Neurol* **5**, 331–342 (2009).
15. Forsaa, E. B., Larsen, J. P., Wentzel-Larsen, T. & Alves, G. What predicts mortality in Parkinson disease?: a prospective population-based long-term study. *Neurology* **75**, 1270–1276 (2010).
16. Marinus, J., Zhu, K., Marras, C., Aarsland, D. & van Hilten, J. J. Risk factors for non-motor symptoms in Parkinson's disease. *The Lancet Neurology* **17**, 559–568 (2018).
17. Goetz, C. G., Fan, W., Leurgans, S., Bernard, B. & Stebbins, G. T. The malignant course of 'benign hallucinations' in Parkinson disease. *Arch. Neurol.* **63**, 713–716 (2006).
18. Pagonabarraga, J. *et al.* Minor hallucinations occur in drug-naive Parkinson's disease patients, even from the premotor phase. *Mov. Disord.* **31**, 45–52 (2016).
19. Kulick, C. V., Montgomery, K. M. & Nirenberg, M. J. Comprehensive identification of delusions and olfactory, tactile, gustatory, and minor hallucinations in Parkinson's disease psychosis. *Parkinsonism Relat. Disord.* **54**, 40–45 (2018).
20. Fernandez, H. H. *et al.* Scales to assess psychosis in Parkinson's disease: Critique and recommendations. *Movement Disorders* **23**, 484–500 (2008).
21. Ravina, B. *et al.* Diagnostic criteria for psychosis in Parkinson's disease: Report of an NINDS, NIMH Work Group. *Movement Disorders* **22**, 1061–1068 (2007).
22. Holroyd, S., Currie, L. & Wooten, G. F. Prospective study of hallucinations and delusions in Parkinson's disease. *Journal of Neurology, Neurosurgery & Psychiatry* **70**, 734–738 (2001).

23. Weil, R. S. *et al.* Visual dysfunction in Parkinson's disease. *Brain* **139**, 2827–2843 (2016).
24. Bejr-Kasem, H. *et al.* Disruption of the default mode network and its intrinsic functional connectivity underlies minor hallucinations in Parkinson's disease. *Mov. Disord.* **34**, 78–86 (2019).
25. Hecaen & De Ajuriaguerra. Misconstructions and hallucinations with respect to the body image; integration and disintegration of somatognosi. *L' Evolution Psychiatrique* 745–750 (1952).
26. Blanke, O. *et al.* Report Neurological and Robot-Controlled Induction of an Apparition. *Current Biology* **24**, 2681–2686 (2014).
27. Weiskrantz, L., Elliott, J. & Darlington, C. Preliminary observations on tickling oneself. *Nature* **230**, 598–599 (1971).
28. Blakemore, S. J., Wolpert, D. & Frith, C. Why can't you tickle yourself? *Neuroreport* **11**, R11-16 (2000).
29. Ehrsson, H. H., Holmes, N. P. & Passingham, R. E. Touching a rubber hand: feeling of body ownership is associated with activity in multisensory brain areas. *J Neurosci* **25**, 10564–10573 (2005).
30. Pozeg, P., Rognini, G., Salomon, R. & Blanke, O. Crossing the Hands Increases Illusory Self-Touch. *PLoS One* **9**, (2014).
31. Shergill, S. S., Samson, G., Bays, P. M., Frith, C. D. & Wolpert, D. M. Evidence for sensory prediction deficits in schizophrenia. *Am J Psychiatry* **162**, 2384–2386 (2005).
32. Blakemore, S.-J., Wolpert, D. M. & Frith, C. D. Central cancellation of self-produced tickle sensation. *Nat Neurosci* **1**, 635–640 (1998).
33. Blakemore, S.-J., Wolpert, D. M. & Frith, C. D. Abnormalities in the awareness of action. *Trends in Cognitive Sciences* **6**, 237–242 (2002).
34. Wolpert, D. M., Ghahramani, Z. & Jordan, M. I. An internal model for sensorimotor integration. *Science* **269**, 1880–1882 (1995).
35. Miall, R. C. & Wolpert, D. M. Forward Models for Physiological Motor Control. *Neural Networks* **9**, 1265–1279 (1996).
36. Corlett, P. R. *et al.* Disrupted prediction-error signal in psychosis: evidence for an associative account of delusions. *Brain* **130**, 2387–2400 (2007).
37. Fletcher, P. C. & Frith, C. D. Perceiving is believing: a Bayesian approach to explaining the positive symptoms of schizophrenia. *Nat. Rev. Neurosci.* **10**, 48–58 (2009).
38. Ford, J. M. & Mathalon, D. H. Electrophysiological evidence of corollary discharge dysfunction in schizophrenia during talking and thinking. *Journal of Psychiatric Research* **38**, 37–46 (2004).
39. Conte, A., Khan, N., Defazio, G., Rothwell, J. C. & Berardelli, A. Pathophysiology of somatosensory abnormalities in Parkinson disease. *Nature Reviews Neurology* **9**, 687–697 (2013).
40. Pagonabarraga, J. *et al.* Neural correlates of minor hallucinations in non-demented patients with Parkinson's disease. *Parkinsonism & Related Disorders* **20**, 290–296 (2014).
41. Hara, M. *et al.* A novel manipulation method of human body ownership using an fMRI-compatible master-slave system. *Journal of Neuroscience Methods* **235**, 25–34 (2014).
42. Leube, D. T. *et al.* The neural correlates of perceiving one's own movements. *NeuroImage* **20**, 2084–2090 (2003).
43. Sperduti, M., Delaveau, P., Fossati, P. & Nadel, J. Different brain structures related to self- and external-agency attribution: a brief review and meta-analysis. *Brain Struct Funct* **216**, 151–157 (2011).
44. David, N., Newen, A. & Vogeley, K. The “sense of agency” and its underlying cognitive and neural mechanisms. *Consciousness and Cognition* **17**, 523–534 (2008).
45. Blakemore, S. J., Wolpert, D. M. & Frith, C. D. Central cancellation of self-produced tickle sensation. *Nature neuroscience* **1**, 635–640 (1998).

46. Yomogida, Y. *et al.* The neural basis of agency: an fMRI study. *Neuroimage* **50**, 198–207 (2010).
47. Ehrsson, H. H., Holmes, N. P. & Passingham, R. E. Touching a rubber hand: feeling of body ownership is associated with activity in multisensory brain areas. *The Journal of neuroscience : the official journal of the Society for Neuroscience* **25**, 10564–73 (2005).
48. Farrer, C. *et al.* Modulating the experience of agency: A positron emission tomography study. *NeuroImage* **18**, 324–333 (2003).
49. Blakemore, S. J. & Sirigu, A. Action prediction in the cerebellum and in the parietal lobe. *Experimental Brain Research* **153**, 239–245 (2003).
50. Boes, A. D. *et al.* Network localization of neurological symptoms from focal brain lesions. *Brain* **138**, 3061–3075 (2015).
51. Nooner, K. B. *et al.* The NKI-Rockland Sample: A Model for Accelerating the Pace of Discovery Science in Psychiatry. *Front Neurosci* **6**, (2012).
52. Friston, K. J. The disconnection hypothesis. *Schizophr. Res.* **30**, 115–125 (1998).
53. Friston, K., Brown, H. R., Siemerikus, J. & Stephan, K. E. The dysconnection hypothesis (2016). *Schizophrenia Research* **176**, 83–94 (2016).
54. Frith, C. The neural basis of hallucinations and delusions. *C. R. Biol.* **328**, 169–175 (2005).
55. Aarsland, D., Hutchinson, M. & Larsen, J. P. Cognitive, psychiatric and motor response to galantamine in Parkinson's disease with dementia. *Int J Geriatr Psychiatry* **18**, 937–941 (2003).
56. Ramirez-Ruiz, B., Junque, C., Marti, M.-J., Valldeoriola, F. & Tolosa, E. Cognitive changes in Parkinson's disease patients with visual hallucinations. *Dement Geriatr Cogn Disord* **23**, 281–288 (2007).
57. Morgante, L. *et al.* Psychosis associated to Parkinson's disease in the early stages: relevance of cognitive decline and depression. *J. Neurol. Neurosurg. Psychiatry* **83**, 76–82 (2012).
58. Pagonabarraga, J. *et al.* Parkinson's disease-cognitive rating scale: a new cognitive scale specific for Parkinson's disease. *Mov. Disord.* **23**, 998–1005 (2008).
59. Blakemore, S. J. & Frith, C. Self-awareness and action. *Curr. Opin. Neurobiol.* **13**, 219–224 (2003).
60. Friston, K. J. Theoretical neurobiology and schizophrenia. *Br. Med. Bull.* **52**, 644–655 (1996).
61. Goetz, C. G., Vaughan, C. L., Goldman, J. G. & Stebbins, G. T. I finally see what you see: Parkinson's disease visual hallucinations captured with functional neuroimaging. *Mov. Disord.* **29**, 115–117 (2014).
62. Meppelink, A. M. *et al.* Impaired visual processing preceding image recognition in Parkinson's disease patients with visual hallucinations. *Brain* **132**, 2980–2993 (2009).
63. Weintraub, D., Kales, H. C. & Marras, C. The Danger of Not Treating Parkinson Disease Psychosis-Reply. *JAMA Neurol* **73**, 1156–1157 (2016).
64. Rana, A. Q., Vaid, H. M., Edun, A., Dogu, O. & Rana, M. A. Relationship of dementia and visual hallucinations in tremor and non-tremor dominant Parkinson's disease. *J. Neurol. Sci.* **323**, 158–161 (2012).
65. Reijnders, J. S. A. M., Ehrt, U., Lousberg, R., Aarsland, D. & Leentjens, A. F. G. The association between motor subtypes and psychopathology in Parkinson's disease. *Parkinsonism Relat. Disord.* **15**, 379–382 (2009).
66. Bates, D., Mächler, M., Bolker, B. & Walker, S. Fitting Linear Mixed-Effects Models Using lme4. *Journal of Statistical Software* **67**, 1–48 (2015).
67. Kuznetsova, A., Brockhoff, P. B. & Christensen, R. H. B. lmerTest Package: Tests in Linear Mixed Effects Models. *Journal of Statistical Software* **82**, 1–26 (2017).
68. Luo, D., Ganesh, S & Koolaard, J. predictmeans: Calculate Predicted Means for Linear Models, <http://cran.r-project.org/package=predictmeans>. (2014).

69. Power, J. D., Barnes, K. A., Snyder, A. Z., Schlaggar, B. L. & Petersen, S. E. Spurious but systematic correlations in functional connectivity MRI networks arise from subject motion. *Neuroimage* **59**, 2142–2154 (2012).
70. Tzourio-Mazoyer, N. *et al.* Automated Anatomical Labeling of Activations in SPM Using a Macroscopic Anatomical Parcellation of the MNI MRI Single-Subject Brain. *NeuroImage* **15**, 273–289 (2002).
71. Eickhoff, S. B. *et al.* A new SPM toolbox for combining probabilistic cytoarchitectonic maps and functional imaging data. *NeuroImage* **25**, 1325–1335 (2005).
72. Fox, M. D. Mapping Symptoms to Brain Networks with the Human Connectome. *New England Journal of Medicine* **379**, 2237–2245 (2018).
73. Whitfield-Gabrieli, S. & Nieto-Castanon, A. Conn: a functional connectivity toolbox for correlated and anticorrelated brain networks. *Brain Connect* **2**, 125–141 (2012).
74. Kuhn, M. caret: Classification and Regression Training. *Astrophysics Source Code Library* ascl:1505.003 (2015).
75. Friedman, J., Hastie, T. & Tibshirani, R. Regularization Paths for Generalized Linear Models via Coordinate Descent. *J Stat Softw* **33**, 1–22 (2010).
76. Revelle, W. R. psych: Procedures for Personality and Psychological Research. (2017).

Supplementary Information of Sensorimotor hallucinations in  
Parkinson's disease

**Study 1.1: Robot-induced presence hallucinations (riPH) in patients with PD**

*Supplementary S1: Participants: Inclusion/Exclusion criteria*

Participants in the present study consisted of patients with PD and the symptom of PH (PD-PH, n=13), patients with PD without the symptom of PH (PD-nPH, n=13), and age-matched healthy controls (HC, n=21). Demographic and clinical data are summarized in Table S1. Patients with cognitive impairments (defined as a MoCA score<sup>1</sup> lower than 24<sup>2</sup>), treated with neuroleptics, affected by other central neurological co-morbidities, affected by psychiatric co-morbidities unrelated to PD, and patients with recent (< one month) changes in their medical treatment were not included in the study. The HC included in the study never experienced PH, did not suffer from a neurological or psychiatric disease, and had no objective sign of cognitive impairment.

*Supplementary S2: Demographic and disease-related variables*

For every PD patient, the doses of anti-parkinsonian medication were converted to the levodopa equivalent daily dose<sup>3</sup>. The severity of motor symptoms was assessed by the score at the Movement Disorders Society - Unified Parkinson Disease Rating Scale (MDS-UPDRS) - part III (Goetz et al., 2008), in “ON” state. In addition, impulsive-compulsive disorders were assessed by the score at the “Questionnaire for Impulsive-Compulsive Disorders in Parkinson's Disease” (QUIP-RS<sup>4</sup>). We also assessed for PD-PH, PD-nPH, and HC apathy scale<sup>5</sup> and the risk for psychosis (Prodromal Questionnaire PQ-16<sup>6</sup>; which was divided in part I (hallucinations, and negative symptoms-like experiences), and part II (level of distress linked to the experiences). Hallucinations were assessed with a semi-structured interview adapted from the psychosensory hallucinations Scale (PSAS) for Schizophrenia and Parkinson's disease<sup>7</sup>. Next to PH, we also inquired about other hallucinations possibly experienced by patients with PD, e.g. passage hallucinations (i.e., animal, person or indefinite object passing in the peripheral visual field), visual illusion and complex hallucinations (structured visual, auditory or tactile hallucinations) as well as delusional ideas.

	PD-PH (N = 13)	PD-nPH (N = 13)	<i>p-values</i>
Age	60.69 ± 13.19	65.69 ± 7.60	0.25
Gender	9 (M)	4 (M)	0.05 ( $\chi^2$ )
UPDRS-III	20 ± 12.09	19 ± 17.51	0.87
MoCA	26.85 ± 1.82	28.15 ± 1.57	0.08
PQ16	4.00 ± 2.00	0.69 ± 1.32	< 0.001
PQ16-2	3.54 ± 4.86	1.08 ± 2.63	0.1
Apathy	12.69 ± 8.06	10.23 ± 4.64	0.37
LEDD (mg/day)	727.77 ± 410.46	786.23 ± 657.23	0.8
Disease Duration (years)	9.46 ± 4.22	9.38 ± 5.72	0.5

Table S1. Clinical variables between PD-PH and PD-nPH.

	PD-PH (N = 13)	HC (N = 21)	<i>p-values</i>
Age	60.69 ± 13.19	66.90 ± 5.75	0.06
Gender	9 (M)	11 (M)	0.9 ( $\chi^2$ )
MoCA	26.85 ± 1.82	28.52 ± 1.03	<0.001
PQ16	4.00 ± 2.00	0.24 ± 0.44	<0.001
PQ16-2	3.54 ± 4.86	0 ± 0	<0.001
Apathy	12.69 ± 8.06	6.33 ± 4.05	0.01

Table S2. Clinical variables between PD-PH and HC.

*Supplementary S3: Experimental procedure*

Each PD patient underwent study1 at a similar time (10am), after having received their usual anti-parkinsonian medication and were in their “best ON” state for the whole duration of study1 as well as the psychological and neuropsychological assessments<sup>8</sup>. To investigate the riPH in patients with PD (and HC), we used the same experimental setup and device as our previous research<sup>9</sup>. The robotic stimulation was administered through a robotic system<sup>10</sup> that has previously been used to induce the PH and other bodily illusions in healthy subjects<sup>9</sup>. The experimental design consisted in factors Synchrony (synchronous/asynchronous), Side (most/less affected) and Group (PD-PH/PD-nPH).



*Supplementary S4: Questionnaire results: PH*

Detailed ratings for all questions can be seen on Table S3 (below).

*Robot-induced PH (“I felt as if someone was close-by”)*

*PD-PH vs. PD-nPH.* No main effect of Side (permutation p-value=0.37). No interactions were observed, all permutation p-values>0.05.

*PD-PH vs. HC.* By comparing PD-PH and HC, we confirmed the importance of conflicting sensorimotor stimulation to induced PH, as both groups gave higher PH ratings in the asynchronous versus synchronous condition (p-value=0.033). The intensity of riPH ratings did not differ statistically between PD-PH and HC (permutation p-value=0.48). The Side did not significantly modulate the riPH ratings (permutation p-value=0.38). No interactions were observed, all permutation p-values>0.05.

*Supplementary S5: Questionnaire results: Other robot-induced perceptions*

*Passivity experience (“I felt as if someone else was touching my back.”)*

*PD-PH vs. PD-nPH.* The two sub-groups of patients did not report difference in passivity experiences in the asynchronous condition (permutation p-value = 0.1, main effect of Synchrony), the ratings did not differ significantly between the groups of patients (permutation p-value = 0.38, main effect of Group), and the Side did not modulate the passivity experience (permutation p-value=0.41). No interactions were observed, all permutation p-values>0.05.

*PD-PH vs. HC.* We observed a trend for a main effect of synchrony where higher passivity experiences were induced in the asynchronous condition (permutation p-value=0.06). The ratings were not statistically different between the groups (permutation p-value=0.86, main effect of Group). The Side modulated the passivity experience (permutation p-value<0.01). No interactions were observed, all other permutation p-values>0.05.

*Self-touch ("I felt as if I was touching my back." )*

PD-PH vs. PD-nPH. In line with previous work<sup>9</sup>, the two sub-groups of patients reported higher self-touch experiences in the synchronous condition (permutation p-value=0.043, main effect of Synchrony). The ratings did not differ significantly neither between the groups of patients (permutation p-value=0.65, main effect of Group), nor between the Side (permutation p-value=0.51). No interactions were observed, all other permutation p-values>0.05.

PD-PH vs. HC. We observed that participants reported a trend for higher self-touch experiences in the synchronous condition (permutation p-value=0.054, main effect of Synchrony). The rating did not differ significantly neither between the groups (permutation p-value=0.92, main effect of Group), nor between the Side (permutation p-value=0.4). No interactions were observed (all other permutation p-values>0.05).

*Loss of agency ("I felt as if I was not controlling my movements or actions." )*

PD-PH vs. PD-nPH. The robotic stimulation was associated with a stronger loss of agency in PD-PH than PD-nPH (permutation p-value=0.045, main effect of Group). Neither the sensorimotor conditions (permutation p-value=0.26, main effect of Synchrony), nor the Side (permutation p-value=0.67) modulated significantly the rating. No interactions were observed, all other permutation p-values>0.05.

PD-PH vs. HC. No statistical difference was observed between the two sub-groups (permutation p-value=0.073, main effect of Group). Neither the sensorimotor conditions (permutation p-value=0.6, main effect of Synchrony) nor the Side (permutation p-value=0.28) modulated significantly the ratings. No interactions were observed, all other permutation p-values>0.05.

*Bodily sensations (“I felt as if I had two bodies”) (Control item 1).*

PD-PH vs. PD-nPH. The robotic stimulation did not modulate significantly this bodily sensation (permutation p-value=0.98, main effect of Synchrony), we did not observe statistically significant differences between the two sub-groups (permutation p-value=0.26, main effect of Group), and did not observed a difference due to the Side (permutation p-value=0.88). No interactions were observed, all other permutation p-values>0.05.

PD-PH vs. HC. The robotic stimulation neither modulated this bodily sensation (permutation p-value=0.85, main effect of Synchrony) nor did the two sub-groups (permutation p-value=0.79, main effect of Group), and we did not observe a difference due to the Side (permutation p-value=0.71). No interactions were observed, all other permutation p-values>0.05.

*Control Question (“I felt someone was standing in front of me.”) (Control item 2).*

For each of the three sub-groups, all the raw ratings were zeros for the question front-PH (permutation p-value=1).

**Chapter 3. Sensorimotor hallucinations in Parkinson's disease – Supplementary**

<b>Question</b>	<b>Group</b>	<b>Synchrony</b>	<b>Side</b>	<b>Mean</b>	<b>Standard Deviation</b>
PH	PD-PH	Async	Less affected side	1.67	2.31
PH	PD-PH	Async	Most affected side	2.23	2.17
PH	PD-PH	Sync	Less affected side	0.42	0.9
PH	PD-PH	Sync	Most affected side	1.31	1.93
PH	PD-nPH	Async	Less affected side	0.62	1.56
PH	PD-nPH	Async	Most affected side	0.23	0.83
PH	PD-nPH	Sync	Less affected side	0	0
PH	PD-nPH	Sync	Most affected side	0	0
PH	HC	Async	Less affected side	1.05	1.96
PH	HC	Async	Most affected side	1.33	2.15
PH	HC	Sync	Less affected side	0.52	1.66
PH	HC	Sync	Most affected side	0.86	1.93
Loss of agency	PD-PH	Async	Less affected side	1.83	2.25
Loss of agency	PD-PH	Async	Most affected side	2.25	2.14
Loss of agency	PD-PH	Sync	Less affected side	1.17	1.7
Loss of agency	PD-PH	Sync	Most affected side	1.75	1.71
Loss of agency	PD-nPH	Async	Less affected side	0.85	1.63
Loss of agency	PD-nPH	Async	Most affected side	0.54	0.97
Loss of agency	PD-nPH	Sync	Less affected side	0.08	0.28
Loss of agency	PD-nPH	Sync	Most affected side	0.23	0.6
Loss of agency	HC	Async	Less affected side	0.48	1.25
Loss of agency	HC	Async	Most affected side	0.81	1.47
Loss of agency	HC	Sync	Less affected side	0.24	0.89
Loss of agency	HC	Sync	Most affected side	0.9	1.7
Passivity experience	PD-PH	Async	Less affected side	2.33	2.31
Passivity experience	PD-PH	Async	Most affected side	3.08	2.43
Passivity experience	PD-PH	Sync	Less affected side	1.25	2.05
Passivity experience	PD-PH	Sync	Most affected side	2.08	2.14
Passivity experience	PD-nPH	Async	Less affected side	2.54	2.37
Passivity experience	PD-nPH	Async	Most affected side	1.77	2.05
Passivity experience	PD-nPH	Sync	Less affected side	1.54	2.22
Passivity experience	PD-nPH	Sync	Most affected side	1.38	1.94
Passivity experience	HC	Async	Less affected side	1.81	2.5
Passivity experience	HC	Async	Most affected side	3.29	2.31
Passivity experience	HC	Sync	Less affected side	1.29	2.22
Passivity experience	HC	Sync	Most affected side	2.33	2.61
Self-touch	PD-PH	Async	Less affected side	1.92	2.35
Self-touch	PD-PH	Async	Most affected side	1.38	1.66
Self-touch	PD-PH	Sync	Less affected side	2.08	2.27
Self-touch	PD-PH	Sync	Most affected side	3	2.24
Self-touch	PD-nPH	Async	Less affected side	0.85	1.57
Self-touch	PD-nPH	Async	Most affected side	0.85	1.57
Self-touch	PD-nPH	Sync	Less affected side	1.46	2.37
Self-touch	PD-nPH	Sync	Most affected side	1.92	2.56
Self-touch	HC	Async	Less affected side	2.38	2.69
Self-touch	HC	Async	Most affected side	1.86	2.46
Self-touch	HC	Sync	Less affected side	2.43	2.84
Self-touch	HC	Sync	Most affected side	2.81	2.84

Question	Group	Synchrony	Side	Mean	Standard Deviation
PH front	PD-PH	Async	Less affected side	0	0
PH front	PD-PH	Async	Most affected side	0	0
PH front	PD-PH	Sync	Less affected side	0	0
PH front	PD-PH	Sync	Most affected side	0	0
PH front	PD-nPH	Async	Less affected side	0	0
PH front	PD-nPH	Async	Most affected side	0	0
PH front	PD-nPH	Sync	Less affected side	0	0
PH front	PD-nPH	Sync	Most affected side	0	0
PH front	HC	Async	Less affected side	0	0
PH front	HC	Async	Most affected side	0	0
PH front	HC	Sync	Less affected side	0	0
PH front	HC	Sync	Most affected side	0	0
Control	PD-PH	Async	Less affected side	0.25	0.62
Control	PD-PH	Async	Most affected side	0.54	1.2
Control	PD-PH	Sync	Less affected side	0.25	0.87
Control	PD-PH	Sync	Most affected side	0.38	0.96
Control	PD-nPH	Async	Less affected side	0	0
Control	PD-nPH	Async	Most affected side	0	0
Control	PD-nPH	Sync	Less affected side	0	0
Control	PD-nPH	Sync	Most affected side	0	0
Control	HC	Async	Less affected side	0.19	0.87
Control	HC	Async	Most affected side	0.19	0.87
Control	HC	Sync	Less affected side	0	0
Control	HC	Sync	Most affected side	0.24	1.09

Table S3. Mean ratings for all questions, and experimental conditions

*Supplementary S6: Post-experiment debriefing: riPH mimic sPH (in PD-PH)*

*Patients reports.* One PD-PH patient reported that he could feel the robot-induced presence on the side (not on the back) and added (after being asked to compare s- and riPH) “it is slightly similar, but it is not exactly the same because the presence (symptomatic) is all of a sudden, while here (the riPH) it is built-up”. Although, the riPH was strong felt, another PD-PH patient noted that the PH lacked some aspects of his symptomatic PH (sPH). He described that “when I feel the symptomatic PH it’s like a chewing gum with a lot of taste, while here (the riPH) it was still like chewing gum but without the taste”. Another PD-PH patient compared his riPH to “an adrenaline rush. Like something or someone was behind me, although there is not the possibility to have someone behind” and “I really had the impression that someone was doing something behind me”. Another PD-PH patient reported that “I honestly have the impression to have someone behind me”. Just after the stimulation and removal of the blindfold she added “I was surprised to see you all in front of me”.

*Supplementary S7: Post-experiment debriefing: Spatial location of the riPH*

We further determined the experienced spatial location of the riPH and whether this differed across the three participant groups. Analyzing all trials for which a participant positively rated the PH during the robotic procedure (i.e., value > 0 on Likert scale) we found that PD-PH patients reported a higher number of lateralized riPH (n=24; i.e. instances of a riPH with a value > 0; across all trials and conditions) than HC (n=18) (Chi-square: p-value = 0.003,  $\chi^2(1)=9$ ) and PD-nPH (n=3) (Chi-square: p-value = 0.001,  $\chi^2(1)=11.26$ ), Table S2). PD-PH reported riPH either to the side (n=14) or behind them (n=6), with no predominant location (Chi-square: p-value = 0.11,  $\chi^2(1)=3.22$ ), while HC predominantly reported riPH behind them (n=14, and n=2 lateralized) (Chi-square: p-value = 0.006,  $\chi^2(1)=9$ ). The most affected side did not influence the location of the riPH (all p-values>0.05). The very few instances in PD-nPH patients did not differ (behind: n=2; lateralized: n=1) (Chi-square: p-value = 1,  $\chi^2(1)=0.33$ ). These data show that similarly to the sPH, PD-PH patients experienced riPH more often on the side, even if the tactile feedback was provided on the back, differing from HC, who always reported the location of the robot-induced presence behind them. Debriefing data also suggest that 38% of PD-PH patients report robotic-induced PH that are associated with a state that is comparable in intensity to sPH. Interestingly, these robotic-induced sPH only occurred in the asynchronous stimulation condition.

*Supplementary S8: sPH in PD-PH (semi-structured interview data).*

Previous studies observed that most patients with PD who experience PH report them as neutral, as not distressing (except when it occurred for the first time), and usually short-lasting. Moreover, PH are typically felt beside or behind the patient's body (rarely also in an adjacent room)<sup>11</sup>. In the current study, the semi-structured interview data confirmed that sPH in PD-PH patients were in 54% neutral or positive and were in 62% of undetermined gender. In 69% the presence was either felt on the side of the patient's body and/or on the back (for other variables see Table S2). Collectively, these results are compatible with previously reported sPH in PD. Overall sPH were not predominantly located in one spatial position. That is, ~38% of the patients experienced the sPH on either sides (not simultaneously) and/or in the back,

confirming that sPH are not associated with the predominantly affected side of the disease 11 (Table S4 for details).

	Number of patients	%
<b>PH Valence</b>		
• Positive/Neutral	7	54
• Negative	6	46
<b>PH Gender</b>		
• Female only	2	15
• Male only	1	8
• Both sex	2	15
• Undetermined	8	62
<b>PH Lateralisation</b>		
• Side only	6	46
• Back only	3	23
• Back and Side	2	15
• Front	1	8
• Other room	5	38
<b>Occurrence (moment)</b>		
• Day	3	23
• Night	4	31
• Anytime	6	46
<b>Occurrence (place)</b>		
• Home only	8	62
• Outside home only	0	0
• Both	6	46
<b>Distance of PH</b>		
• Less than 1m	5	38
• More than 1m	8	62

Table S4. Phenomenology of the symptomatic PH in PD.

*Study 1.2: riPH in PD-PH patients depend on sensorimotor delay*

*Supplementary S9: Participants*

The same participants of study1.1 took part in study1.2. In total, 10 PD-PH and 12 PD-nPH and 21 HC participated to study1.2. Because of fatigue and/or tremor, two PD-PH and one PD-nPH could not participate in study1.2. One PD-PH and one PD-nPH were excluded from the analysis because they performed less than 18 trials (i.e. one session) before definitively interrupting the experiment, due to fatigue and/or excessive tremor.

*Supplementary S10: Experimental procedure*

For each patient, the task of study1.2 was done exclusively with the hand that was most affected by PD. HC did the task with their dominant hand. Each participant was asked to perform three sessions; each session consisted of 18 trials (3 repetitions per delay). In total, each delay was repeated 9 times. The overall experiment lasted approximately 20 minutes. Between each session, the participant could take a break according to his/her needs. One PD-PH patient performed longer sessions. In total, PD-PH completed  $57.8 \pm 16.9$  (mean  $\pm$  SD) trials, PD-nPH completed  $45 \pm 12.8$  (mean  $\pm$  SD) trials, and HC completed  $53.3 \pm 3.91$  (mean  $\pm$  SD) trials. No statistically difference across groups was observed (Welch two Sample t-test, two-tailed): PD-PH vs. PD-nPH:  $t(17) = 1.97$ , p-value = 0.065; PD-PH vs. HC:  $t(-9) = 0.89$ , p-value = 0.39.

*Supplementary S11: Degree of sensorimotor conflict modulates riPH*

Study1.2 confirmed that PD-PH patients experienced stronger riPH than PD-nPH patients (main effect of group: permutation p-value = 0.016; Fig.1D). Comparing the intensity of riPH between PD-PH and HC, we observed that PD-PH patients have a stronger bias in experiencing riPH than HC (main effect of group: permutation p-value=0.046t), and that the intensity of riPH increased with increasing delays for both groups (main effect of delay: p-value<0.001, two-tailed permutation test; Fig. S1). Although PD-PH patients have a stronger bias in riPH, there was no significant difference in sensitivity (slope) between these two groups (p-value=0.6, two-tailed permutation test). On average PD-PH rated the riPH for the delays: 0ms:  $35.1 \pm 33.8$  (percentage mean  $\pm$  SD), 100ms:  $34.8 \pm 33.8$ , 200ms:  $45.7 \pm 38$ , 300ms:  $39.8 \pm 37$ , 400ms:  $48.1 \pm 39.5$ , 500ms:  $48.4 \pm 43.3$ . PD-nPH rated on average the riPH: 0ms:  $6.75 \pm 16.1$ , 100ms:  $5.56 \pm 19.2$ , 200ms:  $8.33 \pm 25.6$ , 300ms:  $7.41 \pm 22.4$ , 400ms:  $8.33 \pm 28.9$ , 500ms:  $7.41 \pm 25.7$ . HC rated on average the ri PH: 0ms:  $14.3 \pm 26.3$ , 100ms:  $14.8 \pm 28$ , 200ms:  $15.3 \pm 29.1$ , 300ms:  $15.2 \pm 28.3$ , 400ms:  $23.8 \pm 38.9$ , 500ms:  $23.5 \pm 34.9$ .



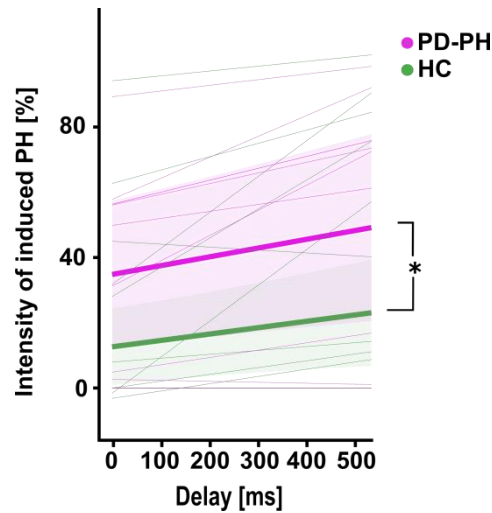


**Figure S1. riPH (PD patient & HC). Study1.2.** riPH were modulated by delay (permutation  $p$ -value $<0.001$ ) and PD-PH vs. HC had a stronger bias in experiencing riPH. The thicker lines indicate the mean of the fitted models, the thinner lines indicate the individual fit, and the shaded are indicates the 95% confidence interval.

#### *Supplementary S12: Movement analysis*

To assess whether the spatio-temporal pattern of the movement could explain the difference in rating of the riPH among groups, we calculated: i) the Inter-poke-interval (time between the end of the touch on the back of poke  $n$  and the beginning of the following touch – poke  $n+1$ ), ii) duration of the poke and iii) the spatial distance between poke  $n$  and poke  $n+1$ . Data were analyzed with linear mixed effects models `lme4` and `lmerTest` both R packages<sup>12,13</sup>. The significance of fixed effects was estimated with a permutation test (5000 iterations; predicted mean R package).

*Inter-poke-interval (ipi).* To assess the temporal aspects of the sensorimotor integration we computed the ipi for each individual and for each trial independently. Models were performed on the ipi for each subject, with Groups (i.e., PD-PH vs. PD-nPH; PD-PH vs. HC) as fixed effects, and random intercepts for the participant.

*Poke duration.* To assess a second temporal aspects of the sensorimotor integration we computed the duration of each poke, for each individual and for each trial independently. Models were performed on the duration for each subject, with Groups (i.e., PD-PH vs. PD-nPH; PD-PH vs. HC) as fixed effects, and random intercepts for the participant.

*Spatial distance between pokes.* To further investigate the spatial aspects of the sensorimotor integration we computed the Euclidean distance between pokes for each trial and subject. Models were performed on each distance values for each subject, with Groups (i.e., PD-PH vs. PD-nPH and PD-PH vs. HC) as fixed effects, and random intercepts for the participant.

*Supplementary S13: Movement analysis*

Are bias and delay effect related to differences in the upper arm movements of PD-PH vs. PD-nPH patients during the robotic procedure? During Study1.2 we measured the movements performed by all participants, allowing us to analyze whether PD-PH, PD-nPH, and HC moved differently, calculating the inter-poke-interval (i.e., time between the end of the touch on the back (poke  $n$ ) and the beginning of the following poke  $n+1$ ) and the spatial distance between successive pokes (poke  $n$  and poke  $n+1$ ).

The analysis of the movement data of Study1.2 exclude differences in movement patterns (neither temporal nor spatial aspects) between the two sub-groups of patients. No difference in the inter-poke-interval between PD-PH and PD-nPH (permutation p-value = 0.29). Average duration of the inter-poke-interval for PD-PH was  $2.06 \pm 1.97$  seconds (mean  $\pm$  SD) and  $1.55 \pm 2.26$  sec for PD-nPH (mean  $\pm$  SD). The duration of each poke did not different between PD-PH and PD-nPH (permutation p-value=1). The average duration of the poke duration for PD-PH was  $0.75 \pm 5.24$  seconds (mean  $\pm$  SD) and  $0.73 \pm 2.82$  seconds (mean  $\pm$  SD) for PD-nPH (Fig.S2A-B). Spatial analysis of the movement revealed no difference in the distance between the pokes between PD-PH and PD-nPH (permutation p-value = 0.3). Average surface explication for PD-PH was  $17.83 \pm 18.4$  mm (mean  $\pm$  SD) and  $23.89 \pm 21.05$  mm for PD-nPH (mean  $\pm$  SD)

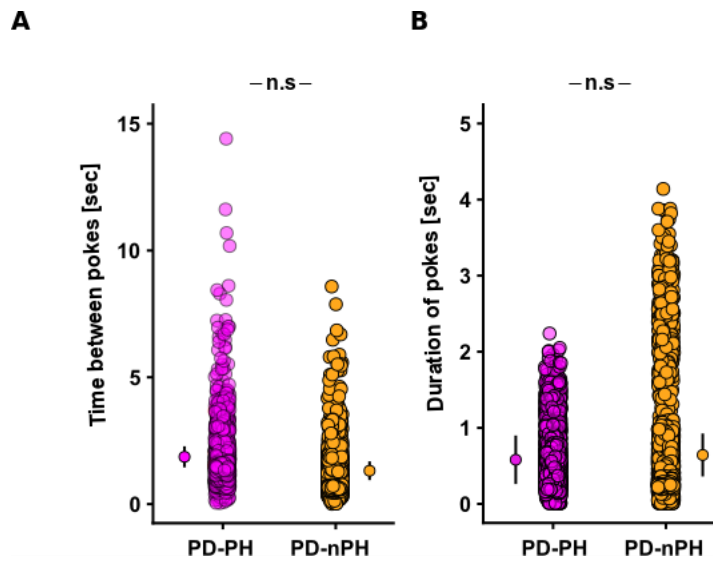


**Figure S2. Analysis of the movement patterns during the sensorimotor stimulation.** A. Mixed effects linear regression between the time between pokes for PD-PH (purple) and PD-nPH (yellow). The duration did not differ significantly (permutation p-value=0.29) in the time between two pokes (inter-pokes-interval). B. Mixed effects linear regression between duration of the pokes. The duration of the pokes did not differ significantly (p-value=1). Error bar represent 95% confidence interval.

PD-PH were not significantly slower in performing poking movement than HC ( $1.57 \pm 2.08$ ; mean  $\pm$  SD) (permutation p-value=0.097). The duration of each poke did not differ between PD-PH and HC (permutation p-value=0.076), the average duration of the poke duration for HC was  $0.49 \pm 0.39$  seconds (mean  $\pm$  SD). No differences were observed in the spatial aspects of the movement between PD-PH and HC (permutation p-value = 0.067). The average surface explored for HC was  $29.45 \pm 25.78$  mm (mean  $\pm$  SD).

These movement data show that both PD groups and the elderly HC were well able to carry out sensorimotor stimulation during the robotic procedure and, importantly, that movement patterns did not differ between both patient groups.

#### *Supplementary S14: riPH are not due to clinical differences between PD-PH and PD-nPH*

All patients were treated with anti-parkinsonian medications, but there was no significant difference in medication between both patient groups (Table S1). Although clinical experience and research has associated hallucinations with dopaminergic

treatment<sup>11,14</sup>, the exact role between the dopaminergic system and hallucinations is currently debated<sup>15,16</sup>. Thus, PD patients can experience PH before starting any dopaminergic medication<sup>17</sup> and the use of levodopa and dopamine agonists was not found to modulate occurrence of PH<sup>15</sup>. Motor fluctuations have also been linked to PH<sup>18</sup> (for a review<sup>15</sup>) and it is known that PH and other hallucinations occur more frequently in advanced stages of PD<sup>16</sup>. Thus, the difference in riPH between the two PD groups was not related to differences in disease duration, motor impairment, motor complications, or to dopaminergic treatment or hyperdopaminergic behavior (no significant differences between PD-PH and PD-nPH: all p-values>0.05; two-tailed permutation test; Table S1-2). Analyzing several other clinical and demographic variables (including motor impairment, dopaminergic treatment, and) that have been associated with symptomatic hallucinations in PD (e.g.<sup>18</sup>). We found no evidence for a difference between the two sub-groups of patients (all p-values>0.05; Table S1 for demographic of sub-groups).

Between the two sub-groups of patients with PD, there were no statistically significant differences (p-values>0.05) in the performance on the Montreal Cognitive Assessment (MoCA), disease duration, dopaminergic treatments (levodopa daily equivalent dosage), apathy, hyperdopaminergic behavior (QUIP-RS), motor impairment (MDS-UPDRS-III) and motor complications (MDS-UPDRS-IV). Patients that felt the presence as a symptom of the disease, PD-PH (vs. PD-nPH), had a higher score on the score for risk of psychosis (PQ-16, part 1- assessing hallucinations, but not for part 2 - assessing the level of distress associated with the occurrence of hallucinations).

Collectively, these results suggest that the differences in robot induced-PH between PD-PH and PD-nPH cannot be explained by differences in the degree of neurodegeneration, dopaminergic treatment, or motor fluctuations (or any of the other clinical variables we measured).

*Study 2.1: riPH are associated with activation of a subcortical-cortical sensorimotor network in healthy subjects*

*Supplementary S15: Robotic system*

The MR-compatible robotic system used to generate the sensorimotor conflicts was composed of a front and a back robot (Fig.2A in the main text;<sup>19</sup>). The front-robot of the MR-compatible robot contained a carbon-fiber rod attached to a slider allowing the participant to move along two directions (Fig.2A in the main text) and measured the movements. Movements of the carbon-fiber rod were electronically translated into movements of the back-robot. The back-robot was composed of a roller that touched the participant's back with stroking and tapping movements (for general performance of the robotic system see <sup>19</sup>). The back-robot's shape was adapted to the spatial dimensions of the scanner bore and a wooden mattress structure with a central slit was designed to allow the contact part of the back-robot to touch the back of the participants. The performance of the robotic system was previously validated inside a 3T and 7T MR scanner with a phantom<sup>19</sup>. Visual Studio 2013 interface (Microsoft) was used to control the robotic system.

The robotic system used in this study differed from the one used in the study 1 and of Blanke and colleagues<sup>9</sup> in multiple aspects. First, the participants were in the supine position compared to the standing position. Secondly, due to the spatial constraints of the MR-environment, the movement of the participants were limited to the middle back and not the whole back and participants had less degree of freedom: they could only move in X (along the body) and Z (towards the body) directions. All these different aspects might have led to the decrease of intensity of the PH induction compared to the standing robot used in the previous study<sup>9</sup>.

*Supplementary S16: Mock scanner: pilot study*

Here, we tested whether we could induce PH in supine position in a mock scanner using the MRI robot (i.e. riPH). All participants (n=24; 16 women, mean age±SD: 24.6±2.8 years old) had no history of neurological or psychiatric disorders. All participants were right handed as assessed by the Edinburgh Handedness Inventory <sup>20</sup> (mean index: 81.0± 16.3 (SD) and range: 40-100). All participants provided written informed consent prior to the experiment. The study was approved by the Cantonal

Ethics Committee of Geneva (Commission Cantonale d'Ethique de la Recherche-CCER). The Mock scanner (MRI Simulator, Psychology Software Tools, Inc.) mimicked the scanner environment as well as the noise of the echo-planar imaging sequence. Participants were asked to perform repetitive movements with their right hand and this operated the front-robot, the movements of which were translated to the back-robot that provided tactile feedback to our participants' backs. In two conditions, tactile feedback was delivered either synchronously with the participants' movements (synchronous control condition, sync) or with a delay (asynchronous condition, async) that was previously shown to induce the PH in healthy participants (Video S2). In a third condition (desynchronous condition, desync), movements of the back-robot consisted of a pre-recorded sequence. Each condition lasted for 3 minutes, was repeated once, and given in random order. After each condition, a questionnaire adapted from <sup>9</sup> was filled where participants were asked to rate their degree of agreement or disagreement on a Likert scale from 0 to 6.

*Supplementary S17: Mock Scanner (pilot study): Questionnaire results*

All the ratings are summarized in Table S5.

*Passivity experience ("I felt as if someone else was touching my body")*

In line with prior work<sup>21</sup>, we found that asynchronous robotic stimulations were associated with higher passivity experience than synchronous stimulation (main effect of Synchrony: permutation p-value < 0.001) with higher ratings in the async and desync conditions compared to the sync condition (post-hoc test:  $t(46) = 2.16$ , p-value = 0.035 and  $t(46) = 4.75$ , p-value < 0.001, respectively) and higher ratings in the desync compared to the async condition (post-hoc test:  $t(46) = 2.59$ , p-value = 0.012). These results further indicate a difference in the passivity experience between the desync and the async condition. This can be explained by the fact that the desync condition is a pre-recorded movement sequence played on the back of the participants which is being completely decoupled with the participant's movement.

*PH ("I felt as if a presence or someone was behind me")*

A main effect of Synchrony was also found for PH (permutation p-value < 0.001) with higher ratings in the desync and async condition compared to the sync condition post-hoc test: ( $t(46) = 4.14$ , p-value < 0.001 and  $t(46) = 2.92$ , p-value = 0.00053, respectively). No significant difference between the async and desync ratings was found (post-hoc test:  $t(46) = 1.13$ , p-value = 0.26). Contrary to passivity experience, the desync condition did not elicit significantly higher ratings than the async condition suggesting that both condition generating sensorimotor conflicts can equally induce PH. Taken together, these results confirm previous findings in showing that passivity experience and PH are induced in the presence of strong sensorimotor conflicts, in line with the results found by Blanke and colleagues <sup>9</sup>.

*Self-touch ("I felt as if I was touching my body")*

Regarding self-touch, only a trend for a main effect of Synchrony was found (permutation p-value=0.062), with a tendency for higher ratings in the sync condition compared to async and desync (Table S5 for ratings).

<b>Question</b>	<b>Synchrony</b>	<b>Mean</b>	<b>Standard deviation</b>
Self-touch	Desync	1.58	1.84
Self-touch	Async	2.08	2.10
Self-touch	Sync	2.54	2.48
I felt as if I was touching someone else's body	Desync	0.71	1.55
I felt as if I was touching someone else's body	Async	0.75	1.62
I felt as if I was touching someone else's body	Sync	0.50	1.29
Passivity experience	Desync	3.96	1.97
Passivity experience	Async	2.71	2.14
Passivity experience	Sync	1.67	1.97
PH	Desync	2.08	1.82
PH	Async	1.67	1.81
PH	Sync	0.67	1.55
Control (I felt as if I had no body)	Desync	0.67	1.09
Control (I felt as if I had no body)	Async	0.42	0.88
Control (I felt as if I had no body)	Sync	0.33	0.64
Control (I felt as if I had two right hands)	Desync	0.83	1.40
Control (I felt as if I had two right hands)	Async	0.75	1.51
Control (I felt as if I had two right hands)	Sync	0.63	1.06

Table S5. Mean ratings for all questions used in the mock scanner study

*Movement analysis*

To ensure that riPH were not due to any movement differences across experimental conditions, we calculated the total distance that each participant moved the front-robot. Analysis revealed no significant difference between the total distance covered in the synchronous versus asynchronous condition (permutation p-value = 0.96).

*Supplementary S18: fMRI behavioral study 2.1: Questionnaire results*

The questionnaire included only the first six questions of the mock scanner pilot study: “I felt as if I was touching my body”, “I felt as if I was touching someone else’s body”, “I felt as if I had no body”, “I felt as if I had two right hands”, “I felt as if someone else was touching my body” and “I felt as if a presence or someone was behind me”.

*Passivity experience*

Participants reported stronger passivity experiences in the asynchronous condition compared to the synchronous condition (main effect of Synchrony, permutation p-value < 0.001; Table S6).

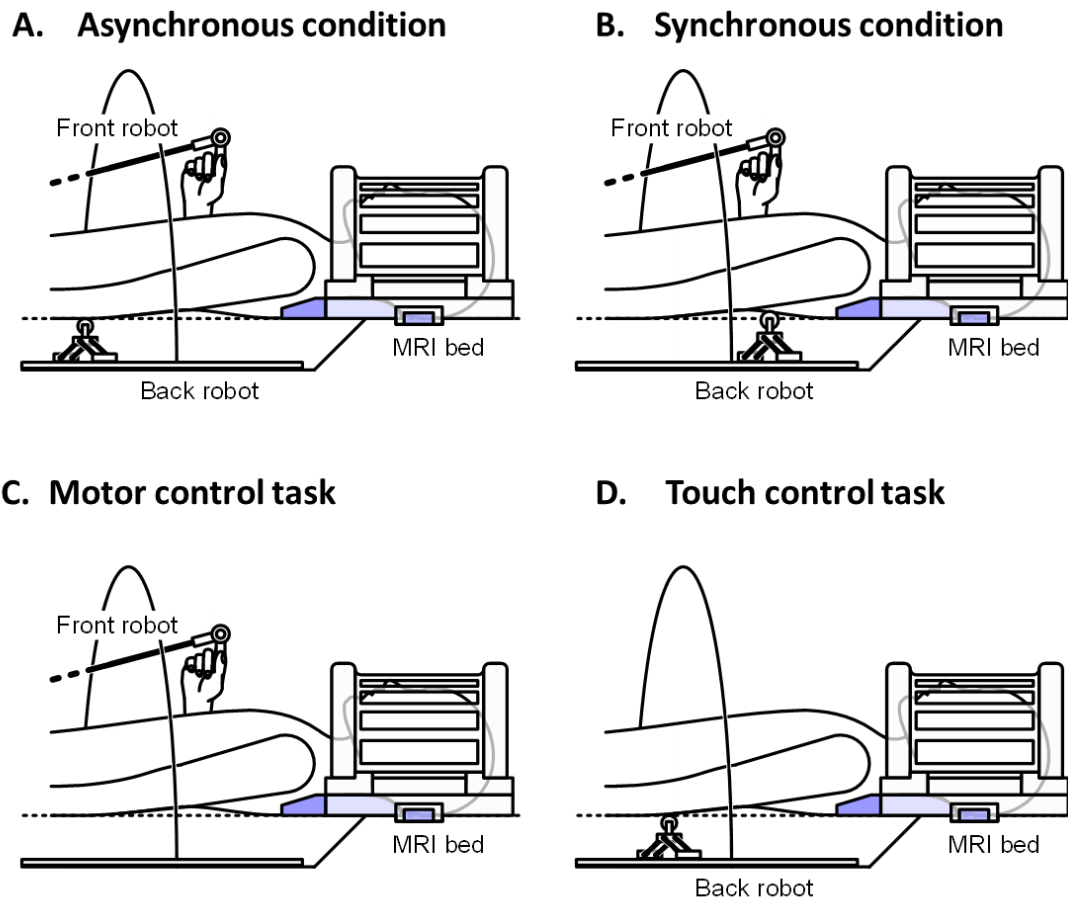
Question	Synchrony	Mean	Standard deviation
Self-touch	Async	3.28	2.25
Self-touch	Sync	3.72	2.23
I felt as if I was touching someone else's body	Async	1.12	1.81
I felt as if I was touching someone else's body	Sync	0.88	1.59
Passivity experience	Async	3.40	2.25
Passivity experience	Sync	2.08	2.14
PH	Async	1.68	1.86
PH	Sync	1.04	1.65
Control (I felt as if I had no body)	Async	1.04	1.62
Control (I felt as if I had no body)	Sync	0.80	1.76
Control (I felt as if I had two right hands)	Async	0.56	1.33
Control (I felt as if I had two right hands)	Sync	0.36	0.76

Table S6. Mean ratings for all questions of the fMRI questionnaire



*Supplementary S19: riPH-network in healthy subjects*

We also analyzed fMRI data recorded in two control conditions that allowed us to control for two aspects of sensorimotor stimulation that are not related to PH and determined the brain regions that were commonly activated by either of the sensorimotor conditions (synchronous, asynchronous; Fig.S3A-B) vs. the control conditions (motor, touch; Fig.S3C-D). In the motor control condition, participants were asked to repeatedly move the front-robot with their right hand but did not receive any tactile feedback on their back (Fig.S3C). In the touch control condition, participants received touch feedback on their backs, but were not performing any movement with their right hand (the back-robot was actuated by a previously recorded movement sequence) (Fig.S3D).

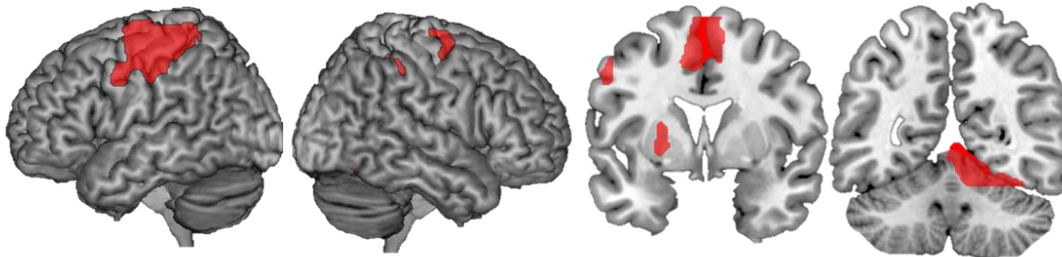


**Figure S3. The different conditions assessed with MR-compatible robotic system.** The MR robotic system consisted of two parts: a front robot composed by a carbon fibre rod with which the participants performed the movement in 2 directions (X and Z) and a back robot that reproduced the movement of the front robot in the back of the participants. Different conditions were tested: (A) an asynchronous condition where the back robot was delayed of 500 ms compared to the front robot, (B) a synchronous condition in which no delay was introduced between the front robot and the back robot. In addition, in the fMRI study, two conditions were added: a motor control task, in which the participant was just performing the movements without any tactile feedback on the back (C) and a touch control task in which the participant only received the tactile feedback on the back without any movement (D). The contact part is composed of a roller effector that enables to touch the back of the participant. Two ultrasonic motors (USR60-E3NT, Shinsei) enable the effector to move. A home-made mattress was designed with an aperture to allow robotic stroking on the participant's back, while lying down.

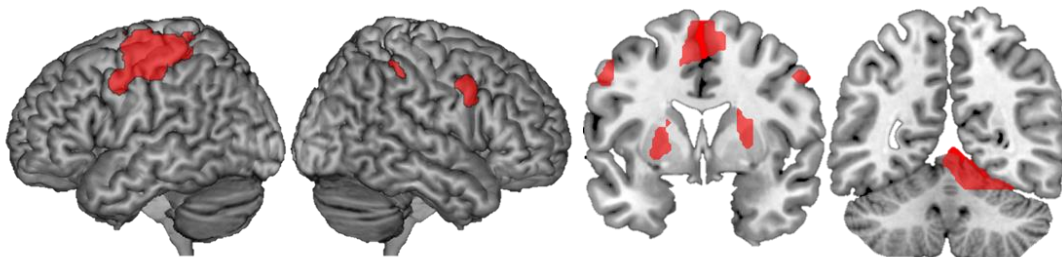
*Supplementary S20: riPH are associated with activation of two sensorimotor networks in healthy subjects*

Fig.S4B shows the activations when comparing the asynchronous condition with the motor plus touch control condition, revealing a large cortical-subcortical network including the left sensorimotor cortex (including adjacent parts of premotor cortex and superior parietal cortex), bilateral SMA and adjacent parts of cingulate cortex, bilateral putamen, the right ventral premotor cortex, the right inferior parietal cortex (IPL) and the right cerebellum (Table S8). Similar regions were found for the contrast between the synchronous and the motor plus touch control condition (Fig.S4A; Table S8). The synchronous versus asynchronous contrast did not show any significant brain activations. We also correlated riPH ratings or passivity experiences with brain regions activated more during the asynchronous condition compared to the synchronous condition and found no significant correlation (all p-values > 0.05 after correcting for multiple comparisons). Activations from the conjunction analysis (Fig.2E main text) also did not correlate with PH ratings or passivity experiences (all p-values > 0.05 after correcting for multiple comparisons).

**A. Sync > motor + touch**



**B. Async > motor + touch**



**Figure S4. Robot-induced PH network.** **A.** Brain regions responding to spatial sensorimotor conflict between the right-hand movement and the feedback on the back of the participants. **B.** Brain regions reflecting the spatio-temporal sensorimotor conflict.

Regions	Voxels	BA	MNI			Peak level t value	Cluster-level p value FWE
			x	y	z		
R. medial prefrontal cortex (mPFC)	770	8/9/32	5	41	47	6.2	0.001
R. ventral premotor cortex (vPMC)/ Inferior Frontal Gyrus (Opercularis and triangularis) (IFG)	708	45/48	51	18	29	5.53	0.001
R. Anterior Insula (Ins)	566	47	36	24	-2	4.78	0.004
R. posterior Middle Temporal Gyrus (pMTG)	479	37	54	-54	0	4.99	0.01

**Table S7. Spatio-temporal sensorimotor conflict PH regions.** Regions activated during the contrast asynchronous > synchronous.

Regions	Voxels	BA	MNI coordinates			Peak level t value	Cluster-level p value FWE
			x	y	z		
<b>Asynchronous &gt; motor + touch</b>							
L. Sensorimotor cortex (primary motor cortex (M1), primary somatosensory cortex (SI), supplemental motor area (SMA), middle cingulate cortex (MCC), Superior parietal lobe (SPL))	9894	2/3/4/6/40	-26	-16	58	7.93	p<0.001
R. Cerebellum	2840		11	-58	-14	7.99	p<0.001
R. Putamen / Globus pallidum	599		22	3	8	6.33	p<0.01
L. Putamen / Globus pallidum	560		-22	1	5	6.07	p<0.01
R. Inferior parietal lobe/supramarginal gyrus (SMG)	503	2/40	41	-37	47	4.1	p<0.01
R. ventral premotor cortex	357	6	55	8	38	5.58	p<0.05
<b>Synchronous &gt; motor + touch</b>							
L. Sensorimotor cortex (primary motor cortex (M1), primary somatosensory cortex (SI), supplemental motor area (SMA), middle cingulate cortex (MCC), Superior parietal lobe (SPL))	12843	2/3/4/6/40	-25	-18	57	8.85	p<0.001
R. Cerebellum	3057		12	-57	-14	8.17	p<0.001
R. Inferior parietal lobe/supramarginal gyrus (SMG)	600	2/40	40	-34	45	4.8	p<0.01
L. Putamen / Globus pallidum	449		-22	0	5	7.34	p<0.05
R. Superior frontal gyrus / dorsal premotor cortex	385	6	28	-8	65	4.62	p<0.05
<b>Conjunction between the asynchronous &gt; motor + touch and synchronous &gt; motor + touch</b>							
L. Sensorimotor cortex (primary motor cortex (M1), primary somatosensory cortex (SI), middle cingulate cortex (MCC), Superior parietal lobe (SPL))	12026	2/3/4/6/40	-26	-18	57	9.99	p<0.001
Supplemental motor area (SMA)		6	-5	-6	56	8.32	p<0.001
R. Cerebellum	2687		11	-57	-14	9	p<0.001
R. Inferior parietal lobe/supramarginal gyrus (SMG)	593	2/40	40	-34	45	4.59	p<0.01
L. Putamen / Globus pallidum	517		-23	0	4	6.44	p<0.01

**Table S8. Robotically induced brain activations.**

*Study 2.2: Common PH-network for sPH and riPH*

*Supplementary S21: Lesion network mapping analysis*

In order to assess the functional network derived from PH, we applied lesion network mapping<sup>22</sup>. This method has the advantage of not requiring functional neuroimaging data from patients and of accounting for the possibility that symptoms may arise from remote brain regions connected to the lesioned brain region rather than the damaged area itself<sup>23,24</sup>. The PH-lesions reported by Blanke and colleagues<sup>21</sup> were used as seed

ROIs except one lesion which was covering the whole brain, resulting in eleven lesions for the analysis.

#### *fMRI acquisition*

Resting state and T1-weighted structural data from 151 healthy participants obtained from the publicly available Enhanced Nathan Kline Institute Rockland Sample<sup>25</sup> was used. All participants were right-handed and aged between 19 to 40 years ( $25.8 \pm 5.5$  years, 83 females). Scans were acquired with a 3T Siemens Magnetom TrioTim syngo. For the resting state data, a multiband EPI sequence was used (multiband factor = 4, 64 continuous slices, TR = 1.4 s, TE = 30 ms, flip angle =  $65^\circ$ , slice thickness = 2 mm) and 404 scans were collected. For each participant, an anatomical image was recorded using a T1-weighted MPRAGE sequence (TR = 1.9 s, TE = 2.52 ms, Inversion time = 900 ms, flip angle =  $9^\circ$ , 1 mm isotropic voxels, 176 slices per slab and FOV = 250 mm).

#### *Data analysis*

The pre-processing steps were performed using SPM12 toolbox (Wellcome Department of Cognitive Neurology, Institute of Neurology, UCL, London, UK) in Matlab (R2016b, Mathworks). The first four functional scans were discarded from the analysis to allow for magnetic saturation effects: the analysis was performed on the 400 remaining scans. Slice timing correction and spatial realignment was applied to individual functional images. The anatomical image was then co-registered with the mean functional image and segmented into grey matter, white matter and cerebrospinal fluid tissue. The functional and anatomical scans were then normalized to the Montreal Neurological Institute space (MNI space). Finally, the functional scans were spatially smoothed with a 5 mm full-width at half-maximum isotropic Gaussian kernel.

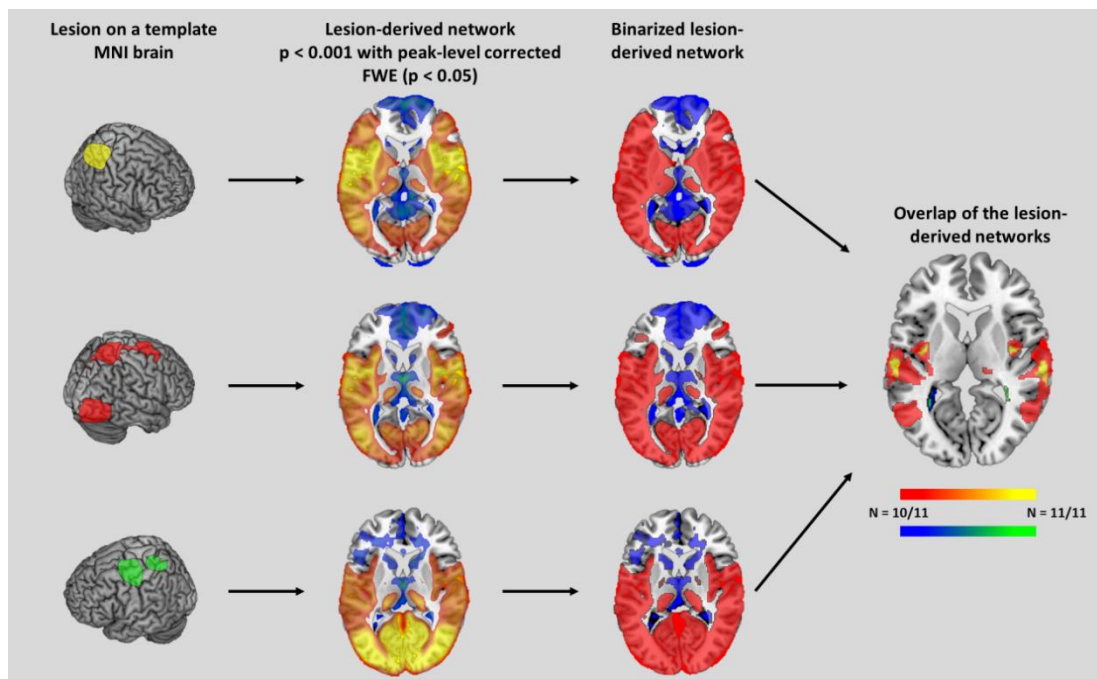


**Figure S5. Lesion network mapping analysis.** The steps of the lesion network mapping analysis are shown: first the lesion is mapped to a template brain, then this lesion is used as a seed ROI in a resting state functional analysis performed on a normative database. The network obtained for each lesion is thresholded at  $p < 0.001$  with peak level corrected FWE ( $p < 0.05$ ). All the lesions-derived networks are binarized and overlap to identify the regions functionally connected to most of the lesions.

#### *Supplementary S22: Lesion network mapping: control analysis*

To exclude that these regions are involved in hallucinations more generally, the same method was applied to a control group of eleven patients suffering from structured visual hallucination (VH)<sup>26</sup>. The sPH-network was defined as those PH regions that were not overlapping with the visual hallucination derived network.

In addition, we determine whether the riPH-network was specifically connected to the lesions causing PH as opposed to the lesions causing VH. Therefore, for each of the 126 subjects in the database, the regionally-averaged resting-state BOLD signal time courses were extracted from each PH and VH lesion and riPH-network (Fig.2D-E in the main text) and were pairwise correlated (Fisher Z-transformed Pearson correlation) to establish the functional connectivity matrix. For each lesion location, we averaged the connectivity measures for the riPH-networks. Then, we compared statistically the connectivity between the two groups (PH vs. VH) using two sample t-test.

*Supplementary S23: Results of lesion network mapping control analysis*

To exclude that these regions are involved in hallucinations more generally, the same method was applied to a control group of eleven patients suffering from structured visual hallucination (VH)<sup>26</sup>, revealing a VH derived network consisting of mostly distinct regions (in bilateral TPJ, dorsal premotor cortex (dPMC), the left middle and superior occipital cortex, left thalamus and hippocampus (Table S11), as well as three common regions (bilateral posterior to middle STG and adjacent parts of parietal cortex; left PMC). Further analysis showed that the brain lesions causing sPH were more strongly connected with the riPH-network (as defined in healthy participants; study2.1) than the lesions causing visual hallucinations (difference between the two groups of lesions:  $t(18)=2.74$ ,  $p\text{-value}=0.013$ , Fig.S6). A sPH-network was defined as those PH regions that were not overlapping with the visual hallucination derived network.

Regions	Overlap	Hemisphere	Voxels	BA	MNI coordinates		
					x	y	z
<b>Positive correlation</b>							
Superior temporal gyrus (STG)	11	Right	770	22	62	25	13
	11	Left	582	22	-58	-29	13
Insula	11	Right	124	48	37	-6	12
	11	Left	135	48	-37	-7	9
	11	Left	81	48	-35	-9	-8
Postcentral sulcus	11	Left	111	48	-58	-16	19
Middle cingulate cortex (MCC)	11	Right	53		9	-11	38
	11	Left	100		-9	-11	37
Inferior frontal operculum/ ventral premotor cortex (vPMC)	11	Right	86	45/48	42	17	23
Temporo-parietal junction (TPJ): STG, MTG (only right), supramarginal gyrus (SMG), rolandic operculum, vPMC	10	Right	7153	21/22/48	56	-18	18
	10	Left	5318	21/22/48	-52	-16	16
Fusiform area	10	Right	2842	19/37	37	-52	-16
	10	Left	2916	19/37	-36	-53	-15
Middle temporal gyrus (MTG)	10	Left	1292	37	-48	-62	11
Dorsal premotor cortex (dPMC)	10	Right	370	6	44	-5	53
	10	Left	308	6	-40	-8	51
Amygdala	10	Right	295	36	29	3	-24
	10	Left	112	36	-26	2	-26
Thalamus	10	Right	126		15	-25	2
	10	Left	120		-12	-27	-2
Cerebellum	10	Left	107		-10	-65	-46
Hippocampus	10	Righth	70		23	-36	-2
	10	Left	90		-20	-37	-1
Putamen	10	Right	69		36	-10	-8
Cuneus	10	Right	68	18	17	-70	26
	10	Left	68	18	-14	-72	22
Supplemental motor area (SMA)/Superior frontal gyrus	10	Left	58	6	-18	-8	68
<b>Negative correlation</b>							
Caudate	10	Right	70		17	-13	27

**Table S9. Symptomatic PH-derived network.** Brain areas that showed positive and negative correlation with most of the lesions (100% or 90% of overlap). Regions in the white matter were not reported.

Regions	Overlap	Hemisphere	Voxels	BA	MNI coordinates		
					x	y	z
<b>Positive correlation</b>							
Superior temporal cortex (TPJ)	10	Right	734	22/48	60	-14	9
	10	Left	148	42/22	-61	-32	14
	10	Left	147	22	-59	-9	-8
	10	Left	92	48	-51	-21	5
Middle and superior occipital cortex/ Inferior parietal lobule	10	Left	326	39/19	-38	-70	28
Hippocampus/parahippocampus	10	Left	118	20	-27	-31	-14
Thalamus/lingual area	10	Left	108	27	-14	-30	-2
Precentral cortex (dPMC)	10	Right	74	6	53	-3	44
	10	Left	51	6	-45	-7	51

**Table S10. VH-derived network.** Brain areas that showed positive correlation with 90 % of the VH lesion locations (only the regions in the grey matter are reported). There was no overlap for all the lesions.

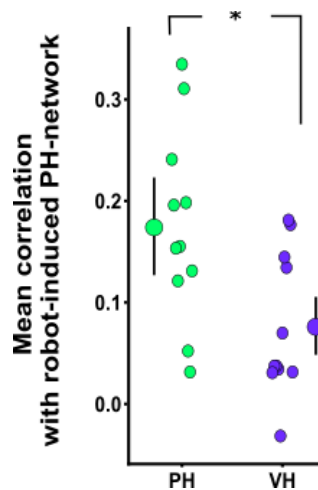


**Figure S6. Lesion connectivity with the robot-induced PH-network.** Lesions causing PH had greater functional connectivity with the riPH-network compared to VH lesions. \* p-value<0.05.

*Supplementary S24: Common PH-network*

The common PH-network (cPH-network) was composed of regions overlapping between the sPH-network and the riPH-network and consisted in three anatomical regions in right IFG, right pMTG and two almost continuous PMC clusters (considered as one ROI for the following analysis).



*Study 3.1: Disrupted functional connectivity in cPH-network accounts for sPH in patients with Parkinson's disease*

*Supplementary S25: Participants*

Data from thirty participants were analyzed in this study. All patients were prospectively recruited from a sample of outpatients regularly attending to the Movement Disorders Clinic at Hospital de la Santa Creu i Sant Pau (Barcelona) based on the fulfilling of MDS new criteria for PD with minor hallucinations (PD-PH) — sense of presence and/or passage hallucinations (n=15) — and without hallucinations (PD-nPH; n=15). Informed consent to participate in the study was obtained from all participants. The study was approved by the local ethics committee. The same dataset has been previously used in <sup>27</sup>. Patients were diagnosed by a neurologist with expertise in movement disorders. Each patient was interviewed regarding years of formal education, disease onset, medication history, current medications, and dosage (levodopa daily dose). Motor status and stage of illness were assessed by the MDS-UPDRS-III<sup>28</sup>. The PD-PH and PD-nPH groups did not differ for age, disease duration, dopaminergic doses, motor severity, cognition, depression, anxiety, and apathy (Table S11). All participants were on stable doses of dopaminergic drugs during the 4 weeks before inclusion. Patients were included if the hallucinations remained stable during the 3 months before inclusion in the study. No participant had used or was using antipsychotic medication.

	<b>PD-PH (N = 15)</b>	<b>PD-nPH (N = 15)</b>	<b><i>p-values</i></b>
Age	70.9 ± 1.5	65.9 ± 1.94	0.06
Gender	9 (M)	10 (M)	0.7 ( $\chi^2$ )
MoCA	25.3 ± 0.8	24 ± 1	0.3
PD-CRS	91.5 ± 4	94.2 ± 4.1	0.67
PD-CRS (frontal)	62.9 ± 3.8	65.7 ± 3.9	0.62
PD-CRS (posterior)	28.7 ± 0.4	28.5 ± 0.4	0.83
UPDRS III	21.7 ± 2.4	25.3 ± 2.03	0.2
LEDD (mg/day)	722.1 ± 73.8	581 ± 80.2	0.2
Dopamine agonists (mg/day)	151.3 ± 31.7	151.3 ± 31.7	0.9
Disease Duration (years)	5.3 ± 0.9	3.7 ± 0.6	0.2

**Table S11. Clinical variables.**

Exclusion criteria were history of major psychiatric disorders, cerebrovascular disease, conditions known to impair mental status other than PD, and the presence of factors that prevented MRI scanning (e.g. claustrophobia, MRI non-compatible prosthesis). Patients with focal abnormalities in MRI or non-compensated systemic diseases (e.g. diabetes, hypertension) were also excluded. In patients with motor fluctuations, cognition was examined during the “on” state. All participants were on stable doses of dopaminergic drugs during the 4 weeks before inclusion. Patients were included if the hallucinations remained stable during the 3 months before inclusion in the study. No participant had used or was using antipsychotic medication. All subjects had normal or corrected-to-normal vision. Informed consent to participate in the study was obtained from all participants. The study was approved by the local ethics committee.

Presence and type of minor hallucinations was assessed using the Hallucinations and Psychosis item of the MDS-UPDRS Part I. Participants with a sense of presence and/or passage hallucinations at least weekly during the last month were categorized as minor hallucinations. Cognitive functions were assessed by the Parkinson's Disease-Cognitive Rating Scale (PD-CRS)<sup>29</sup>. Apathy was assessed with the Starkstein Apathy Scale<sup>5</sup>.

We favored the analysis of resting state fMRI over performing the robotic stimulation within the MRI, because for PD patient performing long motor task (as required by the MRI to have a good signal to noise ratio) can be particularly tiring, and therefore exacerbating the tremor. Thus, the probability to have poor data quality and a high rate of patient willing to interrupt the experiment prematurely was too high.

#### *Supplementary S26: Image acquisition & Image processing*

MRI scans were acquired with a 3T Philips Achieva. T1 weighted scans were obtained using a Magnetization Prepared Rapid Acquisition Gradient Echo (MPRAGE) sequence (TR = 500 ms, TE = 50 ms, flip angle = 8, field of view [FOV] = 23 cm with in-plane resolution of 256 × 256 and 1mm slice thickness). Resting-state functional MRI images were collected using an 8-minute sequence (TR = 2000 ms, TE = 30 ms, flip angle = 78, FOV = 240 mm, slice thickness = 3 mm).

Data analysis and standard pre-processing was performed using the functional connectivity toolbox CONN (<https://www.nitrc.org/projects/conn/>) and Statistical

Parametrical Mapping (SPM 12) (<http://www.fil.ion.ucl.ac.uk/spm/>) for Matlab. Functional images were corrected for slice time and motion, co-registered with a high-resolution anatomical scan, normalised into Montreal Neurological Institute (MNI) space, resampled to  $2 \times 2 \times 2 \text{ mm}^3$ , and smoothed with an  $8 \text{ mm}^3$  full width at half maximum (FWHM) Gaussian kernel for each subject. To estimate the excessive movement, the mean frame-wise displacement (FD) during the scanning was estimated with the exclusion threshold of 0.5 mm. The groups did not differ by the movement over the scanning period ( $t = 1.18$ ,  $p = 0.12$  with the mean FD of  $0.29 \pm 0.15 \text{ mm}$  and  $0.23 \pm 0.16 \text{ mm}$  for PD-PH and PD-nPH groups respectively) and did not reach the excessive movement threshold. Following the standard pipeline for confound removal of the CONN toolbox, the individual time courses of the segmented white matter and cerebrospinal fluid, the 6 motion parameters with rigid body transformations and their first-order derivatives, and global signal time courses were extracted and regressed out of the data. Regressions were performed for the entire time-series. The blood oxygenation level dependent (BOLD) signal data were passed through a band filter of 0.01-0.1 Hz. A whole-brain grey matter mask in MNI space restricted data analysis.

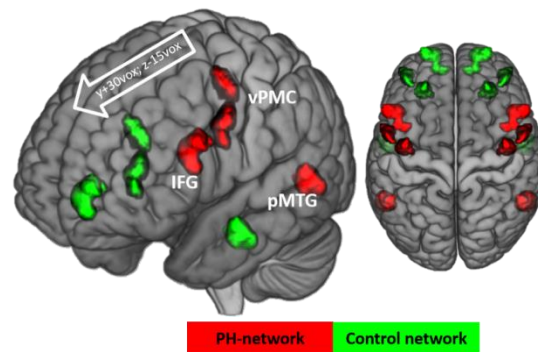


**Figure S7.** Control regions for the resting state fMRI analysis of PD patients. Bilateral PH-network areas (red) shifted forward (green): Inferior frontal gyrus (IFG)  $x \pm 20$   $y + 30$   $z - 15$ ; ventral premotor cortex (vPMC)  $x \pm 10$   $y + 30$   $z - 15$ ; posterior middle temporal gyrus (pMTG)  $x$   $y + 30$   $z - 15$ .

Connections	Variable Importance
Left-IFG - Left pMTG	1
Left pMTG - Right vPMC	0.913
Left IFGlh - Right vPMC	0.797
Left pMTG - Right pMTG	0.710
Left IFG - Right pMTG	0.652
Left IFGlh - Left vPMC	0.348
Right IFG - Right vPMC	0.333
Right pMTG - Right vPMC	0.333
Left pMTG - Left vPMC	0.319
Right IFG - Right pMTG	0.225
Right pMTG - Left vPMClh	0.203
Left vPMC - Right vPMC	0.188
Left IFG - Right IFG	0.174
Right IFG - Left vPMC	0.123
Right IFG - Left pMTG	0

**Table S12.** Contribution of each connectivity to the classification of PD-PH, values scaled between zero and one.

*Supplementary References*

1. Nasreddine, Z. S. *et al.* The Montreal Cognitive Assessment, MoCA: a brief screening tool for mild cognitive impairment. *J Am Geriatr Soc* **53**, 695–699 (2005).
2. Carson, N., Leach, L. & Murphy, K. J. A re-examination of Montreal Cognitive Assessment (MoCA) cutoff scores. *International Journal of Geriatric Psychiatry* **33**, 379–388 (2018).
3. Tomlinson, C. L. *et al.* Systematic review of levodopa dose equivalency reporting in Parkinson's disease. *Movement Disorders* **25**, 2649–2653 (2010).
4. Weintraub, D. *et al.* Questionnaire for Impulsive-Compulsive Disorders in Parkinson's Disease-Rating Scale. *Mov. Disord.* **27**, 242–247 (2012).
5. Starkstein, S. E. *et al.* Reliability, validity, and clinical correlates of apathy in Parkinson's disease. *J Neuropsychiatry Clin Neurosci* **4**, 134–139 (1992).
6. Loewy, R. L., Bearden, C. E., Johnson, J. K., Raine, A. & Cannon, T. D. The prodromal questionnaire (PQ): preliminary validation of a self-report screening measure for prodromal and psychotic syndromes. *Schizophr. Res.* **77**, 141–149 (2005).
7. de Chazeron, I. *et al.* Validation of a Psycho-Sensory hAllucinations Scale (PSAS) in schizophrenia and Parkinson's disease. *Schizophr. Res.* **161**, 269–276 (2015).
8. Cilia, R. *et al.* Dopamine dysregulation syndrome in Parkinson's disease: from clinical and neuropsychological characterisation to management and long-term outcome. *J. Neurol. Neurosurg. Psychiatry* **85**, 311–318 (2014).
9. Blanke, O. *et al.* Report Neurological and Robot-Controlled Induction of an Apparition. *Current Biology* **24**, 2681–2686 (2014).
10. Hara, M. *et al.* A novel approach to the manipulation of body-parts ownership using a bilateral master-slave system. in *2011 IEEE/RSJ International Conference on Intelligent Robots and Systems* 4664–4669 (2011). doi:10.1109/IROS.2011.6094879.
11. Fénelon, G., Soulas, T., De Langavant, L. C., Trinkler, I. & Bachoud-Lévi, A.-C. Feeling of presence in Parkinson's disease. *J Neurol Neurosurg Psychiatry* **82**, 1219–1224 (2011).
12. Bates, D., Mächler, M., Bolker, B. & Walker, S. Fitting Linear Mixed-Effects Models Using lme4. *Journal of Statistical Software* **67**, 1–48 (2015).
13. Kuznetsova, A., Brockhoff, P. B. & Christensen, R. H. B. lmerTest Package: Tests in Linear Mixed Effects Models. *Journal of Statistical Software* **82**, 1–26 (2017).
14. Ravina, B. *et al.* Diagnostic criteria for psychosis in Parkinson's disease: Report of an NINDS, NIMH Work Group. *Movement Disorders* **22**, 1061–1068 (2007).
15. Lenka, A., Pagonabarraga, J., Pal, P. K., Bejr-Kasem, H. & Kulisvesky, J. Minor hallucinations in Parkinson disease: A subtle symptom with major clinical implications. *Neurology* (2019) doi:10.1212/WNL.0000000000007913.
16. Ffytche, D. H. *et al.* The psychosis spectrum in Parkinson disease. *Nat Rev Neurol* **13**, 81–95 (2017).
17. Pagonabarraga, J. *et al.* Minor hallucinations occur in drug-naive Parkinson's disease patients, even from the premotor phase. *Mov. Disord.* **31**, 45–52 (2016).
18. Kataoka, H. & Ueno, S. Predictable Risk Factors for the Feeling of Presence in Patients with Parkinson's Disease. *Mov Disord Clin Pract* **2**, 407–412 (2015).
19. Hara, M. *et al.* A novel manipulation method of human body ownership using an fMRI-compatible master-slave system. *Journal of Neuroscience Methods* **235**, 25–34 (2014).
20. Oldfield, R. C. The assessment and analysis of handedness: The Edinburgh inventory. *Neuropsychologia* **9**, 97–113 (1971).
21. Blanke, O. *et al.* Neurological and Robot-Controlled Induction of an Apparition. *Curbio* **24**, 2681–2686 (2014).
22. Boes, A. D. *et al.* Network localization of neurological symptoms from focal brain lesions. *Brain* **138**, 3061–3075 (2015).
23. Boes, A. D. *et al.* Network localization of neurological symptoms from focal brain lesions. *Brain* **138**, 3061–3075 (2015).

24. Fox, M. D. Mapping Symptoms to Brain Networks with the Human Connectome. *New England Journal of Medicine* **379**, 2237–2245 (2018).
25. Nooner, K. B. *et al.* The NKI-Rockland Sample: A Model for Accelerating the Pace of Discovery Science in Psychiatry. *Front Neurosci* **6**, (2012).
26. Heydrich, L. & Blanke, O. Distinct illusory own-body perceptions caused by damage to posterior insula and extrastriate cortex. *Brain* **136**, 790–803 (2013).
27. Bejr-Kasem, H. *et al.* Disruption of the default mode network and its intrinsic functional connectivity underlies minor hallucinations in Parkinson's disease. *Mov. Disord.* **34**, 78–86 (2019).
28. Movement Disorder Society Task Force on Rating Scales for Parkinson's Disease. The Unified Parkinson's Disease Rating Scale (UPDRS): status and recommendations. *Mov. Disord.* **18**, 738–750 (2003).
29. Pagonabarraga, J. *et al.* Parkinson's disease-cognitive rating scale: a new cognitive scale specific for Parkinson's disease. *Mov. Disord.* **23**, 998–1005 (2008).

## Chapter 4: Individuals with the 22q11.2 deletion syndrome show lack of sensitivity to sensorimotor conflicts

**Authors:** Eva Blondiaux<sup>1</sup>, Jevita Potheegadoo<sup>1</sup>, Giedre Stripeikyte<sup>1</sup>, Laurent Jenni<sup>1</sup>, Johanna Maeder<sup>2</sup>, Virginie Pouillard<sup>2</sup>, Fosco Bernasconi<sup>1</sup>, Corrado Sandini<sup>2</sup>, Eva Micol<sup>2</sup>, Maude Schneider<sup>2</sup>, Stephan Eliez<sup>2</sup>, and Olaf Blanke<sup>1,3</sup>.

**Status:** in preparation

### *Affiliations*

**1.** Laboratory of Cognitive Neuroscience, Center for Neuroprosthetics and Brain Mind Institute, School of Life Sciences, Ecole Polytechnique Fédérale de Lausanne (EPFL), Geneva, Switzerland. **2.** Developmental Imaging and psychopathology Lab, Department of Psychiatry, University of Geneva School of Medicine, Geneva, Switzerland. **3.** Department of Neurology, University of Geneva, Switzerland

**Personal contributions:** Experimental design, data collection, data analysis and writing.

### **Acknowledgments**

All the authors thank the psychologists from the DIPL lab and Dr. Mathilde Millot for their assistance in testing the participants. We kindly thank Mrs. Atena Fadaejouybari for making the illustration of the robotic setup. We thank all the families for their motivation in participating in this study.

## Abstract

**Objective:** The 22q11.2 deletion syndrome (22q11DS) represents one of the highest risk factors for developing schizophrenia. About 30% of individuals with 22q11DS develop symptoms such as hallucinations, thought disorders and passivity experiences (PE) including loss of agency (LoA). These symptoms might arise from abnormal sensorimotor processing leading to the misattribution of self-generated actions to external sources.

**Methods:** We used a robotic device generating sensorimotor conflicts to safely induce mild to moderate subjective experiences that are phenomenologically similar to psychotic symptoms such as presence hallucination (PH), PE and LoA. We assessed the sensitivity of 22q11DS individuals to sensorimotor conflicts and their proneness in experiencing robot-induced PH and related PE as compared to age-matched controls. Also, we evaluated the functional connectivity at rest within a network recently associated with PH (bilateral ventral premotor cortex (vPMC), inferior frontal gyrus (IFG) and posterior middle temporal gyrus (pMTG)).

**Results:** We showed a lack of sensitivity in sensorimotor modulation for LoA in 22q11DS individuals compared to controls. With varying degrees of sensorimotor conflicts, 22q11DS individuals again showed a lack of delay dependency in experiencing robot-induced PH and PE. We found reduced functional connectivity between the right pMTG and right IFG, vPMC and left pMTG. Connectivity between the right pMTG and right IFG significantly correlated to performance at the semantic verbal fluency task.

**Conclusions:** The present study highlights a fronto-temporal disconnection in 22q11DS subjects asymptomatic for psychosis, and a lack of sensorimotor modulation compared to controls.

**Keywords:** velocardiofacial syndrome; functional connectivity; presence hallucination; passivity experiences; loss of agency; executive dysfunctions.



## Introduction

The 22q11.2 microdeletion syndrome (22q11DS or velocardiofacial syndrome) is a well-established genetic condition that gives rise to very heterogeneous clinical manifestations. Important developmental delays, cognitive deficits and neuropsychiatric disorders evince structural and functional brain abnormalities in individuals with 22q11DS (1,2). Importantly, 22q11DS represents one of the highest genetic risk factors for developing schizophrenia (3–5). Up to 60% of the individuals with 22q11DS have subthreshold psychotic symptoms as from late childhood or early adolescence, and 25% to 30% of the individuals develop well-structured symptoms such as hallucinations, delusions or passivity symptoms (thought disorders, loss of agency (LoA) or somatic passivity) (6–8).

One possible explanation for the occurrence of hallucinations and passivity symptoms in schizophrenia resides in the fronto-temporal disconnection hypothesis supported by the forward model (9–11). This model posits that deficits in self-monitoring are linked to abnormal sensorimotor integration and predictions in schizophrenia. The underlying mechanism is based on the comparison between the expected (efference copy) and the actual sensory outcome of self-generated actions. When the expected and the actual sensory outcome match, the sensory signals are attenuated and the corresponding feedback is experienced as self-generated. However, when incongruent, sensory signals fail to attenuate, resulting in the misattribution of one's own actions to external sources. Such discrepancy can lead to abnormal perceptions such as hallucinations and passivity experiences (e.g., LoA, feeling of an alien presence) (10,12–14).

In 22q11DS, deficits in sensorimotor processing have been studied in the visual and auditory domain, and mainly linked with deficits in executive functions (working memory, visual attention) (15,16). However, the potential link between sensorimotor dysfunction, hallucinations and passivity symptoms is sparsely studied in 22q11DS. Only a few studies examined the relationship between deficits in self-monitoring in 22q11DS, showing that adolescents with the microdeletion exhibit source monitoring (i.e., attributing the origin to mental events) impairment when performing an action monitoring paradigm and a speech-monitoring task (17,18). The pattern of results corresponds to what is observed in patients with schizophrenia, but these studies did not find any significant correlations between deficits in self-monitoring and

schizotypal symptoms (e.g., thought disorders, unusual perceptual experiences, which are similar to passivity symptoms). However, the link between sensorimotor processing and occurrence of psychotic symptoms in 22q11DS has not been addressed experimentally.

On the neural level, 22q11DS individuals present abnormal structural and functional connectivity, which can be indicative of an early expression of prodromal or clear psychotic symptoms. Studies mostly show alterations in resting state (rs) functional connectivity in the default mode network (DMN), namely a reduction of connectivity between the anterior and posterior cingulate cortex (ACC and PCC) and the left superior frontal gyrus region (19,20). Altered connectivity to ACC was linked to the presence of psychotic symptoms (21,22). Still, little is known on the neural correlates associated with self-monitoring in 22q11DS.

Recently, we have designed a non-invasive experimental paradigm during which a specific hallucination - the presence hallucination (PH) was safely induced in healthy and clinical populations (23–25) by using a robotic device generating sensorimotor conflicts. PH is the sensation that another person is nearby when no one is actually present and is frequently observed in epilepsy, Parkinson's disease, schizophrenia or bereavement (26–28). PH is suggested to be associated with passivity symptoms of schizophrenia (29) and recent work (24,25) demonstrated that its study is feasible in controlled experimental settings. These studies showed that it is possible to create disturbances in self- or source monitoring and sensorimotor integration of own bodily signals to induce PH and associated passivity experiences (PE) such as LoA. Moreover, we defined a PH-network comprising mainly fronto-temporal areas bilaterally (i.e., posterior middle temporal gyrus (pMTG), inferior frontal gyrus (IFG) and the ventral premotor cortex (vPMC)) obtained from the combination of brain regions from healthy subjects experiencing robot-induced PH (riPH) and a network derived from neurological patients with brain lesions causing PH (24).

Do individuals with the 22q11DS have symptomatic PH? To date, the occurrence of PH in 22q11DS is not documented. To answer this question, we have studied PH under laboratory-controlled conditions in 22q11DS. We aimed at investigating whether there is a causal link between sensorimotor integration, self-monitoring and the occurrence of psychotic symptoms. First, we tested the sensitivity of 22q11DS subjects to varying

degrees of robot-induced sensorimotor conflicts, and their proneness to experience riPH and related PE similar to other positive symptoms. We expected individuals with 22q11DS to show higher sensitivity to sensorimotor conflicts than healthy age-matched controls, with an earlier riPH occurrence due to less sensory attenuation. Second, we analyzed the rs functional connectivity of the PH-network in individuals with 22q11DS and its relationship with riPHs. We predicted reduced functional connectivity within the PH-network based on our recent study on psychotic patients with passivity symptoms showing lower functional connectivity within this network (Stripeikyte et al., personal communication). Finally, we examined neuropsychological and psychopathological correlates of riPHs and associated PE, and within the defined PH-network. We hypothesized that impairment in executive functions modulates sensorimotor integration, and is linked to decreased functional connectivity within the PH-network.

## Methods

### **Participants**

Twenty-six individuals with 22q11DS (9 females) and 16 age-matched healthy controls (22q11DS subjects' siblings) (10 females) took part in the study. Both groups were recruited via the Developmental Imaging and psychopathology Lab, (Department of Psychiatry, University of Geneva). Participants were between 7 to 25 years old and both groups did not differ significantly in terms of age. Control subjects did not have any history of neurological or psychiatric disorders, and were not under medication. Written informed consent was obtained either from all participants or from their parents (when minors were included). The study was approved by the Swiss Ethics Committee of Geneva (CCER, Switzerland) and conducted in accordance to the Declaration of Helsinki. Demographic, psychiatric, neuropsychological measures as well as medication are presented in Table 1.

### **Psychiatric measures**

All participants were assessed with the Prodromal Questionnaire (PQ-16) (30), a self-report questionnaire screening for prodromal signs of psychosis. For 22q11DS subjects only, psychotic symptoms were evaluated by means of the Structured Interview for Prodromal Syndromes (SIPS) (31), and indicated that the individuals with 22q11DS were mostly asymptomatic. Their global functioning in daily life was assessed with the Global Assessment of Functioning (GAF) scale (32). Besides, through a semi-structured interview, we also assessed the occurrence of PH (and its phenomenology) in all participants.

**Table 1. Demographic, psychiatric and neuropsychological data in the 22q11DS and control groups.**

	22q11DS		Controls		Statistics		
	N = 26		N = 16		t	df	p
	Mean	SD	Mean	SD			
Age (years)	14.89	(4.03)	16.62	(4.03)	1.23	28.51	0.22
Schooling (years)	8.46	(2.88)	10.62	(4.20)	1.81	23.75	0.08
Total IQ	74.34	(13.59)	111.68	(12.47)	9.09	34.03	<0.001
Verbal IQ	80.00	(14.43)	116.81	(10.86)	9.38	38.22	<0.001
Performance IQ	73.26	(12.27)	102.23	(11.9)	6.93	25.68	<0.001
<b>Clinical scores</b>							
<i>PQ16 (Prodromal Questionnaire)</i>							
• True items	2.19	(2.00)	1.06	(0.68)	2.64	33.31	0.01
• Distress	2.07	(2.87)	0.75	(1.06)	2.15	34.77	0.04
<i>SIPS positive (Structured Interview for Prodromal Syndromes)</i>							
• P1 (Unusual thought disorder)	0.75	(1.25)	n.a	n.a			
• P2 (Suspiciousness/persecutory ideas)	1.08	(1.01)	n.a	n.a			
• P3 (Grandoise ideas)	0.04	(0.2)	n.a	n.a			
• P4 (Perceptual abnormalities/hallucinations)	1.26	(1.42)	n.a	n.a			
• P5 (Disorganized communication)	0.30	(0.7)	n.a	n.a			
<i>GAF (General Assessment of Functioning)</i>	77.82	(11.55)	n.a	n.a			
<b>Neuropsychological scores</b>							
<i>Stroop Test</i>							
• Inhibition (T-score)	0.56	(0.17)	0.64	(0.13)	1.50	37.26	0.14
<i>Semantic fluency (Animals)</i>							
• Self-monitoring, cognitive control	13.88	(4.05)	19.93	(5.35)	3.88	25.51	<0.001
<i>Letter-Number sequencing</i>							
• Working memory	4.42	(0.98)	5.50	(1.41)	4.45	35.99	0.01
<i>CPT</i>							
• Attention (% commission errors)	58.88	(8.53)	53.06	(9.24)	2.03	29.91	0.05
<b>Medication</b>							
	<b>n</b>	<b>%</b>					
Neuroleptics	1	3.85	n.a	n.a			
Psychostimulant	9	34.6	n.a	n.a			
Antidepressant	3	11.5	n.a	n.a			
Anxiolytics	1	3.85	n.a	n.a			
Antiepileptics	1	3.85	n.a	n.a			

n.a – not applicable

### Neuropsychological evaluations

*General intelligence.* Depending on the age of participants, their general intelligence and reasoning abilities were examined by either the Wechsler Intelligence Scale for

Children (WISC-III) (33) or the Wechsler Intelligence Scale for Adults (WAIS-III) (34).

*Attention.* Sustained attention and impulsivity were assessed by the Continuous Performance Test (35). Participants had to press a button when a letter appeared on the screen, except for the letter X for which they had to refrain themselves from answering.

#### *Executive functions*

1. *Inhibition*, the ability to inhibit a behavior and resisting to interference was evaluated by the Stroop task (36) during which participants are presented name of colors whose printed color is different. They had to say aloud the color of the ink instead of reading the words.

2. *Self-monitoring and cognitive control* was assessed by the semantic verbal fluency (SVF) for the Animal category, which evaluates verbal fluency by giving as many animal names as possible in 1 minute without repeating several times the same name or giving proper names. It also tests different components of executive functions such as initiation and inhibition or strategic search of information (37).

3. *Working memory* was assessed with the letter-number sequencing from WISC III and WAIS III (33,34). The task consists of hearing a series of letters-numbers and reporting them back with the letters in alphabetical order and digits in ascending numerical order. This test evaluates the ability to manipulate and update information mentally.

#### **Experiment 1: robot-induced PH and PE through sensorimotor stimulations**

Based on previous studies (23–25), we used the robot-based experimental paradigm. In practice, participants were seated, blind-folded and acoustically isolated (with white noise) (Figure 1). They were asked to manipulate a front-robot (located in front of them) with their dominant hand and to perform repetitive poking movements. This actuated another robot (located in the back of the participants), which replicated participants' movements and touched them on their back. The sensory feedback generated by the back-robot could be either synchronous (0ms of delay between movements and touch on the back) or asynchronous (500 ms delay) to the participant's movement. One acoustic signal (400 Hz, 100ms duration) notified the participants to

start, and two sounds to stop the movements. Both conditions (i.e., synchronous (sync) and asynchronous (async)) were randomly assessed and lasted two minutes each. After running each condition, a questionnaire evaluated the subjective robot-induced bodily experiences (23) felt by subjects on a 7-point Likert scale from 0 (not at all) to 6 (very strongly): 1. Feeling of self-touch; 2. Passivity Experience; 3. Presence hallucination, 4. Loss of agency; 5. Anxiety; 6. PH in front (control question 1); and 7. Impression of having 2 bodies (control question 2).

### **Experiment 2: robot-induced PH and PE based on varying degrees of sensorimotor conflicts**

Keeping the same setting as in Experiment 1, we further assessed how the degree of sensorimotor conflicts modulated the robot-induced PH and PE. In a first part, after every 6-poking movements (automatically counted), subjects were instructed to stop their movements and say aloud “Yes” or “No” if they experienced PH (“*Did you feel as if someone was close to you, behind or next to you?*”) and in a second part if they experienced passivity (“*Did you feel as if someone else was touching your back?*”). Six delays of sensorimotor conflicts (varying from 0ms to 500ms with steps of 100ms) were tested randomly in each trial. Participants had to start the movements when they heard one auditory signal and stop when they heard 2. Each part consisted of three sessions of 18 trials (3 trials per delay).

### **Experiment 3: resting-state fMRI acquisition**

*Image acquisition.* All participants were scanned with a 3T Siemens Magnetom Prisma scanner using 64 head-channel. The 200 functional scans were acquired using a 8 min EPI sequence (TR=2.4 s, TE=30 ms, flip angle=85°, field of view=235 mm, slice thickness=3.2 mm, 38 slices) and the anatomical image with a T1-weighted sequence (TR=2.5 s, TE=3 ms, flip angle=8°, field of view=23.5 cm<sup>2</sup>, 192 slices).

*Image preprocessing.* Resting state data was analyzed and preprocessed using the CONN-fMRI Functional Connectivity toolbox (v.18.a) (38) and SPM12 in Matlab 2018. The standard pipeline of preprocessing was applied (i.e. slice time and motion correction, co-registration of the anatomical scan, normalization into MNI space and smoothing with a 6 mm<sup>3</sup> FWHM Gaussian kernel) for each subject. The mean frame-wise displacement (FD) was calculated for every participant to ensure subjects did not

move excessively during the resting state acquisition (all participants had a mean  $FD < 0.25$ ) (39). No difference in movement over the acquisition was observed between the two groups ( $t(43)=1.23$ ,  $p=0.22$  with mean  $FD \pm SD$ : 22q11DS subjects= $0.15 \pm 0.048$ ; Controls= $0.14 \pm 0.044$ ). In addition, we extracted and regressed out of the data the individual time courses of the segmented white matter and cerebrospinal fluid, the global signal time courses as well as the six motion parameters and their first-degree derivatives. Finally, the data was filtered with a bandwidth of 0.01-0.1 Hz.

*Regions of interest (ROI).* Based on previous work (24), we defined a PH-network including the following six ROIs: the posterior middle temporal gyrus (pMTG), the inferior frontal gyrus (IFG) and the ventral premotor cortex (vPMC) in both hemispheres. In addition, we defined two control networks: the first one consisted in shifting each region of the PH-network (conserving the same shape and same number of voxels) and the second one was composed of a visual network (including the calcarine sulcus, left thalamus, left and right middle / superior occipital gyri) (40) as done previously (24).

### **Statistical analysis**

*Demographic, psychiatric and neuropsychological data.* The difference between 22q11DS subjects and the controls in terms of demographics and neuropsychological and psychiatric scores was assessed using independent two-sample t-tests. Since our interest was mainly on passivity symptoms, we reported and analyzed the scores obtained on the positive symptoms scale of the SIPS.

*Experiment 1 and 2.* Ratings of the robot-induced bodily experiences questionnaire were analyzed using linear mixed effect models with permutation test (5000 iterations) to estimate significance (lmerTest and predictmeans R package (41)) with Condition as a fixed effect and Subjects as a random factor for each question of Experiment 1. We reported permutation p values. For Experiment 2, Group (22q11DS vs. controls) and Delays (6 delays: 0ms, 100ms, 200ms, 300ms, 400ms and 500ms) were considered as fixed effects, Subject as random effects. Age was added as a covariate for both experiments. PH and PE ratings were combined to create a PH/PE combined score, since both are described as manifestations of a disrupted demarcation between self and other in schizophrenia (25).



*Resting-state neuroimaging.* For each subject, the mean time course of each ROI was extracted and correlated (Pearson correlation) to the time course of the remaining ROIs creating a connectivity matrix of correlation values (z-transformed) of the PH-network for all possible connections for each subject. Connectivity values were extracted and analyzed using R software (<https://www.R-project.org/>, version 3.4.0). First, we removed the connectivity outliers (4.7% of all data points) based on 1.5 IQR from the connectivity median value for each connection. Then linear mixed model with (22q11DS vs. controls) and Connections (15 connections in total for the PH-network) as fixed effects, by-subject random intercepts were applied. Age was also included as a covariate in the analysis according to the model selection based on the Akaike information criterion (AIC). Post-hoc analysis for the between group differences was performed using two-sample t-tests (two-tailed), FDR  $p=0.05$  corrected for multiple comparisons.

*Correlation analyses.* The relationship between functional connectivity of the connections showing altered functional connectivity in 22q11DS subjects compared to controls and the neuropsychological measures were investigated. We performed a spearman 2-tailed correlation analysis using FDR correction for multiple comparisons. Correlations between the ratings collected from Experiment 1 were also correlated with the neuropsychological scores using the same method (FDR correction for multiple comparisons for each item independently).

## Results

### *Occurrence of PH in 22q11DS*

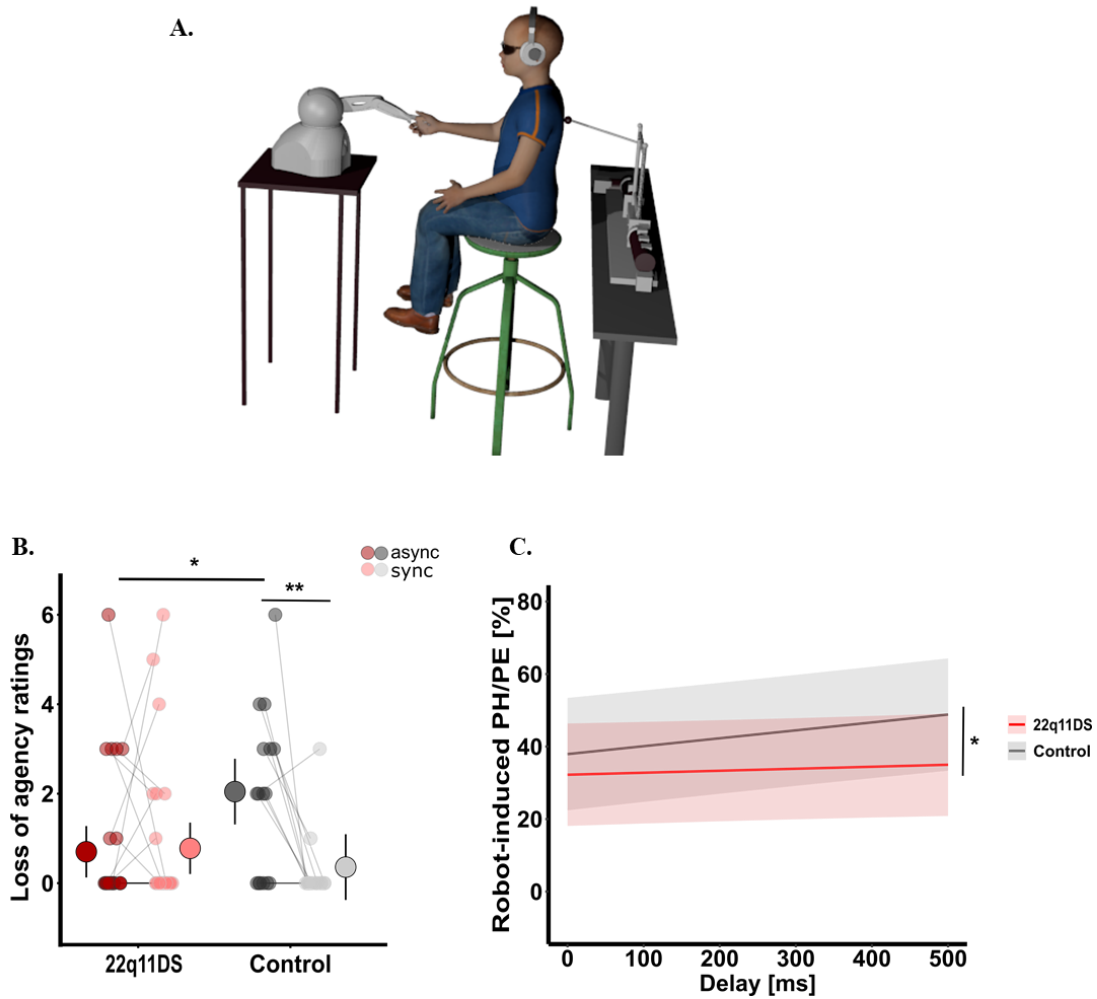
We assessed the symptomatic PH in all the subjects included in the study. While none of the controls presented symptomatic-PH, 31% of the 22q11DS subjects reported PH at least once in their life (Table 2).

Table 2. Phenomenological characteristics of the symptomatic PH in 22q11DS individuals.

<b>Symptomatic PH</b>	<b>22q11DS</b>
	<b>N = 26</b>
<i>Occurrence</i>	8/26 (31 %)
<i>Emotions towards PH</i>	
• Negative	3/8
• Positive	1/8
• None	4/8
<i>Sex of PH</i>	
• Male	2/8
• Female	1/8
<i>Place of occurrence</i>	
• Home	7/8
• Outside home	1/8
<i>Time of occurrence</i>	
• Daytime	1/8
• Afternoon	3/8
• Night	1/8
• Anytime	1/8
• Unknown	2/8
<i>Location of PH</i>	
• Right only	0/8
• Left only	1/8
• Back	5/8
• Bilateral	1/8
• Above	1/8
• Unknown	1/8

*Experiment 1: robot-induced PH and PE through sensorimotor stimulations*

We showed a main effect of Condition for the questionnaire item “loss of agency” (I felt as if I was not controlling the movements) with higher ratings in the asynchronous condition for both groups ( $p=0.006$ ) as well as a main effect of Group ( $p=0.012$ ) with lower ratings in 22q11DS subjects than in controls. A significant interaction between Group and Condition was also observed for loss of agency ( $p=0.008$ ). Post-hoc analysis revealed that 22q11DS individuals did not present any difference in experiencing the loss of agency between asynchronous and synchronous conditions compared to age-matched controls. Conversely, the control group reported higher ratings for the asynchronous condition compared to the synchronous condition and to the 22q11DS individuals (22q11DS, async vs. sync:  $t(78)=0.19$ ,  $p=0.99$ ; Controls, async vs. sync:  $t(40)=3.38$ ,  $p=0.0084$ ; 22q11DS async vs. Controls async:  $t(78)=2.81$ ,  $p=0.031$ ) (Figure 1B, Table 3). Contrary to our predictions, we did not find any main effect of Condition, Group or interaction between Group and Condition (all  $p>0.13$ ) for the PH/PE combined score (PH: I felt as if someone was standing close to me, behind or besides; PE: I felt as if someone else was touching my back). In addition, a main effect of Condition ( $p=0.023$ ) was observed for the item “self-touch” with higher ratings in the synchronous condition considering both groups together, as previously reported (23,25). Age was included as a covariate in the analysis and was found to be related to PH/PE combined score ( $p<0.001$ ) and to loss of agency ( $p=0.018$ ). No other main effects or interactions were significant (all  $ps>0.16$ ) (Table 3).



**Figure 1. Experimental robotic setup and main behavioral results.** **A.** The robotic device consisted of a front robot, which participants moved with their dominant hand and a back robot that translated the movements in the back of the participants either synchronously (sync) or asynchronously (async; with 500 ms delay between the movement generated in the front and the sensory feedback on the back). **B.** Individuals with 22q11DS did not show any difference in loss of agency ratings (LoA) between the conditions where the controls rated higher for the LoA in the asynchronous as compared to synchronous condition. Further, 22q11DS group rated lower compared to controls in asynchronous condition. **C.** Lack of modulation of PH/PE combined score with varying delay in subjects with 22q11DS compared to controls in whom an increase of delay led to increase PH/PE experience.

**Table 3. Mean ratings and standard deviations of questionnaire items of the robot task for both groups and conditions.**

Items	Group	Conditions	Mean	SD
Self-touch	22q11DS	Async	1.77	2.34
Self-touch	22q11DS	Sync	2.15	2.09
Self-touch	Controls	Async	1.19	1.52
Self-touch	Controls	Sync	1.94	1.91
Passivity experience	22q11DS	Async	3.15	2.44
Passivity experience	22q11DS	Sync	2.58	2.35
Passivity experience	Controls	Async	3.19	2.26
Passivity experience	Controls	Sync	2.94	2.17
Presence hallucination	22q11DS	Async	1.50	2.06
Presence hallucination	22q11DS	Sync	1.04	1.59
Presence hallucination	Controls	Async	2.06	1.81
Presence hallucination	Controls	Sync	1.19	2.01
Loss of agency	22q11DS	Async	0.77	1.53
Loss of agency	22q11DS	Sync	0.85	1.69
Loss of agency	Controls	Async	1.94	1.84
Loss of agency	Controls	Sync	0.25	0.77
Anxiety	22q11DS	Async	0.19	0.49
Anxiety	22q11DS	Sync	0.12	0.43
Anxiety	Controls	Async	0.50	1.10
Anxiety	Controls	Sync	0.25	1.00
PH in front (Control)	22q11DS	Async	0.38	1.24
PH in front (Control)	22q11DS	Sync	0.35	1.23
PH in front (Control)	Controls	Async	0.00	0.00
PH in front (Control)	Controls	Sync	0.00	0.00
Impression of two bodies (Control)	22q11DS	Async	0.65	1.67
Impression of two bodies (Control)	22q11DS	Sync	0.88	2.01
Impression of two bodies (Control)	Controls	Async	0.13	0.50
Impression of two bodies (Control)	Controls	Sync	0.06	0.25

***Experiment 2: robot-induced PH and PE based on varying degrees of sensorimotor conflicts***

For this part, only 18 22q11DS subjects and 15 controls completed the task. A main effect of Delay ( $p=0.002$ ), Group ( $p=0.039$ ) and Age ( $p=0.001$ ) were observed. An interaction between Group and Delay ( $p=0.022$ ) was found (Figure 1C), in which 22q11DS individuals did not show any modulation in their responses for PH/PE with respect to the delay compared to the controls in whom higher delays induced higher PH/PE experience.

***Experiment 3: resting-state functional connectivity within the PH-network***

Functional connectivity within the PH-network showed a significant main effect of Group ( $F(1,19)=5.10$ ,  $p=0.036$ ) where 22q11DS individuals had a lower functional connectivity within the network compared to the control group (22q11DS, Mean=0.21; SD=0.27; Controls, Mean=0.26, SD=0.27). We also observed a significant main effect of Connection ( $F(14,530)=31.74$ ,  $p<0.001$ ) and an interaction between the Connection and Group ( $F(14,530)=3.92$ ,  $p<0.001$ ). Post-hoc analyses revealed reduced functional connectivity in 22q11DS individuals compared to controls for the bilateral pMTG connection, the right pMTG and right IFG, as well as right pMTG and right vPMC (Figure 2 and Table 4). These effects were not observed for the two control networks (shifted control network and standard visual network) where no significant main effect of Group nor interaction between the Connections and Group were found (all  $p_s>0.18$ ).

***Correlations with clinical and neuropsychological scores***

*Functional connectivity.* When correlating the neuropsychological scores specific to executive functions (SVF, working memory, inhibition and attention), we found a significant positive correlation between the functional connectivity between the right pMTG and the right IFG and the SVF scores (FDR corrected  $p=0.0018$ ,  $R=0.57$ ). Lower functional connectivity was associated with lower SVF performance independently of the groups (Figure 3). Other clinical and behavioral measures did not significantly relate with decreased functional connectivity in the 22q11DS group (all  $p_s>0.05$ ).

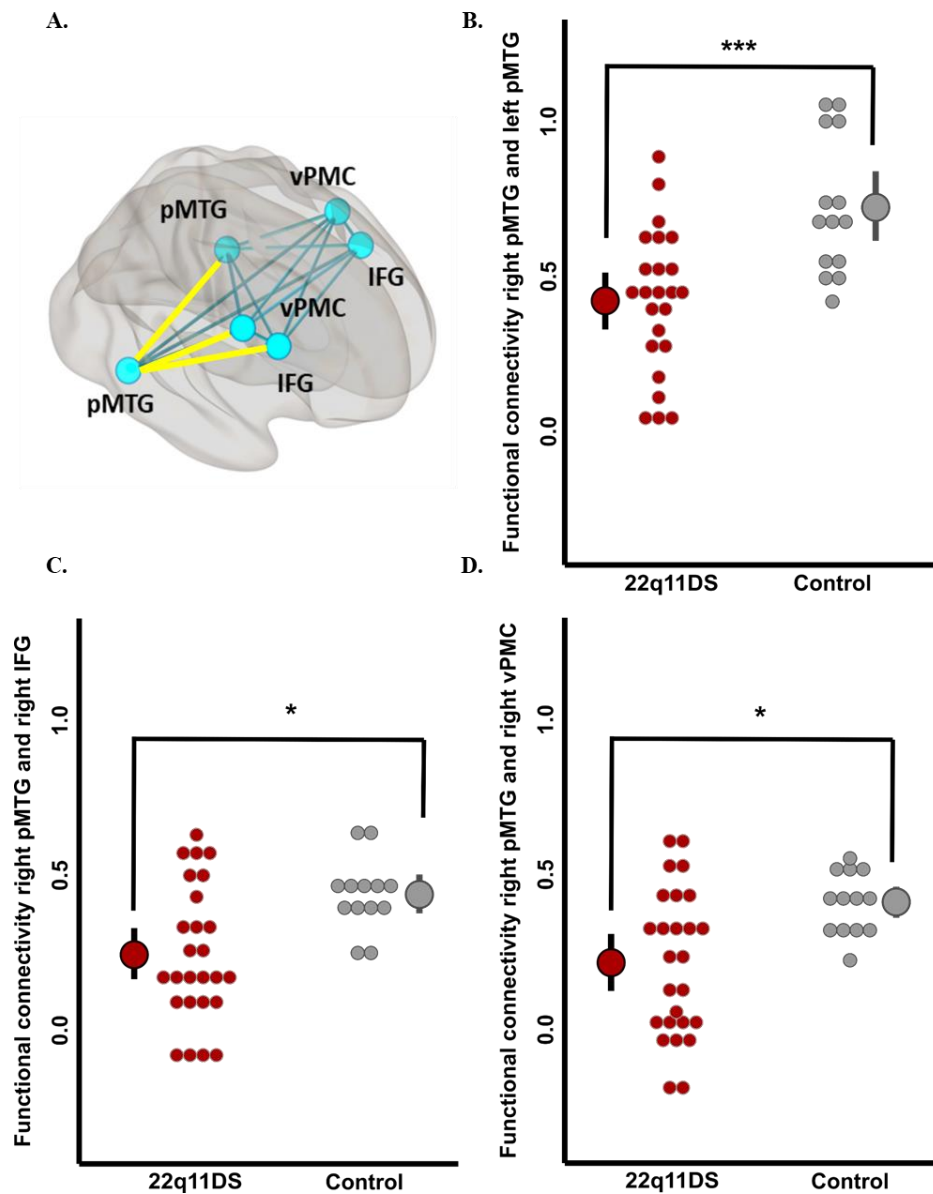


**Figure 2. Functional connectivity within the PH-network.** A. Brain rendering representing the seed regions and connections of the PH-network. Connections depicted in yellow were significantly different in 22q11DS individuals compared to age-matched controls. Reduced functional connectivity was observed in 22q11DS individuals compared to controls between the bilateral pMTG (B), the right pMTG and right IFG (C) and the right pMTG and the right vPMC (D). \*\*\*:  $p < 0.001$ , \*:  $p < 0.05$ .

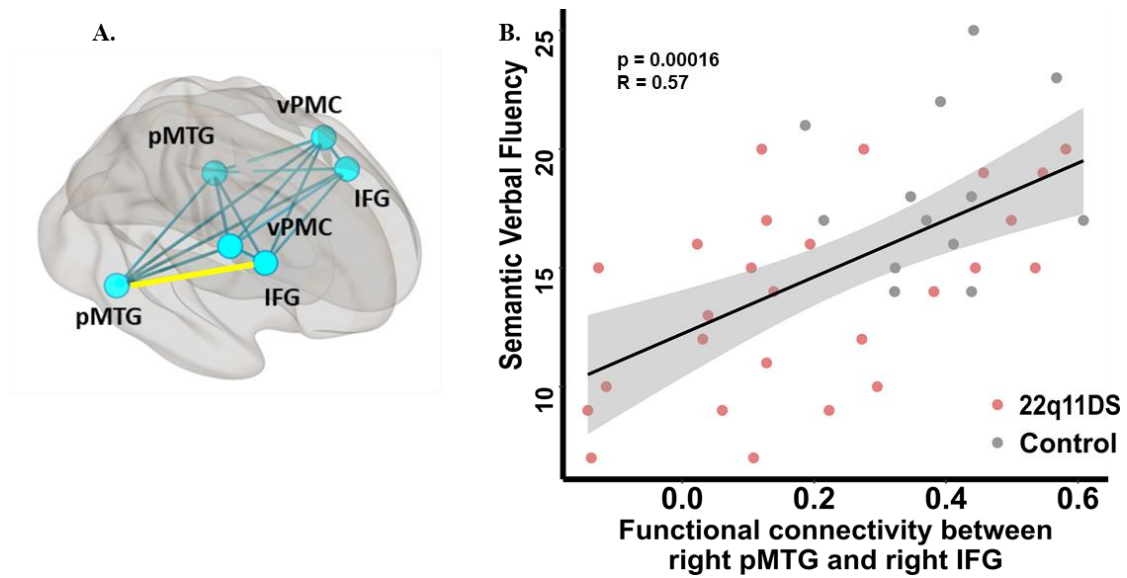


**Figure 3.** Correlations between the right pMTG and right IFG (A) and the semantic verbal fluency (B). Reduced functional connectivity was found between the right IFG and the right pMTG for the 22q11DS subjects compared to controls. The connectivity between those two regions further correlated with the semantic verbal fluency performance with lower connectivity associated to lower performance.

**Table 4.** Significant functional connectivity within the PH-network.

Functional connectivity	22q11DS N = 26		Controls N = 16		Statistics		
	Mean	SD	Mean	SD	t	df	p-value FDR corrected
Right pMTG - right IFG	0.19	0.22	0.38	0.12	3.07	142.00	0.01
Right pMTG - right vPMC	0.17	0.24	0.36	0.1	3.18	123.00	0.01
Right pMTG - left pMTG	0.37	0.23	0.67	0.22	4.60	142.00	p<0.001



## Discussion

PH was assessed for the first time in the present study in individuals with 22q11DS, a genetic disorder associated with very high risk of developing schizophrenia. PH is a specific hallucination and has been proposed to be linked to disturbed sensorimotor integration of own body signals (23,24). Here, we report that actually 31% of the individuals with 22q11DS included in our study experienced symptomatic PH at least once.

Through our robot-based experimental paradigm, we tested the sensitivity of 22q11DS individuals to sensorimotor conflicts and their proneness to experience riPH in a controlled setting. Our main result showed that, contrary to our hypothesis, 22q11DS individuals did not present increased sensitivity to the robotic stimulations. They did not experience stronger riPH and associated PE, even when varying degrees of sensorimotor conflict were applied. We also observed that their sense of agency was not further altered by the sensorimotor stimulation compared to controls whose sense of agency was affected by the asynchronous stimulation.

On the neural level, as expected, the results revealed reduced functional connectivity within the PH-network in 22q11DS individuals compared to controls, namely between the right pMTG and right IFG, right pMTG and right vPMC and bilateral pMTG. Although the 22q11DS individuals were asymptomatic for psychotic symptoms, especially positive ones, these findings are in line with previous work showing reduced connectivity between the right IFG and right pMTG in psychotic patients with vs. without PE (Stripeikyte et al., personal communication). The same connection on the left hemisphere was found reduced in Parkinson's patients with PH compared to those without (24). These findings are in favor of the fronto-temporal disconnection (supported by the forward model) described in schizophrenia (9–11).

Taken together, our results could be explained by an altered sensorimotor integration and prediction in the 22q11DS group. According to the forward model, the initiation of a motor command generates an efference copy to predict or anticipate the sensory consequences of one's action. When the prediction matches the actual sensory feedback, the action is considered as self-generated, and its perception is considered normal. However, when a mismatch between the expected outcome and the actual

sensory feedback occurs, the sensory signals are less attenuated and the event is considered as originating from an external source and not as self-generated. In 22q11DS, the lack of sensitivity to sensorimotor conflicts, as shown by the absence of difference in responses between the synchronous and asynchronous conditions (Experiment 1) and between the different delays of asynchrony (Experiment 2), could indicate source monitoring confusions (18) or rapid (earlier) sensory attenuation of signals in these individuals. A recent study showed that 22q11DS individuals exhibit preserved prediction but rather reduced adaptations in response to repeated auditory stimuli (42). In that case, we could speculate that altered repetition suppression (i.e., the reduced neural response to repeated stimuli) may cause inaccurate sensory predictions and the inability to monitor and adapt to stimulus conflict. Maladaptive conflict monitoring in 22q11DS has been linked to executive dysfunctions, namely deficits in inhibition and cognitive control (43).

Interestingly, the interpretation of our results could be supported, though indirectly, by the reduced functional connectivity between the right IFG and right pMTG which is associated with low performance in the SVF task. Besides assessing language abilities, the SVF task also involves executive functions such as self-monitoring, cognitive control and initiation/inhibition abilities (44). In 22q11DS subjects, an atypical developmental trajectory was observed for the SVF task, and this was not explained by poor lexical level, but most likely due to executive dysfunctions according to the authors (45). Proposed as a potential marker of psychosis among many other executive functions components (46), low SVF performance is also associated with reduced activity in the right IFG and bilateral temporal cortex in high-risk for psychosis in adolescents (47). Based on these findings, it is possible that deficits in self-monitoring and cognitive control affect sensitivity of 22q11DS individuals to sensorimotor conflicts.

Our study has a few limitations to consider. The absence of direct correlations between ratings from the robot task with both functional connectivity and executive dysfunctions makes it difficult to unravel the underlying mechanisms of PH and related PE in 22q11DS. Although 31% of 22q11DS individuals had symptomatic PH, it was not possible to directly compare subjects with vs. without PH, nor were we able to stratify and compare the group of 22q11DS according to the presence of attenuated positive symptoms since most individuals were asymptomatic. Future studies with

larger cohorts could overcome this selection bias and determine whether PH would precede marked positive symptoms, and give insight into the behavioral and neural mechanisms.

Our work brings novel data regarding sensorimotor prediction and integration in 22q11DS. Using a robot-based experimental paradigm, we found a lack of sensorimotor modulation in 22q11DS individuals asymptomatic for psychosis, but presenting executive dysfunctions and reduced fronto-temporal connectivity compared to age-matched controls. Deficits in cognitive control and self-monitoring could be further studied to determine whether they represent possible markers for specific psychotic symptoms such as passivity symptoms before their onset. To conclude, now that we showed that individuals with 22q11DS can experience symptomatic PH in daily life, it would also be of clinical relevance to better characterize the phenomenological aspects of PH and related PE in a larger sample of individuals with 22q11DS.

## References

1. Fomin AB, Pastorino AC, Kim CA, Pereira AC, Carneiro-Sampaio M, Abe Jacob CM. DiGeorge Syndrome: a not so rare disease. *Clinics (Sao Paulo)*. 2010 Sep;65(9):865–869.
2. McDonald-McGinn DM, Sullivan KE, Marino B, Philip N, Swillen A, Vorstman JAS, et al. 22Q11.2 Deletion Syndrome. *Nature Reviews Disease Primers*. 2015;1(November).
3. Debbané M, Glaser B, David MK, Feinstein C, Eliez S. Psychotic symptoms in children and adolescents with 22q11.2 deletion syndrome: Neuropsychological and behavioral implications. *Schizophr Res*. 2006 Jun;84(2–3):187–193.
4. Schneider M, Schaer M, Mutlu AK, Menghetti S, Glaser B, Debbané M, et al. Clinical and cognitive risk factors for psychotic symptoms in 22q11.2 deletion syndrome: a transversal and longitudinal approach. *Eur Child Adolesc Psychiatry*. 2014 Jun;23(6):425–436.
5. Chow EWC, Zipursky RB, Mikulis DJ, Bassett AS. Structural Brain Abnormalities in Patients with Schizophrenia and 22q11 Deletion Syndrome. *Biol Psychiatry*. 2002 Feb 1;51(3):208–15.
6. Bassett AS, Chow EWC. Schizophrenia and 22q11.2 Deletion Syndrome. *Curr Psychiatry Rep*. 2008 Apr;10(2):148–157.
7. Schneider M, Debbané M, Bassett AS, Chow EWC, Fung WLA, van den Bree M, et al. Psychiatric disorders from childhood to adulthood in 22q11.2 deletion syndrome: results from the International Consortium on Brain and Behavior in 22q11.2 Deletion Syndrome. *Am J Psychiatry*. 2014 Jun;171(6):627–639.
8. Kook SD, An SK, Kim KR, Kim WJ, Lee E, Namkoong K. Psychotic Features as the First Manifestation of 22q11.2 Deletion Syndrome. *Psychiatry Investig*. 2010 Mar;7(1):72–4.
9. Friston K, Brown HR, Siemerkus J, Stephan KE. The dysconnection hypothesis (2016). *Schizophrenia Research*. 2016 Oct;176(2):83–94.
10. Frith C. Explaining the symptoms of schizophrenia: Abnormalities in the awareness of action. *Brain Research Reviews*. 2000 Mar;31(2–3):357–63.
11. Kendler KS, Mishara A. The Prehistory of Schneider’s First-Rank Symptoms: Texts From 1810 to 1932. *Schizophr Bull*. 2019 11;45(5):971–90.
12. Blakemore SJ, Smith J, Steel R, Johnstone CE, Frith CD. The perception of self-produced sensory stimuli in patients with auditory hallucinations and passivity experiences: evidence for a breakdown in self-monitoring. *Psychol Med*. 2000 Sep;30(5):1131–9.
13. Graham-Schmidt KT, Martin-Iverson MT, Waters FAV. Self- and other-agency in people with passivity (first rank) symptoms in schizophrenia. *Schizophr Res*. 2018;192:75–81.
14. Werner J-D, Trapp K, Wüstenberg T, Voss M. Self-attribution bias during continuous action-effect monitoring in patients with schizophrenia. *Schizophrenia Research*. 2014 Jan;152(1):33–40.
15. Sobin C, Kiley-Brabeck K, Karayiorgou M. Lower Prepulse Inhibition in Children With the 22q11 Deletion Syndrome. *Am J Psychiatry*. 2005 Jun;162(6):1090–1099.
16. Cunningham AC, Hill L, Mon-Williams M, Peall KJ, Linden DEJ, Hall J, et al. Using kinematic analyses to explore sensorimotor control impairments in children with 22q11.2 deletion syndrome. *J Neurodev Disord*. 2019 Jun;11(1):8.
17. Debbané M, Van Der Linden M, Glaser B, Debbané M, Eliez S. Monitoring of self-generated speech in adolescents with 22q11 . 2 deletion syndrome. *British Journal of clinical psychology*. 2010;49:373–86.
18. Debbané M, Linden MV der, Glaser B, Eliez S. Source monitoring for actions in adolescents with 22q11.2 deletion syndrome (22q11DS). *Psychological Medicine*. 2008

- Jun;38(6):811–20.
19. Padula MC, Schaer M, Scariati E, Schneider M, Van De Ville D, Debbané M, et al. Structural and functional connectivity in the default mode network in 22q11.2 deletion syndrome. *J Neurodev Disord* [Internet]. 2015 [cited 2020 Feb 28];7(1). Available from: <https://www.ncbi.nlm.nih.gov/pmc/articles/PMC4522079/>
  20. Debbané M, Lazouret M, Lagioia A, Schneider M, Van De Ville D, Eliez S. Resting-state networks in adolescents with 22q11.2 deletion syndrome: associations with prodromal symptoms and executive functions. *Schizophr Res*. 2012 Aug;139(1–3):33–39.
  21. Scariati E, Schaer M, Richiardi J, Schneider M, Debbané M, Van De Ville D, et al. Identifying 22q11.2 deletion syndrome and psychosis using resting-state connectivity patterns. *Brain Topogr*. 2014 Nov;27(6):808–821.
  22. Zöllner D, Schaer M, Scariati E, Padula MC, Eliez S, van de Ville D. Disentangling resting-state BOLD variability and PCC functional connectivity in 22q11.2 deletion syndrome. *NeuroImage*. 2017;149:85–97.
  23. Blanke O, Pozeg P, Hara M, Heydrich L, Serino A. Neurological and Robot - Controlled Induction of an Apparition. *Current Biology*. 2014;24.
  24. Bernasconi F, Blondiaux E, Potheegadoo J, Stripeikyte G, Pagonabarraga J, Bejr-Kasem H, et al. Sensorimotor hallucinations in Parkinson’s disease [Internet]. *Neuroscience*; 2020 May [cited 2020 May 16]. Available from: <http://biorxiv.org/lookup/doi/10.1101/2020.05.11.054619>
  25. Salomon R, Progin P, Griffa A, Rognini G, Do KQ, Conus P, et al. Sensorimotor Induction of Auditory Misattribution in Early Psychosis. *Schizophrenia Bulletin*. 2020 Feb 11;sbz136.
  26. Arzy S, Seeck M, Ortigue S, Spinelli L, Blanke O. Induction of an illusory shadow person. *Nature*. 2006 Sep 21;443(7109):287.
  27. Ratcliffe M. Sensed presence without sensory qualities: a phenomenological study of bereavement hallucinations. *Phenom Cogn Sci* [Internet]. 2020 Mar 24 [cited 2020 May 28]; Available from: <https://doi.org/10.1007/s11097-020-09666-2>
  28. Llorca PM, Pereira B, Jardri R, Chereau-Boudet I, Brousse G, Misdrahi D, et al. Hallucinations in schizophrenia and Parkinson’s disease: an analysis of sensory modalities involved and the repercussion on patients. *Sci Rep*. 2016 Dec 1;6(1):1–9.
  29. Jaspers K. Über leibhaftige Bewußtheiten (Bewußtheitstäuschungen), ein psychopathologisches Elementarsymptom. In: Jaspers K, editor. *Gesammelte Schriften zur Psychopathologie* [Internet]. Berlin, Heidelberg: Springer Berlin Heidelberg; 1913 [cited 2019 Jan 23]. p. 413–20. Available from: [https://doi.org/10.1007/978-3-642-62027-0\\_8](https://doi.org/10.1007/978-3-642-62027-0_8)
  30. Ising HK, Veling W, Loewy RL, Rietveld MW, Rietdijk J, Dragt S, et al. The Validity of the 16-Item Version of the Prodromal Questionnaire (PQ-16) to Screen for Ultra High Risk of Developing Psychosis in the General Help-Seeking Population. *Schizophr Bull*. 2012 Nov;38(6):1288–96.
  31. Miller TJ, McGlashan TH, Rosen JL, Cadenhead K, Cannon T, Ventura J, et al. Prodromal assessment with the structured interview for prodromal syndromes and the scale of prodromal symptoms: predictive validity, interrater reliability, and training to reliability. *Schizophr Bull*. 2003;29(4):703–715.
  32. Endicott J, Spitzer RL, Fleiss JL, Cohen J. The Global Assessment Scale: A Procedure for Measuring Overall Severity of Psychiatric Disturbance. *Arch Gen Psychiatry*. 1976 Jun 1;33(6):766–71.
  33. Wechsler D. *The Wechsler intelligence scale for children—third edition: administration and scoring manual*. Psychological corporation. San Antonio; 1991.
  34. Wechsler D. *Wechsler adult intelligence scale-III: administration and scoring manual*. Psychological Corporation. San Antonio; 1997.
  35. Conners CK, Staff MHS. *Conner’s continuous performance test II: computer program for windows technical guide and software manual*. Multi-Health Systems. North

- Tonawanda; 2000.
36. 36. Stroop JR. Studies of interference in serial verbal reactions. *J Exp Psychol.* 1935;643–62.
  37. 37. Cardebat D, Démonet JF, Viallard G, Faure S, Puel M, Celsis P. Brain Functional Profiles in Formal and Semantic Fluency Tasks: A SPECT Study in Normals. *Brain and Language.* 1996 Feb;52(2):305–313.
  38. 38. Whitfield-Gabrieli S, Nieto-Castanon A. Conn: A Functional Connectivity Toolbox for Correlated and Anticorrelated Brain Networks. *Brain Connectivity.* 2012;2(3):125–141.
  39. 39. Power JD, Barnes KA, Snyder AZ, Schlaggar BL, Petersen SE. Spurious but systematic correlations in functional connectivity MRI networks arise from subject motion. *NeuroImage.* 2012;59(3):2142–2154.
  40. 40. Shirer WR, Ryali S, Rykhlevskaia E, Menon V, Greicius MD. Decoding subject-driven cognitive states with whole-brain connectivity patterns. *Cerebral Cortex.* 2012;22(1):158–65.
  41. 41. Kuznetsova A, Brockhoff PB, Christensen RHB. lmerTest Package: Tests in Linear Mixed Effects Models. *Journal of Statistical Software.* 2017;82(13).
  42. 42. Larsen KM, Mørup M, Birkenow MR, Fischer E, Olsen L, Didriksen M, et al. Individuals with 22q11.2 deletion syndrome show intact prediction but reduced adaptation in responses to repeated sounds: Evidence from Bayesian mapping. *Neuroimage Clin* [Internet]. 2019 Feb 13 [cited 2020 May 14];22. Available from: <https://www.ncbi.nlm.nih.gov/pmc/articles/PMC6383326/>
  43. 43. Bish JP, Ferrante SM, McDonald-McGinn D, Zackai E, Simon TJ. Maladaptive conflict monitoring as evidence for executive dysfunction in children with chromosome 22q11.2 deletion syndrome. *Developmental Science.* 2005;8(1):36–43.
  44. 44. Whitney C, Kirk M, O’Sullivan J, Lambon Ralph MA, Jefferies E. The Neural Organization of Semantic Control: TMS Evidence for a Distributed Network in Left Inferior Frontal and Posterior Middle Temporal Gyrus. *Cereb Cortex.* 2011 May 1;21(5):1066–75.
  45. 45. Maeder J, Schneider M, Bostelmann M, Debbané M, Glaser B, Menghetti S, et al. Developmental trajectories of executive functions in 22q11.2 deletion syndrome. *J Neurodev Disord.* 2016;8:10–10.
  46. 46. Becker HE, Nieman DH, Dingemans PM, Fliert JR [van de, Haan L [De, Linszen DH. Verbal fluency as a possible predictor for psychosis. *European Psychiatry.* 2010;25(2):105–10.
  47. 47. Jacobson S, Kelleher I, Harley M, Murtagh A, Clarke M, Blanchard M, et al. Structural and functional brain correlates of subclinical psychotic symptoms in 11–13 year old schoolchildren. *NeuroImage.* 2010;49(2):1875–85.

## **Chapter 5: Fronto-temporal functional disconnection within the presence hallucination network in psychotic patients with passivity experiences**

**Authors:** Giedre Stripeikyte<sup>1\*</sup>, Jevita Potheegadoo<sup>1</sup>, Pierre Progin<sup>1,2</sup>, **Eva Blondiaux<sup>1</sup>**, Giulio Rognini<sup>1</sup>, Kim Do<sup>2</sup>, Philippe Conus<sup>2</sup>, Patric Hagmann<sup>3,4</sup>, Nathan Faivre<sup>5</sup>, Olaf Blanke<sup>1,6</sup>

**Status:** in preparation

### ***Affiliations***

**1.** Laboratory of Cognitive Neuroscience, Centre for Neuroprosthetics and Brain Mind Institute, Faculty of Life Sciences, Swiss Federal Institute of Technology (EPFL), Switzerland. **2.** Department of General Psychiatry, CHUV, Switzerland. **3.** Signal Processing Laboratory 5 (LTS5), Ecole Polytechnique Fédérale de Lausanne (EPFL), Lausanne, Switzerland. **4.** Department of Radiology, Centre Hospitalier Universitaire Vaudois (CHUV) and University of Lausanne (UNIL), Lausanne, Switzerland. **5.** Laboratoire de Psychologie et Neurocognition, LPNC CNRS 5105 Université Grenoble Alpes, France. **6.** Department of Neurology, University of Geneva, Switzerland

**Personal contributions:** Data analysis of the ROI-to-ROI resting state fMRI analysis

### **Acknowledgments**

The authors are grateful for all the patients and clinical staff for data collection

## Abstract

Psychosis corresponds to a group of symptoms leading to abnormal mental states including hallucinations and delusions, typical of schizophrenia. Theories posit that psychosis is driven by inaccurate sensorimotor predictions causing the misattribution of self-related events to external sources. This misattribution has been linked to passivity experiences (PE), such as loss in the sense of agency and, particularly, the intervention of an alien agent. The subjective experience of feeling an alien agent in the immediate surrounding while no one is actually there is called presence hallucination (PH). PH has been observed in schizophrenia, Parkinson's disease, and neurological patients with focal brain lesions or healthy subjects under extreme conditions. Recently, the presence hallucination network (PH-network) was established and included bilateral posterior middle temporal gyrus (pMTG), inferior frontal gyrus (IFG), and ventral premotor cortex (vPMC). Given that experiencing the presence of an alien agent is a specific feature of PE, we analyzed whether the functional connectivity in the PH-network can specifically differentiate psychotic patients with versus without PE. We observed reduced functional connectivity in patients with PE (N = 39) compared to patients without PE (N = 26) between the right pMTG and the IFG bilaterally. When seeding from these three areas separately to the whole brain, patients with PE compared to without had functional disconnection with areas that overlap with the PH-network and extended clusters. Functional disconnectivity within the PH-network stands in line with the theories suggesting that psychosis is linked to sensorimotor prediction errors and reduced fronto-temporal functional connectivity.

**Keywords:** psychosis, hallucinations, functional connectivity, resting-state fMRI



## Introduction

Psychosis is an abnormal mental state including hallucinations and delusions, typical of psychiatric conditions such as schizophrenia<sup>1</sup>. It has been proposed that a critical aspect of psychosis is a disturbed perception of the self and the external world whereby patients fail to correctly attribute and recognize their own motor actions, thoughts or emotions<sup>2,3</sup>. Patients can experience abnormal sensations such as delusions of control, somatic passivity, thought withdrawal, thought insertion or auditory verbal hallucinations. This group of psychotic symptoms, formerly known as Schneiderian first-rank symptoms<sup>4</sup>, is termed as “passivity experiences (PE)”<sup>5</sup>. PE have been suggested to ensue with an impairment in self-monitoring<sup>6</sup>, an essential aspect of sensorimotor functioning as it allows anticipation and control of actions based upon sensorimotor integration and prediction mechanisms (i.e., the expected sensory consequences related to self-generated actions)<sup>7,8</sup>. Disturbances in self-monitoring reflect a diminished demarcation of self-other boundaries where one’s thoughts, perceptions, and actions are not sensed as self-generated, but rather attributed to an external source due to the abnormal sensorimotor prediction mechanisms<sup>9-12</sup>, therefore giving rise to PE. PE strongly suggest a loss of self-agency and the attribution of perceptions and actions to the alien source. It has been argued that such self-monitoring deficits cause patients to believe that they are not the authors of the feelings, thoughts, and actions they are experiencing. However, there is lacking evidence and mechanistic explanations that would account for the attribution of thoughts, feelings, and actions to an external source or alien agent (alienation), characteristic of PE.

A recent growing body of work<sup>5,13-15</sup> shows that disturbances in self-monitoring and sensorimotor prediction can also account for another symptom frequently observed in patients with schizophrenia, relevant for understanding alienation, and related to PE: the presence hallucination (PH)<sup>16-18</sup>. The PH is defined as the vivid sensation that another person is nearby when no one is actually present. It has been reported that PHs occur in around 50% of patients with schizophrenia<sup>18</sup>, albeit in clinical practice it still remains overlooked and not investigated in more detail. This particular hallucination is also frequent in neurological illnesses such as Parkinson’s disease, epilepsy, and dementia<sup>19-21</sup> but can also be experienced by healthy individuals in particular in emotional or extreme conditions<sup>22,23</sup>. Moreover, PHs share common mechanisms with PE in terms of defective integration of one’s own bodily signals (tactile, proprioceptive and motor) leading to misattribution of the experienced sensation to external

sources<sup>13</sup>. A novel study by Bernasconi, Blondiaux et al.<sup>15</sup> have investigated neural underpinnings of PHs in healthy subjects and neurological patients by establishing the presence hallucination network (PH-network). They have defined the PH-network by looking for common brain regions involved in two independent data samples of robot-induced PHs in healthy subjects and symptomatic PHs in neurological patients. The clinical relevance of this PH-network was tested in patients with Parkinson's disease (PD), where functional disconnectivity was observed in fronto-temporal areas within the PH-network in patients with PD reporting symptomatic PHs. The relevance of the PH-network in patients experiencing a broader spectrum of psychotic symptoms like PE has not been addressed yet.

In this study, we investigated, for the first time, the functional connectivity of PH-network in psychotic patients with and without PE. First, we hypothesized functional disconnection within the PH-network, as many studies have supported the disconnectivity hypothesis in schizophrenia<sup>24-27</sup>. Functional disconnectivity in schizophrenia has also been linked to impaired sensorimotor integration, which could give rise to PE and PHs. Therefore, we also expected that brain regions from the PH-network altered in patients with PE compared to those without would show functional dysconnectivity to an extended network reflecting PE.

## Methods

### Participants

Sixty-five psychotic patients were included in this study. Part of the patients were recruited from the outpatient clinic of the department of psychiatry, Lausanne University Hospitals, Switzerland, and met DSM-IV criteria for schizophrenia or schizoaffective disorder<sup>28</sup>. Another part of the patients, who met threshold criteria for psychosis, as defined by the ‘Psychosis threshold’ subscale of the Comprehensive Assessment of At-Risk Mental States, were recruited from the TIPP Program (Treatment and Early Intervention in Psychosis Program, University Hospital, Lausanne, Switzerland)<sup>29</sup>. Neurological disorders and severe head trauma were exclusion criteria for all patients. Informed written consent in accordance with institutional guidelines (protocol approved by the Cantonal Ethics Commission of Vaud, Switzerland) was obtained for all patients.

Patients underwent an in-depth clinical assessment by a trained psychiatrist where the frequency and severity of symptoms were evaluated. Lifetime occurrence of passivity experiences (PE) (auditory verbal hallucinations; somatic passivity; thought broadcasting; thought insertion; thought withdrawal) inspired from the Scale for the Assessment of Positive Symptoms (SAPS)<sup>5,30–33</sup> were assessed. Patients were considered PE+ if they had presented at least one of these experiences (N = 39, Figure 1). Twenty-six patients did not show these symptoms and were thus included in the PE- group. Symptom severity was assessed using the Positive and Negative Syndrome Scale (PANSS)<sup>34</sup> and did not differ between the groups (Table 1 for the details). The patient groups did not differ significantly by any demographic trait (Table 1 for the details).

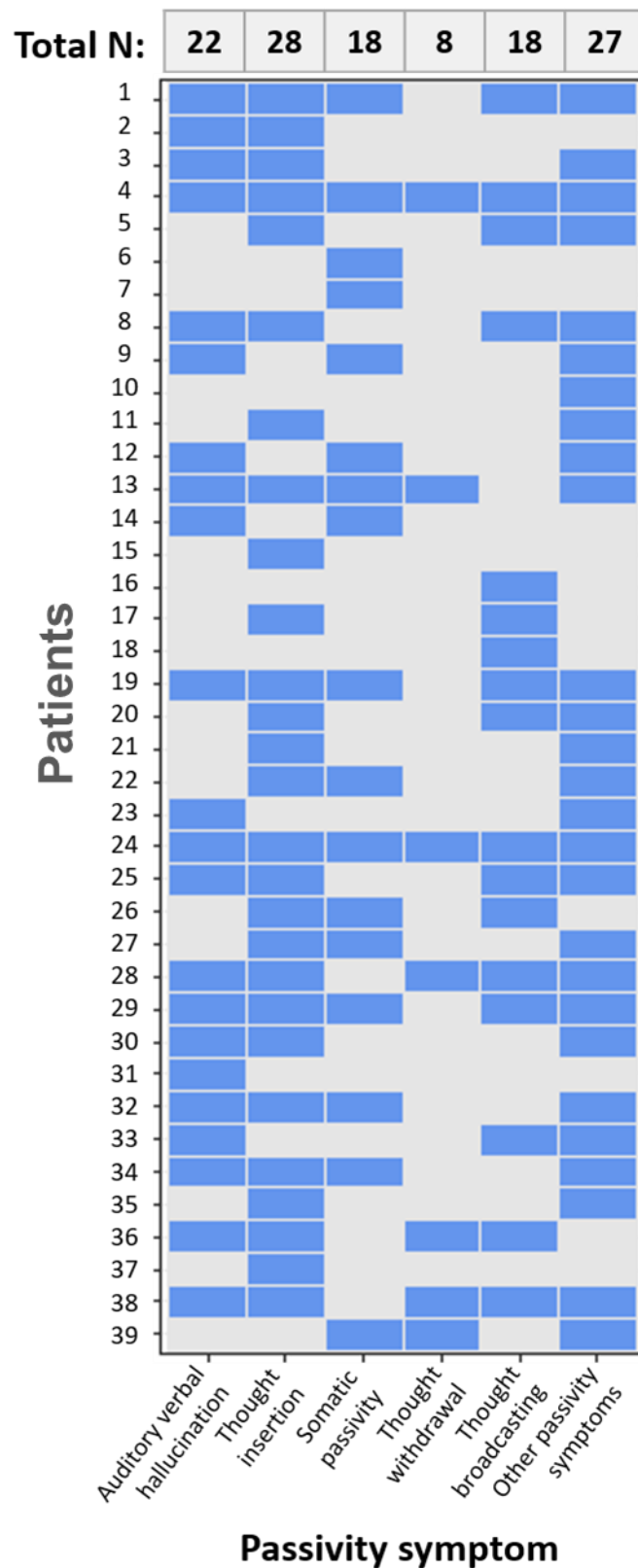


**Figure 1. Passivity symptoms per patient.** The list of the passivity symptoms per patient, presence of the symptom is depicted in the blue color. The total number of patients having each symptom is depicted at the top of the graph.

Characteristic/test	PE-	PE+	p(t / $\chi^2$ )
Group size	26	39	
Gender, M/F	20/6	23/16	0.1 (2.2)
Handedness, R/L	23/3	34/3	0.4 (1.5)
Age, y	29.9 $\pm$ 10	30.5 $\pm$ 9.7	0.9 (-0.08)
Education, y	12.9 $\pm$ 2.5	12.3 $\pm$ 3.5	0.6 (0.55)
Illness duration, y	6.2 $\pm$ 7.7	5.2 $\pm$ 5.1	0.6 (0.6)
Chlorpromazine, mg/day	275 $\pm$ 247	365 $\pm$ 262	0.2 (-1.4)
PANSS total	65.5 $\pm$ 17.3	59.8 $\pm$ 16	0.2 (1.3)
PANSS positive	14 $\pm$ 4.9	13.5 $\pm$ 4.3	0.6 (0.4)
PANSS negative	17.5 $\pm$ 6	14.6 $\pm$ 5.8	0.06 (1.9)

**Table 1: Demographic and clinical data of the patients.** Data are presented in mean  $\pm$  standard deviation. 2-tailed t-tests and  $\chi^2$  tests performed when appropriate. Abbreviations: M – male; F – female; R – right handed; L – left handed; y – years; PANSS – positive and negative symptom scale; PE – passivity experiences.

### MR image acquisition

MRI data were acquired using a 3 Tesla scanner (Magnetom TrioTim, Siemens Medical Solutions), equipped with a 32-channel head coil. Each MRI session included a magnetization-prepared rapid acquisition gradient echo (MPRAGE) sequence and a 9 minutes gradient echo-planar imaging (EPI) sequence sensitive to BOLD (blood-oxygen-level-dependent) contrast. The MPRAGE acquisition had a 1 mm in-plane resolution and 1.2 mm slice thickness, covering  $240 \times 257 \times 160$  voxels (TR = 2.30 ms, TE = 2.98 ms and TI = 900 ms). The functional MRI (EPI) acquisition had isotropic 3.3 mm voxel size, with a 0.3 mm inter-slice gap and covering a total of  $64 \times 58 \times 32$  voxels (TR = 1920 ms and TE = 30ms). Resting-state fMRI (rs-fMRI) was recorded, patients were lying in the scanner with eyes open, resting but awake and cognitively alert. The acquisition process resulted in a sequence of 280 BOLD images for each patient. Two patients were excluded from further imaging analysis due to poor image quality (these patients are excluded from the data shown in Table 1).

## Functional image preprocessing

Functional data analysis and standard pre-processing was performed using the functional connectivity toolbox CONN (conn-toolbox.org/) and SPM 12 (fil.ion.ucl.ac.uk/spm/) for Matlab (mathworks.com). Functional images were corrected for slice time and motion, co-registered with a high-resolution anatomical scan, normalized into MNI space, resampled to  $1.5 \times 1.5 \times 1.5 \text{ mm}^3$ , and smoothed with a  $6 \text{ mm}^3$  full-width at half maximum (FWHM) Gaussian kernel for each subject. To estimate the excessive movement, the mean frame-wise displacement (FD)<sup>35</sup> during the scanning was estimated with the exclusion threshold of 0.5 mm. The groups did not differ in terms of the movements over the scanning period ( $t = -0.35$ ,  $p = 0.7$  with the mean FD of  $0.18 \pm 0.09 \text{ mm}$  and  $0.19 \pm 0.1 \text{ mm}$  for PE- and PE+ groups respectively). Following the standard pipeline for confound removal of the CONN toolbox, the individual time courses of the segmented white matter and cerebrospinal fluid, the 6 motion parameters with rigid body transformations and their first-order derivatives, and global signal time courses were extracted and regressed out of the data. Regressions were performed for the entire time-series. The BOLD signal data were passed through a band filter (0.009-0.08 Hz).

## Networks

*Presence hallucination network.* Presence hallucination network (PH-network; Figure 2A) was defined as an overlap of the brain regions associated with the robot-induced PH and the symptomatic PH-network derived from neurological patients experiencing PH (for more details see Bernasconi, Blondiaux et al., 2020<sup>15</sup>). The overlapping areas of these two experiments are the right posterior middle temporal gyrus (pMTG right;  $x = 54$ ,  $y = -54$ ,  $z = 0$ ), the right inferior frontal gyrus (IFG right;  $x = 51$ ,  $y = 18$ ,  $z = 29$ ) and left ventral premotor cortex (vPMC left;  $x = 51$ ,  $y = 18$ ,  $z = 29$ ). Those areas were transposed bilaterally.

*Control networks.* Control regions were derived by shifting each region of the PH-network but keeping the same shape and the same number of voxels as an original network<sup>15</sup> (Figure S1A). The areas were shifted to fit in the brain mask and do not comprise white matter. The areas were shifted by the following coordinates: IFG  $x \pm 20$   $y + 30$   $z - 15$ ; vPMC  $x \pm 10$   $y + 30$   $z - 15$ ; pMTG  $x$   $y + 30$   $z - 15$ . Visual network from resting-state fMRI network atlas<sup>36</sup> (Figure S1B) was analyzed as a second control network. It is composed of four regions of interests (ROIs): calcarine sulcus, left thalamus, left and right middle / superior occipital gyri.

## Statistical analyses

Differences in demographic characteristics and clinical data between the two groups of patients were examined by unpaired t-tests and Pearson's  $\chi^2$  tests when applicable.

ROI-to-ROI analyses were conducted by extracting bivariate correlation values (z-transformed) of the PH-network for all possible connections for each subject. Connectivity values were exported and subjected to statistical analysis in R (R-project.org/). Linear mixed-effects model using group (PE+, PE-) and connection (15 connections) as fixed effects and subjects as a random effect was applied in order to investigate whether an interaction effect between the groups and all possible connections was present within the PH network. Post-hoc analyses for the between-group differences were performed with FDR (p=0.05) correction for multiple comparisons. Data outliers (6% of all data points) were removed based on 1.5 IQR from the functional connectivity mean value for each connection. Patients' age and medication dose were included in the analysis as covariates of no interest due to considerable variance between the patients, which can influence functional coupling<sup>37,38</sup>.

To further study functional connectivity associated with PH-network, we performed ROI-to-whole-brain analysis. The ROIs from the PH-network, which showed significant functional connectivity differences between groups, were used as seed ROIs. Individual correlation maps were created by extracting the mean resting state BOLD time course from the seed region and correlating it with the time course of each voxel of the whole brain. Subsequently, correlation coefficients were normalized using Fisher-z-transformation to create individual single-patient maps of voxel-wise functional connectivity. The resulting maps were then entered in a second-level analysis. T-contrasts for group comparisons with p<0.001 peak voxel-level uncorrected and cluster level FDR p<0.05 corrected thresholds were analyzed. Age and medication dose of the patients were included as covariates of no interest to control for possible confounds in functional brain coupling.

## Results

### *Functional disconnection within the presence hallucination network*

We investigated the functional connectivity within the PH-network between PE+ and PE- patients to determine whether the PH-network is relevant for a broader spectrum of psychotic symptoms like PE. The linear mixed-effects model showed no main effect of group ( $F_{(1,56)} = 2.4$ ,  $p = 0.12$ ), meaning that there was no global difference of PH-network functional connectivity between groups (PE+ patients  $r_{PH\_total} = 0.21 \pm 0.26$ ,  $CI = [0.23, 0.19]$ , PE- patients  $r_{PH\_total} = 0.24 \pm 0.28$ ,  $CI = [0.27, 0.22]$ ). We observed a significant main effect of connection ( $F_{(14,786)} = 52.4$ ,  $p < 0.0001$ ) and a significant interaction between patient group and connection ( $F_{(14,786)} = 3.4$ ,  $p < 0.0001$ ). Post-hoc analysis revealed that the interaction was driven by functional connectivity differences between the right pMTG and the right IFG ( $r_{PE+} = 0.235 \pm 0.172$ ,  $CI = [0.29, 0.17]$ ;  $r_{PE-} = 0.481 \pm 0.165$ ,  $CI = [0.56, 0.40]$ ;  $t = -4.1$ ,  $p = 0.0007$ ), and between the right pMTG and the left IFG ( $r_{PE+} = -0.029 \pm 0.223$ ,  $CI = [0.04, -0.10]$ ;  $r_{PE-} = -0.152 \pm 0.206$ ,  $CI = [0.24, 0.07]$ ;  $t = -3.49$ ,  $p = 0.004$ ) (Figure 2B,C). Functional connectivity was reduced for both connections in PE+ group as compared to PE- group. Similar analyses in control regions (main effect of group  $F_{(1,59)} = 0.03$ ,  $p = 0.85$ , group by connection interaction:  $F_{(14,794)} = 1.4$ ,  $p = 0.14$ ) and visual network (main effect of group:  $F_{(1,54)} = 0.57$ ,  $p = 0.45$ , group by connection interaction:  $F_{(5,276)} = 0.53$ ,  $p = 0.75$ ) revealed no significant differences between the patient groups (for more details see supplementary information).



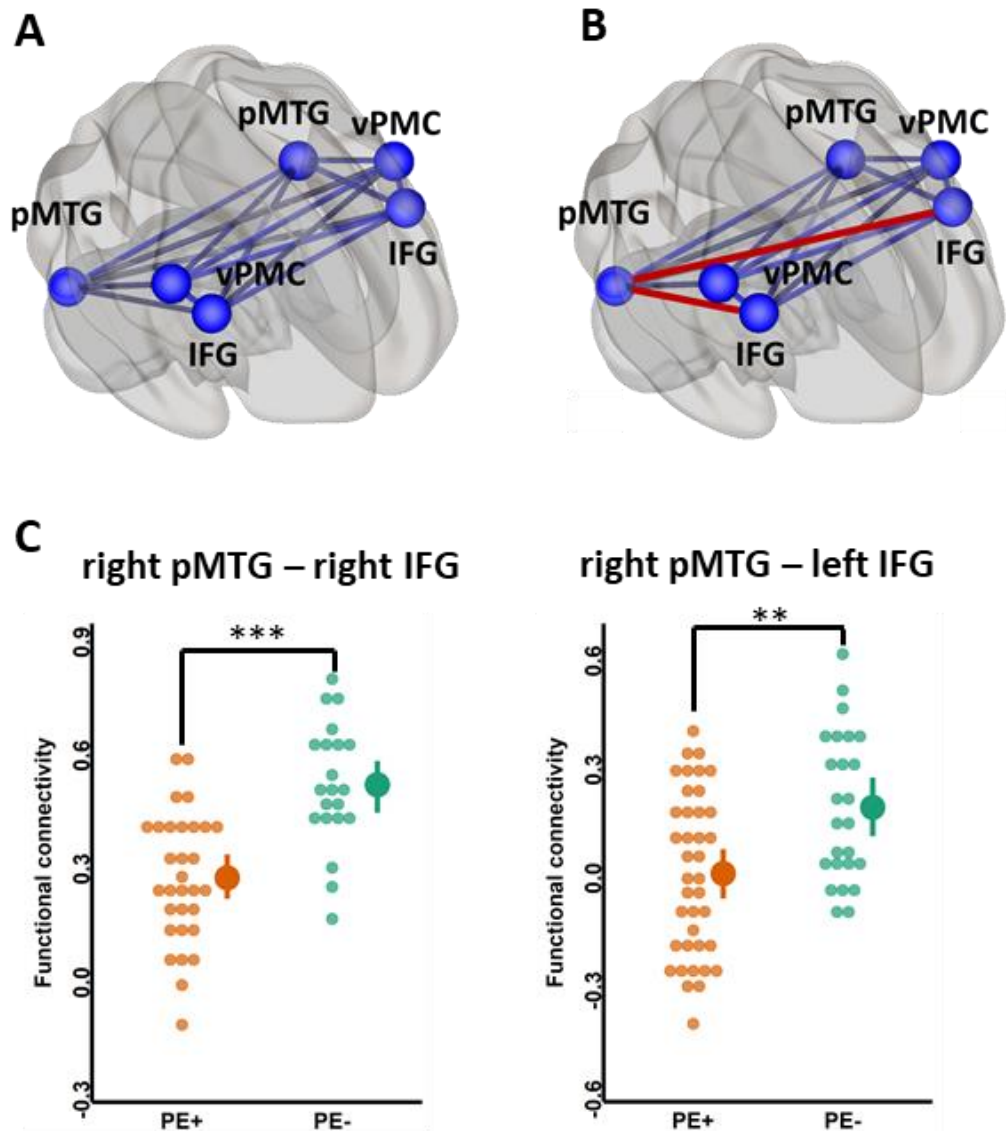


**Figure 2. Functional disconnection within the presence hallucination network comparing patients with (PE +) and without (PE -) passivity experiences.** **A.** PH-network projection on the brain surface. Six regions of interest were used as seeds for functional connectivity analysis bilaterally: inferior frontal gyrus (IFG), posterior middle temporal gyrus (pMTG), ventral premotor cortex (vPMC). **B.** Connections marked in red are hypoconnected in PE+ patients compared to PE- ones. **C.** Functional connectivity between the right pMTG and the right IFG is presented on the left and the right pMTG and the left IFG (on the right). Post-hoc FDR corrected at threshold of  $p=0.05$ . \*\* $p<0.01$ , \*\*\* $p<0.001$ . Dots represent individual connectivity values of each patient.

### *Extended PH-network functional connectivity changes*

To investigate network changes associated with the PH-network, we conducted three seed-based analyses using the right pMTG, bilateral IFG as seed regions. Seeding from the right pMTG, a decreased functional connectivity was observed with the right middle frontal gyrus and the left inferior frontal gyrus in PE+ group compared to PE-. These two areas partly overlapped with the PH-network ROIs (108 voxels with the left IFG and 2 voxels with the right IFG; Figure 3A). Using the left IFG as a seed, a decreased functional connectivity was observed in the right medial superior frontal gyrus and the left Heschl gyrus (superior temporal gyrus) in the PE+ group as compared to PE- group (Figure 3B). When seeding from the right IFG, an increased functional connectivity with the left putamen and decreased functional connectivity with the left lateral occipital cortex (inferior occipital gyrus), and the right middle temporal gyrus were found in the PE+ group (Figure 3C). Moreover, the cluster in the right middle temporal gyrus has been identified as part of the PH-network area (59 voxels overlap with the right pMTG; Figure 3A). The details of the clusters are described in Table 2.

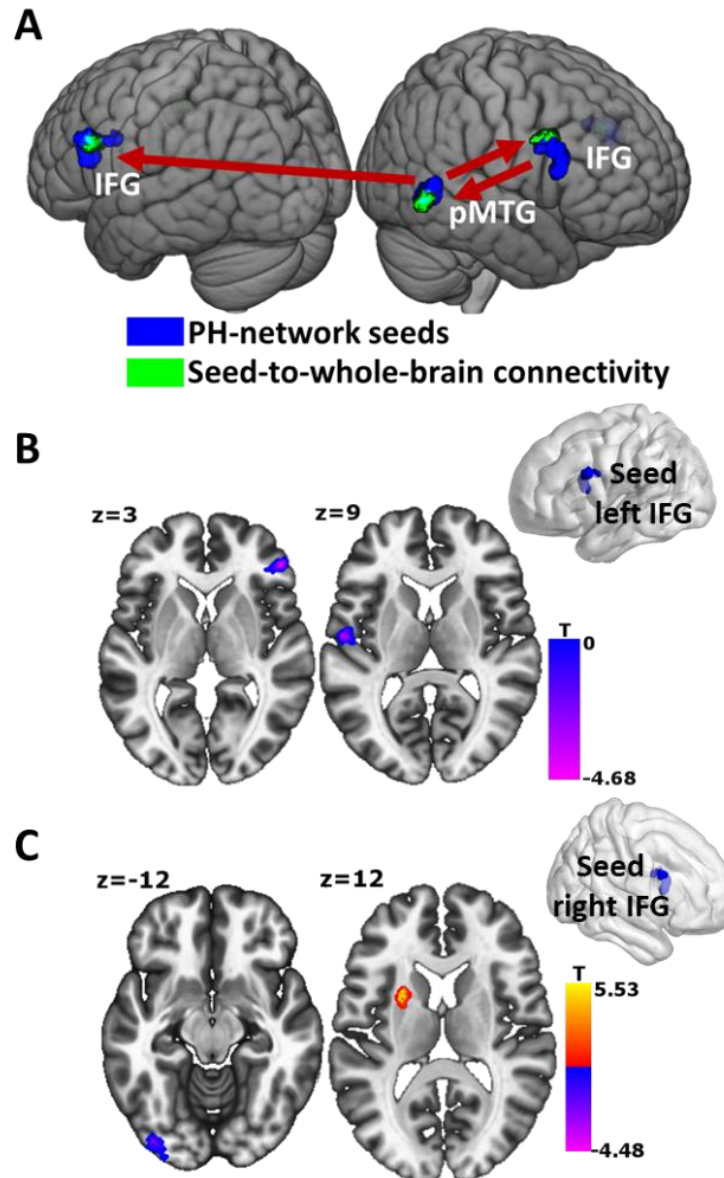


**Figure 3. Functional connectivity changes in PE+ patients seeding from the PH-network areas to the whole brain.** **A.** PH-network seeds (in blue) were traced back during whole brain functional connectivity analysis (areas in green). The red arrows represent from which seed (blue) the decreased functional connectivity in PE+ patients was observed. **B.** Decreased functional connectivity in PE+ patients seeding from the left IFG with the right medial superior frontal gyrus and the left Heschl gyrus. **C.** Decreased functional connectivity in PE+ patients seeding from the right IFG with the left inferior occipital gyrus and increased functional connectivity with the left putamen. Voxel level  $p < 0.001$  uncorrected, cluster threshold at  $p < 0.05$  FDR corrected.

<b>Seed-to-whole-brain</b>								
<b>PE+ vs. PE-</b>								
MNI coordinates								
BA	Anatomic Label		k (vox)	x	y	z	$\beta$	T
<b>right pMTG</b>								
9	Middle frontal gyrus	R	189	35	06	32	-0.22	-4.58
9	Inferior frontal gyrus	L	161	-53	17	27	-0.22	-4.47
<b>left IFG</b>								
8	Medial superior frontal gyrus (frontal pole)	R	137	48	39	03	-0.22	-4.64
43, 22	Heschl gyrus (part of superior temporal gyrus)	L	149	-57	-11	09	-0.17	-4.06
<b>right IFG</b>								
	Putamen	L	178	-24	08	14	0.14	5.34
18	Lateral occipital cortex, inferior division (inferior occipital gyrus)	L	211	-39	-87	-12	-0.16	-4.18
21, 37	Middle temporal gyrus, temporooccipital part	R	147	63	-53	-03	-0.19	-4.13

**Table 2: Details of the clusters from seed-to-whole-brain functional connectivity analysis.** BA – Broadman area, k – cluster size in voxels, PE – passivity experiences

## Discussion

We have investigated the functional connectivity changes within the PH-network in psychotic patients with and without PE. Our key finding was the observed reduced fronto-temporal functional connectivity within the PH-network, namely between the right pMTG and IFG bilaterally in patients with PE as compared to the patients without PE. We have shown that functional disconnectivity is specific to the PH-network compared to two control networks, where no significant differences between the groups were observed. Further, we investigated the seed-to-the whole-brain connectivity and we traced back the disconnectivity of the PH-network without *a priori* restriction of the connections. Fronto-temporal disconnection stands in line with recent works showing reduced functional connectivity within the PH-network in patients with Parkinson's disease experiencing symptomatic PHs<sup>15</sup>. Furthermore, patients with Lewy Body Dementia suffering from PHs have decreased glucose intake (PET study) in the fronto-parietal areas (including the temporo-parietal junction)<sup>39</sup>.

This decrease in functional connectivity was predicted and extends earlier findings of reduced functional connectivity in psychotic patients<sup>26,27,40,41</sup> to the PH-network, suggesting that PH is an essential aspect in the symptomatology of psychosis and relevant for the mechanisms involved in the occurrence of passivity symptoms. It could represent a building block discrepancy, giving rise and interacting with different hallucinations where internal actions, thoughts and sensations are misattributed to an external agent. PH is similar to the passivity symptoms in terms of an erroneous interpretation of self-related sensorimotor processing<sup>7,13,15,42</sup>. Taken as an example, one of the most abundant passivity symptoms is auditory verbal hallucination, where self-generated inner speech is misattributed to an external agent<sup>43,44</sup>. Both these hallucinations share a fundamental aspect of disturbed self-monitoring in different sensory domains. Notably, studies that have induced mild sensations of PHs under controlled conditions concurrently have reported elevated levels of PE in healthy subjects<sup>13,15</sup> and first episode psychosis<sup>5</sup>. Based on these studies, we could argue that PHs and PE are intertwined and suggest that PH is sub-part of PE, and current findings confirm this at the neural level. Nonetheless, despite the existing relationship between the passivity symptoms and PH, the latter was never included in the same categorization. Indeed, the occurrence of PH was not investigated until recently in daily clinical practices, and only now is it gaining interest as a frequent symptom in psychotic patients<sup>18</sup>.

Since we investigated the PH-network in psychotic patients with PE, we were expecting to find an extended network from PH-network between the patients due to the broader range of the symptoms. Indeed, we have observed additional functional connectivity changes with the frontal areas (bilateral IFG). Decreased functional connectivity in patients with PE has been found between left IFG and left Heschl gyrus, which could account for the PH-network association with auditory verbal hallucinations. Altered functional connectivity to the Heschl gyrus has been reported in patients with auditory verbal hallucinations<sup>41,45,46</sup>. This is in line with our findings, since one of the criteria for patients to be grouped as PE+ was the presence of auditory verbal hallucinations (more than half of the patients tested in this study displayed this symptom (see Figure 1)). We also observed increased functional connectivity between the right IFG (from the PH-network) and the left putamen in patients with PE. Changes in putamen activity have also been related to the auditory verbal hallucinations<sup>47-49</sup>. These findings allow us to link the PH-network with passivity symptoms, more specifically, with auditory-verbal hallucinations, which are very frequent in psychotic patients<sup>18</sup>.

The current study has some limitations. The evaluation of the symptoms was not conducted at the time as the data acquisition and PH was not specifically assessed in those patients. Further studies should investigate more in-depth into the similarities and differences of various passivity symptoms and their relation with PH-network. Additionally, it would be interesting to assess in more details the occurrence of PH, which could give us a unique insight into the specific characteristics and allow to disentangle PH and PE.

Altogether this work showed that functional connectivity within the PH-network, more precisely between the right pMTG and bilateral IFG, was different in psychotic patients with PE compared to those without. PH seemed to be part of a broader PE network. Future should investigate in more details the relation between PH and PE. Taken together, these findings strengthen the relevance of the PH-network for clinical populations suffering from psychosis, suggesting that the PH-network could be a potential biomarker for various passivity symptoms.

## References

1. Lysaker PH, Lysaker JT. Narrative Structure in Psychosis. *Theory Psychol.* 2002;12(2):207-220. doi:10.1177/0959354302012002630
2. Graham-Schmidt KT, Martin-Iverson MT, Waters FAV. Self- and other-agency in people with passivity (first rank) symptoms in schizophrenia. *Schizophr Res.* 2017;192:75-81. doi:10.1016/j.schres.2017.04.024
3. Waters FAV, Badcock JC, Dragović M, Jablensky A. Neuropsychological functioning in schizophrenia patients with first-rank (passivity) symptoms. *Psychopathology.* 2009;42(1):47-58. doi:10.1159/000187634
4. Schneider K. Primary & secondary symptoms in schizophrenia. *Fortschr Neurol Psychiatr Grenzgeb.* 1957;25(9):487-48790.
5. Salomon R, Progin P, Griffa A, Rognini G, Do KQ, Conus P. Sensorimotor Induction of Auditory Misattribution in Early Psychosis. *Schizophr Bull.* 2020:1-8. doi:10.1093/schbul/sbz136
6. Blakemore S-J, Smith J, Steel R, Johnstone EC, Frith CD. The perception of self-produced sensory stimuli in patients with auditory hallucinations and passivity experiences: evidence for a breakdown in self-monitoring. *Psychol Med.* 2000;30(5):1131-1139. doi:10.1017/S0033291799002676
7. Blakemore S-J, Goodbody SJ, Wolpert DM. Predicting the Consequences of Our Own Actions : The Role of Sensorimotor Context Estimation. 1998;18(18):7511-7518.
8. Ford JM, Palzes VA, Roach BJ, Mathalon DH. Did I Do That? Abnormal Predictive Processes in Schizophrenia When Button Pressing to Deliver a Tone. *Schizophr Bull.* 2014;40(4):804-812. doi:10.1093/schbul/sbt072
9. Fletcher PC, Frith CD. Perceiving is believing: a Bayesian approach to explaining the positive symptoms of schizophrenia. *Nat Rev Neurosci.* 2009;10(1):48-58. doi:10.1038/nrn2536
10. Frith CD. The self in action: Lessons from delusions of control. *Conscious Cogn.* 2005;14(4):752-770. doi:10.1016/j.concog.2005.04.002
11. Frith CD, Done DJ. Experiences of alien control in schizophrenia reflect a disorder in the central monitoring of action. *Psychol Med.* 1989;19(2):359-363. doi:10.1017/S003329170001240X
12. Bansal S, Ford JM, Sperling M. The function and failure of sensory predictions. *Ann N Y Acad Sci.* 2018;1426(1):199-220. doi:10.1111/nyas.13686
13. Blanke O, Pozeg P, Hara M, et al. Neurological and Robot-Controlled Induction of an Apparition. *Curr Biol.* 2014;24(22):2681-2686. doi:10.1016/j.cub.2014.09.049
14. Serino A, Pozeg P, Rognini G, et al. Robot-controlled induction of thought insertion. *submitted.* 41(0):1-30.
15. Bernasconi F, Blondiaux E, Potheegadoo J, et al. *Sensorimotor Hallucinations in Parkinson's Disease.* doi:https://doi.org/10.1101/2020.05.11.054619
16. James W. *The Principles of Psychology.* New York: Henry Holt and Company; 1890.
17. Jaspers K. Über leibhaftige Bewußtheiten (Bewußtheitstäuschungen), ein psychopathologisches Elementarsymptom. In: *Gesammelte Schriften zur Psychopathologie.* Berlin, Heidelberg: Springer Berlin Heidelberg; 1913:413-420.
18. Llorca PM, Pereira B, Jardri R, et al. Hallucinations in schizophrenia and Parkinson's disease: an analysis of sensory modalities involved and the repercussion on patients. *Sci Rep.* 2016;6(1):38152. doi:10.1038/srep38152
19. Arzy S, Seeck M, Ortigue S, Spinelli L, Blanke O. Induction of an illusory shadow person. *Nature.* 2006;443(7109):287. doi:10.1038/443287a
20. Fénelon G, Soulas T, Cleret de Langavant L, Trinkler I, Bachoud-Lévi A-C. Feeling of presence in Parkinson's disease. *J Neurol Neurosurg Psychiatry.* 2011;82(11):1219-1224. doi:10.1136/jnnp.2010.234799
21. Reckner E, Cipolotti L, Foley JA. Presence Phenomena in Parkinsonian Disorders: Phenomenology and Neuropsychological Correlates. *Int J Geriatr Psychiatry.* 2020. doi:10.1002/gps.5303
22. Barnby JM, Bell V. The Sensed Presence Questionnaire (SenPQ): initial psychometric validation of a measure of the "Sensed Presence" experience. *PeerJ.* 2017;5:e3149. doi:10.7717/peerj.3149

23. Hayes J, Leudar I. Experiences of continued presence: On the practical consequences of “hallucinations” in bereavement. *Psychol Psychother.* 2016;89(2):194-210. doi:10.1111/papt.12067
24. Friston KJ. The disconnection hypothesis. *Schizophr Res.* 1998;30(2):115-125. doi:10.1016/S0920-9964(97)00140-0
25. Hahamy A, Calhoun V, Pearlson G, et al. Save the Global: Global Signal Connectivity as a Tool for Studying Clinical Populations with Functional Magnetic Resonance Imaging. *Brain Connect.* 2014;4(6):395-403. doi:10.1089/brain.2014.0244
26. Skudlarski P, Jagannathan K, Anderson K, et al. Brain Connectivity Is Not Only Lower but Different in Schizophrenia: A Combined Anatomical and Functional Approach. *Biol Psychiatry.* 2010;68(1):61-69. doi:10.1016/j.biopsych.2010.03.035
27. Karbasforoushan H, Woodward ND. Resting-State Networks in Schizophrenia. *Curr Top Med Chem.* 2013;12(21):2404-2414. doi:10.2174/1568026611212210011
28. American Psychiatric Association. *DSM-IV.*; 2000.
29. Baumann PS, Crespi S, Marion-Veyron R, et al. Treatment and early intervention in psychosis program (TIPP-Lausanne): Implementation of an early intervention programme for psychosis in Switzerland. *Early Interv Psychiatry.* 2013;7(3):322-328. doi:10.1111/eip.12037
30. Schnell K, Heekeren K, Daumann J, et al. Correlation of passivity symptoms and dysfunctional visuomotor action monitoring in psychosis. *Brain.* 2008;131(10):2783-2797. doi:10.1093/brain/awn184
31. Franck N, O’Leary DS, Flaum M, Hichwa RD, Andreasen NC. Cerebral Blood Flow Changes Associated With Schneiderian First-Rank Symptoms in Schizophrenia. *J Neuropsychiatry Clin Neurosci.* 2002;14(3):277-282. doi:10.1176/jnp.14.3.277
32. Farrer C, Franck N, Frith CD, et al. Neural correlates of action attribution in schizophrenia. *Psychiatry Res Neuroimaging.* 2004;131(1):31-44. doi:10.1016/j.psychres.2004.02.004
33. Andreasen NC. *The Scale for the Assessment of Positive Symptoms (SAPS).* Iowa City, University of Iowa; 1984.
34. Kay SR, Fiszbein A, Opler LA. The positive and negative syndrome scale (PANSS) for schizophrenia. *Schizophr Bull.* 1987;13(2):261-276. doi:10.1093/schbul/13.2.261
35. Power JD, Barnes KA, Snyder AZ, Schlaggar BL, Petersen SE. Spurious but systematic correlations in functional connectivity MRI networks arise from subject motion. *Neuroimage.* 2012;59(3):2142-2154. doi:10.1016/j.neuroimage.2011.10.018
36. Shirer WR, Ryali S, Rykhlevskaia E, Menon V, Greicius MD. Decoding subject-driven cognitive states with whole-brain connectivity patterns. *Cereb Cortex.* 2012;22(1):158-165. doi:10.1093/cercor/bhr099
37. Ferreira LK, Regina ACB, Kovacevic N, et al. Aging effects on whole-brain functional connectivity in adults free of cognitive and psychiatric disorders. *Cereb Cortex.* 2016;26(9):3851-3865. doi:10.1093/cercor/bhv190
38. H. Roder C, Marie Hoogendam J, M. van der Veen F. FMRI, Antipsychotics and Schizophrenia. Influence of Different Antipsychotics on BOLD-Signal. *Curr Pharm Des.* 2010;16(18):2012-2025. doi:10.2174/138161210791293088
39. Nicastro N, Eger AF, Assal F, Garibotto V. Feeling of presence in dementia with Lewy bodies is related to reduced left frontoparietal metabolism. *Brain Imaging Behav.* 2018. doi:10.1007/s11682-018-9997-7
40. Crossley N a., Mechelli A, Fusar-Poli P, et al. Superior temporal lobe dysfunction and frontotemporal dysconnectivity in subjects at risk of psychosis and in first-episode psychosis. *Hum Brain Mapp.* 2009;30(12):4129-4137. doi:10.1002/hbm.20834
41. Oertel-Knöchel V, Knöchel C, Matura S, et al. Association between symptoms of psychosis and reduced functional connectivity of auditory cortex. *Schizophr Res.* 2014;160(1-3):35-42. doi:10.1016/j.schres.2014.10.036
42. Frith CD, Blakemore SJ, Wolpert DM. Explaining the symptoms of schizophrenia: Abnormalities in the awareness of action. *Brain Res Rev.* 2000;31(2-3):357-363. doi:10.1016/S0165-0173(99)00052-1
43. Jones SR, Fernyhough C. Neural correlates of inner speech and auditory verbal hallucinations: A critical review and theoretical integration. *Clin Psychol Rev.* 2007;27(2):140-154. doi:10.1016/j.cpr.2006.10.001



44. Tracy DK, Shergill SS. Mechanisms Underlying Auditory Hallucinations-Understanding Perception without Stimulus. *Brain Sci.* 2013;3(2):642-669. doi:10.3390/brainsci3020642
45. Shinn AK, Baker JT, Cohen BM, Öngür D. Functional connectivity of left Heschl's gyrus in vulnerability to auditory hallucinations in schizophrenia. *Schizophr Res.* 2013;143(2-3):260-268. doi:10.1016/j.schres.2012.11.037
46. Dierks T, Linden DE, Jandl M, Formisano E, Goebel R. Activation of Heschl's Gyrus during Auditory Hallucinations of these studies could directly differentiate between the hallucinatory and nonhallucinatory states within one scanning session. Because of this restriction, they did. *Neuron.* 1999;22:615-621.
47. Cui LB, Liu K, Li C, et al. Putamen-related regional and network functional deficits in first-episode schizophrenia with auditory verbal hallucinations. *Schizophr Res.* 2016;173(1-2):13-22. doi:10.1016/j.schres.2016.02.039
48. Hoffman RE, Fernandez T, Pittman B, Hampson M. Elevated functional connectivity along a corticostriatal loop and the mechanism of auditory/verbal hallucinations in patients with schizophrenia. *Biol Psychiatry.* 2011;69(5):407-414. doi:10.1016/j.biopsych.2010.09.050
49. Hoffman RE, Hampson M. Functional connectivity studies of patients with auditory verbal hallucinations. *Front Hum Neurosci.* 2012;6(January):1-7. doi:10.3389/fnhum.2012.00006

Supplementary information of fronto-temporal functional disconnection within the PH-network in psychotic patients with passivity experiences

**ROI-to-ROI analysis**

*PH-network.* Linear mixed model analyses were performed for the PH-network investigation (all connections' functional connectivity is depicted in Figure S2). Model included covariates of no interest which did not have any significant effect on the functional connectivity differences between the groups: patient's age ( $F_{(1,1)} = 0.1$ ,  $p = 0.3$ ) and dosage of medication ( $F_{(1,1)} = 0.04$ ,  $p = 0.84$ ).

*Control networks.* The same analysis was applied to the control networks. Statistical analysis in control regions, which were derived by shifting PH-network areas (see Figure S1A), showed no significant effect of group ( $F_{(1,1)} = 0.10$ ,  $p = 0.74$ ;  $PE+ r_{total} = 0.09 \pm 0.36$ ,  $CI = [0.12, 0.05]$ ;  $PE- r_{total} = 0.09 \pm 0.35$ ,  $CI = [0.13, 0.06]$ ) nor interaction between group and connection ( $F_{(1,14)} = 1.4$ ,  $p=0.15$ ). The main effect connections ( $F_{(1,14)} = 100.6$ ,  $p<0.0001$ ) was significant. Covariates of no interest patient's age ( $F_{(1,1)} = 0.06$ ,  $p = 0.8$ ) and dosage of medication ( $F_{(1,1)} = 0.77$ ,  $p = 0.15$ ) did not have significant effect.

Visual network from resting state fMRI network atlas<sup>36</sup> was analyzed as a second control (Figure S1B). Statistical analysis in visual network showed no significant effect of group ( $F_{(1,1)} = 0.57$ ,  $p = 0.45$ ;  $PE+ r_{total} = 0.38 \pm 0.42$ ,  $CI = [0.44, 0.32]$ ;  $PE- r_{total} = 0.36 \pm 0.44$ ,  $CI = [0.43, 0.29]$ ) and group by connection interaction ( $F_{(1,5)} = 0.53$ ,  $p=0.75$ ). The main effect connections ( $F_{(1,5)} = 278.3$ ,  $p < 0.001$ ) was significant. The age of patients, which was used in the model as a covariate of no interest, had a significant effect:  $F_{(1,1)} = 5.92$ ,  $p = 0.02$  while the dosage of medication had no significant effect ( $F_{(1,1)} = 0.60$ ,  $p = 0.44$ ).

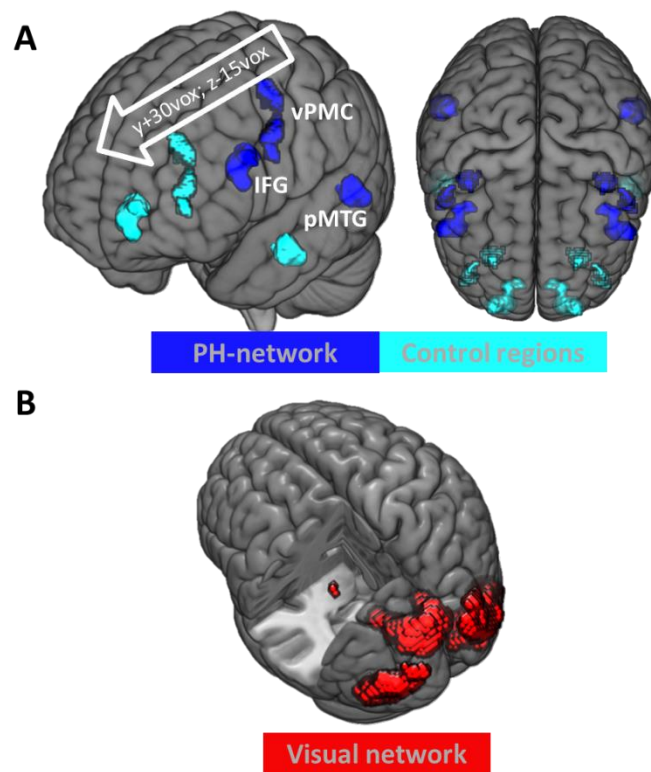


**Figure S1. Control networks.** **A.** PH-network (blue) and shifted regions of PH-network (cyan) projection on the brain surface left hemisphere and top brain surface view. IFG - inferior frontal gyrus, pMTG - posterior middle temporal gyrus, vPMC - ventral premotor cortex. **B.** Visual network projection on the brain surface.

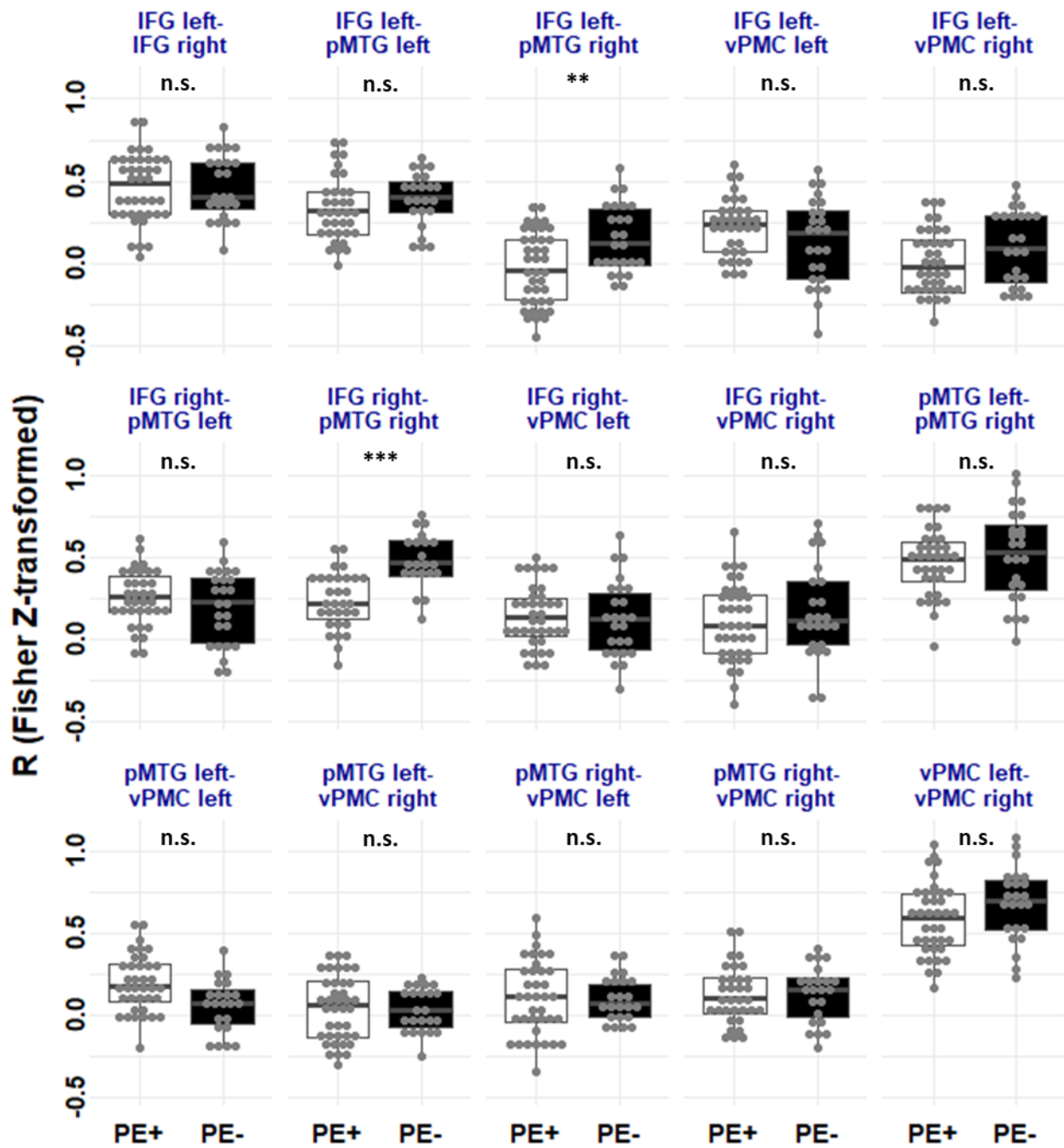


Figure S2. Functional connectivity all PH-network connections. IFG - inferior frontal gyrus, pMTG - posterior middle temporal gyrus, vPMC - ventral premotor cortex.

## Chapter 6: General Discussion

The present thesis investigated the brain networks associated with complex autoscopic phenomena with an emphasis on PH, by merging robotic technologies, cognitive neuroscience and neuroimaging. Prior this work, the understanding of the neural origins of PH was limited to the anatomical analysis of idiosyncratic brain lesions (Blanke et al., 2003, 2014; Landtblom, 2006; Nicastro et al., 2018; Picard, 2010) or to electrical stimulation in the absence of neural recordings (Arzy et al., 2006; Zijlmans et al., 2009). Here, we implemented an experimental paradigm enabling safe induction of PH, in a controlled manner, in healthy subjects. This led to the identification of a PH-network relevant for clinical populations. Our findings can lead, amongst others, to novel methods of early stage diagnosis. For example, in PD, reduced functional connectivity within a specific connection of the PH-network was associated with stronger cognitive decline in PD patients with PH and could enable the detection of more severe forms. Therefore, identifying the patients at an early stage can lead to early treatment intervention. In the next sections, I will summarize and discuss the main findings of my thesis. Future perspectives based on the work presented in this thesis will also be provided.

### 6.1 Summary of scientific contributions

#### 6.1.1 *Studying AP towards a better understanding of BSC*

**Chapter 2** described my study of the brain networks associated with each AP in neurological patients, as well as their common brain networks using recent advances in neuroimaging analysis and open access databases (Boes et al., 2015; Fox, 2018; Nooner et al., 2012). This study included the largest sample of patients with AP to date, and showed that all AP shared common brain networks including connectivity to bilateral TPJ, identified as a key region in BSC by previous studies (Blanke, 2012; Blanke et al., 2015). Indeed, TPJ has been involved in different processes important for self-consciousness such as multisensory integration (e.g. visual, tactile and vestibular signals), self-processing of agency, self-recognition, visual perspective and self-location (Apps et al., 2012, 2015; Ionta et al., 2011; Leube et al., 2003a; Nahab et al., 2011; Ruby and Decety, 2001; Salomon et al., 2016; Schurz et al., 2013; Uddin et al., 2005). This result is also in line with the classification of the four symptoms (AH,

HAS, OBE and PH) as AP and the common feature they all share: the illusory reduplication of one's own body in the extrapersonal space (Blanke et al., 2004; Brugger, 2002; Brugger et al., 1997). AP are phenomena in which the sense of self is altered and the present involvement of TPJ provides further evidence of the importance of this region in BSC (Blanke, 2012; Blanke et al., 2015; Ionta et al., 2011). Common involvement of TPJ is also in agreement with the suggested idea of continuum between AP experiences (Hécaen and Ajuriaguerra, 1952; Maillard et al., 2004). As such, a few patients reported experiencing more than one type of AP (Arias et al., 2007; Maillard et al., 2004; Martínez-Horta et al., 2020; Tadokoro et al., 2006).

We also found specific brain networks associated with each AP reflecting their own and unique characteristics that phenomenologically distinguish them from each other, i.e. AH are visual AP, OBE involve mainly vestibular components associated with disembodiment and perspective changes, HAS has prominent interoceptive, motor, and language-related aspects and PH relies mostly on sensorimotor components. Altogether, these results suggest that AP share common brain networks but that different functional sub-systems are involved in each of them. Our findings could be used in clinics to better identify which brain networks are altered depending on the AP experienced by the patients. Indeed, the brain networks associated with AP might also be involved in the underlying disease of the patients and could help identifying which brain regions are involved in focal epilepsies for example.

### *6.1.1.1 Outlook*

It would also be interesting to understand how the brain changes from one AP network to another and whether functional connectivity to some networks are more widespread than others. One way to investigate such questions would be to experimentally induce the different AP states in a controlled manner while measuring brain activity. Recent neuroimaging studies and the present **Chapter 3** have applied conflicting sensorimotor or multisensory stimulation through the use of new technologies (e.g. robotic device and virtual reality) to induce altered mental states comparable to OBE and PH (Guterstam et al., 2015; Ionta et al., 2011; Petkova et al., 2011). Combination of those experimental paradigms and dynamical functional connectivity methods could lead to a better understanding of how these networks (that are important for BSC since they capture its key aspects: self-identification, self-location and first-person perspective)

interact with each other to construct this unitary sense of self. The present findings shed light on new possibilities to investigate BSC and its complex brain mechanisms.

### *6.1.2 PH brain network across populations*

This section will summarize the main findings of **Chapter 3**, **Chapter 4** and **Chapter 5** (depicted in Figure 6.1). The next part of the discussion will address in more details the induction of PH in healthy subjects and its mechanisms, as well as the PH-network across clinical populations.

In **Chapter 3**, we adapted the paradigm used to induce PH in a safe and controlled manner (Blanke et al., 2014) to the MR scanner environment to investigate the brain networks associated to PH in healthy subjects. We found two different networks: the first one that was more activated during the asynchronous condition compared to the synchronous condition composed of four brain regions: right IFG, right pMTG, right superior frontal gyrus and right insula. The second network was more global and included all regions commonly activated by asynchronous and synchronous conditions compared to control conditions (i.e. the left sensorimotor cortex, bilateral supplemental motor area (SMA), right IPL, left putamen and right cerebellum). Both networks were found functionally more connected to the lesion locations causing PH than to control lesion locations causing visual hallucinations, providing further specificity of these networks (found in healthy subjects) with PH. These two networks were further overlapped with the symptomatic PH-network derived from eleven neurological patients with PH using the lesion network mapping analysis described in **Chapter 2**. This allowed me to determine the common brain regions associated to PH. Those regions were identified as the PH-network and included: the right IFG, the right pMTG and the right vPMC. The relevance of the PH-network was then assessed in an independent group of neurological patients (patients with PD). Functional connectivity within the PH-network predicted, with 94% accuracy, whether a patient with PD showed PH symptoms or not in his daily life. Patients with PD experiencing PH in daily life had a reduced functional connectivity between the left pMTG and the left IFG compared to PD patients without PH in daily life. The PH-network was found very selective since no differences between the two PD patients' groups (PH vs. no PH) were found in the control networks. In addition, the functional connectivity between pMTG and IFG was correlated with fronto-subcortical cognitive decline. This

work also extends the internal forward model to hallucinations in patients with PD experiencing PH and further supports that PH is an own-body schema disorder associated with altered sensorimotor self-monitoring (Arzy et al., 2006; Brugger et al., 1996; Corlett et al., 2007; Critchley, 1979; Fletcher and Frith, 2009). The results will be discussed in more details in section 6.5.

In **Chapter 4**, we studied a population with a 22q11DS, who has a very high risk of developing schizophrenia. In the first part of the study, we tested the sensitivity and the proneness of these subjects to experience PH and related PE; we found that 22q11DS individuals had a lack of sensitivity in sensorimotor modulation for the loss of agency (LoA) and a lack of delay dependency in experiencing robot-induced PH and PE compared to age-matched controls. Reduced functional connectivity within the PH-network was found for the 22q11DS subjects compared to controls, specifically in right fronto-temporal connections and bilateral pMTG. These results could represent potential behavioral and neural markers for specific psychotic symptoms (such as passivity experiences) since they were found in asymptomatic 22q11DS subjects.

Finally, in **Chapter 5**, we assessed the PH-network in psychotic patients with and without PE. We found again a fronto-temporal disconnection between the right pMTG and bilateral IFG. Connectivity from the PH-network to the whole brain showed functional disconnection with areas that overlap with the PH-network as well as with additional clusters that have been shown to be altered in auditory verbal hallucinations (the latter are comprised among the PE) (Cui et al., 2016; Dierks et al., 1999; Hoffman and Hampson, 2012; Hoffman et al., 2011; Oertel-Knöchel et al., 2014; Shinn et al., 2013).

Altogether, I have identified a PH-network that is affected in all clinical populations (more details in section 6.5). These results are important because, in clinical practices, hallucinations such as PH are assessed through post-hoc interviews and are described sometimes days or weeks after the occurrence, potentially resulting in sub-optimal treatments. More generally, the present work provides researchers and clinician new tools to assess PH more objectively either by quantifying online robot-induced PH across controlled conditions or by detecting functional connectivity changes in PH-networks. Early detection of those patients could help in providing the appropriate preventive care at an early stage of the illness before the apparition of more severe



symptoms. In the following sections, I will discuss in more details the induction of PH in healthy subjects and PH across clinical populations, as well as future perspectives.

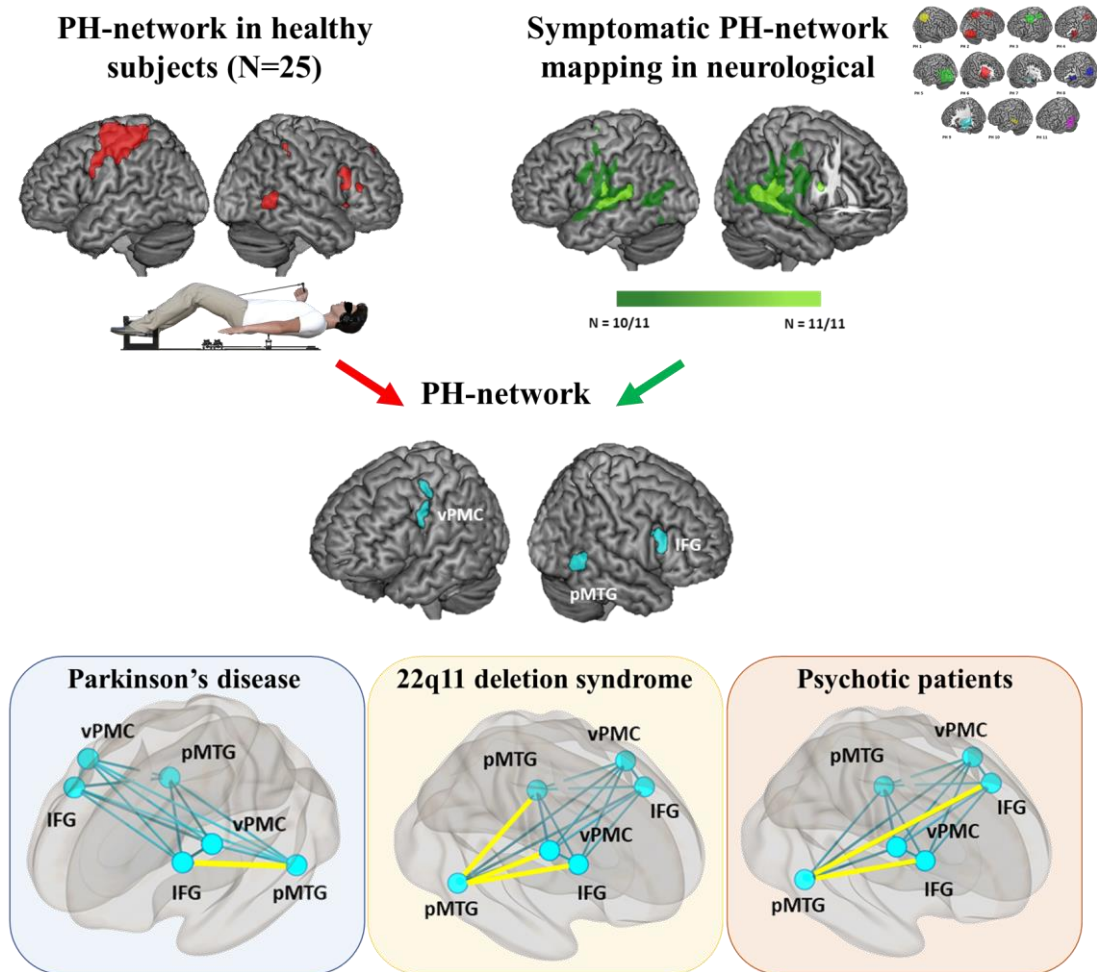


Figure 6.1: Overview of the brain regions associated with PH in different populations discovered during my thesis.

## 6.2 Induction of PH in healthy subjects

Previous neuroimaging studies have mainly focused on upper limb conflicts, more particularly on visuo-tactile or visuo-motor conflicts, assessing either body-part ownership or agency (Ehrsson et al., 2004, 2005; Farrer and Frith, 2002; Farrer et al., 2003; Fink et al., 1999; Nahab et al., 2011; Sperduti et al., 2011; Tsakiris et al., 2006, 2010; Yomogida et al., 2010). A meta-analysis on the brain regions associated to external-agency attribution revealed involvement of STG, dorsomedial prefrontal cortex, pre-SMA and inferior parietal lobe (IPL) while self-agency was related to the insula, primary somatosensory cortex and premotor cortex (Sperduti et al., 2011). Regarding body-part ownership, different brain regions were associated with the

illusory feeling of ownership towards a body part such as the premotor cortex, the intraparietal sulcus (IPS), the cerebellum and the insula (Ehrsson et al., 2004; Lloyd et al., 2006; Tsakiris et al., 2007). Although most of these studies relied on visuo-tactile conflicts, one study also relied on somatosensory conflicts between the two upper limbs to induce illusory ownership while measuring fMRI (Ehrsson et al., 2005). The authors found activation in IFG (called ventral premotor cortices in their study but similar to our IFG ROI), intraparietal sulcus and cerebellum to be associated with the illusory condition of the hand ownership and the strength of the illusion correlated with the activity in IFG and cerebellum. This suggests that IFG and cerebellum are important structures for the detection and integration of multisensory signals (tactile and proprioceptive).

More recently, neuroimaging studies manipulating the global aspects of BSC (which we also studied through the PH) through visuo-tactile conflicts started to emerge. This manipulation aimed at providing a better understanding on how the brain integrates multisensory and sensorimotor signals to create a global and coherent representation of the self (Blanke, 2012; Blanke and Metzinger, 2009; Blanke et al., 2015; Guterstam et al., 2015; Ionta et al., 2011; Petkova et al., 2011; Tsakiris et al., 2010). Ionta and colleagues manipulated self-location and self-identification of healthy subjects by generating visuo-tactile and visuo-vestibular conflicts using virtual reality combined with a robotic device (Ionta et al., 2011). They found bilateral involvement of the TPJ for self-location and the right middle-inferior temporal cortex for self-identification (Ionta et al., 2011). The experimental design presented in **Chapter 3** also involved the full-body but differed from the previous studies in the sense that we applied sensorimotor conflicts (and not visuo-tactile conflicts) between the right-hand movement and the sensory feedback on the back of the participants. During the condition eliciting PH (i.e. asynchronous condition with 500 ms delay between the hand movement and the sensory feedback), different sensorimotor conflicts were present. The first conflict was a spatial one (also present in the synchronous condition) where movements performed in the front space had consequences in the back space. The second conflict was a spatio-temporal conflict, where the generated right hand movements were delayed by 500 ms before being reproduced on the back. This generated both a temporal conflict and an additional spatial conflict generating another spatial conflict between the movement and sensory feedback received (Figure 6.2A).

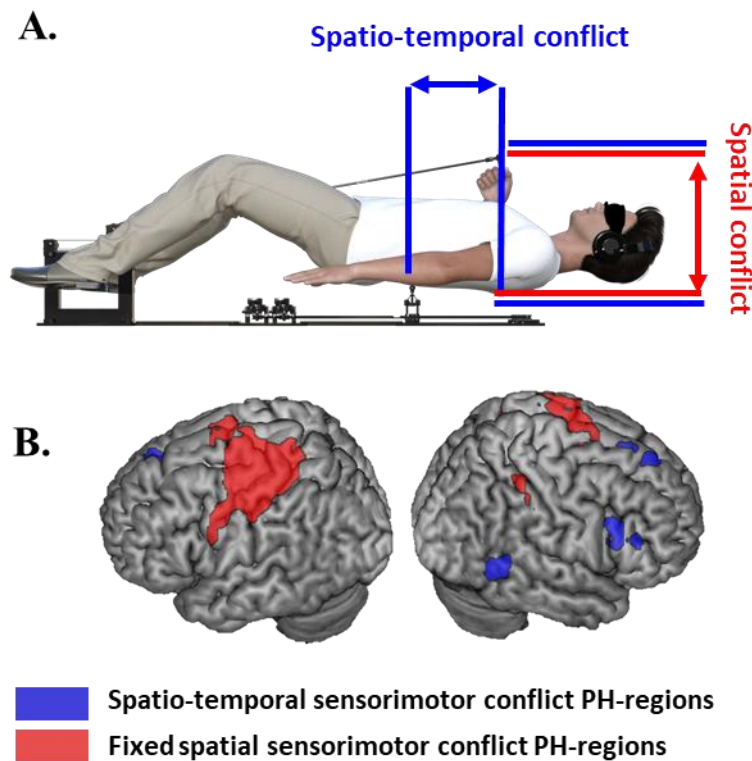


**Figure 6.2: Robot-induced PH relies on sensorimotor conflicts.** **A.** Spatio-temporal sensorimotor conflicts applied during the experimental paradigm used for robot-induced PH. In red, a fixed spatial conflict is present in both condition (asynchronous and synchronous) where a movement in the front space is reproduced in the back space. An additional spatio-temporal conflict is present in the asynchronous condition where the generated movement is delayed before being reproduced on the back of the participants generating another spatial conflict between the current position of the hand and the touch on the back (in blue). **B.** The brain regions associated to the different conflicts: in blue the regions specifically more activated during the asynchronous condition compared to the synchronous condition and in red the brain regions commonly activated during the asynchronous and synchronous conditions compared to control conditions.

**Chapter 3** attempted to determine the networks underlying both spatial and spatio-temporal conflicts by specifically looking at the brain regions more activated in the asynchronous condition compared to the synchronous condition. We identified regions on the right hemisphere (right IFG, right pMTG, right superior frontal gyrus (SFG) and right insula (in blue in Figure 6.2B). Brain regions activated both by the asynchronous and the synchronous condition compared to two controls conditions (one motor where no sensory feedback was perceived and one sensory condition where no movement was performed) were also found and comprised mainly the left sensorimotor cortex, bilateral supplemental motor area (SMA), right IPL, left putamen and right cerebellum (regions depicted in red in Figure 6.2B; cerebellum not shown).

This network is in line with previous literature on agency and sensorimotor processing (Blakemore and Sirigu, 2003; Farrer and Frith, 2002; Farrer et al., 2003; Leube et al., 2003b; Lewis and Van Essen, 2000; Sperduti et al., 2011; Yomogida et al., 2010). The activation of this network might be necessary but not sufficient to induce PH by itself. Additional functional connectivity analysis was carried out in the two networks to underlie their connectivity according to the condition (i.e. asynchronous or synchronous). Reduced functional connectivity within the brain regions activated by the fixed spatial conflict (Figure 6.2B in red) was found in the asynchronous versus synchronous condition, compatible with their involvement in the PH, which is stronger in the asynchronous condition (see **Annexes 8.1** for more details). However, the dynamics and interaction between those two networks still remain unclear and future studies should try to examine more precisely the role and interactions of both networks by using dynamical functional connectivity methods for example (Dhanis, Blondiaux et al., in preparation) and more detailed psychophysical conditions for robot-induced PH in the scanner.

### **6.3 PH and PE: independent processes?**

As mentioned, the robotic device I used also allowed to induce passivity experiences (PE, i.e. the sensation of not being in control of one's own actions) in the asynchronous condition (i.e. condition eliciting PH). This was shown in healthy subjects and psychotic patients (Blanke et al., 2014; Salomon et al., 2020). **Chapter 3** confirmed these findings in healthy subjects with the MR-compatible robotic device. Participants did not only feel someone near them but also have the sensation of being touched by someone else (PE) in the asynchronous condition. PE and PH have been proposed to arise from a failure in self-monitoring that would lead to misattributing one's own action to an external source (Blakemore et al., 2000a, 2002; Blanke et al., 2014; Fletcher and Frith, 2009; Ford et al., 2014; Salomon et al., 2020). This would suggest that PE and PH share common brain mechanisms. However, neuroimaging studies where sensorimotor conflicts between two upper limbs were applied, did not induce PH in the participants (Blakemore et al., 2000b; Ehrsson et al., 2005). A recent study from the lab showed that when the robotic feedback was applied on the hand (rather than the trunk) only PE was induced (not PH) (Franza, Bernasconi, Dhanis et al., in prep). This provides evidence for distinct brain mechanisms even though PH and PE

might share common brain structures. Altogether, spatio-temporal sensorimotor conflicts involving the trunk seem to be necessary to induce PH in line with prominent accounts that PH is a global own-body schema disorder (Brugger et al., 1996). PH and PE might share similar parts of their brain networks and mechanisms but still seem to possess their own network specificity since PE is not always associated with PH. Whether PE is necessary to induce PH still remains an open question and future research should attempt to address it.

Clinical research may also help to disentangle PH from PE. Although **Study 2.1 of Chapter 3** did not allow us to dissociate PH and PE (no correlations between the questionnaire scores and the brain regions were found), combination with the network derived from neurological patients with focal brain damage causing PH (**Chapter 3 study 2.2**) enabled to refine the network only to the brain regions associated to PH. The importance of this network was confirmed in patients with PD experiencing PH in daily life. In **Chapter 5**, we investigated whether functional connectivity from the PH-network was also different in psychotic patients with PE compared to those without. Here, it should be noted that the occurrence of PH in those patients was not assessed (retrospective imaging study) and might have co-occurred with PE. We found reduced fronto-temporal functional connectivity within PH-network in psychotic patients with PE compared to those without. This study showed that the PH-network shares brain mechanisms with PE.

Future clinical studies should characterize both PH and PE (as well as the sense of agency) in patients through detailed clinical interviews and quantify both phenomena using the robotic device. This will allow to better classify the patients according to the presence of symptomatic PE (PE+), the presence of symptomatic PH (PH+), the presence of both (PE+PH+) or none (PH-PE-). Evaluation of their sensitivity to the robot-induced PH and PE could also be investigated across groups and compared to their symptomatic PH and PE. We could further compare the functional connectivity within the PH-network across those different groups of patients and investigate additional differences in resting state connectivity.

## 6.4 Current and future studies in healthy subjects

### 6.4.1 *Using dynamic functional connectivity*

**Study 2.1 of Chapter 3** represents the first evidence that brain correlates of robot-induced PH can be assessed with fMRI. A follow up study that is currently being conducted consists in assessing the dynamic functional connectivity during the robot-induced PH (Dhanis, Blondiaux, et al., *in prep*). The aim is to better characterize the dynamic interactions of the brain regions involved in PH. For this, recurring co-activation patterns (CAPs) were identified and extracted during task-based fMRI on the data sample than **Study 2.1 of Chapter 3** (Liu et al., 2018). This method has the advantage to capture at single time points the different brain patterns associated with a seed region. Here, given the importance of the pMTG and IFG in the clinical populations, we further investigated these two regions. This study has the potential to provide further insights about the brain networks underlying PH and PE in healthy subjects and refine the networks in improved spatio-temporal terms.

### 6.4.2 *Whole versus body parts*

As mentioned previously, PH was induced by applying sensorimotor conflicts between the hand and the back of the participants and hence involved the whole body. When such conflicts are applied between the hands (meaning when the sensory feedback is reproduced on the other hand of the participants instead of their back), PH has not been induced or reported (Blakemore et al., 1998; Ehrsson et al., 2005). PH was linked to the internal forward model (Blanke et al., 2014), however, the model underlying PH might be more complex since PH only arises when conflicting sensorimotor stimulation occurs between the hand and the trunk. Therefore, the PH model should consider the prediction signals from the hand action and their integration with sensory feedback from a different body part (the trunk). Hierarchical Bayesian models may well underlie this process by relying both on the sensory inputs and on prior knowledge of what are usually the consequences of generating a hand movement (Corlett et al., 2007; Fletcher and Frith, 2009). According to this theory, low-level systems integrate and send prediction errors to higher level systems, which then send back prior beliefs to the low-level systems. The higher-level system will be adjusted in order to reduce the prediction error, increase accuracy and maintain a coherent internal representation.

Therefore, it would be interesting to investigate and compare PH in many more systematically varied trials as well as the underlying brain networks associated to sensory feedback delivered either to the hand or on the back within the same participants. This would enable to identify the brain regions or brain connections that differ depending on where the tactile feedback was delivered (to hand or back). Since PH is not induced during conflicts between the upper limbs while PE is, this experiment can also help to disentangle the two processes. In addition, this experiment will show the brain regions that are commonly activated for both the body part and the trunk and, importantly, allow to extend the internal forward model to go beyond external causation (classical model) to external other (PH).

In terms of neural correlates, the present findings in clinical populations highlighted mainly the IFG and pMTG. These two regions have been implicated in different self-related processes and BSC such as conflict monitoring, self-other distinction and self-recognition (David et al., 2008; Fink et al., 1999; Hodzic et al., 2009; Van Kemenade et al., 2019; Leube et al., 2010; Nahab et al., 2011; Uddin et al., 2005). As mentioned above, IFG was also found during upper limb somatosensory conflicts and might therefore be sensitive to body-related sensorimotor conflicts and may play a role in body ownership (Ehrsson et al., 2005). pMTG was associated with detection of multisensory conflicts when an action is self-generated and was suggested to communicate with the cerebellum, which has been involved in generating prediction errors (Blakemore et al., 1999, 2001; Van Kemenade et al., 2019; Schlerf et al., 2012). Connectivity between the IFG and pMTG might reflect integration between sensorimotor signals and self-related processes, which could in turn lead to PH in case of strong discrepancies. Therefore, it would be interesting to investigate whether the activity of these two brain regions (IFG and pMTG) and their connectivity are different when applying the sensorimotor conflict to the hand or to the trunk.

### **6.5 PH across clinical populations**

PH has been reported in different clinical populations, e.g. in Parkinson's disease (40%) and schizophrenia (46%) (Llorca et al., 2016). Although PH is frequent in these population, it is often understudied and not systematically assessed by clinicians. In the case of PD, patients also do not spontaneously report PH to their medical doctors (Ravina et al., 2007). Here, by merging cognitive neuroscience and robotics, we

designed a paradigm able to assess and induce PH in patients with Parkinson's disease (**Chapter 3 study 1**) and subjects prone to develop schizophrenia (i.e. 22q11DS subjects, **Chapter 4**). In PD patients, the robot-induced PH was similar to the phenomenology of symptomatic PH experienced in daily life. PD patients with PH showed higher sensibility and stronger bias than PD patients without PH when strong sensorimotor conflicts were applied. These results do not only extend the internal forward model to hallucination in PD patients with PH but also provide a potential behavioral marker that can be used for early diagnosis of PD patients more prone to develop hallucinations, psychosis and cognitive decline (**Chapter 3, study 3**). This would enable earlier treatment administration and/or close monitoring of the evolution of the psychotic symptoms in the patient.

Compared to PD patients, 22q11DS subjects showed a lack of sensitivity to the modulation of the sensorimotor conflicts compared to age-matched controls. The tested 22q11DS subjects were still asymptomatic (no psychotic symptoms) when tested but their response profile already differed from those of the controls. A follow-up study should try to assess 22q11DS with and without psychotic symptoms or more particularly with or without PH and measure again their response to the robotic paradigm. This would enable to monitor the evolution of the response profile in the robotic task in function of the apparition of the psychotic symptoms. PH is now also being assessed in a cohort of subjects with 22q11DS during clinical interviews and a questionnaire has been developed to assess PH more systematically. Preliminary data including 76 patients of the longitudinal cohort shows that around 20% of the individuals with 22q11DS experience PH.

I also assessed the functional connectivity at rest within the PH-network in three different clinical populations: PD (**Chapter 3, study 3**), 22q11DS subjects (**Chapter 4**) and schizophrenic patients (**Chapter 5**). This is discussed next.

### ***6.5.1 Fronto-temporal disconnection***

All three clinical populations showed consistent fronto-temporal disconnection in the PH-network, particularly between the pMTG and IFG. These results are in line with the fronto-temporal disconnection hypothesis suggested for schizophrenia and associated to psychotic symptoms (Friston, 1998; Friston and Frith, 1995; Friston et



al., 2016; Lawrie et al., 2002; Wolf et al., 2007). More recent studies also found reduced structural connectivity between these two regions in patients with schizophrenia compared to controls but also in subjects at high risk of psychosis and in first-episode psychosis (Crossley et al., 2009; van den Heuvel et al., 2010; Skudlarski et al., 2010). These results are also in line with a recent study that investigated the brain differences using positron emission tomography (PET) imaging in patients with dementia with Lewy Body with and without PH (Nicastro et al., 2018). The authors found also a reduction in glucose metabolism in left fronto-parietal regions, including a region close to TPJ.

All three assessed clinical populations showed reduced functional connectivity between the pMTG and IFG. In PD patients, this connection was found on the left hemisphere while in subjects with 22q11DS and psychotic patients this specific connection was found on the right hemisphere (also some bilateral connections were found). A study has shown early cortical susceptibility in the left hemisphere in PD patients compared to late stage PD patients in which right predominant cortical areas and bilateral occipital areas were more impaired (Claassen et al., 2016). These results are consistent with the present findings. It should be noted that the PD patients included in our study only presented minor hallucinations (i.e. PH) and no visual hallucinations, which have been more linked to the right hemisphere (Cronin-Golomb, 2010). Conversely, positive psychotic symptoms have been related to the right hemisphere in schizophrenia (Caligiuri et al., 2005). Interestingly, subjects with 22q11DS showed reduced functional connectivity between the right IFG and right pMTG compared to age-matched controls, a result that was also found in psychotic patients with PE. 22q11DS subjects were asymptomatic for psychotic symptoms at the time of data collection. This finding could represent a vulnerability marker for developing psychotic symptoms. Follow-up longitudinal studies would be interesting to monitor the evolution of the functional connectivity within the PH-network as well as the presence of psychotic symptoms.

The three clinical populations also displayed different patterns of dysconnectivity. In psychotic patients and 22q11DS subjects, even though a right hemispheric predominance was found, bilateral disconnection connections were also found: between the left IFG and right pMTG (for psychotic patients with PE) and bilateral pMTG (for 22q11DS subjects), while in PD, only the left hemisphere was affected.

The different connections affected within the PH-network might reflect the different brain alterations underlying their pathology.

Overall, these results showed different alterations in the PH-network that might reflect different mechanistic origins all leading to PH. The present findings suggest that the PH-network could be a potential predictor of psychosis more generally. This approach can also be applied in different clinical populations (Lewy body dementia for example). In addition, our results are consistent with fronto-temporal disconnections found in schizophrenia and associated to psychotic symptoms.

### **6.5.2 *Future studies in patients***

In this thesis, I have presented and validated a novel paradigm using an MR-compatible robotic device enabling the induction of PH and PE through sensorimotor conflicts in healthy subjects. This MR-robotic paradigm can now also be adapted to clinical populations to directly assess the brain networks of patients during the robot-induced PH and PE. This would enable to refine and map the brain networks for each patient. This approach would allow to more precisely compare and contrast networks across different clinical populations. The robot-induced PH and symptomatic PH of the patients can therefore be directly compared. This can also lead to tailored therapy and novel non-invasive therapeutic treatments using real-time fMRI neurofeedback to train the patients to restore normal brain activity in the specific brain regions.

## **6.6 Conclusion**

In conclusion, the novelty of this work resides in the combination of novel techniques across fields (robotics, neuroimaging, cognitive neuroscience) to unravel the brain networks of complex AP, with a focus on PH. This work highlights the importance of mainly two brain regions: IFG and TPJ (mainly the pMTG) in altered sense of self. These two brain regions were part of the identified PH-network, and their connectivity was altered in clinical populations. Therefore, this thesis revealed a previously unknown PH-network that is relevant to different populations. These findings provide new tools for PH diagnosis and can lead to a plethora of follow-up studies.

---

## 7. References

- Alais, D., and Burr, D. (2004). The Ventriloquist Effect Results from Near-Optimal Bimodal Integration. *Curr. Biol.* *14*, 257–262.
- American Psychiatric Association (2013). *Diagnostic and statistical manual of mental disorders* (5th ed.) (American Psychiatric Publishing, Arlington, VA: APA.).
- Andreasen, N.C., and Pierson, R. (2008). The Role of the Cerebellum in Schizophrenia. *Biol. Psychiatry* *64*, 81–88.
- Anzellotti, F., Onofrj, V., Maruotti, V., Ricciardi, L., Franciotti, R., Bonanni, L., Thomas, A., and Onofrj, M. (2011). Autoscopical phenomena: case report and review of literature. *Behav. Brain Funct.* *7*, 2.
- Apps, Tajadura-Jiménez, A., Turley, G., and Tsakiris, M. (2012). The different faces of one's self: An fMRI study into the recognition of current and past self-facial appearances. *Neuroimage* *63*, 1720–1729.
- Apps, M., Tajadura-Jimenez, A., Sereno, M., Blanke, O., and Tsakiris, M. (2015). Plasticity in Unimodal and Multimodal Brain Areas Reflects Multisensory Changes in Self-Face Identification. *Cereb. Cortex* *25*, 46–55.
- Ardila, A., and Gómez, J. (1988). Paroxysmal “Feeling of Somebody Being Nearby.” *Epilepsia* *29*, 188–189.
- Arias, M., Constela, I.R., Iglesias, S., Arias-Rivas, S., Dapena, D., and Sesar, Á. (2007). The autoscopical phenomena in neurological clinic: A study of two cases. *J. Neurol. Sci.* *263*, 223–225.
- Arzy, S., Seeck, M., Ortigue, S., Spinelli, L., and Blanke, O. (2006). Induction of an illusory shadow person. *Nature* *443*, 287.
- Barnby, J.M., and Bell, V. (2017). The Sensed Presence Questionnaire (SenPQ): initial psychometric validation of a measure of the “Sensed Presence” experience. *PeerJ* *5*, e3149.
- Bassett, A.S., and Chow, E.W.C. (1999). 22q11 deletion syndrome: A genetic subtype of schizophrenia. *Biol. Psychiatry* *46*, 882–891.
- Bates, E., Wilson, S.M., Saygin, A.P., Dick, F., Sereno, M.I., Knight, R.T., and Dronkers, N.F. (2003). Voxel-based lesion–symptom mapping. *Nat. Neurosci.* *6*, 448–450.
- Bernard, J.A., Goen, J.R.M., and Maldonado, T. (2017). A case for motor network contributions to schizophrenia symptoms: Evidence from resting-state connectivity. *Hum. Brain Mapp.* *38*, 4535–4545.
- Biswas, A.B., and Furniss, F. (2016). Cognitive phenotype and psychiatric disorder in 22q11.2 deletion syndrome: A review. *Res. Dev. Disabil.* *53–54*, 242–257.
- Blackmore (1982). *Beyond the Body. An Investigation of Out-of-Body Experiences* (Heinemann, London.).
- Blackmore (1986). Out-of-body experiences in schizophrenia. A questionnaire survey. *J. Nerv. Ment. Dis.* *174*, 615–619.
- Blakemore, S.-J. (2003). Deluding the motor system. *Conscious. Cogn.* *12*, 647–655.
- Blakemore, S.-J., and Sirigu, A. (2003). Action prediction in the cerebellum and in the parietal lobe. *Exp. Brain Res.* *153*, 239–245.
- Blakemore, S.-J., Wolpert, D.M., and Frith, C.D. (1998). Central cancellation of self-produced tickle sensation. *Nat. Neurosci.* *1*, 635–640.
- Blakemore, S.-J., Wolpert, D.M., and Frith, C.D. (1999). The cerebellum contributes to somatosensory cortical activity during self-produced tactile stimulation. *Neuroimage* *10*, 448–459.
- Blakemore, S.-J., Smith, J., Steel, R., Johnstone, E.C., and Frith, C.D. (2000a). The perception of self-produced sensory stimuli in patients with auditory hallucinations and passivity experiences: evidence for a breakdown in self-monitoring. *Psychol. Med.* *30*, 1131–1139.
- Blakemore, S.-J., Wolpert, D., and Frith, C. (2000b). Why can't you tickle yourself? *Neuroreport* *11*, R11–R16.
- Blakemore, S.-J., Frith, C.D., and Wolpert, D.M. (2001). The cerebellum is involved in predicting the sensory consequences of action. *Neuroreport* *12*, 1879–1884.
- Blakemore, S.-J., Wolpert, D.M., and Frith, C.D. (2002). Abnormalities in the awareness of action. *Trends Cogn. Sci.* *6*, 237–242.

- Blanke, O. (2012). Multisensory brain mechanisms of bodily self-consciousness. *Nat. Rev. Neurosci.* *13*, 556–571.
- Blanke, O., and Metzinger, T. (2009). Full-body illusions and minimal phenomenal selfhood. *Trends Cogn. Sci.* *13*, 7–13.
- Blanke, O., and Mohr, C. (2005). Out-of-body experience, heautoscopy, and autoscopic hallucination of neurological origin: Implications for neurocognitive mechanisms of corporeal awareness and self-consciousness. *Brain Res. Rev.* *50*, 184–199.
- Blanke, O., Ortigue, S., Coeytaux, A., Martory, M.-D., and Landis, T. (2003). Hearing of a presence. Neurocase Case Stud. Neuropsychol. Neuropsychiatry, Behav. Neurol. *9*, 329–339.
- Blanke, O., Landis, T., Spinelli, L., and Seeck, M. (2004). Out-of-body experience and autoscopia of neurological origin. *Brain* *127*, 243–258.
- Blanke, O., Arzy, S., and Landis, T. (2008). Illusory perceptions of the human body and self. *Neuropsychology* *88*, 429–458.
- Blanke, O., Pozeg, P., Hara, M., Heydrich, L., Serino, A., Yamamoto, A., Higuchi, T., Salomon, R., Seeck, M., Landis, T., et al. (2014). Neurological and Robot-Controlled Induction of an Apparition. *Curr. Biol.* *24*, 2681–2686.
- Blanke, O., Slater, M., and Serino, A. (2015). Behavioral, Neural, and Computational Principles of Bodily Self-Consciousness. *Neuron* *88*, 145–166.
- Boes, A.D., Prasad, S., Liu, H., Liu, Q., Pascual-Leone, A., Caviness, V.S., and Fox, M.D. (2015). Network localization of neurological symptoms from focal brain lesions. *Brain* *138*, 3061–3075.
- Bottini, G., Bisiach, E., Sterzi, R., and Vallar, G. (2002). Feeling touches in someone else’s hand. *Neuroreport* *13*, 249–252.
- Britain, G., Senior, W., Trust, W., Miall, R.C., and Wolpert, D.M.D.M. (1996). Forward Models for Physiological Motor Control. *Neural Networks* *9*, 1265–1279.
- Brocca, P. (1865). Sur le siège et la nature de la faculté du langage. *Bull. La Société d’anthropologie Paris* *1*, 369–385.
- Brugger (2002). Reflective mirrors: Perspective-taking in autoscopic phenomena. *Cogn. Neuropsychiatry* *7*, 179–194.
- Brugger, P. (1994). Are “Presences” Preferentially Felt along the Left Side of One’s Body? *Percept. Mot. Skills* *79*, 1200–1202.
- Brugger, P., Regard, M., and Landis, T. (1997). Illusory Reduplication of One’s Own Body: Phenomenology and Classification of Autoscopic Phenomena. *Cogn. Neuropsychiatry* *2*, 19–38.
- Brugger, P., Agosti, R., Regard, M., Wieser, H.G., and Landis, T. (1994). Heautoscopy, epilepsy, and suicide. *J. Neurol. Neurosurg. Psychiatry* *57*, 838–839.
- Brugger, P., Regard, M., and Landis, T. (1996). Unilaterally Felt “Presences”: The Neuropsychiatry of One’s Invisible Doppelgänger. *Neuropsychiatry. Neuropsychol. Behav. Neurol.* *9*, 114–122.
- Brugger, P., Regard, M., Landis, T., and Oelz, O. (1999). Hallucinatory experiences in extreme-altitude climbers. *Neuropsychiatry. Neuropsychol. Behav. Neurol.* *12*, 67–71.
- Brugger, P., Blanke, O., Regard, M., Bradford, D.T., and Landis, T. (2006). Polyopic heautoscopy: Case report and review of the literature. *Cortex* *42*, 666–674.
- Bychowski, G. (1943). Disorders in the body-image in the clinical pictures of psychoses. *J. Nerv. Ment. Dis.* *97*, 310–335.
- Caligiuri, M.P., Hellige, J.B., Cherry, B.J., Kwok, W., Lulow, L.L., and Lohr, J.B. (2005). Lateralized cognitive dysfunction and psychotic symptoms in schizophrenia. *Schizophr. Res.* *80*, 151–161.
- Case, L.K., Solcà, M., Blanke, O., and Faivre, N. (2020). Disorders of body representation. In *Multisensory Perception*, (Elsevier), pp. 401–422.
- Claassen, D.O., McDonnell, K.E., Donahue, M., Rawal, S., Wylie, S.A., Neimat, J.S., Kang, H., Hedera, P., Zald, D., Landman, B., et al. (2016). Cortical asymmetry in Parkinson’s disease: early susceptibility of the left hemisphere. *Brain Behav.* *6*, e00573.
- Cohen, A.L., Soussand, L., Corrow, S.L., Martinaud, O., Barton, J.J.S., and Fox, M.D. (2019). Looking beyond the face area: lesion network mapping of prosopagnosia. *Brain* *142*, 3975–3990.

- Corlett, P.R., Murray, G.K., Honey, G.D., Aitken, M.R.F., Shanks, D.R., Robbins, T.W., Bullmore, E.T., Dickinson, A., and Fletcher, P.C. (2007). Disrupted prediction-error signal in psychosis: Evidence for an associative account of delusions. *Brain* 130, 2387–2400.
- Corp, D.T., Joutsa, J., Darby, R.R., Delnooz, C.C.S., Van De Warrenburg, B.P.C., Cooke, D., Prudente, C.N., Ren, J., Reich, M.M., Batla, A., et al. (2019). Network localization of cervical dystonia based on causal brain lesions. *Brain* 142, 1660–1674.
- Critchley, M. (1950). The body-image in neurology. *Lancet* 1, 335–340.
- Critchley, M. (1955). The idea of a presence. *Acta Psychiatr. Scand.* 30, 155–168.
- Critchley, M. (1979). The divine banquet of the brain.
- Cronin-Golomb, A. (2010). Parkinson’s Disease as a Disconnection Syndrome. *Neuropsychol. Rev.* 20, 191–208.
- Crossley, N. a., Mechelli, A., Fusar-Poli, P., Broome, M.R., Matthiasson, P., Johns, L.C., Bramon, E., Valmaggia, L., Williams, S.C.R., and McGuire, P.K. (2009). Superior temporal lobe dysfunction and frontotemporal dysconnectivity in subjects at risk of psychosis and in first-episode psychosis. *Hum. Brain Mapp.* 30, 4129–4137.
- Cui, L.B., Liu, K., Li, C., Wang, L.X., Guo, F., Tian, P., Wu, Y.J., Guo, L., Liu, W.M., Xi, Y. Bin, et al. (2016). Putamen-related regional and network functional deficits in first-episode schizophrenia with auditory verbal hallucinations. *Schizophr. Res.* 173, 13–22.
- Darby, R.R., Laganriere, S., Pascual-Leone, A., Prasad, S., and Fox, M.D. (2017a). Finding the imposter: Brain connectivity of lesions causing delusional misidentifications. *Brain* 140, 497–507.
- Darby, R.R., Horn, A., Cushman, F., and Fox, M.D. (2017b). Lesion network localization of criminal behavior. *Proc. Natl. Acad. Sci.* 201706587.
- Darby, R.R., Joutsa, J., Burke, M.J., and Fox, M.D. (2018). Lesion network localization of free will. *Proc. Natl. Acad. Sci.* 115, 10792–10797.
- David, N., Newen, A., and Vogeley, K. (2008). The “ sense of agency ” and its underlying cognitive and neural mechanisms. *Conscious. Cogn.* 17, 523–534.
- Debbané, M., Glaser, B., David, M.K., Feinstein, C., and Eliez, S. (2006). Psychotic symptoms in children and adolescents with 22q11.2 deletion syndrome: Neuropsychological and behavioral implications. *Schizophr. Res.* 84, 187–193.
- Debbané, M., Van Der Linden, M., Glaser, B., Debbané, M., and Eliez, S. (2010). Monitoring of self-generated speech in adolescents with 22q11.2 deletion syndrome. *Br. J. Clin. Psychol.* 49, 373–386.
- Devinsky, O., Feldmann, E., Burrowes, K., and Bromfield, E. (1989). Autoscopy phenomena with seizures. *Arch. Neurol.* 46, 1080–1088.
- Dierks, T., Linden, D.E., Jandl, M., Formisano, E., Goebel, R., Lanfermann, H., and Singer, W. (1999). Activation of Heschl’s Gyrus during Auditory Hallucinations. *Neuron* 22, 615–621.
- Ehrsson, H.H. (2007). The Experimental Induction of Out-of-Body Experiences. *Science* (80-. ). 317, 1048–1048.
- Ehrsson, H.H., Spence, C., and Passingham, R.E. (2004). That’s my hand! Activity in premotor cortex reflects feeling of ownership of a limb. *Science* 305, 875–877.
- Ehrsson, H.H., Holmes, N.P., and Passingham, R.E. (2005). Touching a rubber hand: feeling of body ownership is associated with activity in multisensory brain areas. *J. Neurosci.* 25, 10564–10573.
- Ernst, M.O., and Banks, M.S. (2002). Humans integrate visual and haptic information in a statistically optimal fashion. *Nature* 415, 429–433.
- Farrer, C., and Frith, C.D. (2002). Experiencing Oneself vs Another Person as Being the Cause of an Action: The Neural Correlates of the Experience of Agency. *Neuroimage* 15, 596–603.
- Farrer, C., Franck, N., Georgieff, N., Frith, C.D., Decety, J., and Jeannerod, M. (2003). Modulating the experience of agency: A positron emission tomography study. *Neuroimage* 18, 324–333.
- Fasano, A., Laganriere, S.E., Lam, S., and Fox, M.D. (2017). Lesions causing freezing of gait localize to a cerebellar functional network. *Ann. Neurol.* 81, 129–141.
- Fénelon, G., and Alves, G. (2010). Epidemiology of psychosis in Parkinson’s disease. *J. Neurol. Sci.* 289, 12–17.

- Fénelon, G., Mahieux, F., Huon, R., and Ziegler, M. (2000). Hallucinations in Parkinson's disease: prevalence, phenomenology and risk factors. *Brain* 123, 733–745.
- Fénelon, G., Soulas, T., Cleret de Langavant, L., Trinkler, I., and Bachoud-Lévi, A.-C. (2011). Feeling of presence in Parkinson's disease. *J. Neurol. Neurosurg. Psychiatry* 82, 1219–1224.
- Ferguson, M.A., Lim, C., Cooke, D., Darby, R.R., Wu, O., Rost, N.S., Corbetta, M., Grafman, J., and Fox, M.D. (2019). A human memory circuit derived from brain lesions causing amnesia. *Nat. Commun.* 10, 1–9.
- Ffytche, D.H., Pereira, J., Ballard, C., Chaudhuri, K.R., Weintraub, D., and Aarsland, D. (2017). Risk factors for early psychosis in PD: insights from the Parkinson's Progression Markers Initiative. *J. Neurol. Neurosurg. Psychiatry* 88, 325–331.
- Fink, G.R., Marshall, J.C., Halligan, P.W., Frith, C.D., Driver, J., Frackowiak, R.S.J., and Dolan, R.J. (1999). The neural consequences of conflict between intention and the senses. *Brain* 122, 497–512.
- Fischer, D., Boes, A., Demertzi, A., Evrard, H., Laureys, S., Edlow, B., Liu, H., Saper, C., Pascual-Leone, A., Fox, M., et al. (2016). A human brain network based on coma-causing brainstem lesions. *Neurology* 87, 2427–2434.
- Fletcher, P.C., and Frith, C.D. (2009). Perceiving is believing: a Bayesian approach to explaining the positive symptoms of schizophrenia. *Nat. Rev. Neurosci.* 10, 48–58.
- Ford, J.M., Gray, M., Faustman, W.O., Heinks, T.H., and Mathalon, D.H. (2005). Reduced gamma-band coherence to distorted feedback during speech when what you say is not what you hear. *Int. J. Psychophysiol.* 57, 143–150.
- Ford, J.M., Roach, B.J., Faustman, W.O., and Mathalon, D.H. (2008). Out-of-Synch and Out-of-Sorts: Dysfunction of motor-sensory communication in schizophrenia. *Biol. Psychiatry* 63, 736–743.
- Ford, J.M., Palzes, V.A., Roach, B.J., and Mathalon, D.H. (2014). Did I Do That? Abnormal Predictive Processes in Schizophrenia When Button Pressing to Deliver a Tone. *Schizophr. Bull.* 40, 804–812.
- Fox, M.D. (2018). Mapping Symptoms to Brain Networks with the Human Connectome. *N. Engl. J. Med.* 379, 2237–2245.
- Friston, K.J. (1998). The disconnection hypothesis. *Schizophr. Res.* 30, 115–125.
- Friston, K.J. (1999). Schizophrenia and the disconnection hypothesis. *Acta Psychiatr. Scand. Suppl.* 395, 68–79.
- Friston, K.J., and Frith, C.D. (1995). Schizophrenia: a disconnection syndrome? *Clin. Neurosci.* 3, 89–97.
- Friston, K., Buechel, C., Fink, G., Morris, J., Rolls, E., and Dolan, R. (1997). Psychophysiological and Modulatory Interactions in Neuroimaging. *Neuroimage* 6, 218–229.
- Friston, K.J., Brown, H.R., Siemerkus, J., and Stephan, K.E. (2016). The dysconnection hypothesis (2016). *Schizophr. Res.* 176, 83–94.
- Frith, C. (2000). Explaining the symptoms of schizophrenia: Abnormalities in the awareness of action. *Brain Res. Rev.* 31, 357–363.
- Frith, C.D. (1992). *The cognitive neuropsychology of schizophrenia* (Hove, U.K.: Lawrence Erlbaum).
- Frith, C.D. (2005). The self in action: Lessons from delusions of control. *Conscious. Cogn.* 14, 752–770.
- Gallagher, S. (2000). Philosophical conceptions of the self: Implications for cognitive science. *Trends Cogn. Sci.* 4, 14–21.
- Geiger, J. (2009). *The Third Man Factor: Surviving the Impossible* (New York: Weinstein Books).
- Graham-Schmidt, K.T., Martin-Iverson, M.T., and Waters, F.A.V. (2017). Self- and other-agency in people with passivity (first rank) symptoms in schizophrenia. *Schizophr. Res.* 192, 75–81.
- Guterstam, A., Björnsdotter, M., Gentile, G., and Ehrsson, H.H.H. (2015). Posterior Cingulate Cortex Integrates the Senses of Self-Location and Body Ownership. *Curr. Biol.* 25, 1416–1425.
- Hayes, J., and Leudar, I. (2016). Experiences of continued presence: On the practical consequences of “hallucinations” in bereavement. *Psychol. Psychother.* 89, 194–210.
- Hécaen, H., and Ajuriaguerra, J. (1952). *Meconnaissances et Hallucinations Corporelles: Intégration et Désintégration de la Somatognosie* (Masson (in French)).

- Hécaen, H., De Ajuriaguerra, J., and David, D. (1952). Les déficits fonctionnels après lobectomie occipitale. 239–291.
- van den Heuvel, M.P., Mandl, R.C.W., Stam, C.J., Kahn, R.S., and Hulshoff Pol, H.E. (2010). Aberrant Frontal and Temporal Complex Network Structure in Schizophrenia: A Graph Theoretical Analysis. *J. Neurosci.* 30, 15915–15926.
- Van Den Heuvel, M.P., and Fornito, A. (2014). Brain networks in schizophrenia. *Neuropsychol. Rev.* 24, 32–48.
- Heydrich, L., and Blanke, O. (2013). Distinct illusory own-body perceptions caused by damage to posterior insula and extrastriate cortex. *Brain* 136, 790–803.
- Heydrich, L., Lopez, C., Seeck, M., and Blanke, O. (2011). Partial and full own-body illusions of epileptic origin in a child with right temporoparietal epilepsy. *Epilepsy Behav.* 20, 583–586.
- Hodzic, A., Kaas, A., Muckli, L., Stirn, A., and Singer, W. (2009). Distinct cortical networks for the detection and identification of human body. *Neuroimage* 45, 1264–1271.
- Hoffman, R.E., and Hampson, M. (2012). Functional connectivity studies of patients with auditory verbal hallucinations. *Front. Hum. Neurosci.* 6, 1–7.
- Hoffman, R.E., Fernandez, T., Pittman, B., and Hampson, M. (2011). Elevated functional connectivity along a corticostriatal loop and the mechanism of auditory/verbal hallucinations in patients with schizophrenia. *Biol. Psychiatry* 69, 407–414.
- Holroyd, S., Currie, L., and Wooten, G.F. (2001). Prospective study of hallucinations and delusions in Parkinson's disease. *J. Neurol. Neurosurg. Psychiatry* 70, 734–738.
- Ionta, S., Heydrich, L., Lenggenhager, B., Mouthon, M., Fornari, E., Chapuis, D., Gassert, R., and Blanke, O. (2011). Multisensory mechanisms in temporo-parietal cortex support self-location and first-person perspective. *Neuron* 70, 363–374.
- James, W. (1961). *The variety of religious experience* (Coller McMillan, New York).
- Jaspers, K. (1913). Über leibhaftige Bewusstheiten (Bewusstheitstauschungen), ein psychopathologisches Elementarsymptom. *Zeitschrift Für Pathopsychologie* 2, 150–161.
- Jastorff, J., Clavagnier, S., Gergely, G., and Orban, G.A. (2011). Neural mechanisms of understanding rational actions: Middle temporal gyrus activation by contextual violation. *Cereb. Cortex* 21, 318–329.
- Jeannerod, M. (2003). The mechanism of self-recognition in humans. *Behav. Brain Res.* 142, 1–15.
- Joutsa, J., Horn, A., Hsu, J., and Fox, M.D. (2018). Localizing parkinsonism based on focal brain lesions. *Brain* 2445–2456.
- Kalckert, A., and Ehrsson, H.H. (2012). Moving a Rubber Hand that Feels Like Your Own: A Dissociation of Ownership and Agency. *Front. Hum. Neurosci.* 6, 40.
- Kannape, O.A., Schwabe, L., Tadi, T., and Blanke, O. (2010). The limits of agency in walking humans. *Neuropsychologia* 48, 1628–1636.
- Karnath, H.-O., Sperber, C., and Rorden, C. (2018). Mapping human brain lesions and their functional consequences. *Neuroimage* 165, 180–189.
- Keen, C., Murray, C.D., and Payne, S. (2013). A qualitative exploration of sensing the presence of the deceased following bereavement. *Mortality* 18, 339–357.
- Van Kemenade, B.M., Arikani, B.E., Podranski, K., Steinsträter, O., Kircher, T., and Straube, B. (2019). Distinct Roles for the Cerebellum, Angular Gyrus, and Middle Temporal Gyrus in Action-Feedback Monitoring. *Cereb. Cortex* 29, 1520–1531.
- Kilteni, K., and Ehrsson, H.H. (2020). Functional Connectivity between the Cerebellum and Somatosensory Areas Implements the Attenuation of Self-Generated Touch. *J. Neurosci.* 40, 894–906.
- Kim, N.Y., Hsu, J., Talmasov, D., Joutsa, J., Soussand, L., Wu, O., Rost, N.S., Morenas-Rodríguez, E., Martí-Fàbregas, J., Pascual-Leone, A., et al. (2019). Lesions causing hallucinations localize to one common brain network. *Mol. Psychiatry*.
- Klingbeil, J., Wawrzyniak, M., Stockert, A., Karnath, H.-O., and Saur, D. (2020). Hippocampal diaschisis contributes to anosognosia for hemiplegia: Evidence from lesion network-symptom-mapping. *Neuroimage* 208, 116485.

- Kuceyeski, A., Maruta, J., Relkin, N., and Raj, A. (2013). The Network Modification (NeMo) Tool: Elucidating the Effect of White Matter Integrity Changes on Cortical and Subcortical Structural Connectivity. *Brain Connect.* 3, 451–463.
- Laganieri, S., Boes, A.D., and Fox, M.D. (2016). Network localization of hemichorea-hemiballismus. *Neurology* 86, 2187–2196.
- Landtblom, A.M. (2006). The “sensed presence”: An epileptic aura with religious overtones. *Epilepsy Behav.* 9, 186–188.
- Lawrie, S.M., Buechel, C., Whalley, H.C., Frith, C.D., Friston, K.J., and Johnstone, E.C. (2002). Reduced frontotemporal functional connectivity in schizophrenia associated with auditory hallucinations. *Biol. Psychiatry* 51, 1008–1011.
- Lenggenhager, B., Tadi, T., Metzinger, T., and Blanke, O. (2007). Video ergo sum: manipulating bodily self-consciousness. *Science* 317, 1096–1099.
- Lenggenhager, B., Mouthon, M., and Blanke, O. (2009). Spatial aspects of bodily self-consciousness. *Conscious. Cogn.* 18, 110–117.
- Leube, D.T., Knoblich, G., Erb, M., and Kircher, T.T.J. (2003a). Observing one’s hand become anarchic: An fMRI study of action identification. *Conscious. Cogn.* 12, 597–608.
- Leube, D.T., Knoblich, G., Erb, M., Grodd, W., Bartels, M., and Kircher, T.T.J. (2003b). The neural correlates of perceiving one’s own movements. *Neuroimage* 20, 2084–2090.
- Leube, D.T., Knoblich, G., Erb, M., Schlotterbeck, P., and Kircher, T.T.J. (2010). The neural basis of disturbed efference copy mechanism in patients with schizophrenia. *Cogn. Neurosci.* 1, 111–117.
- Lewis, J.W., and Van Essen, D.C. (2000). Corticocortical connections of visual, sensorimotor, and multimodal processing areas in the parietal lobe of the macaque monkey. *J. Comp. Neurol.* 428, 112–137.
- Lhermitte, J. (1939). L’image de notre corps.
- Lhermitte, J. (1951). Visual Hallucination of the Self. *Br. Med. J.* 431–434.
- Li, S., Hu, N., Zhang, W., Tao, B., Dai, J., Gong, Y., Tan, Y., Cai, D., and Lui, S. (2019). Dysconnectivity of Multiple Brain Networks in Schizophrenia: A Meta-Analysis of Resting-State Functional Connectivity. *Front. Psychiatry* 10, 1–11.
- Lindner, A., Thier, P., Kircher, T.T.J., Haarmeier, T., and Leube, D.T. (2005). Disorders of agency in schizophrenia correlate with an inability to compensate for the sensory consequences of actions. *Curr. Biol.* 15, 1119–1124.
- Lippman (1992). Hallucinations of physical duality in migraine. 345–350.
- Liu, X., Zhang, N., Chang, C., and Duyn, J.H. (2018). Co-activation patterns in resting-state fMRI signals. *Neuroimage* 180, 485–494.
- Llorca, P.M., Pereira, B., Jardri, R., Chereau-Boudet, I., Brousse, G., Misdrahi, D., Fénelon, G., Tronche, A.-M., Schwan, R., Lançon, C., et al. (2016). Hallucinations in schizophrenia and Parkinson’s disease: an analysis of sensory modalities involved and the repercussion on patients. *Sci. Rep.* 6, 38152.
- Lloyd, D., Morrison, I., and Roberts, N. (2006). Role for human posterior parietal cortex in visual processing of aversive objects in peripersonal space. *J. Neurophysiol.* 95, 205–214.
- Lukianowicz (1958). Autoscopic phenomena. *Arch. Neurol. Psychiatry* 80, 199.
- Lunn, V. (1970). Autoscopic phenomena. *Acta Psychiatr. Scand.* 46, 118–125.
- Maillard, L., Vignal, J.P., Anxionnat, R., Taillandier, L., and Vespignani, H. (2004). Semiologic Value of Ictal Autoscopy. *Epilepsia* 45, 391–394.
- Martínez-Horta, S., Perez-Perez, J., Pagonabarraga, J., Sampedro, F., Horta-Barba, A., Blanke, O., and Kulisevsky, J. (2020). Autoscopic phenomena as an atypical psychiatric presentation of Huntington’s disease: A case report including longitudinal clinical and neuroimaging data. *Cortex* 125, 299–306.
- de Maupassant, G. (1886). Le Horla.
- McDonald-McGinn, D.M., Sullivan, K.E., Marino, B., Philip, N., Swillen, A., Vorstman, J.A.S.S., Zackai, E.H., Emanuel, B.S., Vermeesch, J.R., Morrow, B.E., et al. (2015). 22q11.2 deletion syndrome. *Nat. Rev. Dis. Prim.* 1, 15071.
- McGuire, P.K., and Frith, C.D. (1996). Disordered functional connectivity in schizophrenia. *Psychol. Med.* 26, 663–667.



- Menninger-Lerchenthal, E. (1935). *Das Truggebilde der eigenen Gestalt (Heautoscopy, Doppelgänger)* (Berlin, Karger).
- Messner, R. (2003). *The Naked Mountain* (Seattle: Cambridge University Press, 2003).
- Miall, R.C., and Wolpert, D.M. (1996). Forward models for physiological motor control. *Neural Networks* 9, 1265–1279.
- Murphy, K.C., Jones, L.A., and Owen, M.J. (1999). High rates of schizophrenia in adults with velo-cardio-facial syndrome. *Arch. Gen. Psychiatry* 56, 940–945.
- Nagahama, Y., Okina, T., Suzuki, N., and Matsuda, M. (2010). Neural correlates of psychotic symptoms in dementia with Lewy bodies. *Brain* 133, 557–567.
- Nahab, F.B., Kundu, P., Gallea, C., Kakareka, J., Pursley, R., Pohida, T., Mileta, N., Friedman, J., and Hallett, M. (2011). The neural processes underlying self-agency. *Cereb. Cortex* 21, 48–55.
- Nicastro, N., Eger, A.F., Assal, F., and Garibotto, V. (2018). Feeling of presence in dementia with Lewy bodies is related to reduced left frontoparietal metabolism. *Brain Imaging Behav.*
- Nightingale, S. (1982). Somatoparaphrenia: A Case Report. *Cortex* 18, 463–467.
- Nooner, K.B., Colcombe, S.J., Tobe, R.H., Mennes, M., Benedict, M.M., Moreno, A.L., Panek, L.J., Brown, S., Zavitz, S.T., Li, Q., et al. (2012). The NKI-Rockland Sample: A Model for Accelerating the Pace of Discovery Science in Psychiatry. *Front. Neurosci.* 6, 1–11.
- Northoff, G., and Duncan, N.W. (2016). How do abnormalities in the brain’s spontaneous activity translate into symptoms in schizophrenia? From an overview of resting state activity findings to a proposed spatiotemporal psychopathology. *Prog. Neurobiol.* 145–146, 26–45.
- Oertel-Knöchel, V., Knöchel, C., Matura, S., Stäblein, M., Prvulovic, D., Maurer, K., Linden, D.E.J., and van de Ven, V. (2014). Association between symptoms of psychosis and reduced functional connectivity of auditory cortex. *Schizophr. Res.* 160, 35–42.
- Pagonabarraga, J., Martínez-Horta, S., Fernández de Bobadilla, R., Pérez, J., Ribosa-Nogué, R., Marín, J., Pascual-Sedano, B., García, C., Gironell, A., and Kulisevsky, J. (2016). Minor hallucinations occur in drug-naïve Parkinson’s disease patients, even from the premotor phase. *Mov. Disord.* 31, 45–52.
- Parnas, J., and Handest, P. (2003). Phenomenology of anomalous self-experience in early schizophrenia. *Compr. Psychiatry* 44, 121–134.
- Petkova, V.I., Björnsdotter, M., Gentile, G., Jonsson, T., Li, T.-Q., and Ehrsson, H.H. (2011). From Part- to Whole-Body Ownership in the Multisensory Brain. *Curr. Biol.* 21, 1118–1122.
- Phillips, J.R., Hewedi, D.H., Eissa, A.M., and Moustafa, A.A. (2015). The Cerebellum and Psychiatric Disorders. *Front. Public Heal.* 3, 66.
- Picard, F. (2010). Epileptic feeling of multiple presences in the frontal space. *Cortex* 46, 1037–1042.
- Podoll, K., and Robinson, D. (1999). Out-of-body experiences and related phenomena in migraine art. *Cephalalgia* 19, 886–896.
- Pozeg, P., Rognini, G., Salomon, R., and Blanke, O. (2014). Crossing the Hands Increases Illusory Self-Touch. *PLoS One* 9, e94008.
- Pynn, L.K., and DeSouza, J.F.X. (2013). The function of efference copy signals: Implications for symptoms of schizophrenia. *Vision Res.* 76, 124–133.
- Ravina, B., Marder, K., Fernandez, H.H., Friedman, J.H., McDonald, W., Murphy, D., Aarsland, D., Babcock, D., Cummings, J., Endicott, J., et al. (2007). Diagnostic criteria for psychosis in Parkinson’s disease: Report of an NINDS, NIMH Work Group. *Mov. Disord.* 22, 1061–1068.
- Rees, W.D. (1971). Hallucinations of widowhood. *Br. Med. J.* 4, 304.
- Rohde, M., Scheller, M., and Ernst, M.O. (2014). Effects can precede their cause in the sense of agency. *Neuropsychologia* 65, 191–196.
- Rorden, C., and Karnath, H.O. (2004). Using human brain lesions to infer function: A relic from a past era in the fMRI age? *Nat. Rev. Neurosci.* 5, 812–819.
- Rorden, C., Karnath, H.-O., and Bonilha, L. (2007). Improving lesion-symptom mapping. *J. Cogn. Neurosci.* 19, 1081–1088.
- Rubinov, M., and Sporns, O. (2010). Complex network measures of brain connectivity: Uses and interpretations. *Neuroimage* 52, 1059–1069.

- Ruby, P., and Decety, J. (2001). Effect of subjective perspective taking during simulation of action: A PET investigation of agency. *Nat. Neurosci.* 4, 546–550.
- Salomon, R., Galli, G., Łukowska, M., Faivre, N., Ruiz, J.B., and Blanke, O. (2016). An invisible touch: Body-related multisensory conflicts modulate visual consciousness. *Neuropsychologia* 88, 131–139.
- Salomon, R., Progin, P., Griffa, A., Rognini, G., Do, K.Q., and Conus, P. (2020). Sensorimotor Induction of Auditory Misattribution in Early Psychosis. *Schizophr. Bull.* 1–8.
- Schlerf, J., Ivry, R.B., and Diedrichsen, J. (2012). Encoding of sensory prediction errors in the human cerebellum. *J. Neurosci.* 32, 4913–4922.
- Schneider, M., Schaer, M., Mutlu, A.K., Menghetti, S., Glaser, B., Debbané, M., and Eliez, S. (2014). Clinical and cognitive risk factors for psychotic symptoms in 22q11.2 deletion syndrome: A transversal and longitudinal approach. *Eur. Child Adolesc. Psychiatry* 23, 425–436.
- Schurz, M., Aichhorn, M., Martin, A., and Perner, J. (2013). Common brain areas engaged in false belief reasoning and visual perspective taking: a meta-analysis of functional brain imaging studies. *Front. Hum. Neurosci.* 7, 712.
- Shergill, S.S., Samson, G., Bays, P.M., Frith, C.D., and Wolpert, D.M. (2005). Evidence for sensory prediction deficits in schizophrenia. *Am. J. Psychiatry* 162, 2384–2386.
- Shergill, S.S., White, T.P., Joyce, D.W., Bays, P.M., Wolpert, D.M., and Frith, C.D. (2013). Modulation of somatosensory processing by action. *Neuroimage* 70, 356–362.
- Shergill, S.S., White, T.P., Joyce, D.W., Bays, P.M., Wolpert, D.M., and Frith, C.D. (2014). Functional magnetic resonance imaging of impaired sensory prediction in schizophrenia. *JAMA Psychiatry* 71, 28–35.
- Shinn, A.K., Baker, J.T., Cohen, B.M., and Öngür, D. (2013). Functional connectivity of left Heschl’s gyrus in vulnerability to auditory hallucinations in schizophrenia. *Schizophr. Res.* 143, 260–268.
- Skudlarski, P., Jagannathan, K., Anderson, K., Stevens, M.C., Calhoun, V.D., Skudlarska, B.A., and Pearlson, G. (2010). Brain Connectivity Is Not Only Lower but Different in Schizophrenia: A Combined Anatomical and Functional Approach. *Biol. Psychiatry* 68, 61–69.
- Smythe (1940). *Adventures of a Mountaineer* (Dent).
- Snider, S.B., Hsu, J., Darby, R.R., Cooke, D., Fischer, D., Cohen, A.L., Grafman, J.H., and Fox, M.D. (2020). Cortical lesions causing loss of consciousness are anticorrelated with the dorsal brainstem. *Hum. Brain Mapp.* 41, 1520–1531.
- Sperduti, M., Delaveau, P., Fossati, P., and Nadel, J. (2011). Different brain structures related to self- and external-agency attribution: A brief review and meta-analysis. *Brain Struct. Funct.* 216, 151–157.
- Suedfeld, P., and Mocellin, J.S.S.P. (1987). The “Sensed Presence” in Unusual Environments. *Environ. Behav.* 19, 33–52.
- Sutterer, M.J., Bruss, J., Boes, A.D., Voss, M.W., Bechara, A., and Tranel, D. (2016). Canceled connections: Lesion-derived network mapping helps explain differences in performance on a complex decision-making task. *Cortex* 78, 31–43.
- Tadokoro, Y., Oshima, T., and Kanemoto, K. (2006). Postictal autoscopia in a patient with partial epilepsy. *Epilepsy Behav.* 9, 535–540.
- Tsakiris, M., Prabhu, G., and Haggard, P. (2006). Having a body versus moving your body: How agency structures body-ownership. *Conscious. Cogn.* 15, 423–432.
- Tsakiris, M., Hesse, M.D., Boy, C., Haggard, P., and Fink, G.R. (2007). Neural signatures of body ownership: A sensory network for bodily self-consciousness. *Cereb. Cortex* 17, 2235–2244.
- Tsakiris, M., Longo, M.R., and Haggard, P. (2010). Having a body versus moving your body: Neural signatures of agency and body-ownership. *Neuropsychologia* 48, 2740–2749.
- Uddin, L.Q., Kaplan, J.T., Molnar-Szakacs, I., Zaidel, E., and Iacoboni, M. (2005). Self-face recognition activates a frontoparietal “mirror” network in the right hemisphere: An event-related fMRI study. *Neuroimage* 25, 926–935.
- Vallar, G., and Ronchi, R. (2009). Somatoparaphrenia: A body delusion. A review of the neuropsychological literature. *Exp. Brain Res.* 192, 533–551.

- Wawrzyniak, M., Klingbeil, J., Zeller, D., Saur, D., and Classen, J. (2018). The neuronal network involved in self-attribution of an artificial hand: A lesion network-symptom-mapping study. *Neuroimage* 166, 317–324.
- Weiskrantz, L., Elliott, J., and Darlington, C. (1971). Preliminary observations on tickling oneself. *Nature* 230, 598–599.
- WHO (2018). International Classification of Diseases, 11th Revision (ICD-11),.
- Williams, D.R., Warren, J.D., and Lees, A.J. (2008). Using the presence of visual hallucinations to differentiate Parkinson’s disease from atypical parkinsonism. *J. Neurol. Neurosurg. Psychiatry* 79, 652–655.
- Wolf, D.H., Gur, R.C., Valdez, J.N., Loughhead, J., Elliott, M.A., Gur, R.E., and Ragland, J.D. (2007). Alterations of fronto-temporal connectivity during word encoding in schizophrenia. *Psychiatry Res.* 154, 221–232.
- Wolpert, D.M., Ghahramani, Z., and Jordan, M. (1995). An Internal Model for Sensorimotor Integration. *Am. Assoc. Adv. Sci. Stable* 269, 1880–1882.
- Wolpert, D.M., Miall, R.C., and Kawato, M. (1998). Internal models in the cerebellum. *Trends Cogn. Sci.* 2, 338–347.
- Wood, R.A., Hopkins, S.A., Moodley, K.K., and Chan, D. (2015). Fifty Percent Prevalence of Extracampine Hallucinations in Parkinson’s Disease Patients. *Front. Neurol.* 6, 1–9.
- Woodward, N.D., Baxter, R., and Heckers, S. (2012). Functional resting-state networks are differentially affected in schizophrenia. *Schizophr. Res.* 130, 86–93.
- Yomogida, Y., Sugiura, M., Sassa, Y., Wakusawa, K., Sekiguchi, A., Fukushima, A., Takeuchi, H., Horie, K., Sato, S., and Kawashima, R. (2010). The neural basis of agency: An fMRI study. *Neuroimage* 50, 198–207.
- Zamboni, G., Budriese, C., and Nichelli, P. (2005). “Seeing oneself”: A case of autoscopia. *Neurocase* 11, 212–215.
- Zijlmans, M., Van Eijsden, P., Ferrier, C.H., Kho, K.H., Van Rijen, P.C., and Leijten, F.S.S. (2009). Illusory shadow person causing paradoxical gaze deviations during temporal lobe seizures. *J. Neurol. Neurosurg. Psychiatry* 80, 686–688.

## 8. Annexes

I have also been involved in other projects during my thesis, which are listed in my CV. These include different ongoing projects that will only be briefly mentioned here. First, more details on an additional analysis conducted in **Chapter 3** is presented, then a full study that investigate the peri-personal space (PPS) which is the reaching space around the body relevant for BSC is described (Blanke, 2012; Blanke et al., 2015).

I have also been involved in two pharmacological longitudinal studies in 22q11DS individuals conducted by the laboratory of Developmental Imaging and Psychopathology directed Professor Stephan Eliez (NCCR-synapsy project). The aim of these projects was to better understand the role of the dopaminergic system in multisensory integration and in the induction of psychosis-like states. To this purpose, we used the same paradigm as described in **Chapter 4**, and assessed the robot-induced PH and related PE at three different time points (before, during and after treatment). The data collection is still ongoing.

### 8.1 Psycho-physiological analysis

To attempt to investigate the relation between the two networks found in healthy subjects (i.e. the brain regions responding to the fixed spatial conflict and the ones specifically more activated in the asynchronous condition), I present here an additional analysis that was not mentioned in **Chapter 3**. We investigated whether the two conditions (i.e. asynchronous and synchronous conditions) differently modulated the communication between the different regions activated by either the fixed spatial or the spatio-temporal sensorimotor conflicts.

#### Methods

To this purpose, we applied psycho-physiological interaction (PPI) analysis, which takes into account the moment-to-moment fluctuations in connectivity (Friston et al., 1997). We used the 4 regions of the spatio-temporal sensorimotor conflict PH-network and the 5 regions of the fixed spatial sensorimotor conflict PH-network (see **Chapter 3**). In order to extract their BOLD signal time courses, we performed another general linear model where the two experimental runs were concatenated together to have one time course per ROI per subject. The time courses were extracted from a sphere of

8 mm around the peak level group coordinates of each ROI (see Supplementary Table S7 and S8 of **Chapter 3** for the coordinates) and the search radius for local maxima from the group analysis was restricted to 16 mm using  $p < 0.05$  uncorrected and adjusted for effects of interest. The spatio-temporal PH regions were extracted from the asynchronous > synchronous contrast while the static spatial PH regions were extracted from the sum of the asynchronous and synchronous conditions. For three subjects, we were unable to extract some ROIs from the contrast asynchronous > synchronous, the analysis was therefore done on the remaining 22 subjects. The PPI interaction term and the task regressor were created for each ROI. These parts were performed using SPM12 toolbox (Wellcome Department of Cognitive Neurology, Institute of Neurology, UCL, London, UK). In the study, we were interested on how the connectivity between those regions was affected by the contrast asynchronous > synchronous, therefore, we performed a ROI-to-ROI PPI analysis. We then performed a one sample t test for each pairwise connection on the PPI beta values. Only the connections surviving Bonferroni correction for multiple comparison were considered as significant.

## Results

ROI-to-ROI PPI analysis revealed, as predicted, that several regions showed functional connectivity decreases in the asynchronous condition. We found that the left sensorimotor area, the left putamen and the right IPL had lower covariance with the right cerebellum in the asynchronous vs. synchronous condition. The left sensorimotor cortex also showed lower covariance during the asynchronous vs. synchronous condition with the right IPL (corrected for multiple comparisons using Bonferroni correction) (see Table 8.1). These data reveal a cortical and subcortical robot-induced PH-network - consisting of sensorimotor cortex, IPL, putamen, and cerebellum – that is linked to PH by showing synchrony-dependent connectivity changes. These decreases in connectivity during the PH-associated asynchronous condition (that was found for all four altered connections) is compatible with previous fMRI data on hallucinations and psychosis that have found frontal-posterior decreases in functional connectivity in patients suffering from hallucinations (e.g., Bernard et al., 2018; Crossley et al., 2009), leading to the disconnection hypothesis of hallucinations (Friston, 1998; Friston et al., 2016). The cerebellum was also found to be hypo-connected with the sensorimotor cortex, IPL and the putamen during the asynchronous

condition compared to the synchronous condition. It has been suggested that the cerebellum is a key element of sensorimotor prediction (Blakemore, 2003; Blakemore et al., 1999, 2001; Wolpert et al., 1998) and it has been shown that its activity is altered in schizophrenia (Andreasen and Pierson, 2008; Phillips et al., 2015). Finally, PPI analysis revealed that only connectivity between regions activated by the fixed spatial sensorimotor conflict were differently modulated between conditions.

<i>Interactions</i>	<i>mean PPI beta value</i>	<i>Peak level t-value</i>	<i>p-value</i>
<b><i>Asynchronous &gt; synchronous</i></b>			
Left sensorimotor cortex			
Right Cerebellum	-0.197	-4.89	0.000054
Right IPL	-0.157	-4.91	0.000052
Right Cerebellum			
Left Putamen	-0.184	-5.3	0.000019
Right IPL	-0.217	-4.47	0.00015

**Table 8.1: Results from the PPI analysis.** Pairwise connections functionally modulated by the asynchronous > synchronous contrast surviving Bonferroni multiple comparison. All pairwise connections had greater coupling during the synchronous condition compared to the asynchronous condition.

## 8.2 Distinct neural mechanisms of temporal and spatial prediction in peripersonal space

**Authors:** Petr Grivaz<sup>1,2,3\*</sup>, **Eva Blondiaux**<sup>1,2,\*</sup>, Michel Akselrod<sup>1,2,3</sup>, Bruno Herbelin<sup>1,2</sup>, Andrea Serino<sup>1,2,3\*\*</sup> & Olaf Blanke<sup>1,2,4,\*\*</sup>

(\*, \*\*) These authors contributed equally to the paper

### *Affiliations*

**1.** Laboratory of Cognitive Neuroscience, Brain Mind Institute, School of Life Science, Ecole Polytechnique Fédérale de Lausanne, Switzerland. **2.** Center for Neuroprosthetics, School of Life Science, Ecole Polytechnique Fédérale de Lausanne, Switzerland. **3.** My Space Lab, University Hospital Lausanne (CHUV), Lausanne, Switzerland. **4.** Department of Neurology, University Hospital Geneva, Switzerland

**Personal contributions:** Designed the paradigms, collected and analysed the data and writing.

### **Acknowledgements**

This work was supported by the Bertarelli foundation, by the National Center of Competence in Research: SYNAPSY – The Synaptic Bases of Mental Disease (financed by the Swiss National Science Foundation), grant 320030\_166643 of the Swiss National Science Foundation to OB and grant PP00P3\_163951 / 1 by the Swiss National Science Foundation to AS. The authors would also like to thank Baptiste Gautier for help with the manuscript.

Abstract

The brain integrates multisensory events occurring within peripersonal space (PPS). The brain's PPS system reacts to touch and to visual stimuli moving towards the body and is believed to predict collisions of external objects with the body, based on temporal and spatial estimates. Whether these two dimensions are implemented in the same brain regions, however, remains unknown. In two separate fMRI and behavioral experiments, we probed the human PPS brain regions by delivering facial touch while looming stimuli were perceived at different depths or while static visual stimuli remained in far space and further manipulated the a priori probability of the virtual ball providing spatial cues. Depth-specific touch-induced activity, stronger for stimuli near the face, was found in parietal (intraparietal sulcus, IPS, S1), dorsal premotor cortex (dPMc) and temporo-parietal (parietal operculum) regions. These areas possessed patterns of activity suggestive of temporal prediction, whereas only the bilateral dPMc, right IPS and right temporo-parietal regions (i.e. right hemispheric predominance) had patterns also suggesting predictive spatial processing. These data describe a PPS network and newly highlight bilateral PPS regions coding for temporal and spatial prediction and regions predominantly in the right hemisphere that specialize in processing of spatial PPS prediction.

**Keywords:** Multisensory integration, human, visuo-tactile, ultra high-field fMRI



## Introduction

Peripersonal space (PPS), or the space immediately surrounding our body, is the fundamental interface between our body and the external world, mediating interactions with the environment and others (Serino, 2019) and is represented by specific populations of multisensory neurons. Electrophysiological recordings in monkeys have demonstrated the presence of neurons in the ventral premotor cortex (vPMc, Graziano, Yap, & Gross, 1994; Rizzolatti, Fadiga, Fogassi, & Gallese, 1997), in the intraparietal sulcus (IPS), in parietal area 5 (Duhamel, Bremmer, Ben Hamed, & Graf, 1997; Graziano, Cooke, & Taylor, 2000), in parietal area 7 (Hyvarinen & Shelepin, 1979; Leinonen & Nyman, 1979) and in the putamen (Graziano & Gross, 1994), responding when a tactile stimulus is delivered on a specific portion of the skin and a visual or auditory stimulus is presented close (but not far) to the same skin region. Such PPS neurons possess visual receptive fields of various sizes (variably extending from the skin by 5 to 100 cm) and cover various body parts (hand, arm, face, etc.) and some even the entire body (Fogassi et al., 1996; Graziano, Hu, & Gross, 1997). A neural system mapping of the PPS in humans has also been described using non-invasive neuroimaging techniques (for reviews, see Blanke, Slater, & Serino, 2015; Brozzoli, Makin, Cardinali, Holmes, & Farnè, 2012; di Pellegrino & Làdavas, 2015; Grivaz, Blanke, & Serino, 2017). Fronto-parietal activations responding to stimuli within the PPS around the hand (e.g. Brozzoli, Gentile, Petkova, & Ehrsson, 2011), the face (Bremmer et al., 2001; Cardini et al., 2011; Sereno & Huang, 2006) and the trunk (Huang, Chen, Tran, Holstein, & Sereno, 2012) were most consistently found in the vPMc, the inferior parietal lobule (IPL), the IPS, the superior parietal lobule (SPL), the supramarginal gyrus, the primary somatosensory cortex (area 2) and the putamen, mirroring monkey findings (for a recent meta-analysis, see Grivaz et al., 2017). A recent study using intracranial electroencephalography also demonstrated multisensory integration for audio-tactile stimuli within the peripersonal space also in humans (Bernasconi et al., 2018). Collectively, this body of evidence suggests that the primate brain has developed a multisensory neural system, located in premotor and different parietal regions, as well as regions at the temporo-parietal junction, which encode the space near specific body parts.

One of the proposed roles of the PPS system is predicting potential collisions of external objects with the body (Cléry, Guipponi, Wardak, & Ben Hamed, 2014;

Graziano & Cooke, 2006; Serino, 2016). Indeed, studies have shown that PPS neurons are particularly sensitive to looming (as opposed to receding) stimuli (Colby, Duhamel, & Goldberg, 1993; Duhamel, Colby, & Goldberg, 1998; Graziano et al., 1997) and increase their firing rate as a function of the speed of the looming stimulus (Colby et al., 1993; Fogassi et al., 1996). Behavioral studies in humans further showed that multisensory processing is anticipated for faster as compared to slower looming stimuli (Noel, Blanke, Magosso, & Serino, 2018) and time to contact for looming stimuli are consistently underestimated, especially when these are perceived as threatening (Ferri, Tajadura-Jiménez, Väljamäe, Vastano, & Costantini, 2015; Vagnoni, Lourenco, & Longo, 2012). Furthermore, the presence of looming stimuli has been shown to directly affect tactile processing accordingly to specific temporal and spatial profiles. For instance, tactile sensitivity on the face is enhanced when touch is delivered at the expected time of contact of a looming visual stimulus (Cléry, Guipponi, Odouard, Wardak, & Ben Hamed, 2015). Perception of a tactile stimulus, both in terms of reaction time (Serino, Noel, et al., 2015) and detection accuracy (Salomon et al., 2017) is also enhanced when concurrent visual (Kandula, Hofman, & Dijkerman, 2015; Kandula, Van der Stoep, Hofman, & Dijkerman, 2017; Salomon et al., 2017) or auditory (Canzoneri, Magosso, & Serino, 2012; Noel et al., 2014; Noel, Pfeiffer, Blanke, & Serino, 2015a; Serino, Noel, et al., 2015) looming stimuli are presented within PPS, and this depth-specific cross-modal facilitation property has been exploited to probe the boundaries of PPS in humans (Blanke et al., 2015; Serino, 2016). These findings suggest that neural representations of PPS not only discriminate where a stimulus is with respect to the body and whether a moving object could potentially collide with the body, but also anticipate when this is likely to occur, thus exploiting predictive mechanisms. While a previous study partially tested PPS-related multisensory prediction in non-human primates (Cléry et al., 2017), previous studies in humans have tested how and where in the brain such temporal and spatial PPS prediction mechanisms are implemented.

Here, we conducted a series of behavioral and fMRI experiments in a total of 56 subjects and investigated human brain regions involved in the processing of multisensory stimuli around the face (i.e., peri-face space) in a spatially and temporally predictive manner. In the present fMRI and behavioral paradigms, we measured responses to tactile stimuli on the face, while visual stimuli were either looming

towards the face (dynamic visuo-tactile conditions, dVT) or remained static in far space (static visuo-tactile conditions, sVT). Furthermore, visuo-tactile interaction was sampled at three temporal offsets of touch delivery, which, in the dVT conditions, resulted in the perception of the visual stimulus at a far, an intermediate or close distance from the face. To further dissociate between temporal and spatial predictive effects, in two different series of otherwise identical experiments, we manipulated the subject's a priori expectations about spatio-temporal associations of the stimuli by manipulating the order of presentation of spatially and temporally predictive cues. Concretely, in experiment 1, trials from the dVT and sVT conditions were fully intermingled and thus occurred with the same probability during the entire experimental block. Therefore, a ball appearing at a far location in space was expected by the participant to loom towards the face, enter the PPS and be associated with touch with an intermediate probability. As a consequence, temporal and spatial cues could both be used to predict touch on the face. Instead, in experiment 2, in the first half of the experiment, the far ball was never associated to a stimulus entering the PPS (only sVT and unimodal visual trials were administered), whereas in the second half, the virtual ball approached the body all the time (only dVT and unimodal visual trials were administered). Thus, touch could be predicted on the basis of primarily temporal information (spatial information was absent) in the first part of experiment 2 and of spatial information (beside temporal) in the second part of experiment 2. In this way, we studied not only which brain areas processed together tactile and dynamic visual stimuli within the PPS, but also whether they did it accordingly to temporal and spatial features.

## Materials and Methods

### Participants

For experiment 1, we recruited 10 subjects (3 female, mean  $\pm$  SD age  $23.7 \pm 3.6$  years) for the fMRI part (experiment 1A) and another 18 subjects (7 female, mean  $\pm$  SD age  $24.4 \pm 4.31$  years) for the behavioral part (experiment 1B). One subject from experiment 1B was excluded from the analysis, due to an excessive number of invalid responses ( $> 40\%$  for three experimental conditions, see below about definition of an invalid trial).

For experiment 2, 10 additional subjects (4 female, mean  $\pm$  SD age  $24.0 \pm 5.64$  years) were recruited for the fMRI part (experiment 2A) and 18 subjects (11 female, mean  $\pm$  SD age  $23.9 \pm 4.80$  years) were recruited for the behavioral part (experiment 2B). One subject from experiment 2B was excluded from the analysis due to a large number of invalid responses ( $> 40\%$  for two experimental conditions).

Finally, 10 additional subjects (5 female, mean  $\pm$  SD age  $28.8 \pm 7.35$  years) participated in the depth estimation experiment.

All participants were right-handed, had normal vision and no history of psychological or neurological disorders. All of them provided their informed consent prior to participating in the experiment, which was conducted in accordance with the principles of the Declaration of Helsinki and authorized by the local ethical committee of the University of Lausanne, Switzerland.

### fMRI sessions

#### *Experimental setup and stimuli*

Participants lay supine on the bed of a short-bore 7 Tesla MR scanner (Siemens Medical, Erlangen, Germany). Visual stimuli were back-projected by a beamer onto a semi-transparent screen located near the end extremity of the bore. Participants viewed the content of this screen through a  $45^\circ$  tilted mirror, allowing for a diagonal field-of-view of approximately  $17^\circ$ . Button responses were collected using an MR-compatible response pad.

The visual stimuli consisted of a permanent white fixation cross in the center of the screen and an occasionally-appearing static or dynamic three-dimensional grey spherical object (virtual ball) on a black background (Figure 1A). The virtual ball was programmed and rendered in OpenGL with virtual lights placed so as to highlight its 3-dimensional shape on an otherwise 2-dimensional surface. The tactile stimuli were delivered with precise timing bilaterally on the cheeks of the participants using a custom-made, air-driven tactile stimulator. The device was composed of three main parts, among which were (i) the compressor, (ii) a control board that triggered, upon incoming instructions from a computer, the opening and closing of relevant air valves to deliver a tactile stimulus, and (iii) two MR-compatible air-driven pistons mounted on the head-coil that delivered touch to the cheeks. Each piston was fitted at the tip with a Q-tip whose length and position were personalized to the size of each participant's head to ensure a comfortable, but clear sensation of bilateral touch on the cheeks (assessed by a self-report before the experiment). A trigger to deliver touch was sent over a serial port from a computer to a programmable electronic board (Arduino Leonardo), which in turn controlled the opening and closing of the relevant air valves to allow the pistons to touch the cheeks for an approximate duration of 300ms. The presentation and timing of the visual and tactile stimuli, as well as the recording of button responses was managed using an in-house software (ExpypVR, <http://lnc0.epfl.ch/expypvr>) running on a desktop computer.

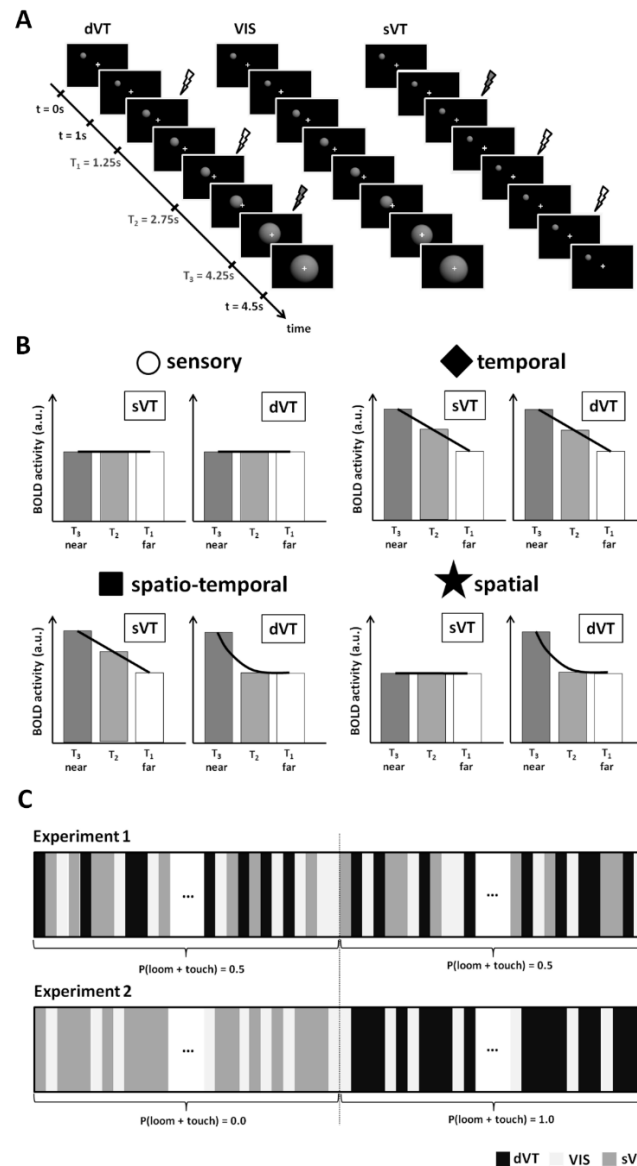


**Figure 1:** Experimental paradigm and ROI classification scheme. (A) Time course of a typical trial and stimuli of the experimental conditions. In all the conditions, the virtual ball appeared in far space; in the dVT and VIS conditions, after 1 sec, it started looming towards the observer, whereas in the sVT condition it remained static in far space. Furthermore, touch to the face was delivered (in dVT and sVT conditions) or not (VIS condition) at different temporal offsets in the dVT and sVT (at T<sub>3</sub>, T<sub>2</sub>, T<sub>1</sub>; T<sub>3</sub> and T<sub>1</sub> are shown as an example by the yellow flash). In addition, the temporal offsets at T<sub>1|2</sub> and T<sub>2|3</sub> (in grey) were only used in the behavioral task (B) Canonical patterns of expected ROI activity based on processing of condition-unspecific sensory information, temporal prediction, spatio-temporal prediction and spatial prediction (see methods section for more details). (C) Illustration of the different ordering of experimental conditions between experiments. In experiment 1, all the three experimental conditions were presented in a fully randomized order, thus a ball appearing at a far location in space had an intermediate probability to loom towards the face, enter the PPS and be associated with touch. In experiment 2, all sVT conditions were presented within the first half of the block (therefore never associated with both looming of the stimulus and touch delivery), whereas all the dVT conditions were presented in the second half of the experiment (the virtual ball approached the body all the time). dVT dynamic visuo-tactile, VIS visual, sVT static visuo-tactile conditions.

*fMRI visuo-tactile interaction paradigm (PPS)*

In order to investigate the neural and behavioral mechanisms of peri-face space using a visuo-tactile interaction task, we adapted a behavioral paradigm previously used for assessing the boundaries of PPS in humans, while reproducing the rationale of neurophysiological recordings in monkeys. The behavioral task (Canzoneri et al., 2012; Serino, Noel, et al., 2015) measures reaction times (RTs) to touch on the skin while a dynamic visual or auditory stimulus is perceived at different distances from the location of touch (Canzoneri et al., 2012; Kandula et al., 2015; Noel et al., 2014, 2015a; Serino, Noel, et al., 2015). Typically, tactile processing is sped up as the dynamic visual or auditory stimulus approaches the body. However, such distance-specific facilitation on the RTs is not linear but occurs only within a given distance from the body. The spatial location dividing the space where such facilitation occurs or does not occur is used as a proxy measure of the PPS boundary. Here, we hypothesized that regions in the fronto-parietal network of the brain, known to be involved in PPS processing (Grivaz et al., 2017), would exhibit patterns of activity in line with the patterns of RTs typically observed in such behavioral paradigms.

The structure of a typical experimental trial used here can be found in Figure 1A. Every trial lasted in total 4.5 sec and was separated from the subsequent one by an inter-stimulus interval (which served as a rest period) lasting between 2.5 and 8.5 sec, randomly selected. The visual stimuli consisted of a virtual ball that appeared equally frequently on the left or on the right of a centered fixation cross in far space for 1 second and then either loomed towards the participant's face at a constant velocity for 3.5 seconds during which the participant either received touch on the cheeks (dynamic visuo-tactile condition, dVT) or not (visual only condition, VIS). In another condition, the visual stimulus remained stationary in far space for 3.5 seconds during which touch was again delivered on the cheeks (static visuo-tactile condition, sVT). In the dVT condition, the trajectory of the virtual ball always ended proximal to the center of the screen in near space. This means that in the dVT and VIS conditions, the ball's trajectory was linear and with constant speed, but slightly oblique. This was done in order to highlight visual depth and dynamics of the virtual ball on an otherwise 2-dimensional screen, as well as to avoid habituation to the stimulus. Crucially, touch was delivered on the cheeks in the dVT and sVT conditions with one of three temporal offsets with respect to the first appearance of the virtual ball on that trial on the screen,

at  $T1 = 1.25$  s,  $T2 = 2.75$  s or  $T3 = 4.25$  s. This corresponded, in the case of the dVT condition, to situations when the virtual ball was observed in far, intermediate or close space from the face at the time of tactile delivery, respectively.

An attention task was added to the experiment in which the participants were instructed to only press a button upon a rare change of color of the fixation cross (constantly present in the center of the screen throughout the whole experiment). An attention trial resembled an experimental condition and allowed to control that the participants were fully involved in the task and that their gaze was centered.

We did not ask participants to perform any task with respect to the main visual and tactile stimuli to avoid contaminating brain imaging data with motor planning and execution-related activity (i.e. the physical button pressing). The fMRI visuo-tactile interaction experiment thus consisted of a 3-by-3 full factorial design with factors Modality (sVT, dVT, VIS) and Temporal offset (T1, T2, T3). In the case of the VIS condition, the temporal offsets only had the effect of shifting the onset time of the visual stimulus with respect to the onset time for acquiring a functional volume by the scanner to be comparable with the analogous dVT and sVT conditions.

Crucially, between the two different experiments conducted on two separate populations, we manipulated the subject's a priori expectations about spatio-temporal associations of the stimuli. Thus, in experiment 1, the order of the three experimental conditions (sVT, dVT, VIS) was fully randomized, whereas in experiment 2, all of the sVT and half of the VIS conditions were randomized within the first half of the block and all of the dVT and the other half of the VIS trials were randomized in the second half of the block (Figure 1C). In this way in experiment 1, we hypothesized that the processing of the visuo-tactile stimuli would implicitly be made based on a mix of both temporal and spatial information. Conversely, in the first part of experiment 2, we expected participants to rely primarily on temporal information as no spatially informative visuo-tactile (i.e. dVT) trials were administered. In the second part of the same experiment, we expected participants to rely primarily on spatial (in addition to temporal) information to predict touch, as only spatially and temporally predictive visuo-tactile dVT conditions were administered. We expected the unimodal visual stimuli to not differentially affect predictions to touch as they were identically distributed between the two experiments and were not informative about touch (i.e.



never coupled to tactile events). For both experiments 1 and 2, the experimental conditions, the number of repetitions per condition (10) and the total length of experiment (approximately 17 minutes) were identical. Only the order of presentation differed.

### *fMRI data acquisition*

Functional and anatomical brain images were acquired on a short-bore 7 Tesla scanner (Siemens Medical, Erlangen, Germany) with a 32-channel Transmit/Receive RF head coil (Nova Medical, Wilmington MA, USA), known to yield a superior signal-to-noise ratio and sensitivity over the standard 8-channel coil (Salomon, Darulova, Narsude, & Van Der Zwaag, 2014). A total of 400 functional volumes were acquired per subject using an echo-planar imaging (EPI) sequence. Each volume was comprised of 46 axial slices covering approximately the superior portion of the brain from the anterior-posterior commissure plane (in-plane resolution 1.5 x 1.5 mm<sup>2</sup>; slice thickness 1.5 mm; no gap, matrix size 140 x 140, FOV = 210 mm, TE = 26 ms, TR = 2.5s, GRAPPA = 2). The choice of this slice placement was based on a priori hypotheses about the location of PPS-sensitive areas, namely the parietal and premotor cortices (Grivaz et al., 2017). To aid coregistration, a single whole-brain EPI volume with 64 slices (1.3 x 1.3 x 1.3 mm<sup>3</sup> resolution) was acquired (as in Akselrod et al., 2017). Finally, in order to locate anatomically activation clusters and to improve normalization, an anatomical volume was recorded using the MR2RAGE sequence (Marques et al., 2010) with TE = 2.63 ms, TR = 7.2 ms, TI1 = 0.9s, TI2 = 3.2 s, TRmprage = 5 s.

### *fMRI data analysis*

#### fmri preprocessing and subject-wise modelling

All preprocessing and statistical analyses were conducted using the SPM12 package (Wellcome Department of Cognitive Neurology, London, UK) running on Matlab (v2014b, Mathworks). Functional images were corrected for acquisition delay (i.e. using slice timing correction) and realigned to the first acquired volume. The anatomical image was coregistered to the whole-brain EPI image, which in turn was coregistered to the mean EPI image from the realignment step, applying the same transformation matrix to the anatomical image to ensure accurate coregistration between the functional images with partial brain coverage and the whole-brain

anatomical image. The anatomical image was segmented into the different tissue types based on tissue probability maps of SPM 12 and the resulting forward deformation fields were applied to both the anatomical and functional images to warp them into Montreal Neurological Institute (MNI) standard space. Finally, all the normalized functional images were smoothed with an isotropic Gaussian kernel (FWHM = 4 mm).

Statistical analysis was conducted using a General Linear Model (GLM) as implemented in SPM12. At the individual level (i.e. 1st level analysis), two separate regressors were created for each one of the 9 experimental conditions (the HRF and its temporal derivative, the latter not being included in the contrast), only modeling the last 3.5 sec of the 4.5 sec trial length. We modeled as a regressor of no interest the first second of the trial (since this part was identical in every condition with a static ball displayed in the far space, and to avoid capturing startle-related effects), the attention condition trials and experimental trials where a button had been (wrongfully) pressed. For each subject, we created a series of T and F contrasts assessing the activity induced by each of the experimental conditions versus rest (which served as an implicit baseline). These subject-wise contrast maps were combined in a 2nd level random-effects group analysis (one sample T-tests) and further used for producing contrasts of interest for the factorial analysis, or for extracting the parameter estimates for the ROI analysis (see below for more details). For the factorial analysis conducted on the whole imaged portion of brain space, we used a significance threshold of  $p < 0.05$ , corrected for multiple comparisons using the false discovery rate (FDR) method (Genovese, Lazar, & Nichols, 2002).

Based on scientific experiments investigating the neural mechanisms of PPS in both monkeys and humans (see above), we expected that activity induced by PPS-sensitive regions should be most pronounced in situations when the looming visual stimulus (in the dVT condition) was closest to the face at the time of touch, as opposed to when it was at an intermediate or far distance. Furthermore, we predicted that larger responses for spatial vs. temporal conditions would vary as a function of the predictability of the association between the appearance of the virtual ball at a far location and its looming behavior, as defined by the protocol difference between experiments 1 and 2.

For experiments 1 and 2, we conducted two types of fMRI analyses: a factorial analysis and a region-of-interest (ROI) analysis.

### Group-level Factorial analysis

For the factorial analysis, we produced linear contrasts to identify regions of the brain which (i) responded differentially to a touch on the face when the virtual ball was perceived in near versus far space  $[(dVTT3 - VIST3) > (dVTT1 - VIST1)]$  and (ii) which showed different activity to the presence of a dynamic virtual ball in near versus far space, while subtracting out the activity induced by touch  $[(dVTT3 - sVTT3) > (dVTT1 - sVTT1)]$ . These contrasts were designed to isolate PPS activity associated to the tactile and visual components, respectively, while controlling for temporal expectancy in the latter case. However, as neither of these contrasts uncovered any brain activity surviving multiple comparison correction ( $p < 0.05$  FDR corrected) for either experiment, we only pursued with the ROI analysis (see below).

### Group-level ROI analysis

The aims of the ROI analysis were to define ROIs that (i) exhibit patterns of activity suggesting PPS processing and (ii) possess patterns of activity that reflect the spatial prediction component of PPS (in addition to or as opposed to the temporal component).

### PPS ROI definition

We, firstly, defined ROIs from the conjunction of activity elicited by any of the experimental conditions versus rest (conjunction of F-contrasts), irrespectively of the Temporal offset of the tactile stimulus:  $(sVT \text{ vs rest}) \cap (dVT \text{ vs rest}) \cap (VIS \text{ vs rest})$ ,  $p < 0.05$  FWE-corrected,  $k \geq 100$ ). Secondly, we extracted, from each of these ROIs, the subject- and condition-wise mean parameter estimates from the GLM analysis. Thirdly, we performed a 3-by-3-by-N repeated measures analysis of variance (rmANOVA), with factors Modality (sVT, dVT, VIS), Temporal offset (T1, T2, T3) and ROI (N ROIs from the conjunction analysis) on the subject- and condition-wise mean parameter estimates from the GLM analysis. The ROI-wise Modality-by-Temporal offset interaction was analyzed only if the 3-way interaction was significant. The rationale is the following: we expected the BOLD signal to be unaffected or less affected as a function of increasing Temporal offset for the sVT condition (where the virtual ball is static in far space), but to increase for the dVT condition (as the virtual ball looms towards the face). The pattern of activity of the VIS condition (with no touch) should be unaffected by the Temporal offset and thus drive the two-way

Modality-by-Offset interaction. So, fourthly, we ran a ROI-wise 2-by-3 rmANOVA with factors Modality (sVT, dVT) and Temporal offset (T1, T2, T3), excluding the VIS conditions. Specifically, we considered that a larger level of activity for the dVT condition at T3 (near) compared to T2 (intermediate) and T1 (close) defines an ROI as coding for visuo-tactile PPS around the face.

#### PPS ROI spatio-temporal tuning definition

We classified the ROIs according to both the main effect of the Temporal offset (time-modulation of activity irrespectively of the Modality defines temporal expectancy) and its interaction with modality (time-modulation of activity differentially affected by the Modality defines spatial processing). Furthermore, to assess which of temporal and/or spatial prediction each ROI was engaged in, we classified each ROI according to its patterns of activity as either “spatial” (significant 2-by-3 interaction, but no significant main effect of Temporal offset), as “spatio-temporal” (significant 2-by-3 interaction and a significant main effect of Temporal offset), as “temporal” (significant main effect of Temporal offset, but no significant interaction), or as “sensory” (no significant main effect of Temporal offset or interaction; i.e. unspecific activation by the experimental conditions, see Figure 1B). To account for multiple comparisons, for every ANOVA conducted separately, we adapted our threshold for significance using a Matlab-based implementation of the algorithm for false discovery rate (FDR) correction (Benjamini & Hochberg, 1995). Thus, any main effect or interaction reported here as significant is such after correction for multiple comparisons.

The presence of a main effect of Temporal offset and/or a Modality-by-Temporal offset interaction does not on its own guarantee that the pattern of activity is the one expected for temporal expectancy and spatial processing in PPS. In order to classify the ROI based on fine criteria, we further conducted a function fitting procedure based on a priori hypotheses about the expected shape of the group-averaged curves in the sVT and dVT conditions, - based on human behavioral data and animal electrophysiological data - (for the canonical patterns of activity, function fitting and ROI classification, see Figure 1B). We expected a pattern of activity reflecting the temporal prediction to be best fitted by a linear function (i.e.  $f(x) = ax + b$ ), as it has been suggested in a recent study (Kandula et al., 2017). This was motivated by the fact that our temporal offsets were separated by an identical temporal interval (1.5 s) and

thus the probability of receiving touch on the face, only once in every sVT and dVT trial, increased linearly with time. On the other hand, the pattern of activity reflecting the processing of the spatial component of PPS is expected to be better approximated by a monotonically descending inverse function (i.e.  $f(x) = a/x + b$ ). This function was chosen because it resembled the characteristics of PPS sensitive neurons in monkeys, where the firing rate in response to a looming object is typically pronounced when the object is close (within PPS), and much less so for intermediate and far distances (e.g. Fogassi et al., 1996). The non-linear profile of the PPS fitting function also reflects the sigmoidal function of modulation of RT as a function of the position of external stimuli typically found in behavioral studies using similar audio-tactile (Canzoneri et al., 2012; Ferri, Costantini, et al., 2015; Ferri, Tajadura-Jiménez, et al., 2015; Noel, Lukowska, Wallace, & Serino, 2016; Salomon et al., 2017; Serino, Canzoneri, Marzolla, di Pellegrino, & Magosso, 2015; Taffou & Viaud-Delmon, 2014; Teneggi, Canzoneri, di Pellegrino, & Serino, 2013) and visuo-tactile (Kandula et al., 2017) paradigms (sampling at more distances). Accordingly, we expected that ROIs coding for spatial characteristics should be better fitted by a linear function for the sVT condition and better fitted by the inverse function for the dVT condition, which would be reflected by a Modality-by-Temporal offset interaction. PPS-sensitive ROIs were therefore defined as coding for spatial characteristics if the linear function fitted better than the inverse function for the sVT condition and if the inverse function fitted better the linear for the dVT. We used R<sup>2</sup> as the index of the goodness of fit. In order to test which regions predominantly processed temporal and/or spatial prediction, we conducted the same ROI analyses as described above with the ROIs defined as the overlap of regions between the two different conjunctions of F-contrasts from experiments 1A and 2A ( $k \geq 30$ ).

### *Behavioral experiments*

#### Experimental setup and stimuli

In the behavioral visuo-tactile interaction task, participants lay supine inside of a mock scanner (MRI Simulator, Psychology Software Tools, Inc) that mimicked the Siemens echo-planar imaging sequence noise and reproduced similar spatial constraints, as those present during the fMRI experiment. Visual stimuli were presented on a computer screen located at the end extremity of the mock scanner bore and participants

observed its contents using a 45°-tilted mirror mounted on a fake head-coil, allowing for a diagonal field-of-view (FoV) of approximately 17°, matched to that available for the fMRI experiment. As in the MRI scanner, participants wore ear protection and their heads were immobilized within the fake head coil using soft foam padding. They delivered their responses using the index finger of their right hand on an external USB number pad.

#### Behavioral visuo-tactile interaction paradigm (PPS)

The aims of these experiments were (i) to probe the boundaries of PPS and (ii) to assess whether and to what extent reaction times to touch were affected by temporal and spatial prediction mechanisms, as implemented by experiment 1 and experiment 2. Indeed, it has previously been shown that the presence of task-irrelevant visual looming stimuli towards the face enhanced tactile detection on the face at the predicted time of impact, although the visual stimulus was no longer present (Clery et al., 2015). We thus adapted a paradigm from previous behavioral experiments that measured the boundaries of PPS using an audio-tactile interaction task (Canzoneri et al., 2012; Ferri, Costantini, et al., 2015; Galli, Noel, Canzoneri, Blanke, & Serino, 2015; Noel et al., 2014; Noel, Pfeiffer, Blanke, & Serino, 2015b; Serino, Canzoneri, et al., 2015; Serino, Noel, et al., 2015), but replaced auditory with visual stimuli (Kandula et al., 2015, 2017; Salomon et al., 2017). In these paradigms, it has been shown that reaction times (RTs) in response to the delivery of a tactile stimulus on a body part was affected by the perceived distance from that body part of the auditory/visual task-irrelevant stimulus at the time touch is delivered. RTs were typically faster when the auditory/visual stimulus was perceived close to, as opposed to far from, the stimulated body part, specifically when the auditory/visual stimulus was looming towards the stimulated body part (Serino, Noel, et al., 2015). The depth beyond which a facilitation on the RTs with respect to the baseline (unimodal tactile only) condition was observed served as a proxy measure of the boundary between PPS and extrapersonal space.

For the behavioral paradigm, we used identical stimuli to those used in the fMRI experiment (Figure 1A). Only minor changes were made. These included shorter inter-trial intervals (randomly selected between 1.0s, 1.5s and 2.0s) and a reduced number of VIS trials. Furthermore, touch was delivered on the cheeks in the dVT and sVT conditions with one of five temporal offsets (as opposed to three) with respect to the

first appearance of the virtual ball on that trial on the screen, at  $T1=1.25s$ ,  $T1|2 = 2.0s$ ,  $T2 = 2.75s$ ,  $T2|3 = 3.5s$  or  $T3 = 4.25s$ , corresponding, in the case of the dVT condition, to situations when the virtual ball was observed in far, far-intermediate, intermediate, close-intermediate or close space from the face at the time of tactile delivery, respectively. The temporal offsets  $T1$ ,  $T2$  and  $T3$  were the same ones used in the fMRI experiment. The participants were instructed to press a button as quickly as possible when and only when one of two events occurred: (i) upon the delivery of a tactile stimulus on the cheeks (experimental conditions), or (ii) when the white centered fixation cross changed briefly color to red for 300ms (attention conditions). The attention conditions, which were identical to a subset of the experimental conditions, served two purposes, namely to (i) ensure that participants were directing their gaze to the middle of the screen and to (ii) ensure that their level of attention was elevated throughout the experiment (comparable to the fMRI task). We report the rate of success in the attention condition as the number of trials in which participants (correctly) pressed a button upon the change of color of the fixation cross, divided by the total number of trials of the attention condition. Furthermore, to ensure that participants do not automatically associate the presence of dynamic stimuli to a button response, we measured the rate of false alarms, which were defined as the number of trials of the VIS condition where a button was (wrongly) pressed divided by the total number of VIS trials. Finally, in order to detect a truly multisensory facilitation effect within the boundaries of PPS in the dVT condition, we also measured in the baseline (unimodal touch only) condition the RTs to tactile stimuli in the absence of a visual stimulus at temporal offsets  $T1$  (BAT1) and  $T3$  (BAT3). To sum up, the behavioral visuo-tactile interaction task consisted of a 2 x 5 full-factorial design with factors Modality (sVT, dVT) and Temporal offset ( $T1$ ,  $T1|2$ ,  $T2$ ,  $T2|3$ ,  $T3$ ). Each condition was repeated in total 10 times within a single block of approximately 17 minutes. Within the same block, the attention, VIS, BAT1, and BAT5 conditions were also uniformly distributed and repeated 10 times.

Crucially, in order to assess how temporal versus temporal/spatial prediction mechanisms could affect RTs, the same experiment was conducted with the sVT and dVT conditions fully randomized (experiment 1B) or sequentially presented (experiment 2B), mirroring the fMRI versions of experiments 1 and 2 respectively. Irrespectively of the group, the VIS, BAT1 and BAT3 conditions were always

uniformly distributed within each block. Indeed, as they were unimodal conditions (only visual or only tactile), they did not provide cues for the multisensory (sVT & dVT) conditions and were not expected to affect RTs for them.

#### Data preprocessing and analysis (PPS)

Prior to conducting statistical tests on the RTs, we conducted some pre-processing on the raw data. For all subjects and all experimental conditions, we excluded all negative RTs (which suggested a button press before the delivery of a tactile stimulus). Based on the residual data, we calculated the condition-wise means and standard deviations and excluded RTs that were more than 2.5 times the standard deviation off from the mean for every condition separately.

Data from both experimental groups was analyzed separately as it was collected in a different sample of subjects, but otherwise the statistical tests remained identical. Concretely, we run two types of analyses on the RTs. The first analysis aimed at assessing whether (and how) the RTs differed between the two levels of the Modality factor as a function of the Temporal offset factor. Accordingly, we performed a 2-by-5 rmANOVA with the factors Modality (sVT, dVT) and Temporal offset (T1, T1|2, T2, T2|3, T3) on the individual condition-wise RTs from which the average baseline times had been subtracted (i.e. baseline-corrected RTs). The baseline, which was unique to each participant, was defined as the arithmetic mean between the mean RT to BAT1 and the mean RT to BAT3 (RTs to unimodal touch delivered to the face at Temporal offsets T1 and T3). Only in case of a Modality-by-Temporal offset interaction, we performed a post-hoc Tukey's honestly significant difference (HSD) test, comparing RTs at the same Temporal offset between the two modalities in order to investigate the origin of the interaction. The second analysis aimed at assessing between which temporal offsets (and thus depths for the dVT conditions) the boundary of PPS was located. For this, we ran a 2-by-6 rmANOVA on the baseline-uncorrected RTs with factors Modality (sVT, dVT) and Temporal offset (T1, T1|2, T2, T2|3, T3, baseline). In the case of an interaction, Tukey's HSD test was used for post-hoc comparisons between the RTs for the baseline with respect to the other levels of the Temporal offset factor. Significance was set for  $p < 0.05$ . Only RTs at temporal offsets that differed significantly from those of the baseline were considered (in the case of dVT) as within PPS.



### Ball depth estimation task

The aim of the depth estimation experiment was to assess the average perceived distances of the virtual balls from the face at the times when the tactile stimulus was delivered in the dVT condition (see above). For this task, the experimental setup was identical to the one used for the behavioral visuo-tactile interaction task, except that no touch was delivered since the task was purely visual. In a typical trial, at time  $t = 0$ s were presented 2 virtual balls at a far and a near location in space. The virtual balls were identical to those used in the visuo-tactile interaction task, but were rendered semi-transparent and served as spatial cues for far and near distance, where in the dVT conditions the virtual ball first appeared and then disappeared respectively in each trial. At  $t = 2$ s, the target virtual ball appeared on the screen at one of the 5 depths where it was located in the dVT condition at the moment touch was delivered, and remained there stationary until the end of the trial. At  $t = 3$ s, the visual cues disappeared and at  $t = 5$ s a scale with a cursor appeared at the bottom of the screen asking participants to estimate the depth of the target virtual ball with respect to the near and far cues. Participants were instructed to bring the cursor to the desired position using a response box held in their right hand and to confirm their choice. The cursor moved on a 100-point scale where the left-most portion (1) signaled that the target virtual ball was perceived at the position of the near cue and right-most portion (100) at the position of the far cue. In each trial, the cursor appeared at a random location on the scale and participants had no time constraints to respond. Each trial was separated from the subsequent one by an inter-stimulus interval of 0.5, 1.0 or 1.5s, randomly selected. The task consisted of 5 conditions where the target virtual ball appeared in one of the 5 depths where touch was delivered in the dVT conditions (DT1, DT1|2, DT2, DT2|3, DT3). Each experimental condition was repeated in total 10 times and the task took approximately 10 min to complete.

For the depth estimation task, for each participant, we calculated the mean rating about depth individually for each of the 5 experimental conditions and subjected these to a one-way rmANOVA with the 5 levels of the factor Distance (DT1, DT1|2, DT2, DT2|3, DT3) that corresponded to the distances at Temporal offsets T1, T1|2, T2, T2|3, and T3 respectively. Only in case of a significant main effect, we used a post-hoc Tukey's HSD test to make pair-wise comparisons.

## Results

### *Experiment 1A - fMRI*

For the ROI analysis, the conjunction of F-contrasts assessing regions activated by any of the experimental conditions versus rest, revealed activity in a total of 13 regions and these were located in fronto-parietal (SPL and dPMc), temporo-parietal (IPL and parietal operculum) and occipital regions (Table 1, Figure 2A). A significant 3-way interaction ( $F(48, 432) = 1.75, p = 0.0021$ ) from the 3-by-3-by-13 rmANOVA with factors Modality (sVT, dVT, VIS), Temporal offset (T1, T2, T3) and ROI (ROIs 1-13) allowed us to pursue with further analyses for every ROI separately. We thus proceeded with a 3-by-3 rmANOVA with factors Modality (sVT, dVT, VIS) and Temporal offset (T1, T2, T3) on the mean parameter estimates from the GLM within each of these ROIs, revealing that in 8 of these 13 ROIs there was a significant interaction.

To exclude the possibility that the interaction was driven by the unisensory VIS condition, we excluded the latter and further conducted a 2-by-3 rmANOVA with factors Modality (sVT, dVT) and Temporal offset (T1, T2, T3) on these 8 ROIs, revealing a main effect of Temporal offset in 7 ROIs, suggesting processing related to temporal prediction, irrespectively of the sVT and dVT conditions. For all these brain regions, the pattern of activity was better fitted by a linear than by an inverse function and was monotonically increasing as a function of increasing temporal offset (see methods section about ROI classification procedure and curve fitting). These 7 regions were thus labeled as “temporal” ROIs (left SPL, right dPMc, bilateral TPJ/IPL and right S1). We did not find for any ROIs either a significant interaction that would signal spatial processing (i.e. “spatial” ROIs; non-linear increase of activity in the dVT condition and no change in the sVT condition) or both spatial and temporal processing (i.e. “spatio-temporal” ROIs, non-linear increase of activity in the dVT and linear increase in the sVT condition). The 6 other ROIs that did not possess any of the expected patterns of activity (see methods) were labeled as “sensory” and were located in the bilateral superior occipital cortex (SOC), right lateral occipital cortex (LOC), right cuneus, right IPS and right precuneus. To summarize, out of the initial 13 ROIs, 6 were categorized as “sensory” and 7 as “temporal” with no regions coding “spatio-temporal” or “spatial” aspects (Figure 3).

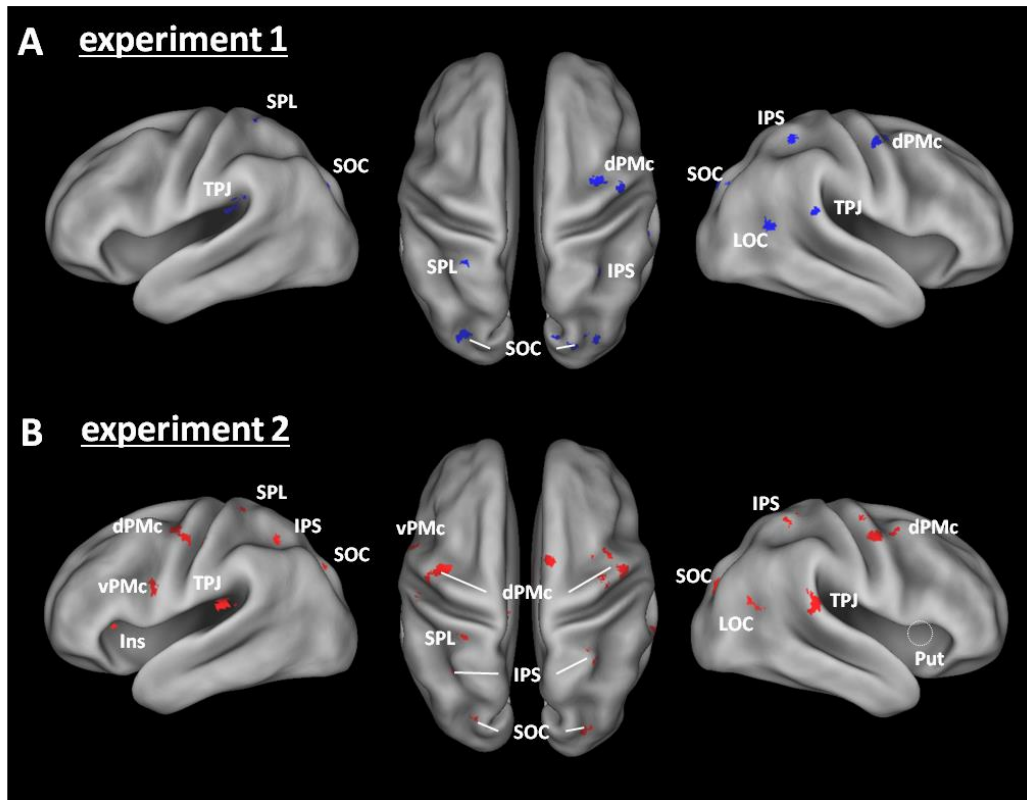


**Figure 2:** Brain regions activated by any of the experimental conditions in experiment 1 (A) and experiment 2 (B). For more details, see Table 1 and Figure 3. IPS intraparietal sulcus, SPL superior parietal lobule, dPMc dorsal premotor cortex, TPJ temporo-parietal junction

Anatomical location	experiment 1*					experiment 2*					overlap†				
	x	y	z	size	BA	x	y	z	size	BA	x	y	z	size	BA
<b>Parietal regions</b>															
R precuneus	1	-42	55	112	5	15	-40	58	500	5					
R intraparietal sulcus (IPS)	29	-43	56	272	2,7,40	33	-44	59	476	2,7,40	31	-43	57	42	2,40
L intraparietal sulcus (IPS)						-31	-52	46	179	7,40					
L postcentral gyrus (SPL)	-32	-41	69	128	5	-28	-34	62	143	3					
L postcentral gyrus (S1)						-32	-23	38	122	3					
R postcentral gyrus (S1)	32	-37	72	279	3										
<b>Frontal regions</b>															
R middle frontal gyrus (dPMc)						39	-4	62	1034	6					
L precentral gyrus (dPMc)						-38	-7	50	917	6					
L precentral gyrus (vPMc)						-51	-1	19	265	6,48					
R precentral gyrus (dPMc)	33	-3	45	709	6	36	-2	41	228	6	49	-8	53	126	6
R supplementary motor area (SMA)						10	4	70	218	6					
L anterior insula						-26	19	6	151	48					
R putamen						25	15	5	117	48					
<b>Parieto-occipular regions</b>															
R parietal operculum (TPJ)	56	-28	16	113	42	61	-33	16	793	22,42,48	65	-34	17	59	22,42
L parietal operculum (TPJ)	-40	-33	17	207	48	-32	-29	19	284	48	-34	-30	19	42	48
R superior temporal gyrus (TPJ)	65	-42	13	395	22,42,48										
L supramarginal gyrus (IPL)	-51	-36	24	150	48										
<b>Occipital regions</b>															
R middle temporal gyrus (LOC)	55	-60	12	257	21,37,39	40	-56	19	502	21,37,39					
R cuneus	23	-66	33	100	7	8	-75	20	201	18					
R middle occipital gyrus (SOC)	23	-83	37	801	19	29	-78	29	170	19					
L superior occipital gyrus (SOC)	-31	-77	25	356	19	-23	-75	37	155	19					

**Table 1:** brain regions activated by the experimental conditions for experiments 1 and 2 and their overlap. \*  $p < 0.05$  FWE,  $k > 100$ ; † only clusters larger than 30 voxels are shown. L left, R right, BA Brodmann area, x y z are MNI coordinates of peak-activation voxels

### Experiment 1B – behavior

Unlike, experiment 2B (see below), behavioral results for experiment 1B (Figure 4C, for full details see SOM) revealed that RTs to touch on the face were affected by increasing temporal offsets of touch delivery, but were not differentially affected between the sVT and dVT conditions. Furthermore, there was no significant facilitation effect on RTs between the visuo-tactile versus tactile (baseline) conditions for any of the tested temporal offsets. This suggests that when the presentation of sVT and dVT conditions is intermingled, participants rely either on a mix of temporal information (present predominantly in the sVT condition) and spatial (present only in the dVT condition) information to make predictions about the delivery of touch. The absence of a facilitation effect of RTs with respect to baseline (thus signaling a boundary of PPS) suggests that temporal information was weighted more strongly. This is also in line with the results from the fMRI part of experiment 1, where no regions possessed patterns of activity suggesting spatial processing (i.e. absence of “spatial” and “spatio-temporal” ROIs) but many possessed patterns of activity, not differentially affected between the sVT and dVT conditions, suggesting temporal processing (i.e. “temporal” ROIs).

### *Experiment 2A - fMRI*

For the ROI analysis, the conjunction analysis of F-contrasts assessing regions activated by any of the experimental conditions versus rest, revealed activity in a total of 21 clusters located mostly in fronto-parietal, temporo-parietal and occipital regions (Figure 2B, Table 1). The 3-by-3-by-21 rmANOVA with factors Modality (sVT, dVT, VIS), Temporal offset (T1, T2, T3) and ROI (ROIs 1-21) revealed a three-way interaction ( $F(80, 720) = 2.20, p < 0.001$ ) and statistical analysis for individual ROIs (3-by-3 rmANOVAs with factors Modality (sVT, dVT, VIS) and Temporal offset (T1, T2, T3)) revealed an interaction in 10 of these ROIs.

In order to exclude the possibility that the interaction was driven by the VIS condition, the subsequent 2-by-3 rmANOVA for these 10 residual ROIs revealed in 6 ROIs only a main effect of Temporal offset (in bilateral TPJ, left SPL, left S1, left posterior cingulate cortex (PCC) and right putamen; “temporal” ROIs). In 3 ROIs we found a significant main effect of Temporal offset and an interaction (bilateral dPMc and right IPS; “spatio-temporal” ROIs) and in one ROI only a significant interaction (right superior occipital cortex (SOC)). All of these ROIs possessed one of the predicted patterns of activity (Figure 1B), except for the cluster in the right SOC, and it was thus classified as “sensory” (see Figure S1 for more detail). Comparisons of the R2 on the group-averaged ROI-specific parameter estimates from the GLM analysis showed that the linear function fitted better the sVT curves and the inverse function fitted better the dVT curve in all of the “spatio-temporal” ROIs (Figure 3). To summarize, in experiment 2, out of the 21 ROIs activated by any of the experimental conditions, 12 were classified as “sensory”, 6 as “temporal”, 3 as “spatio-temporal” and no ROI as pure “spatial”. Thus, when occurrence of tactile stimulation was distinguishable between sVT and dVT condition, a differential role of temporal and spatial predictions could be identified in bilateral dPMc and right IPS regions.

### *Experiment 2B – behavior*

The pattern of fMRI response was also reflected in the behavioral experiment. Indeed, unlike the behavioral data from experiment 1B, the results in experiment 2B (Figure 4C, for full details see SOM) revealed that RTs to touch on the face were differentially affected by the Temporal offset factor between the sVT and dVT conditions, with the two curves dissociating significantly at time T3 (i.e. when visual stimulus in dVT

condition was near the face). Furthermore, only for the dVT conditions, but not for the sVT, the RTs were significantly affected by the Temporal offset factor. Finally, with respect to the unimodal baseline (touch only), only for T3 in the dVT condition there was a facilitation effect on the RTs, suggesting, for the dVT condition, the presence of the PPS boundary between T3 and T2|3 (Figure 4C).

#### *Temporal vs spatial prediction ROI analysis (experiments 1A & 2A)*

In order to directly investigate the brain regions processing primarily temporal versus spatial prediction in the context of PPS, we compared fMRI results from experiments 1 and 2, as for the latter the predictability of ball looming had been manipulated. We first selected those regions that were activated in both experiments (i.e. overlap of the conjunction analyses from both experiments,  $k \geq 30$ ). This analysis uncovered the bilateral TPJ, the right dPMc and the right IPS (Figure 4A). We classified each of these ROIs as “sensory”, “temporal”, “spatio-temporal” or “spatial” in the same manner as in the ROI analyses above, but separately for the data from each experiment. Whereas all the ROIs were classified as “temporal” for the data of experiment 1, they were all except the left TPJ cluster classified as “spatio-temporal” for experiment 2. Furthermore, linear curves fitted better data from all ROIs from experiment 1, suggesting processing of temporal prediction, whereas the inverse curve fitted better the dVT condition (but not the sVT) in experiment 2 in all ROIs (except the left TPJ), suggesting processing of spatial PPS information (Figure 4B). Collectively, this shows that when the online a priori probability (and thus subject expectancy) that the virtual ball looms towards the face is manipulated so as to avoid mutual effects of sVT on dVT and vice-versa, patterns of activity suggesting spatial prediction can be revealed in the dVT condition.

#### *Depth estimation task*

The depth estimation task assessed the subjective perceived depth of the virtual ball at positions corresponding to when touch was delivered in the dVT conditions. Results revealed that subjects perceived these depths as significantly different, although with a distorted near versus far space (Figure S2, for full details see SOM). Concretely, the perceived differences in depths between T3 and T2 (near space, perceived as 50.81% of the total path length) were larger than those between T2 and T1 (far space, perceived

as 18.48% of total path length), despite the fact that they were equally-spaced in virtual space.

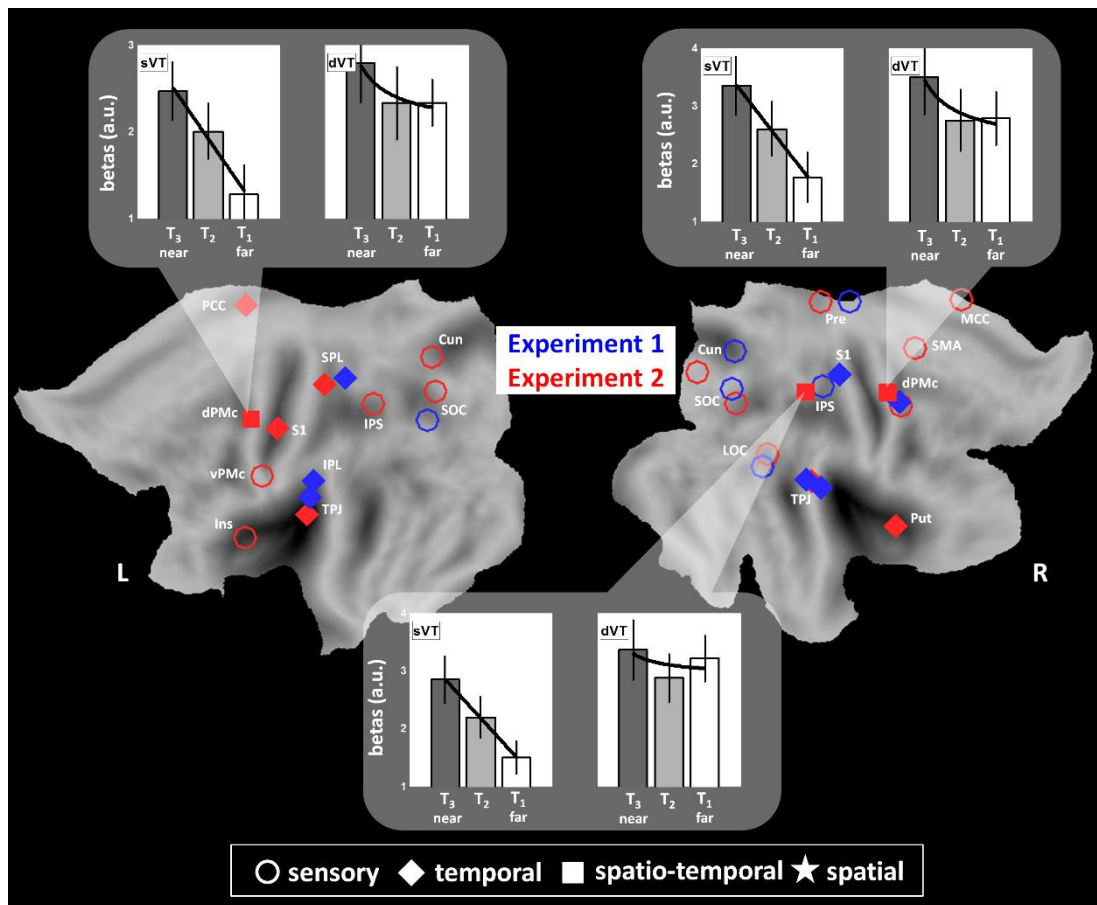


**Figure 3:** Projection on a flat brain surface of the locations of the peak-activation voxels corresponding to the activation clusters for experiment 1 (in blue) and experiment 2 (in red). The symbols represent the classification of that cluster in terms of pattern of activity (see methods section in main text). Thus, clusters activated not specifically by any experimental condition are classified as “sensory” (ring); those modulated exclusively and non-differentially between the sVT and dVT conditions by the Temporal offset factor are classified as “temporal” (diamond); those modulated differentially between the sVT and dVT conditions depending on the distance of the visual stimulus and by the Temporal offset factor are classified as “spatio-temporal” (square); and those only affected differentially between the sVT and dVT conditions are classified as “spatial” (star). On top and at the bottom are represented ROI-specific patterns of activity in the three “spatio-temporal” ROIs from experiment 2. The y-axis represents the mean  $\pm$  s.e.m. parameter estimates from the GLM analysis. Fitted over the bars are either a linear or an inverse function (whichever yielded a higher R<sup>2</sup>, see methods section for more details). L left, R right, v/dPMc ventral/dorsal premotor cortex, S1 primary somatosensory, SPL superior parietal lobule, SOC/LOC superior/lateral occipital cortex, TPJ temporo-parietal junction, Pre precuneus, IPS intraparietal sulcus, Put putamen, Ins insula, IPL inferior parietal lobule, PCC/MCC posterior/mid cingulate cortex

## Discussion

We investigated the neural mechanisms of visuo-tactile PPS processing around the face in healthy subjects by adapting a visuo-tactile interaction paradigm, previously only used in behavioral studies (Pellencin, Paladino, Herbelin, & Serino, 2017; Salomon et al., 2017; Serino, Noel, et al., 2015), to the scanner. This allowed us to manipulate in different conditions the characteristics of visual stimulation so as to provide different spatial information regarding an upcoming tactile event on the face (i.e., the visual stimuli could be far, at an intermediate distance or close to the face at the onset of the tactile stimulus). In addition, in order to assess which brain regions process predominantly spatial versus temporal information related to multisensory tactile stimulation, we manipulated in two distinct experiments the predictability of the looming visual stimulus entering the PPS and thus providing spatial vs. temporal information to predict the occurrence of tactile stimulation. Results highlighted a distributed set of brain regions located mainly in parietal, premotor and superior-temporal areas involved in visuo-tactile multisensory processing. The activity profile of these regions reflected spatial and temporal features of the visual cues to enhance tactile processing when the visual stimulus was close to the face, i.e. PPS processing. Moreover, these activity patterns suggested that all regions processed anticipation to touch based on temporal information (as stressed by our stimulation paradigm), whereas only a subset of them, located in the premotor, parietal and temporo-parietal regions of the right hemisphere, processed in addition spatial information. In the following, we will discuss in detail the involved PPS mechanisms with respect to multisensory, spatial and temporal processing, linking them to current knowledge in the field and proposing a general neural mechanism for PPS processing.

### *Multisensory processing within the face PPS network in fronto-parietal and temporo-parietal areas*

The combination of visual and tactile stimuli activated a broad network of areas located in frontal, parietal, and occipital cortex, as well as the temporo-parietal junction (Figures 2 & 3). All these areas, except those of the occipital cortex, showed patterns of activity suggesting PPS processing (i.e. with a more pronounced touch-induced activity when the looming visual stimulus was near the face, as compared to the intermediate and far distances from the face). Many of these regions have previously



been described as regions of multisensory (mostly visuo-tactile) integration in humans (Driver & Noesselt, 2008; Macaluso & Driver, 2005) and also largely mirror the results from a recent neuroimaging meta-analysis on PPS from studies using a variety of mostly visual and visuo-tactile stimuli to probe PPS around the hand, face and trunk (Grivaz et al., 2017) in healthy participants.

### ***Posterior parietal areas***

The PPS regions in the parietal cortex were centered in and around the SPL/S1 (BAs 5, 7, 2 and 3) and in the IPS (BA 40). Activity associated with unisensory and multisensory PPS has been frequently reported by previous work in and around the IPS region; this has been observed for the PPS around the hand (i.e. the most frequently studied body part, Brozzoli, Gentile, Bergouignan, & Ehrsson, 2013; Brozzoli et al., 2011; Brozzoli, Gentile, & Ehrsson, 2012a; Gentile, Guterstam, Brozzoli, & Ehrsson, 2013; Gentile, Petkova, & Ehrsson, 2011; Makin, Holmes, & Zohary, 2007), around the trunk (Huang et al., 2012) and the face (Bremmer et al., 2001; Holt et al., 2014; Huang et al., 2012; Sereno & Huang, 2006). We argue that these posterior parietal regions represent the homologous regions where PPS neurons have originally been recorded in non-human primates, the IPS, and in particular the ventral intraparietal areal (VIP; Duhamel et al., 1997) and area 5 (Graziano et al., 2000). Collectively, these early neurophysiological studies demonstrated that neurons in VIP and in area 5 respond to both visual and tactile stimuli and possess large tactile receptive fields (RFs) that form a crude somatotopic map of the body. Importantly, associated to their tactile RFs, these multisensory neurons also have visual RFs extending into PPS (i.e. outward from the skin) that are sensitive to objects moving in its vicinity and especially when moving towards the monkey (Colby et al., 1993). In line with the present findings, area VIP has been shown to possess tactile RFs predominantly representing the peri-face regions (Colby et al., 1993; Duhamel et al., 1998).

### ***Primary somatosensory cortex***

Interestingly, we also found visuo-tactile activity in areas 2 and 3 of the primary somatosensory cortex (S1). Although it may seem at first surprising to find visually induced PPS activity in a region generally associated with tactile and proprioceptive processing (Gardner, 1988), the traditional view of modality-specific segregation of

sensory processing in primary sensory cortices has been challenged (Ghazanfar & Schroeder, 2006; Martuzzi et al., 2007; Wallace, Ramachandran, & Stein, 2004). Many behavioral examples exist in humans whereby visual information influences S1 activity. For instance, viewing a body or viewing a body being touched affects tactile processing via the involvement of S1 (Banissy & Ward, 2007; Blakemore, Bristow, Bird, Frith, & Ward, 2005; Cardini et al., 2011; Fiorio & Haggard, 2005; Haggard, Christakou, & Serino, 2007; Longo, Pernigo, & Haggard, 2011; Serino, Pizzoferrato, & Làdavas, 2008; Taylor-Clarke, Kennett, & Haggard, 2002), possibly by means of indirect modulatory projections from multisensory parietal areas (for a review, see Serino & Haggard, 2010). Likewise, modulation of activity in the primary and secondary somatosensory areas has been observed in response not only to direct tactile stimulation of one's own face, but also when viewing touch on another person's face (Blakemore et al., 2005; Cardini et al., 2011), a situation which involved re-mapping of the PPS around another person into one's own PPS (Maister, Cardini, Zamariola, Serino, & Tsakiris, 2015). Likewise, S1 activity has been shown to be affected by the affective significance of physical touch (Gazzola et al., 2012). The involvement of area 2 in primary somatosensory cortex is less surprising, because neurons in this area possess complex and large tactile RFs covering substantial portions of the body and processing proprioceptive signals, as shown in monkeys (Gardner, 1988; Kaas, Nelson, Sur, Lin, & Merzenich, 1979) and humans (Akselrod et al., 2017; Martuzzi, van der Zwaag, Farthouat, Gruetter, & Blanke, 2014). Interestingly, the involvement of area 2 in PPS processing is also corroborated by a recent quantitative meta-analysis investigating the neural correlates of PPS in humans, in which this region was found to be consistently activated and largely overlapped with the region described in the present study (Grivaz et al., 2017). The majority of studies involved in that meta-analysis focused on hand PPS (and not face PPS as done here) and most frequently used unimodal visual stimuli (as opposed to visuo-tactile stimuli used here). The present findings thus extend the results from that meta-analysis and show for the first time the involvement of area 3 and 2 in the multisensory processing of the face-PPS.

### ***Frontal areas***

PPS regions in frontal cortex as found in the present study were located at the border between the dPMc and vPMc (area 6). In humans, face PPS processing has previously been reported in both the vPMc (Bremmer et al., 2001; Cardini et al., 2011) and dPMc

(Holt et al., 2014). Likewise, similar regions have been described in relation to hand PPS (for dPMc: Brozzoli et al., 2013, 2011, Gentile et al., 2013, 2011, for vPMc: Brozzoli et al., 2011; Ferri, Costantini, et al., 2015; Gentile et al., 2013, 2011; Makin et al., 2007). In particular, activity in the left vPMc has been shown to reflect the individual extent of PPS boundaries around the hand using a similar paradigm to the one used here (with the exception that audio-tactile instead of visuo-tactile stimuli were administered) (Ferri, Costantini, et al., 2015). Likewise, activity in the bilateral vPMc has been associated with viewing touch on a front-facing image of a face while receiving physical touch on one's cheeks (Cardini et al., 2011). Finally, non-invasive brain stimulation interfering with vPMc activity has been shown to affect PPS processing around the hand (Avenanti, Annala, & Serino, 2012; Serino, Canzoneri, & Avenanti, 2011). We note that due to the absence of a cytoarchitectonically-defined atlas of area 6 in standard space and its decomposition into its ventral and dorsal aspects, our clusters are most likely in dPMc (i.e. Mayka, Corcos, Leurgans, & Vaillancour, 2006), yet could also reflect vPMc clusters (i.e. Bremner et al., 2001). Research in non-human primates has also described neurons with PPS properties in the vPMc, in area F4 (Fogassi et al., 1996; Graziano & Cooke, 2006; Graziano & Gross, 1994; Graziano et al., 1997; Graziano, Reiss, & Gross, 1999; G. Rizzolatti, Scandolara, Matelli, & Gentilucci, 1981a, 1981b). These have collectively described neurons with similar properties as in the VIP (see above), including tactile RFs frequently representing the upper limb territory (Fogassi et al., 1996; Gentilucci, Scandolara, Pigarev, & Rizzolatti, 1983; Graziano et al., 1994). Unlike the VIP, the visual and tactile RFs of area vPMc were always spatially aligned thus suggesting a mostly arm/hand-centered representation of space in vPMc, whereas they were face/head-centered in VIP. Collectively the VIP-F4 network (the two regions are densely connected; Matelli, Camarda, Glickstein, & Rizzolatti, 1986) has thus been argued to combine information about the location of objects around the body, especially potentially harmful ones around the face, to trigger the most relevant motor response (Avenanti et al., 2012; Makin, Holmes, Brozzoli, Rossetti, & Farnè, 2009; Serino, Annala, & Avenanti, 2009).

### ***Temporo-parietal areas***

We also found that PPS processing involves regions at the TPJ, one of the major human cortical areas associated with multisensory (visual, tactile, auditory and vestibular)

integration (Blanke & Arzy, 2005; Lopez & Blanke, 2011; Macaluso & Driver, 2005), and included the parietal operculum and the IPL (BAs 22, 42, and 48). To the best of our knowledge, neurons with PPS properties have not been described in monkey TPJ. We propose, however, that this portion of IPL processing multisensory PPS cues in humans may correspond to monkey area 7b where neurons with PPS properties have been described (Leinonen, Hyvärinen, Nyman, & Linnankoski, 1979; Jiang, Hu, Wang, Ma, & Hu, 2013). Area 7b is ventral to the IPS in macaque monkeys and has been proposed as the human homologue of the area PF (for a discussion about human macaque homologies of the IPL, see Caspers et al., 2011). Importantly, activity in and around the TPJ has previously been reported in human studies investigating PPS processing on and around the face (Bremmer et al., 2001; Tyll et al., 2013), as well as the hand (Brozzoli et al., 2013; Brozzoli, Gentile, & Ehrsson, 2012; Brozzoli et al., 2011; Gentile et al., 2013, 2011). However, these earlier studies have either only probed PPS using unimodal visual stimuli which are not representative of the multisensory characteristics of PPS (Brozzoli et al., 2013, 2011), used a conjunction of unimodal conditions (Bremmer et al., 2001), or probed super-additivity of uni- and bimodal conditions (Gentile et al., 2011), thus disregarding the crucial depth-specificity of PPS (Van der Stoep, Serino, Farnè, di Luca, & Spence, 2016). Our data extend these previous findings and show, for the first time, that TPJ activity is not only multisensory, but, in addition, is modulated by the distance of the perceived task-irrelevant visual stimulus from the body, thus mirroring characteristics of PPS neurons as described in monkeys.

The present TPJ activations may also relate to processing in secondary somatosensory cortex (SII). The parietal operculum hosts human SII (or area OP1, Eickhoff, Amunts, Mohlberg, & Zilles, 2006; Eickhoff, Schleicher, Zilles, & Amunts, 2006) and is a “core” region of vestibular processing (region OP2, Lopez, Blanke, & Mast, 2012; zu Eulenburg, Caspers, Roski, & Eickhoff, 2012). Area SII possesses large and overlapping tactile receptive fields, covering the whole body (Disbrow, Roberts, & Krubitzer, 2000; Eickhoff, Grefkes, Fink, & Zilles, 2008), has been associated to processing of complex forms of touch and pain (Coghill et al., 1994), and is involved in visuo-tactile integration in humans (Macaluso, Frith, & Driver, 2005). Area OP2 (i.e. the human homologue of monkey area PIVC; Eickhoff, Weiss, Amunts, Fink, & Zilles, 2006), on the other hand, is a crucial region for both vestibular processing

(Lopez & Blanke, 2011; Lopez et al., 2012; Zu Eulenburg et al., 2012) and visuo-vestibular interactions (Roberts et al., 2017). Indeed, it has been shown that graviceptive information affects PPS processing in humans (Bufacchi & Iannetti, 2016) and bodily self-consciousness (Ionta et al., 2011) that have been associated to PPS (Noel, Pfeiffer, Blanke, & Serino, 2015b; Blanke et al., 2015). Whether visuo-tactile activity in TPJ may reflect more complex multisensory processing, including vestibular, nociceptive and social input, has to await further investigations, as this was not the purpose of the present study.

### ***Temporal and spatial prediction of touch to the face***

One of the major novelties of the present study is that we investigated whether and how PPS processing was affected by the predictability of a tactile event, based on temporal or spatial features contained in the visual stimuli. To do so, we manipulated, in fMRI and behavioral experiments, the predictability that the virtual ball appearing in far space either looms towards the face, or remains static in far space, while subjects received touch at one of three different temporal offsets (corresponding to different spatial sectors in the case of the looming ball; Figure 1C). In order to keep the stimuli and the length of the experiment identical, we manipulated the order of presentation of the bimodal experimental conditions so that in experiment 1, sVT and dVT conditions were fully intermingled, making the predictability of a looming versus static virtual ball identical. Thus, predictability of touch was at chance level based on spatial visual cues, whereas the temporal delay between the virtual ball appearance and touch delivery was constantly predictable (touch could occur at one of three delays). Under such conditions we found several brain regions with activations (Figure 3) that were characterized by a linear increase of tactile-related processing for increasing temporal delays and this pattern was indistinguishable between dVT and sVT conditions. Likewise, RT patterns to touch were identical in the corresponding conditions of the behavioral study (Figure 4C; see also Kandula et al., 2017 for similar results and a corresponding model). This suggests that when sVT-trials (only temporal information) and dVT-trials (with temporal and spatial information) are presented in the same context (i.e. intermingled), they mutually affect each other and the corresponding brain activations. The fact that in the behavioral experiment no facilitation on the RTs with respect to the baseline was observed and that in the fMRI experiment the PPS sensitive

regions possessed a pattern of activity compatible with only temporal prediction, suggests that temporal predictions are dominant under such conditions.

This was different in experiment 2, where all sVT conditions were presented in the first half of the block and all dVT conditions in the second half of the block: temporal information was made more relevant to predict touch in the sVT conditions, whereas spatial information was made more relevant for the dVT conditions. This change modulated brain responses, with many regions characterized by a linear activity modulation in the sVT and a non-linear activity modulation for the dVT conditions (Figure 3), with a stronger and consistent response for intermediate and close position, i.e. once the visual stimulus had passed the PPS boundary (see below). This was further corroborated in the corresponding behavioral experiment, where RTs were differentially affected between the sVT and dVT conditions and the latter was associated with a significant facilitation effect on the RTs specifically when the virtual ball was within a given distance from the face, highlighting the spatial location of the PPS boundary (Figure 4C).

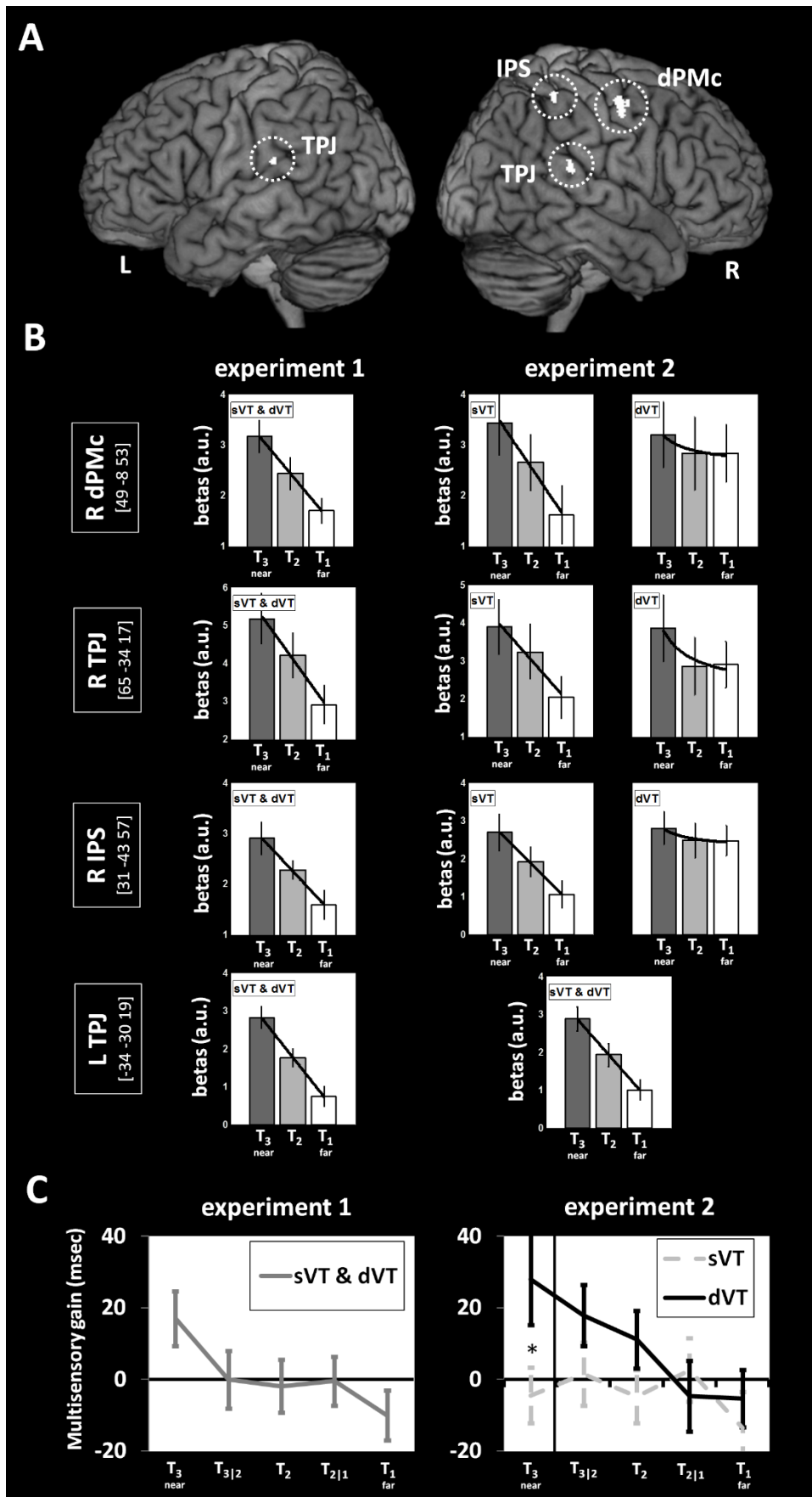


Figure 4: Results from the overlap-based ROI analysis. (A) The four ROIs ( $k \geq 30$ ) used for the overlap-

based ROI analysis (B) ROI-specific patterns of activity elicited as a function of the factors Modality and Temporal offset (in case of significant interaction) or Temporal offset (in case of a main effect) for experiments 1 and 2 separately (left and right columns respectively). The y-axis represents the mean  $\pm$  s.e.m. parameter estimates from the GLM analysis. Either a linear or an inverse function (whichever yielded a higher R2, see methods section for more details) is fitted over the bars (C) Results from the behavioral studies of experiment 1 and experiment 2. For experiment 1, RTs did not differ significantly between the sVT and dVT conditions, as opposed to experiment 2. Only for experiment 2 and only for dVT at T3 did the RTs significantly differ from the baseline (RT to touch alone, zero on the y-axis) suggesting a multisensory integration effect occurring within the boundary of PPS between T3|2 and T3 (black vertical line). L left, R right, IPS intraparietal sulcus, dPMc dorsal premotor cortex, TPJ temporo-parietal junction

Comparing our fMRI results across both experiments, we note that most multisensory PPS regions exhibited an activity pattern that is compatible with temporal prediction. These regions were located in the bilateral S1, left SPL, right IPS, bilateral dPMc, bilateral TPJ, left PCC and the right putamen (Figure 3) and characterized by activity that linearly increased as a function of waiting time to receive the touch (Durstewitz, 2004; Kandula et al., 2017). Many of these regions are associated with temporal processing in humans, such as SPL/S1 (Harrington, Zimelman, Hinton, & Rao, 2010; Murai & Yotsumoto, 2016; van Ede, de Lange, Jensen, & Maris, 2011; Xu et al., 2014), right IPS (Dormal & Pesenti, 2012; Hayashi, Kanai, Tanabe, Yoshida, & Walsh, 2013; Murai & Yotsumoto, 2016; Pouthas et al., 2005; Xu et al., 2014), PMc (Carver, Elvevag, Altamura, Weinberger, & Coppola, 2012; Harrington et al., 2010; Murai & Yotsumoto, 2016; Pouthas et al., 2005), the TPJ (Carver et al., 2012; Harrington et al., 2010) and the putamen (Harrington et al., 2010; Murai & Yotsumoto, 2016; Tipples, Brattan, & Johnston, 2013). Such temporal activity patterns may reflect brain activity that increases in intervals preceding a test stimulus (as observed in our data) in parietal regions of monkeys, in SPL (Chafee & Goldman-Rakic, 1998) and IPS (Janssen & Shadlen, 2005), and have been interpreted as the neural correlates of temporal anticipation (for review, see Coull & Nobre, 2008). Collectively, the present data show that the same regions that engage in temporal processing and/or anticipation are also largely involved in prediction of touch based on visual information and prior expectancy about the visual stimuli in the context of visuo-tactile PPS.



Even more relevant for the present PPS study, a subset of four brain regions further exhibited a pattern of activity compatible with the processing of spatial PPS prediction. These regions were the right IPS, bilateral dPMc and the right TPJ (Figures 3 & 4) and their activity was characterized by a non-linear increase in BOLD response that was present only in the dVT conditions (i.e. with strongest activity when the virtual ball was within the PPS). The same non-linear pattern of multisensory response, with analogous enhancement for within-PPS audio-tactile stimulation, was found in the post-central gyrus and inferior frontal gyrus (plus other sites in the parahippocampal gyrus and insula) in a recent intracranial electroencephalography study (Bernasconi et al., 2018). We argue that these regions integrate both spatial and temporal information present in the stimuli to predict the time and the location of touch delivery. Indeed, previous neuroimaging studies in humans on spatially or temporally driven predictive judgments and on cued attention to spatial locations and temporal intervals have highlighted spatio-temporal integration processing in the bilateral IPS and dPMc (Beudel, Renken, Leenders, & De Jong, 2009; Coull & Nobre, 1998; O'Reilly, Mesulam, & Nobre, 2008). Furthermore, electrical interference of the right IPS has been shown to bias performance in both a line (spatial) and a time interval (temporal) bisection task (Oliveri et al., 2009). Finally, a patient with a right parietal lesion and suffering from hemispatial neglect has been reported to also possess distortions in subjective temporal duration judgments (Basso, Nichelli, Frassinetti, & di Pellegrino, 1996). The present results in humans also complement a recent fMRI study in monkeys showing that conditions in which the temporal and spatial information from a looming stimulus was fully predictive of an upcoming tactile event on the face engaged significantly more areas VIP and F4, as opposed to conditions where the visual stimulus wrongfully predicted either the time or the location of touch (Cléry et al., 2017). These authors further demonstrated that these effects were driven by multisensory integration mechanisms. These previous findings support the notion that temporal and spatial information primarily converges in the right IPS, TPJ and the PMc and further likely relies on multisensory integration mechanisms. The preponderance of right-lateralized spatially-sensitive regions in our experiment is in line with the most accepted view that spatial cognition engages mostly the right hemisphere, in particular the posterior parietal cortex (reviewed in Sack, 2009). Our results thus confirm past findings about regions of spatio-temporal convergence and general right-lateralized spatial processing, but newly link these to the specialized

context of visuo-tactile PPS and shows that activity in the right hemisphere is further modulated by the a priori expectation about the characteristics of the stimuli.

## **Conclusions**

In summary, by probing the neural correlates of visuo-tactile integration for stimuli around the face with ultra high-field fMRI and behavioral experiments, we describe a larger network of brain regions processing temporal predictions that includes a smaller network of regions processing spatial predictions related to PPS. We report a modulation of tactile response based on visual cues, as a function of their distance from the body in depth, in classical PPS areas such as the PMc and IPS, but also in regions such as the primary and secondary somatosensory areas and the IPL. Whereas all PPS regions exhibited activity patterns suggesting the processing of temporal prediction to touch, only a subset of them were also sensitive to the spatial component of visual information. These were located in dPMc, IPS and TPJ with a right hemispheric predominance, and showed differential activity patterns as a function of the a-priori expectation about the characteristics of the visual stimuli when predicting touch on the face. These findings show that the interaction of visual and tactile cues in these multisensory PPS brain regions depends on on-line adapting expectations about the association between a dynamic external stimulus and touch on the body. Extending previous knowledge about the neural mechanisms of visuo-spatial PPS processing around the human face, the present data highlight the major and differential roles that multisensory PPS brain regions have with respect to spatio-temporal predictions.

## References

- Akselrod, M., Martuzzi, R., Serino, A., van der Zwaag, W., Gassert, R., & Blanke, O. (2017). Anatomical and functional properties of the foot and leg representation in areas 3b, 1 and 2 of primary somatosensory cortex in humans: a 7 T fMRI study. *NeuroImage*. <https://doi.org/10.1016/j.neuroimage.2017.06.021>
- Avenanti, A., Annala, L., & Serino, A. (2012). Suppression of premotor cortex disrupts motor coding of peripersonal space. *NeuroImage*, 63(1), 281–288. <https://doi.org/10.1016/j.neuroimage.2012.06.063>
- Banissy, M. J., & Ward, J. (2007). Mirror-touch synesthesia is linked with empathy. *Nature Neuroscience*, 10(7), 815–816. <https://doi.org/10.1038/nn1926>
- Basso, G., Nichelli, P., Frassinetti, F., & di Pellegrino, G. (1996). Time perception in a neglected space. *Neuroreport*, 7(13), 2111–2114. <https://doi.org/10.1097/00001756-199609020-00009>
- Benjamini, Y., & Hochberg, Y. (1995). Controlling the False Discovery Rate : A Practical and Powerful Approach to Multiple Testing. *J. R. Statist. Soc.*, 57(1), 289–300.
- Bernasconi, F., Noel, J. P., Park, H. D., Faivre, N., Seeck, M., Spinelli, L., ... Serino, A. (2018). Audio-tactile and peripersonal space processing around the trunk in human parietal and temporal cortex: An intracranial EEG study. *Cerebral Cortex*, 28(9), 3385–3397. <https://doi.org/10.1093/cercor/bhy156>
- Beudel, M., Renken, R., Leenders, K. L., & De Jong, B. M. (2009). Cerebral representations of space and time. *NeuroImage*, 44(3), 1032–1040. <https://doi.org/10.1016/j.neuroimage.2008.09.028>
- Blakemore, S. J., Bristow, D., Bird, G., Frith, C., & Ward, J. (2005). Somatosensory activations during the observation of touch and a case of vision-touch synaesthesia. *Brain*, 128(7), 1571–1583. <https://doi.org/10.1093/brain/awh500>
- Blanke, O., & Arzy, S. (2005). The out-of-body experience: Disturbed self-processing at the temporo-parietal junction. *Neuroscientist*, 11(1), 16–24. <https://doi.org/10.1177/1073858404270885>
- Blanke, O., Slater, M., & Serino, A. (2015). Behavioral, Neural, and Computational Principles of Bodily Self-Consciousness. *Neuron*, 88(1), 145–166. <https://doi.org/10.1016/j.neuron.2015.09.029>
- Bremmer, F., Schlack, A., Shah, N. J., Zafiris, O., Kubischik, M., Hoffmann, K. P., ... Fink, G. R. (2001). Polymodal motion processing in posterior parietal and premotor cortex: A human fMRI study strongly implies equivalencies between humans and monkeys. *Neuron*, 29(1), 287–296. [https://doi.org/10.1016/S0896-6273\(01\)00198-2](https://doi.org/10.1016/S0896-6273(01)00198-2)
- Brozzoli, C., Gentile, G., & Ehrsson, H. H. (2012). That’s Near My Hand! Parietal and Premotor Coding of Hand-Centered Space Contributes to Localization and Self-Attribution of the Hand. *Journal of Neuroscience*, 32(42), 14573–14582. <https://doi.org/10.1523/JNEUROSCI.2660-12.2012>
- Brozzoli, Claudio, Makin, T. R., Cardinali, L., Holmes, N. P., & Farnè, A. (2012). Peripersonal space: A multisensory interface for body-objects interactions. In *The neural Bases of Multisensory Processes*, Chapter 23, Publisher CRC Press (pp. 447–464).
- Brozzoli, Gentile, G., Bergouignan, L., & Ehrsson, H. H. (2013). A shared representation of the space near oneself and others in the human premotor cortex. *Current Biology*, 23(18), 1764–1768. <https://doi.org/10.1016/j.cub.2013.07.004>
- Brozzoli, Gentile, G., & Ehrsson, H. H. (2012). That’s near my hand! Parietal and premotor coding of hand-centered space contributes to localization and self-attribution of the hand. *The Journal of Neuroscience: The Official Journal of the Society for Neuroscience*, 32(42), 14573–14582. <https://doi.org/10.1523/JNEUROSCI.2660-12.2012>
- Brozzoli, Gentile, G., Petkova, V. I., & Ehrsson, H. H. (2011). fMRI adaptation reveals a cortical mechanism for the coding of space near the hand. *The Journal of Neuroscience: The Official Journal of the Society for Neuroscience*, 31(24), 9023–9031. <https://doi.org/10.1523/JNEUROSCI.1172-11.2011>
- Bufacchi, R. J., & Iannetti, G. D. (2016). Gravitational cues modulate the shape of defensive peripersonal space. *Current Biology*, 26(21), R1133–R1134. <https://doi.org/10.1016/j.cub.2016.09.025>
- Canzoneri, E., Magosso, E., & Serino, A. (2012). Dynamic sounds capture the boundaries of peripersonal space representation in humans. *PloS One*, 7(9), e44306. <https://doi.org/10.1371/journal.pone.0044306>
- Cardini, F., Costantini, M., Galati, G., Romani, G. L., Làdavas, E., & Serino, A. (2011). Viewing one’s

- own face being touched modulates tactile perception: an fMRI study. *Journal of Cognitive Neuroscience*, 23(3), 503–513. <https://doi.org/10.1162/jocn.2010.21484>
- Carver, F. W., Elvevag, B., Altamura, M., Weinberger, D. R., & Coppola, R. (2012). The Neuromagnetic Dynamics of Time Perception. *PLoS ONE*, 7(8), 1–9. <https://doi.org/10.1371/journal.pone.0042618>
- Caspers, S., Eickhoff, S. B., Rick, T., von Kapri, A., Kuhlen, T., Huang, R., ... Zilles, K. (2011). Probabilistic fibre tract analysis of cytoarchitectonically defined human inferior parietal lobule areas reveals similarities to macaques. *NeuroImage*, 58(2), 362–380. <https://doi.org/10.1016/j.neuroimage.2011.06.027>
- Chafee, M. V., & Goldman-Rakic, P. S. (1998). Matching Patterns of Activity in Primate Prefrontal Area 8a and Parietal Area 7ip Neurons During a Spatial Working Memory Task. *Journal of Neurophysiology*, 79(6), 2919–2940.
- Cléry, J., Guipponi, O., Odouard, S., Pinède, S., Wardak, C., & Hamed, S. Ben. (2017). The prediction of impact of a looming stimulus onto the body is subserved by multisensory integration mechanisms. *Journal of Neuroscience*, October(44), 10656–10670. <https://doi.org/10.1523/JNEUROSCI.0610-17.2017>
- Clery, J., Guipponi, O., Odouard, S., Wardak, C., & Ben Hamed, S. (2015). Impact Prediction by Looming Visual Stimuli Enhances Tactile Detection. *Journal of Neuroscience*, 35(10), 4179–4189. <https://doi.org/10.1523/JNEUROSCI.3031-14.2015>
- Cléry, J., Guipponi, O., Wardak, C., & Ben Hamed, S. (2014). Neuronal bases of peripersonal and extrapersonal spaces, their plasticity and their dynamics: Knowns and unknowns. *Neuropsychologia*, 70, 313–326. <https://doi.org/10.1016/j.neuropsychologia.2014.10.022>
- Coghill, R. C., Talbot, J. D., Evans, a C., Meyer, E., Gjedde, a, Bushnell, M. C., & Duncan, G. H. (1994). Distributed processing of pain and vibration by the human brain. *The Journal of Neuroscience : The Official Journal of the Society for Neuroscience*, 14(7), 4095–4108.
- Colby, C. L., Duhamel, J. R., & Goldberg, M. E. (1993). Ventral intraparietal area of the macaque: anatomic location and visual response properties. *Journal of Neurophysiology*, 69(3), 902–914.
- Coull, J. T., & Nobre, a C. (1998). Where and when to pay attention: the neural systems for directing attention to spatial locations and to time intervals as revealed by both PET and fMRI. *J Neurosci*, 18(18), 7426–7435. [https://doi.org/0270-6474/98/187426-10\\$05.00/0](https://doi.org/0270-6474/98/187426-10$05.00/0)
- Coull, J. T., & Nobre, A. C. (2008). Dissociating explicit timing from temporal expectation with fMRI. *Current Opinion in Neurobiology*, 18(2), 137–144. <https://doi.org/10.1016/j.conb.2008.07.011>
- di Pellegrino, G., & Làdavas, E. (2015). Peripersonal space in the brain. *Neuropsychologia*, 66, 126–133. <https://doi.org/10.1016/j.neuropsychologia.2014.11.011>
- Disbrow, E., Roberts, T., & Krubitzer, L. (2000). Somatotopic organization of cortical fields in the lateral sulcus of Homo sapiens: Evidence for SII and PV. *Journal of Comparative Neurology*, 418(1), 1–21. [https://doi.org/10.1002/\(SICI\)1096-9861\(20000228\)418:1<1::AID-CNE1>3.0.CO;2-P](https://doi.org/10.1002/(SICI)1096-9861(20000228)418:1<1::AID-CNE1>3.0.CO;2-P)
- Dormal, G., & Pesenti, M. (2012). A Common Right Fronto-Parietal Network for Numerosity and Duration Processing: An fMRI Study. *Human Brain Mapping*, 33, 1490–1501. <https://doi.org/10.1002/hbm.21300>
- Driver, J., & Noesselt, T. (2008). Multisensory interplay reveals crossmodal influences on “sensory-specific” brain regions, neural responses, and judgments. *Neuron*, 57(1), 11–23. <https://doi.org/10.1016/j.neuron.2007.12.013>
- Duhamel, J. R., Bremmer, F., Ben Hamed, S., & Graf, W. (1997). Spatial invariance of visual receptive fields in parietal cortex neurons. *Nature*, 389(6653), 845–848. <https://doi.org/10.1038/39865>
- Duhamel, J. R., Colby, C. L., & Goldberg, M. E. (1998). Ventral intraparietal area of the macaque: congruent visual and somatic response properties. *Journal of Neurophysiology*, 79(1), 126–136.
- Durstewitz, D. (2004). Neural representation of interval time. *Neuroreport*, 15(5), 5–9.
- Eickhoff, Grefkes, C., Fink, G. R., & Zilles, K. (2008). Functional lateralization of face, hand, and trunk representation in anatomically defined human somatosensory areas. *Cerebral Cortex*, 18(12), 2820–2830. <https://doi.org/10.1093/cercor/bhn039>
- Eickhoff, S. B., Amunts, K., Mohlberg, H., & Zilles, K. (2006). The human parietal operculum. II. Stereotaxic maps and correlation with functional imaging results. *Cerebral Cortex (New York, N.Y. :*

- 1991), 16(2), 268–279. <https://doi.org/10.1093/cercor/bhi106>
- Eickhoff, S. B., Schleicher, A., Zilles, K., & Amunts, K. (2006). The human parietal operculum. I. Cytoarchitectonic mapping of subdivisions. *Cerebral Cortex* (New York, N.Y. : 1991), 16(2), 254–267. <https://doi.org/10.1093/cercor/bhi105>
- Eickhoff, S. B., Weiss, P. H., Amunts, K., Fink, G. R., & Zilles, K. (2006). Identifying human parieto-insular vestibular cortex using fMRI and cytoarchitectonic mapping. *Human Brain Mapping*, 27(7), 611–621. <https://doi.org/10.1002/hbm.20205>
- Ferri, Costantini, M., Huang, Z., Perrucci, M. G., Ferretti, A., Romani, G. L., & Northoff, G. (2015). Intertrial Variability in the Premotor Cortex Accounts for Individual Differences in Peripersonal Space. *Journal of Neuroscience*, 35(50), 16328–16339. <https://doi.org/10.1523/JNEUROSCI.1696-15.2015>
- Ferri, F., Tajadura-Jiménez, A., Väljamäe, A., Vastano, R., & Costantini, M. (2015). Emotion-inducing approaching sounds shape the boundaries of multisensory peripersonal space. *Neuropsychologia*, 70, 468–475. <https://doi.org/10.1016/j.neuropsychologia.2015.03.001>
- Fiorio, M., & Haggard, P. (2005). Viewing the body prepares the brain for touch: Effects of TMS over somatosensory cortex. *European Journal of Neuroscience*, 22(3), 773–777. <https://doi.org/10.1111/j.1460-9568.2005.04267.x>
- Fogassi, L., Gallese, V., Fadiga, L., Luppino, G., Matelli, M., & Rizzolatti, G. (1996). Coding of peripersonal space in inferior premotor cortex (area F4). *Journal of Neurophysiology*, 76(1), 141–157.
- Galli, G., Noel, J. P., Canzoneri, E., Blanke, O., & Serino, A. (2015). The wheelchair as a full-body tool extending the peripersonal space. *Frontiers in Psychology*, 6(May), 639. <https://doi.org/10.3389/fpsyg.2015.00639>
- Gardner, E. P. (1988). Somatosensory cortical mechanisms of feature detection in tactile and kinesthetic discrimination. *Canadian Journal of Physiology and Pharmacology*, 66(4), 439–454. <https://doi.org/10.1139/y88-074>
- Gazzola, V., Spezio, M. L., Etzel, J. A., Castelli, F., Adolphs, R., & Keysers, C. (2012). Primary somatosensory cortex discriminates affective significance in social touch. *PNAS*, 109(25), 1657–1666. <https://doi.org/10.1073/pnas.1113211109>
- Genovese, C. R., Lazar, N. a, & Nichols, T. (2002). Thresholding of statistical maps in functional neuroimaging using the false discovery rate. *NeuroImage*, 15(4), 870–878. <https://doi.org/10.1006/nimg.2001.1037>
- Gentile, G., Guterstam, A., Brozzoli, C., & Ehrsson, H. H. (2013). Disintegration of multisensory signals from the real hand reduces default limb self-attribution: an fMRI study. *The Journal of Neuroscience: The Official Journal of the Society for Neuroscience*, 33(33), 13350–13366. <https://doi.org/10.1523/JNEUROSCI.1363-13.2013>
- Gentile, G., Petkova, V. I., & Ehrsson, H. H. (2011). Integration of visual and tactile signals from the hand in the human brain: an FMRI study. *Journal of Neurophysiology*, 105(December 2010), 910–922. <https://doi.org/10.1152/jn.00840.2010>
- Gentilucci, M., Scandolara, C., Pigarev, I., & Rizzolatti, G. (1983). Visual responses in the postarcuate cortex (area 6) of the monkey that are independent of eye position. *Experimental Brain Research*, 50, 464–468.
- Ghazanfar, A. A., & Schroeder, C. E. (2006). Is neocortex essentially multisensory? *Trends in Cognitive Sciences*, 10(6), 278–285. <https://doi.org/10.1016/j.tics.2006.04.008>
- Graziano, & Cooke, D. F. (2006). Parieto-frontal interactions, personal space, and defensive behavior. *Neuropsychologia*, 44, 2621–2635. <https://doi.org/10.1016/j.neuropsychologia.2005.09.011>
- Graziano, Cooke, D. F., & Taylor, C. S. (2000). Coding the location of the arm by sight. *Science* (New York, N.Y.), 290(5497), 1782–1786. <https://doi.org/10.1126/science.290.5497.1782>
- Graziano, & Gross, C. G. (1994). The representation of extrapersonal space: A possible role for bimodal, visual-tactile neurons. *The Cognitive Neurosciences*.
- Graziano, M. S., Hu, X. T., & Gross, C. G. (1997). Visuospatial properties of ventral premotor cortex. *Journal of Neurophysiology*, 77(5), 2268–2292.
- Graziano, M. S., Reiss, L. a, & Gross, C. G. (1999). A neuronal representation of the location of nearby sounds. *Nature*, 397(6718), 428–430. <https://doi.org/10.1038/17115>
- Graziano, Yap, G. S., & Gross, C. G. (1994). Coding of Visual Space by premotor Neurons. *SCIENCE*.

<https://doi.org/10.1126/science.7973661>

Grivaz, P., Blanke, O., & Serino, A. (2017). Common and distinct brain regions processing multisensory bodily signals for peripersonal space and body ownership. *NeuroImage*, 147(iii), 602–618. <https://doi.org/10.1016/j.neuroimage.2016.12.052>

Haggard, P., Christakou, A., & Serino, A. (2007). Viewing the body modulates tactile receptive fields. *Experimental Brain Research*, 180(1), 187–193. <https://doi.org/10.1007/s00221-007-0971-7>

Harrington, D. L., Zimbelman, J. L., Hinton, S. C., & Rao, S. M. (2010). Neural Modulation of Temporal Encoding, Maintenance, and Decision Processes. *Cerebral Cortex*, 20(June), 1274–1285. <https://doi.org/10.1093/cercor/bhp194>

Hayashi, M. J., Kanai, R., Tanabe, H. C., Yoshida, Y., & Walsh, V. (2013). Interaction of Numerosity and Time in Prefrontal and Parietal Cortex. *Journal of Neurophysiology*, 33(3), 883–893. <https://doi.org/10.1523/JNEUROSCI.6257-11.2013>

Holt, D. J., Cassidy, B. S., Yue, X., Rauch, S. L., Boeke, E. a., Nasr, S., ... Coombs, G. (2014). Neural Correlates of Personal Space Intrusion. *Journal of Neuroscience*, 34(12), 4123–4134. <https://doi.org/10.1523/JNEUROSCI.0686-13.2014>

Huang, R.-S., Chen, C., Tran, A. T., Holstein, K. L., & Sereno, M. I. (2012). Mapping multisensory parietal face and body areas in humans. *Proceedings of the National Academy of Sciences of the United States of America*, 109(44), 18114–18119. <https://doi.org/10.1073/pnas.1207946109>

Hyvarinen, J., & Shelepin, Y. (1979). Distribution of visual and somatic functions in the parietal associative area 7 of the monkey. *Brain Research*, 169, 561–564. [https://doi.org/10.1016/0006-8993\(79\)90404-9](https://doi.org/10.1016/0006-8993(79)90404-9)

Ionta, S., Heydrich, L., Lenggenhager, B., Mouthon, M., Fornari, E., Chapuis, D., ... Blanke, O. (2011). Multisensory mechanisms in temporo-parietal cortex support self-location and first-person perspective. *Neuron*, 70(2), 363–374. <https://doi.org/10.1016/j.neuron.2011.03.009>

Janssen, P., & Shadlen, M. N. (2005). A representation of the hazard rate of elapsed time in macaque area LIP. *Nature Neuroscience*, 8(2), 234–242. <https://doi.org/10.1038/nm1386>

Jiang, H.-H., Hu, Y.-Z., Wang, J.-H., Ma, Y.-Y., & Hu, X.-T. (2013). Visuospatial properties of caudal area 7b in *Macaca fascicularis*. *Zoological Research*, 34(E2), E50–61. <https://doi.org/10.3724/SP.J.1141.2013.E02E50>

Kaas, J., Nelson, R., Sur, M., Lin, C., & Merzenich, M. (1979). Multiple representations of the body within the primary somatosensory cortex of primates. *Science*, 204(May), 1977–1979.

Kandula, M., Hofman, D., & Dijkerman, H. C. (2015). Visuo-tactile interactions are dependent on the predictive value of the visual stimulus. *Neuropsychologia*, 70, 358–366. <https://doi.org/10.1016/j.neuropsychologia.2014.12.008>

Kandula, M., Van der Stoep, N., Hofman, D., & Dijkerman, H. C. (2017). On the contribution of overt tactile expectations to visuo-tactile interactions within the peripersonal space. *Experimental Brain Research*. <https://doi.org/10.1007/s00221-017-4965-9>

Leinonen, L., Hyvärinen, J., Nyman, G., & Linnankoski, I. (1979). I. Functional properties of neurons in lateral part of associative area 7 in awake monkeys. *Experimental Brain Research*, 34(2), 299–320. <https://doi.org/10.1007/BF00235675>

Leinonen, L., & Nyman, G. (1979). II. Functional properties of cells in anterolateral part of area 7 associative face area of awake monkeys. *Experimental Brain Research*, 34(2), 321–333. <https://doi.org/10.1007/BF00235676>

Longo, M. R., Pernigo, S., & Haggard, P. (2011). Vision of the body modulates processing in primary somatosensory cortex. *Neuroscience Letters*, 489(3), 159–163. <https://doi.org/10.1016/j.neulet.2010.12.007>

Lopez, C., & Blanke, O. (2011). The thalamocortical vestibular system in animals and humans. *Brain Research Reviews*, 67(1–2), 119–146. <https://doi.org/10.1016/j.brainresrev.2010.12.002>

Lopez, C., Blanke, O., & Mast, F. W. (2012). The human vestibular cortex revealed by coordinate-based activation likelihood estimation meta-analysis. *Neuroscience*, 212, 159–179. <https://doi.org/10.1016/j.neuroscience.2012.03.028>

Macaluso, E., & Driver, J. (2005). Multisensory spatial interactions: A window onto functional integration in the human brain. *Trends in Neurosciences*, 28(5), 264–271.

<https://doi.org/10.1016/j.tins.2005.03.008>

Macaluso, E., Frith, C., & Driver, J. (2005). Multisensory stimulation with or without saccades : fMRI evidence for crossmodal effects on sensory-specific cortices that reflect multisensory location-congruence rather than task-relevance. *NeuroImage*, 26, 414–425.

<https://doi.org/10.1016/j.neuroimage.2005.02.002>

Maister, L., Cardini, F., Zamariola, G., Serino, A., & Tsakiris, M. (2015). Your place or mine: Shared sensory experiences elicit a remapping of peripersonal space. *Neuropsychologia*, 70, 455–461.

<https://doi.org/10.1016/j.neuropsychologia.2014.10.027>

Makin, T. R., Holmes, N. P., Brozzoli, C., Rossetti, Y., & Farnè, A. (2009). Coding of visual space during motor preparation: Approaching objects rapidly modulate corticospinal excitability in hand-centered coordinates. *The Journal of Neuroscience: The Official Journal of the Society for Neuroscience*, 29(38), 11841–11851. <https://doi.org/10.1523/JNEUROSCI.2955-09.2009>

Makin, T. R., Holmes, N. P., & Zohary, E. (2007). Is that near my hand? Multisensory representation of peripersonal space in human intraparietal sulcus. *The Journal of Neuroscience: The Official Journal of the Society for Neuroscience*, 27(4), 731–740. <https://doi.org/10.1523/JNEUROSCI.3653-06.2007>

Martuzzi, R., Murray, M. M., Michel, C. M., Thiran, J. P., Maeder, P. P., Clarke, S., & Meuli, R. A. (2007). Multisensory interactions within human primary cortices revealed by BOLD dynamics. *Cerebral Cortex*, 17(7), 1672–1679. <https://doi.org/10.1093/cercor/bhl077>

Martuzzi, R., van der Zwaag, W., Farthouat, J., Gruetter, R., & Blanke, O. (2014). Human finger somatotopy in areas 3b, 1, and 2: a 7T fMRI study using a natural stimulus. *Human Brain Mapping*, 35(1), 213–226. <https://doi.org/10.1002/hbm.22172>

Matelli, M., Camarda, R., Glickstein, M., & Rizzolatti, G. (1986). Afferent and efferent projections of the inferior area 6 in the macaque monkey. *Journal of Comparative Neurology*, 251(3), 281–298.

<https://doi.org/10.1002/cne.902510302>

Mayka, M. A., Corcos, D. M., Leurgans, S. E., & Vaillancour, D. E. (2006). Three-dimensional locations and boundaries of motor and premotor cortices as defined by functional brain imaging: A meta-analysis. *NeuroImage*, 31(4), 1453–1474. <https://doi.org/10.1016/j.neuroimage.2006.02.004>

Murai, Y., & Yotsumoto, Y. (2016). Context-Dependent Neural Modulations in the Perception of Duration. *Frontiers in Integrative Neuroscience*, 10(March), 1–11. <https://doi.org/10.3389/fnint.2016.00012>

Noel, J.-P., Blanke, O., Magosso, E., & Serino, A. (2018). Neural adaptation accounts for the dynamic resizing of peripersonal space: Evidence from a psychophysical-computational approach. *Journal of Neurophysiology*, 119(6), 2307–2333. <https://doi.org/10.1152/JN.00652.2017>

Noel, J.-P., Grivaz, P., Marmaroli, P., Lissek, H., Blanke, O., & Serino, A. (2014). Full body action Remapping of Peripersonal Space: The case of walking. *Neuropsychologia*, 1–10. <https://doi.org/10.1016/j.neuropsychologia.2014.08.030>

Noel, J.-P., Lukowska, M., Wallace, M., & Serino, A. (2016). Multisensory simultaneity judgment and proximity to the body. *Journal of Vision*, 16(3), 21. <https://doi.org/10.1167/16.3.21>

Noel, J.-P., Pfeiffer, C., Blanke, O., & Serino, A. (2015a). Peripersonal space as the space of the bodily self. *Cognition*, 144, 49–57. <https://doi.org/10.1016/j.cognition.2015.07.012>

Noel, J.-P., Pfeiffer, C., Blanke, O., & Serino, A. (2015b). Supplementary Online Material: Peripersonal space as the space of the bodily self. *Cognition*, 144, 49–57. <https://doi.org/10.1016/j.cognition.2015.07.012>

O'Reilly, J. X., Mesulam, M. M., & Nobre, A. C. (2008). The Cerebellum Predicts the Timing of Perceptual Events. *Journal of Neuroscience*, 28(9), 2252–2260. <https://doi.org/10.1523/JNEUROSCI.2742-07.2008>

Oliveri, M., Koch, G., Salerno, S., Torriero, S., Gerfo, E. Lo, & Caltagirone, C. (2009). Representation of time intervals in the right posterior parietal cortex: Implications for a mental time line. *NeuroImage*, 46(4), 1173–1179. <https://doi.org/10.1016/j.neuroimage.2009.03.042>

Pellencin, E., Paladino, M. P., Herbelin, B., & Serino, A. (2017). Social perception of others shapes one's own multisensory peripersonal space. *Cortex*, 1–17. <https://doi.org/10.1016/j.cortex.2017.08.033>

Pouthas, V., George, N., Poline, J., Pfeuty, M., Hugueville, L., Ferrandez, A., ... Renault, B. (2005). Neural Network Involved in Time Perception : An fMRI Study Comparing Long and Short Interval

- Estimation. *Human Brain Mapping*, 441, 433–441. <https://doi.org/10.1002/hbm.20126>
- Rizzolatti, G., Scandolara, C., Matelli, M., & Gentilucci, M. (1981a). Afferent properties of periarculate neurons in macaque monkeys. I. Somatosensory responses. *Behavioural Brain Research*, 2, 125–146. [https://doi.org/10.1016/0166-4328\(81\)90052-8](https://doi.org/10.1016/0166-4328(81)90052-8)
- Rizzolatti, G., Scandolara, C., Matelli, M., & Gentilucci, M. (1981b). Afferent properties of periarculate neurons in macaque monkeys. II. Visual responses. *Behavioural Brain Research*, 2, 147–163. [https://doi.org/10.1016/0166-4328\(81\)90053-X](https://doi.org/10.1016/0166-4328(81)90053-X)
- Rizzolatti, Giacomo, Fadiga, L., Fogassi, L., & Gallese, V. (1997). The Space Around Us. *Science*, 277(5323), 190–191. <https://doi.org/10.1126/science.277.5323.190>
- Roberts, R. P., Ahmad, H., Arshad, Q., Patel, M., Dima, D., Leech, R., ... Bronstein, A. (2017). Functional neuroimaging of visuo-vestibular interaction. *Brain Structure and Function*, 222(5), 2329–2343. <https://doi.org/10.1007/s00429-016-1344-4>
- Sack, A. T. (2009). Parietal cortex and spatial cognition. *Behavioural Brain Research*, 202(2), 153–161. <https://doi.org/10.1016/j.bbr.2009.03.012>
- Salomon, R., Noel, J.-P., Łukowska, M., Faivre, N., Metzinger, T., Serino, A., & Blanke, O. (2017). Unconscious integration of multisensory bodily inputs in the peripersonal space shapes bodily self-consciousness. *Cognition*, 166, 174–183. <https://doi.org/10.1016/j.cognition.2017.05.028>
- Sereno, M. I., & Huang, R.-S. (2006). A human parietal face area contains aligned head-centered visual and tactile maps. *Nature Neuroscience*, 9(10), 1337–1343. <https://doi.org/10.1038/nn1777>
- Serino, A. (2016). Variability in Multisensory Responses Predicts the Self-Space. *Trends in Cognitive Sciences*, 20(3), 169–170. <https://doi.org/10.1016/j.tics.2016.01.005>
- Serino, A. (2019). Peripersonal space (PPS) as a multisensory interface between the individual and the environment, defining the space of the self. *Neuroscience and Biobehavioral Reviews*, 99(January), 138–159. <https://doi.org/10.1016/j.neubiorev.2019.01.016>
- Serino, A., Annella, L., & Avenanti, A. (2009). Motor properties of peripersonal space in humans. *PLoS ONE*, 4(8), 1–8. <https://doi.org/10.1371/journal.pone.0006582>
- Serino, A., Canzoneri, E., & Avenanti, A. (2011). Fronto-parietal areas necessary for a multisensory representation of peripersonal space in humans: an rTMS study. *Journal of Cognitive Neuroscience*, 23(10), 2956–2967. [https://doi.org/10.1162/jocn\\_a\\_00006](https://doi.org/10.1162/jocn_a_00006)
- Serino, A., Canzoneri, E., Marzolla, M., di Pellegrino, G., & Magosso, E. (2015). Extending peripersonal space representation without tool-use: evidence from a combined behavioral-computational approach. *Frontiers in Behavioral Neuroscience*, 9(February), 1–14. <https://doi.org/10.3389/fnbeh.2015.00004>
- Serino, A., & Haggard, P. (2010). Touch and the body. *Neuroscience and Biobehavioral Reviews*, 34(2), 224–236. <https://doi.org/10.1016/j.neubiorev.2009.04.004>
- Serino, A., Noel, J. P., Galli, G., Canzoneri, E., Marmaroli, P., Lissek, H., & Blanke, O. (2015). Body part-centered and full body-centered peripersonal space representations. *Scientific Reports*, 5(July), 1–14. <https://doi.org/10.1038/srep18603>
- Serino, A., Pizzoferrato, F., & Làdavias, E. (2008). Viewing a Face (specially one’s own face) being touched enhances tactile perception on the face. *Psychological Science*, 19(5), 434–438. <https://doi.org/10.1111/j.1467-9280.2008.02105.x>
- Taffou, M., & Viaud-Delmon, I. (2014). Cynophobic fear adaptively extends peri-personal space. *Frontiers in Psychiatry*, 5(AUG), 3–9. <https://doi.org/10.3389/fpsy.2014.00122>
- Taylor-Clarke, M., Kennett, S., & Haggard, P. (2002). Vision modulates somatosensory cortical processing. *Current Biology*, 12(3), 233–236. [https://doi.org/10.1016/S0960-9822\(01\)00681-9](https://doi.org/10.1016/S0960-9822(01)00681-9)
- Teneggi, C., Canzoneri, E., di Pellegrino, G., & Serino, A. (2013). Social modulation of peripersonal space boundaries. *Current Biology : CB*, 23(5), 406–411. <https://doi.org/10.1016/j.cub.2013.01.043>
- Tipples, J., Brattan, V., & Johnston, P. (2013). Neural Bases for Individual Differences in the Subjective Experience of Short Durations (Less than 2 Seconds). *PLoS ONE*, 8(1), 1–8. <https://doi.org/10.1371/journal.pone.0054669>
- Tyll, S., Bonath, B., Schoenfeld, M. A., Heinze, H. J., Ohl, F. W., & Noesselt, T. (2013). Neural basis of multisensory looming signals. *NeuroImage*, 65, 13–22. <https://doi.org/10.1016/j.neuroimage.2012.09.056>



- Vagnoni, E., Lourenco, S. F., & Longo, M. R. (2012). Threat modulates perception of looming visual stimuli. *Current Biology*, 22(19), R826–R827. <https://doi.org/10.1016/j.cub.2012.07.053>
- Van der Stoep, N., Serino, A., Farnè, A., di Luca, M., & Spence, C. (2016). Depth : The forgotten dimension in multisensory research. *Multisensory Research*, (JANUARY).
- van Ede, F., de Lange, F., Jensen, O., & Maris, E. (2011). Orienting Attention to an Upcoming Tactile Event Involves a Spatially and Temporally Specific Modulation of Sensorimotor Alpha- and Beta-Band Oscillations. *Journal of Neuroscience*, 31(6), 2016–2024. <https://doi.org/10.1523/JNEUROSCI.5630-10.2011>
- Wallace, M. T., Ramachandran, R., & Stein, B. E. (2004). A revised view of sensory cortical parcellation. *Proceedings of the National Academy of Sciences of the United States of America*, 101(7), 2167–2172. <https://doi.org/10.1073/pnas.0305697101>
- Xu, Z., Wu, Q., Li, Y. K., Wu, J., Li, C., Ohno, S., & Kanazawa, S. (2014). Different Neural Network for Exogenous Temporal Expectations under Sub-second and Supra-second in fMRI. *Proceedings of the 2014 IEEE International Conference on Mechatronics and Automation*, 1734–1739.
- Zu Eulenburg, P., Caspers, S., Roski, C., & Eickhoff, S. B. (2012). Meta-analytical definition and functional connectivity of the human vestibular cortex. *NeuroImage*, 60(1), 162–169. <https://doi.org/10.1016/j.neuroimage.2011.12.032>

## Supplementary information of Distinct neural mechanisms of temporal and spatial prediction in peripersonal space

### Supplementary Results

#### *Experiment 1B – behavior*

The rate of success in the attention condition (i.e. button press in response to a brief change in color of the centered fixation cross) was 97.6% whereas the rate of false alarms (i.e. wrongful button press when ball loomed towards the face but no touch was delivered) was 0.6%, suggesting high compliance. Furthermore, following missed trials and exclusion of invalid and outlier data points (see methods section), 98.9% of all data points were preserved for subsequent analyses.

For the behavioral task associated with experiment 1 (Figure 4C), the 2-by-5 rmANOVA on RTs with factors Modality (sVT, dVT) and Temporal offset (T1, T1|2, T2, T2|3, T3) revealed a main effect of Modality ( $F(1, 16) = 5.18, p = 0.037$ ) and a main effect of Temporal offset ( $F(4, 64) = 5.21, p = 0.001$ ). The Modality-by-Temporal offset interaction was not significant ( $F(4, 64) = 1.86, p = 0.129$ ), suggesting that both modalities were on average affected similarly by the temporal offset.

In order to assess for which temporal offsets there was a multisensory facilitation effect and thus signaling the boundary between peri- and extra-personal space, we checked for which of the bimodal sVT and dVT conditions the reaction times differed significantly from the unimodal baseline condition. To this aim, we ran a 2-by-6 rmANOVA with factors Modality (sVT, dVT) and Temporal offset (T1, T1|2, T2, T2|3, T3, baseline). Such analysis revealed a main effect of Modality ( $F(1,16) = 5.18, p = 0.0370$ ) and of Temporal offset ( $F(5,80) = 4.64, p = 0.0009$ ), but no Modality-by-Temporal offset interaction ( $F(5,80) = 2.08, p = 0.0764$ ). Due to the absence of an interaction, we did not pursue with post-hoc analyses (for each Modality separately), as the RTs for the Modality factors were not influenced differentially by the Temporal offset factors. However, due to the main effect of Temporal offset, we conducted a post-hoc analysis on the pooled data from the sVT and dVT conditions, which showed that none of the mean RTs for any of the temporal offsets were statistically different from the baseline (all  $p > 0.5$ ). Collectively, this suggests that for experiment 1, the

RTs in both sVT and dVT conditions were on average equally affected by the temporal offset of the stimulus. Despite a general speeding up of reaction times with increasing temporal offset, for none of the tested temporal offsets there was a facilitation effect on the RTs with respect to the baseline that would signal the PPS boundary.

### ***Experiment 2B – behavior***

The rate of success in the attention condition (i.e. button press in response to a brief change in color of the centered fixation cross) was 97.1% whereas the rate of false alarms (i.e. wrongful button press when ball loomed towards the face but no touch was delivered) was 4.1%, suggesting high compliance. Furthermore, following missed trials and exclusion of invalid and outlier data points (see methods section), 98.5% of all data points were preserved for subsequent analyses.

For the behavioral task of experiment 2 (Figure 4C), the 2-by-5 rmANOVA on baseline-corrected RTs with factors Modality (sVT, dVT) and Temporal offset (T1, T1|2, T2, T2|3, T3) revealed a main effect of Temporal offset ( $F(4, 64) = 3.97$ ,  $p = 0.006$ ), whereas the main effect of Modality was not significant ( $F(1, 16) = 1.04$ ,  $p = 0.322$ ). Crucially, however, we found a Modality-by-Temporal offset interaction ( $F(4, 64) = 3.30$ ,  $p = 0.016$ ), suggesting that RTs were affected differently depending on the Modality factor. In order to assess the origin of this interaction, we conducted post-hoc pair-wise comparisons on the RTs using Tukey's HSD test, which revealed that RTs in the dVT condition at T3 (when touch was associated to a virtual stimulus close to the face) were significantly faster than RTs in the dVT condition at T1 ( $p = 0.0034$ ), dVT at T1|2 ( $p = 0.0044$ ) and than RTs in all the sVT conditions, namely sVT at T3 ( $p = 0.0047$ ), sVT at T2|3 ( $p = 0.431$ ), sVT at T2 ( $p = 0.0042$ ) and sVT at T1 ( $p = 0.0002$ ). Additionally, dVT at T2|3 was significantly different from dVT at T1 ( $p = 0.0069$ , for all other pairwise comparison  $p > 0.05$ ). Crucially, this shows that when concentrating only on the homologous temporal offsets between the two levels of the Modality factor, only at T3 (virtual ball perceived in near space in the dVT condition) do the RTs differ between the two modalities. Investigating the effects of Temporal offset for each Modality separately yielded a main effect of Temporal offset for the dVT ( $F(4,64) = 5.48$ ,  $p < 0.001$ ) but not the sVT ( $F(4, 64) = 1.37$ ,  $p = 0.253$ ) conditions.

In order to assess the location of the boundary between peri- and extrapersonal space, we ran a 2-by-6 rmANOVA with factors Modality (sVT, dVT) and Temporal offset (T1, T1|2, T2, T2|3, T3, baseline) on the baseline-uncorrected RTs. This analysis revealed a main effect of Temporal offset ( $F(5,80) = 3.47$ ,  $p = 0.0068$ ) but not of Modality ( $F(5,80) = 1.04$ ,  $p = 0.3222$ ). Crucially, there was a Modality-by-Temporal offset interaction ( $F(5,80) = 2.50$ ,  $p = 0.0369$ ). Thus, we ran a one-way rmANOVA on these RTs for each Modality separately, with factors Temporal offset (T1, T1|2, T2, T2|3, T3, baseline), which yielded only for the dVT condition a main effect ( $F(5,80) = 4.45$ ,  $p = 0.0013$ ), but not for the sVT condition ( $F(5,80) = 1.09$ ,  $p = 0.3722$ ). For the prior, we therefore proceeded with pairwise comparisons using Tukey's HSD test, which revealed only a significant difference for RTs between T3 and T1|2 ( $p = 0.0069$ ), T3 and T1 ( $p = 0.0055$ ) and crucially T3 and baseline ( $p = 0.0318$ ), suggesting that the boundary of peri-personal space lies between T3 and T2|3 for the dVT condition (thus between near and near-intermediate perceived distances), whereas the RTs are not significantly different from the baseline for any of the sVT conditions.

### ***Depth estimation task***

A one-way rmANOVA on the factor Distance (DT1, DT1|2, DT2, DT2|3, DT3) showed a main effect ( $F(1, 4) = 163.33$ ,  $p < 0.001$ ), with the position of the virtual ball at the Distance DT1 being perceived furthest from the face and the perceived position at Distance DT3 being perceived as the closest from the face, with a monotonically decreasing perceived distance between T1 and T3. Pairwise post-hoc comparisons using Tukey's HSD test confirmed that the distance perceived at different Temporal offsets were rated as significantly different from their neighbors ( $p < 0.001$ ), except for depths estimated for T1 and T1|2 ( $p < 0.29$ ). Crucially for the fMRI experiment, where only depths corresponding to Temporal offsets T1, T2 and T3 were used, pairwise comparisons showed that they were rated as significantly different between each other (for both T1 and T2, and T2 and T3,  $p < 0.001$ ), although the rated difference in depth between the farther distance (18.48 % of total path length) was perceived smaller than that between the closer distances (50.81 % of total path length).

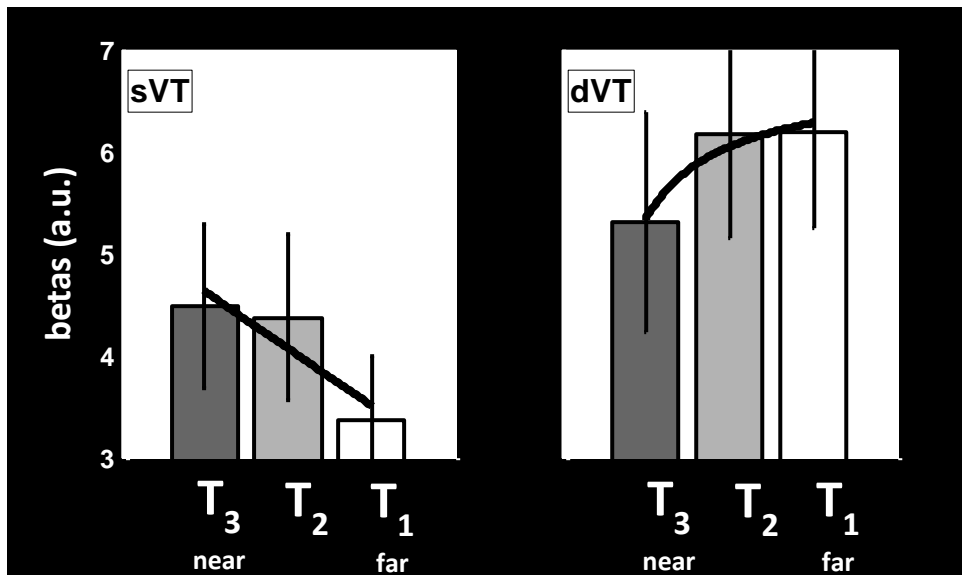


**Figure S1:** Pattern of activity associated to the right superior occipital cortex (SOC). Despite an absence of a main effect of Temporal offset and a presence of a Modality-by-Temporal offset interaction, the pattern of activity was not one that would have been expected for a “spatial” ROI (see classification schemes in Methods and Figure 1B) and was thus classified as “sensory”.

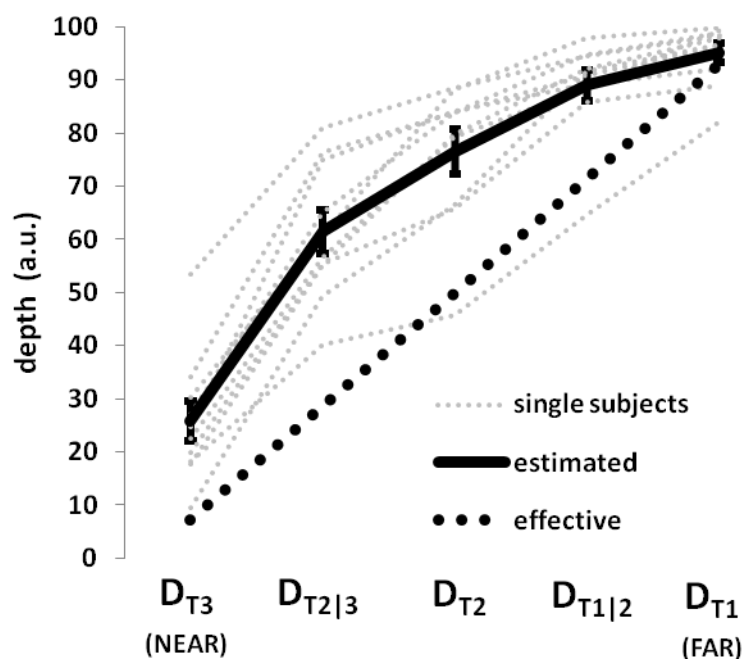


**Figure S2:** Results from the ball depth estimation task. The y-axis represents the percentage of the total length of the trajectory with 0 being close to the face and 100 being far from the face. The “estimated” curve corresponds to the estimated mean  $\pm$  s.e.m. of the virtual ball by the subjects (“single-subjects”). The “effective” curve represents the exact depth of the stimuli in virtual space.

---

## Acknowledgments

I would like to thank my colleagues, my family and friends without whom this work would not have been possible. First, I would like to thank Olaf for the great opportunity he gave me to work in his lab, for his enthusiasm and the meetings which have each time motivated me! I would also like to thank Dimitri for his valuable advices and discussions.

I am very happy to have been part of the great and dynamic team of LNCO! I am grateful to the team of PhDs (Giedre, Herberto, Pavo, Bastien, Julia, June, Myeong, Matteo, Nathalie, Jemina, Atena), with who it is always fun to spend time with! Giedre, for all the early morning coffee breaks and greats talks, Herberto, for his motivation and optimism, Julia for the Thai-food meals and her motivation, Pavo for always sharing good music. I'm grateful to Andrea, Michel and Petr for having helped me at the beginning of my thesis and especially Michel to have taught me everything about fMRI analysis and always helped me with analyses and scripts. I would also like to thank Giulio and Nathan for their supervision and guidance that have always been helpful; Jevita for her valuable advice, help and discussions; Fosco for his challenging comments and discussions.

More generally, I would like to thank all the LNCO lab members with whom it has always been a pleasure to work with and share meals and coffee breaks; and also, all the people from the different fields I had the occasion to work with, Roberto and Loan at the MRI facility, the MIP lab, the DIP lab, Masayuki among others!

I would like to thank the members of the jury for their time and interest in my thesis: Prof. Marie Schaer, Prof. Alice Cronin-Golomb, Prof. Jean-Philippe Thiran, Prof. Friedhelm Hummel.

I would also like to thank all my family, in particular my parents, my brother and sister which have always been there to support me since the beginning!

Finally, I would like to thank my amazing husband Felix that has always been by my side all along my PhD, supporting me and motivating me; and my little sweetheart Eléana that is always there to make me smile!

---

## Curriculum Vitae

### BLONDIAUX EVA

Route du Boiron, 55  
Nyon, 1260, Switzerland  
+41787337821  
blondiaux.eva@gmail.com  
Born on 29.06.1992  
Nationality: French and Spanish



**Languages: French and Spanish (bilingual), English (fluent)**

#### Professional skills

---

- Capable of working in **multidisciplinary** teams (part of a team composed of robotic engineers, medical doctors and psychologists).
- Conduct **independent** research (planning a project from hypothesis to publication).
- **Summarize** results, **simplify** concepts, **present** in clear and efficient way (presentations at national conferences).
- Proficient in **matlab, R** and working knowledge in C/C++, bash.
- Capable of **analyzing large datasets** (e.g. functional magnetic resonance imaging data from preprocessing to statistical analyses).

#### Education

---

- 2015-2020** PhD student in the Laboratory of Cognitive Neuroscience (LNCO) of Prof. Blanke **Swiss Federal Institute of Technology (EPFL)**, Lausanne, Switzerland  
*Neuroscience robotics of altered bodily self-consciousness and hallucinations.*
- 2013-2015** “Ingénieure en Sciences et Technologies du vivant”  
Master of Science (M. Sc.) in Life Sciences and Technology with orientation in Neuroscience and Neuroengineering  
Master project in the Laboratory of Cognitive Neuroscience (LNCO) directed by Prof. Blanke  
*Investigating the neural correlates of the whole-body peri-personal space using ultra high-field fMRI and assessing behaviorally the virtual peri-hand space after manipulation of ownership and agency over that virtual hand*  
**Swiss Federal Institute of Technology (EPFL)**, Lausanne, Switzerland
- 2010- 2013** Bachelor in Life Science and Technology  
**Swiss Federal Institute of Technology (EPFL)**, Lausanne, Switzerland  
Bachelor project in the Laboratory of Molecular Mechanisms of Lung Cancer Development led by Prof. Meylan  
*Screening of important genes for viability in KRas dependent cell line*
- June 2010** “Baccalauréat scientifique à option international espagnol, mention très bien”  
**Lycée International de Ferney-Voltaire**, Ferney-Voltaire, France

---

## PROFESSIONAL EXPERIENCES

---

<b>2016-2019</b>	Management of a website platform to recruit healthy volunteers for experiments for the LNCO
<b>2015-2017</b>	Supervised lectures, prepared and supervised practical sessions in the course “Neuroscience for engineers” (3 <sup>rd</sup> year Bachelor class) and “Neuroscience III: behavioural and cognitive neuroscience” (Master class)
<b>Summer 2014 (Jul-Sept)</b>	Internship at the Laboratory of Neuroimaging research (LREN) Prof. Draganski <i>Automatic pipeline for the pre-processing of MRI images</i> <b>Centre Hospitalier Universitaire Vaudois (CHUV)</b> , Lausanne, Switzerland
<b>Autumn 2013</b>	Teaching-assistant for Analysis I lecture given by Mr. Ruppen <b>Swiss Federal Institute of Technology (EPFL)</b> , Lausanne, Switzerland
<b>Autumn 2012</b>	Teaching-assistant for Analysis I lecture given by Mr. Ruppen <b>Swiss Federal Institute of Technology (EPFL)</b> , Lausanne, Switzerland
<b>2012-2015</b>	Private tuition of mathematics for primary and high school and bachelor students
<b>Apr. 2012 &amp; 2013</b>	Animator at the “Festival de Robotique” 5th and 6th editions
<b>Summer 2010</b>	Commercial employee at Migros in Val Thoiry (France)

---

## PUBLICATIONS, POSTERS & PRESENTATIONS

---

### *Publication*

Sensorimotor hallucinations in Parkinson’s disease. Fosco Bernasconi\*, **Eva Blondiaux\***, Jevita Potheegadoo, Giedre Stripeikyte, Javier Pagonabarraga, Helena Bejr-Kasem, Michela Bassolino, Michel Akselrod, Saul Martinez-Horta, Fred Sampedro, Masayuki Hara, Judit Horvath, Matteo Franza, Stéphanie Konik, Matthieu Bereau, Joseph-André Ghika, Pierre R. Burkhard, Dimitri Van De Ville, Nathan Faivre, Giulio Rognini, Paul Krack, Jaime Kulisevsky, Olaf Blanke *Submitted*, accessible on BioRxiv, <https://doi.org/10.1101/2020.05.11.054619>

Distinct neural mechanisms of temporal and spatial prediction in peripersonal space. Authors: Petr Grivaz\*, **Eva Blondiaux\***, Michel Akselrod, Bruno Herbelin, Andrea Serino & Olaf Blanke. *Submitted*

Bolton, T., Tuleasca, C., Wotruba, D., Rey, G., Dhanis, H., Gauthier, B., Delavari, F., Morgenroth, E., Gaviria, J., **Blondiaux, E.**, Smigielski, L., & Van De Ville, D. (2020). TbCAPs: A toolbox for co-activation pattern analysis. *NeuroImage*, 211, 116621. <https://doi.org/10.1016/j.neuroimage.2020.116621>

(\*) These authors contributed equally to the paper.

### *In preparation*

Common and distinct brain networks of four autoscopic phenomena. **Eva Blondiaux**, Lukas Heydrich & Olaf Blanke

Individuals with the 22q11.2 deletion syndrome show lack of sensitivity to sensorimotor conflicts. **Eva Blondiaux**, Jevita Potheegadoo, Giedre Stripeikyte, Laurent Jenni, Johanna Maeder, Virginie Pouillard, Fosco Bernasconi., Corrado Sandini, Eva Micol, Maude Schneider, Stephan Eliez, and Olaf Blanke

Fronto-temporal functional disconnection within the presence hallucination network in psychotic patients with passivity experiences. Giedre Stripeikyte, Jevita Potheegadoo, Pierre Progin, **Eva Blondiaux**, Giulio Rognini, Kim Do, Philippe Conus, Patric Hagmann, Nathan Faivre, Olaf Blanke



---

Robotically-induced Presence Hallucination hijacks normal brain network dynamics. Herberto Dhanis, **Eva Blondiaux**, Thomas Bolton, Nathan Faivre, Giulio Rognini, Dimitri Van De Ville and Olaf Blanke.

The neural correlates of reduplicative paramnesia – a lesion analysis study. Blanke, O\*, Diamantaras, A\*, **Blondiaux, E**, Müri, R, Heydrich, L

#### Poster

- **Society of Biological Psychiatry meeting (SOBP)** (May 2018): “Neural Mechanisms of Presence Hallucination and Passivity Experience Induced by Sensorimotor Conflicts in Healthy subjects: A Robotics-Fmri Study”
- **Alpine Brain Imaging Meeting** (January 2018): “Fronto-parietal cortices mediate specific psychosis-like states induced by sensorimotor conflicts: a robotics-fMRI study”.
- **Alpine Brain Imaging Meeting** (January 2017): “Neural mechanisms of temporal and spatial prediction in face peripersonal space in humans”.
- **NCCR synapsy Annual meeting** (March 2017): “Brain networks associated with sensorimotor conflicts and presence hallucination using MR-compatible robotics”.
- **BMI retreat** (June 2017): “Right fronto-parietal cortex mediates specific psychosis-like state induced by sensorimotor conflicts: a robotics-fMRI study”.

“Neural correlates of the face peripersonal space using ultra high-field fMRI”, presented at:

- **Alpine Brain Imaging Meeting (ABIM)**, January 2016
- **Swiss Society of Neuroscience (SSN)**, January 2016
- **Human Brain Mapping (HBM)**, June 2016

#### Presentation

- **BBL/CIBM Research day** (June 2017): “Right fronto-parietal cortex mediates specific psychosis-like states induced by sensorimotor conflicts: a robotics-fMRI study”.

#### Other

- Travel grant from the Swiss Society for Neuroscience for the participation in the SOBP (2018)

## SKILLS

---

Cognitive neuroscience, neuroimaging (acquisition and analysis of fMRI, functional resting state (SPM and conn toolbox)), design of behavioral and neuroimaging studies, statistical analysis (R, Statistica)

Basic knowledge in robotics (worked with different robotic systems)

**Programming:** matlab, R, C/C++, MS office and some background in JAVA and PYTHON

## OTHER INTERESTS

---

Dance (Flamenco) for 5 years in Geneva (Switzerland).

Competition in synchronized swimming for 8 years in Meyrin (Switzerland).

Running (10K), Ski

## REFERENCES

---

**Prof. Olaf Blanke**, head of the Laboratory of Cognitive Neuroscience, Brain Mind Institute, EPFL

**Prof. Andrea Serino**, head of My Space Lab, CHUV